Tsogtbaatar Chinzorig

EVOLUTION, DIVERSITY, AND DISPARITY OF ORNITHOMIMOSAURS (DINOSAURIA: THEROPODA) FROM THE UPPER CRETACEOUS OF MONGOLIA

(モンゴルの白亜系から発見されているオルニトミモサウルス類（恐竜類：獣脚類）の進化、多様性、異質性)

Doctoral Dissertation

EVOLUTION, DIVERSITY, AND DISPARITY OF ORNITHOMIMOSAURS (DINOSAURIA: THEROPODA) FROM THE UPPER CRETACEOUS OF MONGOLIA

(モンゴルの白亜系から発見されているオルニトミモサウルス類（恐竜類：獣脚類）の進化、多様性、異質性)

Tsogtbaatar Chinzorig

Graduate School of Science, Hokkaido University
Department of Natural History Sciences

March 2019

ABSTRACT

Ornithomimidae, the derived clade of Ornithomimosauria, are one of the major clades of coelurosaurian dinosaurs and fossil remains of this group have been richly discovered in the Cretaceous sediments of eastern Asia, specifically in the Gobi Desert of Mongolia. In this study, four ornithomimosaur specimens from the Late Cretaceous of Mongolia are newly described in detail. They include a multitaxic bonebed of two potential new ornithomimosaurs from the Bayanshiree Formation (Cenomanian- Turonian), a new taxon, named *Aepyornithomimus tugrikinensis* gen. et sp. nov., from the Djadokhta Formation (Campanian), and a complete articulated ornithomimid skeleton from the Nemegt Formation (late Campanian-early Maastrichtian).

The ornithomimosaur specimens discovered from the Baishin Tsav locality were collected in a single multitaxic bonebed with a different ontogenetic stage of at least five individuals. This bonebed suggests that it is possible that a small pack (<10 individuals) of multispecific ornithomimid herd was herding together in some preferable places.

Aepyornithomimus tugrikinensis gen. et sp. nov. was discovered from the Upper Cretaceous Djadokhta Formation of Mongolia. The phylogenetic position of this new taxon is placed a member of the derived ornithomimosaurs. Hence, it is recovered a missing cap of evolution of the Late Cretaceous Mongolian ornithomimosaurs from the Djadokhta Formation, as well as the first ornithomimid record from eolian influenced environment, indicative of their wide capability to adapt to arid environments.

The Upper Cretaceous Nemegt Formation of Mongolia is rich in well-preserved dinosaurs, and ornithomimosaurs are common dinosaurs in the formation. A complete articulated ornithomimosaur skeleton was recovered from the Upper Cretaceous Nemegt Formation of Bügiin Tsav locality, Mongolia. The morphological features and the phylogenetic analysis of this specimen represent as the definitive new ornithomimid and the fourth ornithomimosaur from the formation, demonstrating a high diversification of this group in Late Cretaceous in Asia. Moreover, the structures of manual elements among Nemegt ornithomimosaurs reveals their remarkable diversity. The results of numerical analyses show that a large diversity of manual morphology may be related to large variety of palaeoecological niches were prevailed in the Nemegt ecosystem.

ACKNOWLEDGMENTS

I would like to thank from my deepest thanks bottom of my heart to my supervisor Prof. Yoshitsugu Kobayashi for first of all that give me the opportunity and chance to study at the Hokkaido University as his student, and his guidance on researches throughout my PhD course. All results and ideas of my research works were discussed with him and gave important points in every statements to make them more interests scientifically.

I am grateful to Drs. Rinchen Barsbold, Philip J. Currie, Shinobu Ishigaki, Khishigjav Tsogtbaatar, Anthony Fiorillo, Mahito Watabe, Mototaka Saneyoshi, and many others who are not included in this list for their help to understand a field of paleontology and geology. I am also thankful to all staff of the Institute of Paleontology and Geology of Mongolian Academy of Sciences for helping me in the laboratory and in the field, specifically Chagnaa Bayardorj for his skillful preparation works of the specimens, Sanjaadash Ulziitseren for taking specimen photos, and helping me to observe more specimens from the collection, and all of others. Moreover, I would gratitude to members of the past Hayashibara Museum of Natural History Sciences, namely Mr. Shigeru Suzuki and Mr. Yasuhiro Kawahara. Mr. Kawahara who are great efforts in the field that discovered the scientifically important specimens during courses of the joint expedition. Without these specimens, my PhD researches wouldn't be accomplished. I am also greatly appreciated Drs. Eva B. Koppelhus and Don Brinkman for their warmth hospitalities and kindness when I travelled to Canada as a collection visit. Drs. David C. Evans, Kevin Seymour, and Caleb Brown of the Royal Ontario Museum, Drs. Mark A. Norell and Carl Mehling of American Museum of Natural History who helped me to access to the collection and provided me to observe hundreds of the specimens during my research visit.

I am also gratitude to my other member of the doctoral committee, professors Mitsuhiro Nakagawa, Toru Takeshita, and Yasuhiro Iba, helped to guidance and instructive technical comments for my dissertation works.

Professors and staffs of the Hokkaido University of Museum, namely Drs. Masahiro Ohara, Masaki Eda, Junichi Yamamoto, Makiko Yuasa, who are always kind to me and always inviting me to participate any activities to make a life fun in Sapporo. I wouldn't forget to express my big thanks

to current lab members, Ryuji Takasaki, Tomonori Tanaka, Kota Kubo, Junki Yoshida, Mui Tanaka, Akira Ota, Suzuki Hana, and other members whose names are not mentioned here, as well as lab alumni, Masaya Iijima, Shoji Hayashi, Kohei Tanaka, Chiba Kentaro, Yoshihiro Tanaka, and Takumi Sakakiyama, for their always helpful any time and informative discussion on my researches, supports in the fieldwork, as well as a life in Sapporo during my doctorate time. Ryuji Takasaki and Masaya Iijima are great contributors for my studies without their critical discussions and helping my research analysis, my dissertation works wouldn't be accepted in peer-review journals. I must hugely thank to Tomonori Tanaka, who was all the time with me to sharing a room for his continuous time-less helps in both in my research and my life in Sapporo. I wouldn't have forgotten the fossil and molding volunteers of the Hokkaido University of Museum for their kindness as well as serving me a hot coffee with snacks in every time and helped me to improve my Japanese which helped me a lot to communicate in Japan. I also wouldn't have forgotten late Mr. Kei Nakano. He always made us some funny things and have told fun stories which were relaxing my brain while I was studying. As well as, he taught me many Japanese words and phrases which I use them every time when I need. Also, I would like to express my thanks to Mrs. Hiroko Nakano for her warmest hospitality and anytime invited my delicious meals. Thanks to the staff of Office for International Academic Support such as Mrs. Hiroko Hori and Mari Igarashi.

I would like to acknowledge my doctoral research funding and financial supports from Japanese Government MEXT Scholarship, a travel grant for collection visit by the Jurassic Foundation, and a 34th International Student Research Grant (Ref# 959) in 2017 of Kobayashi Fund from Fujifilm Xerox Co. Ltd., Tokyo.

Finally, I express my deepest thanks to my parents and my lovely family for their endless supports and cares in many ways and apologize a long period of time to absence from my daughters.

TABLE OF CONTENTS

LIST OF ABBREVIATION

Cranial

an – angular
aof – antorbital fenestra
bs – basisphenoid
d – dentary
dep – depression
ect – ectopterygoid
emf – external mandibular fenestra
eo – exoccipital
f – frontal
fo – fossa
lac – lacrimal
Mand – mandible
m – maxilla
m.fen – maxillary fenestra
n – nasal
nlc – nasolacrimal canal
o – orbit
p – parietal
pal – palatine
pf – prefrontal
po – postorbital
pm – premaxilla
pra – prearticular
ps – parasphenoid
pt – pterygoid
q – quadrate
qj – quadratojugal
racq – ridge for accessory condyle of quadrate
Sk – skull
sa – surangular
sc – sclerotic ring
sp – spenial
sq – squamosal

Axial

as – articular surface
c – centrum
di – diapophysis
ns – neural spine
nst – a tip of the neural spine
pa – parapophysis
prz – prezygapophysis
postz – postzygapophysis

Cervical vertebrae

aic – axial intercentrum
Cv – cervical vertebra
Cvr – cervical rib
pf – pneumatic foramen

Dorsal vertebrae

Dv – dorsal vertebra
hypo – hyposphene
tp – transverse process
sdpl – spinodiapophyseal lamina
spostzl – spinopostzygapophyseal lamina
spzf – spinopostzygapophyseal fossa

Sacral vertebrae

Sv.1 ….. Sv.6 – first sacral …, … sixth sacral

Caudal vertebrae

Ca – caudal vertebra

Appendicular

ca – capitulum

dep – depression

t – tuberculum

Forelimb

ap – acromion process

c – centrale

cf – coracoid fossa

bt – biceps tubercle

d1 – digit I

d2 – digit II

d3 – digit III

dc –distal carpal

Hum – humerus

in – intermedium

igb – infraglenoid buttress

of – olecranon fossa

op – olecranon process

posp – posterior process of coracoid

lcd – lateral condyle

mcd – medial condyle

mc I – metacarpal I

mc II – metacarpal II

mc III – metacarpal III

Ph I-1, Ph I-2, …. Ph III-4 – manual phalanges

r – radiale

ra – radius

scb – scapular blade

scf – flange of the scapula

sgb – supraglenoid buttress

Un – ungual

ul – ulna

Pelvis

aca – acute angle

anp – anterior process of pubic boot

an – antitrochanter

bvf – brevis fossa

cup – cuppedicus fossa

is – ischium

isa – ischial apron

isb – ischial boot

isp – ischial peduncle

iss – ischial shaft

lbvf – lateral wall of brevis fossa

L.IL – left ilium

mbvf – medial wall of brevis fossa

pa – pubic apron

ps – pubic shaft

pu – pubis

pob – posterior blade

pop – posterior process of pubic boot

pub – pubic boot

pisp – proximal end of ischial peduncle

R.IL – right ilium

sac – supracetabular crest

spa – sacral plate

vep – ventral extension of the pubic boot

Hind limb

II-1, II-2, … , IV-5 – pedal phalanges

Aff – anterior region of the fibular facet

a – astragalus

actr – accessory trochanter

asp – ascending process of astragalus

Ca – calcaneum insertion of the astragalus

c – calcaneum

cn – cnemial crest
Ddt – facet of the distal tarsals
d2, d3, d4 – digit 2, digit 3, and digit 4
dt – distal tarsal
f4t – fourth trochanter of femur
Fe – femur
Ff – fibular facet
Ft – flexor tubercle
fic – fibular crest
fgt – greater trochanter of femur
fgt – greater trochanter of femur
fl – fibula
flc – lateral condyle of femur
flt – lesser trochanter of femur
fmc – medial condyle of femur
fs – femur shaft
icgr – intercondylar groove
Ics – intercondylar sulcus
Lc or lc – lateral condyle
Mt II – second metatarsal
Mt III – third metatarsal
Mt IV – fourth metatarsal
Mc or mc – medial condyle
T – flexor tubercle
t – tibia
Pt – protuberance
pgr – popliteal groove
rfl – ridge along posterior of the proximal fibula
II-1 to II-3, III-1 to III-4, and IV-1 to IV-5 – pedal phalanges of digits

Histological terminologies

A – Annulus
po – primary osteon
so – secondary osteon
EFS – External Fundamental System
LAG's or L – Lines of arrested growth

Other word terminologies used in this study

A – anterior
Aa – Archaeornithomimus asiaticus
Ap – Anserimimus planinychus
BTs Ornith BB – Baishin Tsav ornithomimosaur bonebed
Bg – Beishanlong grandis
Con-San – Coniacian – Santonian
Cmp – Campanian
Dm – Deinocheirus mirificus
Gb – Gallimimus bullatus (1, holotype; 2, paratype)
Ho – Harpymimus okladnikovi
km – kilometers
L – lateral
L. – left
M – medial
Ma – million years ago
Maa – Maastrichtian
Mt – mountain
Nt – Nqwebasaurus thwazi
Oe – Ornithomimus edmontonicus (1, holotype; 2, paratype)
Ov – Ornithomimus velox
P – Posterior
PC – principal components
Pp – Pelecanimimus polyodon
R. – right
RW – relative wrap
Sa – Struthiomimus altus
Sd – Sinornithomimus dongi
So – Shenzhousaurus orientalis

LIST OF FIGURES

LIST OF TABLES

LIST OF APPENDICES

LIST OF INSTITUTIONS

AM, Albany Museum, Grahamstown, South Africa,

AMNH, American Museum of Natural History, New York, USA,

CMN, Canadian Museum of Nature, Ottawa, Ontario, Canada,

FRDC-GS GJ, Fossil Research and Development Center, 3rd Geology and Mineral Resources Exploration and Mineral Development, Lanzhou, China,

IVPP, Institute of Vertebrate Paleontology and Paleoanthropology, Beijing, China,

NGMC, National Geological Museum of China, Beijing, China,

MPC-D, **MAS,** Institute of Paleontology and Geology, Mongolian Academy of Sciences, Ulaanbaatar, Mongolia,

ROM, Royal Ontario Museum, Toronto, Ontario, Canada,

TMP, Royal Tyrrell Museum of Palaeontology, Drumheller, Alberta, Canada, UCMZ (VP),

YPM, Yale Peabody Museum of New Haven, Connecticut, U.S.A,

ZPal.No.Mg.D, Zoological Institute of Poland,

CHAPTER I

INTRODUCTION

Ornithomimosauria is a clade of highly specialized theropod dinosaurs that are characterized by edentulous beak-like jaw, lightly built body with long slender forelimb with unusual metacarpal and ungual proportions, and long hind limbs, in which are much resemble modern ground dwelling birds (Osmólska, 1997; Makovicky et al., 2004). The members of this group are best known from the Cretaceous beds of Asia and North America (Makovicky et al., 2004; Weishampel et al., 2004b). Since the first ornithomimosaur, *Ornithomimus velox,* is described based on partial hind limb materials recovered from the late Maastrichtian Denver Formation of North America by Marsh, who also established the family Ornithomimidae (Marsh, 1890), the members of Ornithomimosauria have dramatically increased all around world, including sixteen genera from North America (*Dromiceiomimus brevitertius, Ornithomimus edmontonicus*, *Rativates evadens*, *Struthiomimus altus*, and *Tototlmimus packardensis*), Asia (*Anserimimus planinychus*, *Archaeornithomimus asiaticus*, *Beishanlong grandis*, *Deinocheirus mirificus*, *Gallimimus bullatus*, *Harpymimus okladnikovi*, *Qiupalong henanensis*, *Shenzhousaurus orientalis*, and *Sinornithomimus dongi*), and Africa and Europe (*Nqwebasaurus thwazi*, and *Pelecanimimus polyodon*), (Osmólska et al., 1972; Russell, 1972; Barsbold, 1988; Smith and Galton, 1990; Perėz-Moreno et al., 1994; Ji et al., 2003; Kobayashi and Lü, 2003; Kobayashi and Barsbold, 2005a, 2005b; Makovicky et al., 2009; Xu et al., 2011; Choiniere et al., 2012; Lee et al., 2014; Serrano-Brañas et al., 2016; McFeeters et al., 2016; Ian Macdonald and Currie, 2018).

Cretaceous sediments are widely distributed in southern territory of Mongolia, where ornithomimosaur fossils are abundantly discovered, ranging from the Lower Cretaceous Khukhteeg Formation (Aptian-Albian) to the Upper Cretaceous Nemegt Formation (early Maastrichtian)

(Jerzykiewicz, 2000; Khand et al., 2000; Makovicky et al., 2004). Chronologically, the first ornithomimosaur materials in the Gobi Desert of Mongolia are discovered from the Nemegt Formation by the Polish-Mongolian Paleontological Expedition (PMPE) in late 1960th as well as by the Mongolian Paleontological Expedition (one small skeleton with a skull, lacking the forelimbs) in 1967, which coined a new taxon, *Gallimimus bullatus* (Osmólska et al., 1972). All of these skeletons are different in sizes, the skull of the smallest individual measuring 133 mm, whereas that of the largest reaches 320 mm long. *Gallimimus bullatus* is characterized by a strange bulbous structure, which is a hollowed and formed by parasphenoid, a shovel-like lower jaw, and a short metacarpals with curved manual unguals. *Gallimimus bullatus* is the most common ornithomimid and is the well-known studied taxon among other Nemegt ornithomimosaurs (Kobayashi and Barsbold, 2006). Its fossil specimens have been discovered from localities at Nemegt Basin such as Altan Uul, Bügiin Tsav, Guriliin Tsav, Hermiin Tsav, Khuree Tsav, Tsagaan Khushuu, and Ulaan Khushuu. The second ornithomimosaur, *Deinocheirus mirificus*, was also discovered by PMPE from the Upper Cretaceous Nemegt Formation at Altan Uul-III locality in 1965 and was described as a new genus and species by Osmólska and Roniewicz (1970) based on pectoral girdle and forelimb elements with some other associated skeletal materials. However, the relationship of this taxon to Ornithomimosauria as well as other dinosaur groups, had been contentious due to insufficient skeletal parts (Currie, 2000; Makovicky et al., 2004; Kobayashi and Barsbold, 2006), which remained enigmatic until its recent discovery of additional specimens of this taxon (Lee et al., 2014). The third ornithomimosaur, *Garudimimus brevipes*, is discovered from the Upper Cretaceous Bayanshiree Formation (Cenomanian-Turonian) at Baishin Tsav locality by Soviet-Mongolian Paleontological Expedition (SMPE) in late 1970th and consists of a single partial holotype specimen, missing forelimbs and the most of vertebral series (Barsbold, 1981). The initial description of *Garudimimus brevipes*, Barsbold diagnosed by the following characters, short ilia, non-arctometatarsalian foot, presence of the first pedal digit, and absence of pleurocoels. Later on, this specimen was revised and reexamined by Currie (2000) and Kobayashi and Barsbold (2005a). Currie (2000) suggested that a long postorbital region of the skull relative to other ornithomimosaurs, a more posteriorly positioned jaw articulation than the postorbital bar, and intermediate

degree (between *Harpymimus okladnikovi* and other more derived ornithomimosaurs) of constriction of the proximal end of metatarsal III are diagnostic traits of *Garudimimus brevipes*. Kobayashi and Barsbold (2005a) reexamined the specimen and claimed that some of diagnostic characters presented by Barsbold (1981) were common features in ornithomimosaurs and they were invalid features, such as the ilia being shorter than the pubes and short metatarsals for diagnosis of *Garudimimus brevipes*. They also made some ratio analyses on the appendicular elements and suggested that ratios of ilium length to pubis length and metatarsal III length to femur length are distinctly smaller in *Garudimimus* than other late Late Cretaceous ornithomimids. However, second ratio is may not be diagnostic for the genus because some other ornithomimosaurs, *Anserimimus*, *Gallimimus*, *Sinornithomimus*, and *Struthiomimus* also have small ratio. Moreover, they suggested a cutting-edge of the edentulous dentary which may indicate that the food processing of *Garudimimus* differs from those of toothed ornithomimosaurs (Kobayashi and Barsbold, 2005a). The fourth ornithomimosaur, *Harpymimus okladnikovi*, was discovered from the Lower Cretaceous Shinekhudag Formation (Hauterivian-Barremian) (Kobayashi and Barsbold, 2005b), rather than although originally described as Khukhteeg Formation (Aptian-Albian) in Khuren Dukh locality during SMPE in late 1970 (Barsbold and Perle, 1984). Barsbold and Perle (1984) established the family Harpymimidae for the single holotype specimen of nearly complete skeleton. *Harpymimus* is differentiated from other known ornithomimosaur taxa based on its primitive features, including a presence of the anteriorly restricted 10-11 mandible teeth, distinctly short first metacarpal, and non-arctometatarsalian foot (Barsbold and Perle, 1984). Moreover, Kobayashi and Barsbold (2005b) reexamined the specimen and performed additional analyses, such as a phylogenetic relationship within ornithomimosaurs, a functionality of hand structure, and ratio analyses on the caudal vertebral series for testing tail movements. They made the following emended diagnosis in the holotype of *Harpymimus*: anteriorly positioned eleven dentary teeth, transition point between anterior and posterior caudals at eighteenth caudal, triangular-shaped depression on dorsal surface of supraglenoid buttress of scapula, low ridge dorsal to depression along posterior edge of scapular blade, and small deep collateral ligament fossa on lateral condyle of metatarsal III. The fifth ornithomimosaur, *Anserimimus planinychus*, was discovered from the Upper Cretaceous Nemegt

Formation at Bügiin Tsav during the SMPE in late 1970 (Barsbold, 1988). *Anserimimus planinychus*, a briefly described and named by Barsbold, is characterized by the following diagnostic features, having a strong deltopectoral crest on the humerus, and unusual flattened of the manual unguals (Barsbold, 1988). Because of limited knowledge of this taxon and comparisons with *Gallimimus bullatus* have been restricted so far (Kobayashi and Barsbold, 2006). All of these Mongolian ornithomimosaur taxa are known to date from the Cretaceous sediments, and each of taxa is represent periodically specific geological time (Makovicky et al., 2004).

CHAPTER II

MULTITAXIC BONEBED OF TWO NEW ORNITHOMIMOSAURS (THEROPODA, ORNITHOMIMOSAURIA) FROM THE UPPER CRETACEOUS BAYANSHIREE FORMATION OF SOUTHEASTERN GOBI DESERT, MONGOLIA

Manuscript Information Sheet

Tsogtbaatar Chinzorig, Yoshitsugu Kobayashi, Ryuji Takasaki, Mototaka Saneyoshi, Tomonori Tanaka, Khishigjav Tsogtbaatar, Zorigt Badamkhatan.

Multitaxic bonebed of two new ornithomimosaurs (Theropoda, Ornithomimosauria) from the Upper Cretaceous Bayanshiree Formation of southeastern Gobi Desert, Mongolia.

Status of Manuscript:
_x_ Prepared for submission to a peer-reviewed journal
___ Officially submitted to a peer-reviewed journal
___ Accepted by a peer-reviewed journal
___ Published in a peer reviewed journal

Contribution of Authors and Co-authors
Manuscript in Chapter II
Author: Tsogtbaatar Chinzorig,
Contributions: conceived the study, catalogued and process the specimen, performed the analyses, prepared the figures, and wrote the manuscript.
Co-authors:
Yoshitsugu Kobayashi,
Contributions: provided the useful comments and suggestions and improved to edit earlier drafts of the manuscript.
Mototaka Saneyoshi, Tomonori Tanaka,
Contribution: surveyed the geological analyses of the quarry and a nearby region.
Ryuji Takasaki, Kohei Tanaka, and Zorigt Badamkhatan,
Contributions: discussed and shared informative ideas and help to improve the manuscript story.
Ryuji Takasaki, Tsogtbaatar Chinzorig
Contributions: sampled the histological elements, performed the analysis, and wrote the description.
Khishigjav Tsogtbaatar,
Contributions: organized the joint expedition, allowed to access and study the specimen.

ABSTRACT

Bonebeds can provide us a taphonomic and ontogenetic information about the specimens, which can support paleobiological and paleoecological evidence such as inferred behavior, cause of death, and life strategy. In general, theropod dinosaur bonebeds are rare that compare to ornithischian dinosaurs, and only four ornithomimosaur bonebeds have known to reported in the world, including one from Canada (*Ornithomimus* or *Struthiomimus*), two from China (*Archaeornithomimus* and *Sinornithomimus*), and one from France (*Ornithomimosaur* sp.). Although Mongolia is known as rich country in dinosaur fossils from the Cretaceous sediments, ornithomimosaur bonebed has not been known yet. The bonebed materials described herein consists of partial to nearly complete postcranial skeletons, representing at least five individuals with different ontogenetic stages, basis on the size of the preserved skeletal elements. Based on the morphological differences in postcrania, the material are different than *Garudimimus brevipes* and represent two additional ornithomimosaurs from the formation. At any rate, this bonebed is important to understand the behavior of early Late Cretaceous ornithomimosaurs, because it is the first bonebed record of ornithomimosaur from this time of the Gobi Desert, Mongolia, as well as the first multitaxic bonebed in the worldwide, suggesting the co-existence of multiple groups of ornithomimosaurs in the same niche.

Keywords

The Bayanshiree Formation, ornithomimosaur, Baishin Tsav, bonebed, arctometatarsalian foot, and niche-partitioning.

INTRODUCTION

Ornithomimosaurs are a group of gracile theropods known mainly from the Cretaceous of Asia and North America (Makovicky et al., 2004). Although bonebeds are common for ornithischian dinosaurs, especially ceratopsians and hadrosaurs, theropod dinosaur bonebeds are comparatively rare (Ryan et al., 2001; Dodson et al., 2004; Horner et al., 2004; Eberth and Currie, 2010). Only four ornithomimosaur bonebeds have known date so far in the world, two from China (*Archaeornithomimus* and *Sinornithomimus*) (Smith and Galton, 1990; Kobayashi and Lü, 2003), one from Canada (either *Ornithomimus* or *Struthiomimus*) (Cullen et al., 2013), and one ornithomimosaur sp. bonebed from France (Allain et al., 2011).

Ornithomimosaur specimens are common in the Cretaceous beds of the Gobi Desert of Mongolia (Osmólska, 1980a; Makovicky et al., 2004). The Bayanshiree Formation (Cenomanian-Turonian) is widely distributed in southeastern region of Mongolia and is rich in dinosaur remains, including ankylosaurs, dromaeosaurids, hadrosauroid, ornithomimosaurs, ornithopods, sauropod, therizinosauriods, and tyrannosauroid (Weishampel et al., 2004b; Kobayashi et al., 2009). Although a new material of ornithomimosaur from this formation was briefly reported and was informally called it as "*Gallimimus mongoliensis*" based on the differential morphological features of the skeletal elements (Kobayashi and Barsbold, 2006). Kobayashi et al (2009) are identified a new specimen of arctometatarsalian condition of ornithomimid from the formation and promoted the co-occurrence of Early Late Cretaceous ornithomimosaurs. However, none of these specimens has not been done detail description yet. To date, only known valid taxon from this formation is the deinocheirid *Garudimimus brevipes* (Barsbold, 1981; Kobayashi and Barsbold, 2005a).

Bonebed materials of various dinosaur groups have been commonly discovered from the Gobi Desert sediments during field season. Unfortunately, materials of these bonebeds are not adequately reported or investigated because of insufficient materials or less data collection. Ornithomimosaurs are

represented by relatively few complete skeletons from the Bayanshiree Formation (early Cenomanian-Turonian), compare to that of the Nemegt Formation (late Campanian-early Maastrichtian), (Osmólska, 1980). Isolated postcranial elements, specifically phalanges, fragmentary femur and tibia, and metatarsals, are conversely more common than other elements of the body. On the other hand, monodominant bonebeds are relatively common for either ornithischian and saurischian dinosaurs throughout the Mesozoic, especially in the Late Cretaceous period, but multitaxic bonebed is rare (Smith and Galton, 1990; Jerzykiewicz et al., 1993; Kobayashi and Lü, 2003; Eberth and Currie, 2010; Bell and Campione, 2014; Chiba et al., 2015; Fanti et al., 2015; Funston et al., 2016).

In 2010 summer fieldwork, an ornithomimosaur bonebed was discovered from the Upper Cretaceous Bayanshiree Formation at Baishin Tsav locality (BTs-II, sub-locality main outcrop) in the southeastern part of the Gobi Desert in Mongolia (Figs. 1, 3B) during the Japan-Mongolian (HMNS-MPC) joint paleontological expedition and was assigned the first ornithomimosaur bonebed from the Gobi Desert of Mongolia and the fifth ornithomimosaur bonebed in the world (Cullen et al., 2013).

This bonebed consists of different sizes of partial to semi-articulated postcranial skeletons of at least five individuals based on a number of pubes, and other incomparable size of small skeletal elements, such as ulna and metatarsal V (Fig. 2). Although none of individuals is preserved skull or some of taxonomically important elements such as the femur, the preserved skeletal materials include manual and pedal elements, which are informative for the taxonomic identity. Some elements are similar to *Garudimimus brevipes* such as anteroposteriorly shorter ilium than the pubis length and a ventrally curved pedal ungual. At least one skeleton preserves arctometatarsalian condition of the metatarsals (proximal end of third metatarsal covered by second and fourth metatarsals in anterior view), which is one of the characteristics of the derived clade of ornithomimosaurs, Ornithomimidae. This indicates that this skeleton clearly differs from *Garudimimus brevipes* by the presence of arctometatarsalian foot and a loss of digit I. In addition, two different morphotypes are represent in this study based on the structure of hand morphology. Type I has a proximally positioned medial divergence of metacarpal I and nearly straight slender manual unguals with anteriorly positioned flexor tubercles. Type II has more distally positioned

medial divergence of metacarpal I than Type I and ventrally sharply recurved robust manual unguals. Whether these morphotypes belong to *Garudimimus brevipes* is not clear because its holotype does not preserve hands. Here, we provide the anatomical description of these specimens. Based on a structure of the hand morphology, a bonebed indicates that there are two different ornithomimosaurs, but a distinctive difference on the vertebral column, specifically in the posterior dorsal vertebrae, there might be another ornithomimosaur may have existed in the bonebed other than above two morphotypes. All of these specimens are referred to Ornithomimidae due to subequal metacarpals, a straight pubic shaft, and an arctometatarsalian foot (Osmólska et al., 1972; Russell, 1972; Makovicky et al., 2004; Kobayashi and Barsbold, 2006; Chinzorig et al., 2017a). The bonebed assemblage is the first reported record of a multitaxic bonebed of ornithomimosaur in the world and provides insights on the anatomy and behaviour of ornithomimosaurs from the Upper Cretaceous Bayanshiree Formation of Mongolia.

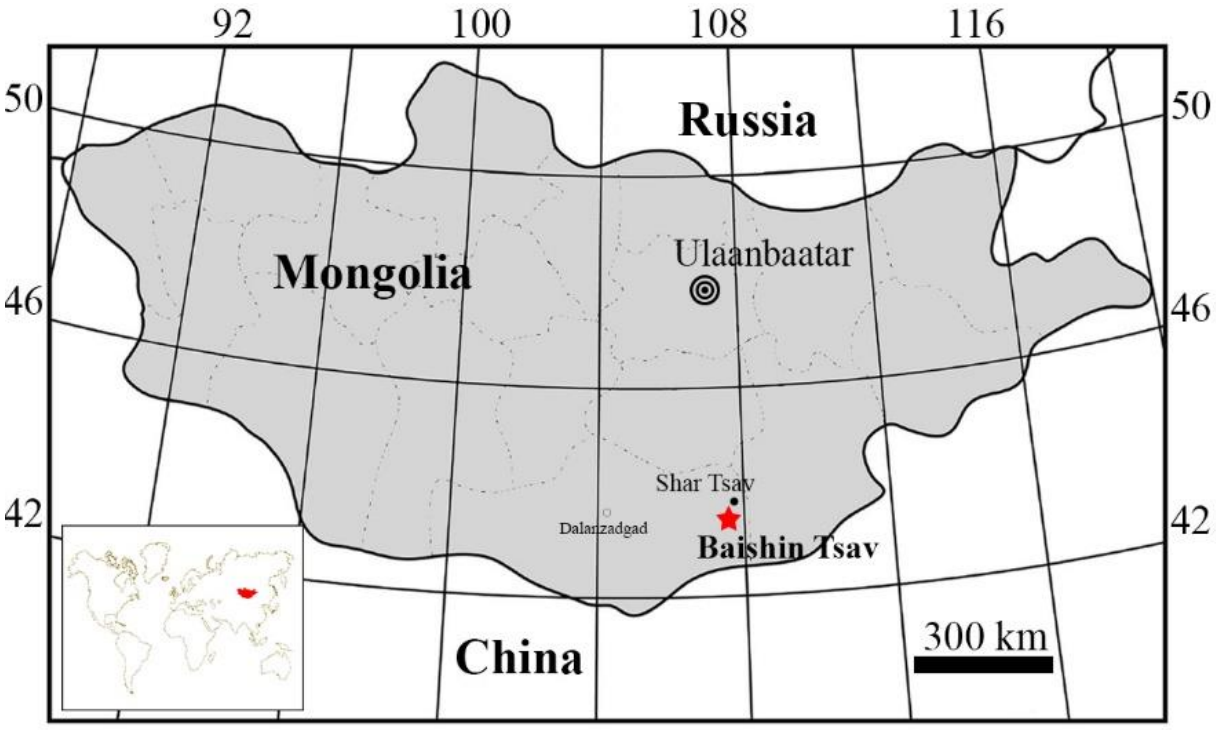

Figure 1. Location map of Baishin Tsav locality (red star).

LOCALITY AND GEOLOGICAL INFORMATION

Baishin Tsav locality is situated in eastern part of the Gobi Desert about 10 km from the dinosaur footprint bearing locality, Shar Tsav, to the south (Fig. 1). Since this locality was first opened by Soviet-Mongolian Paleontological Expeditions in early 1970, several extensive paleontological and geological surveys have done by major joint expeditions, for instance, Soviet-Mongolian, Japan-Mongolian (HMNS-MPC, and OUS-IPG), Korean-Mongolian (KID-IPG) and recently joint expedition between Hokkaido University Museum and Institute of Paleontology and Geology of Mongolia team works in surrounding these areas (Jerzykiewicz and Russell, 1991; Hicks et al., 1999). The outcrop of Baishin Tsav covers area of 1,8 /2,1 km latitudinal and longitudinally and is divided into five sub-localities by HMNS-MPC (Watabe et al., 2010), (Fig. 3).

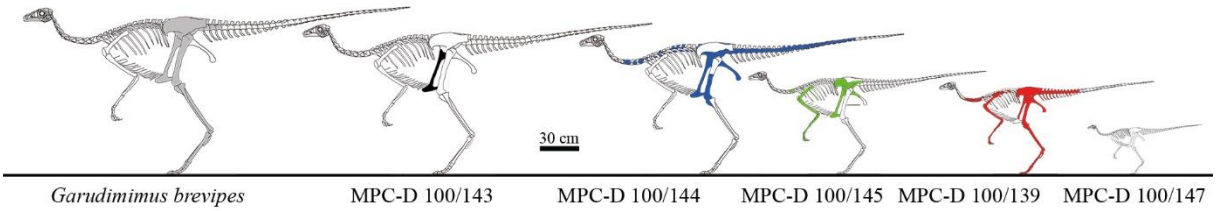

Figure 2. Overview of preserved skeletal elements of each individual in the assemblage and relative body sizes compared with a holotype of *Garudimimus brevipes* based on the size of the pubis. *Explanation:* a color indicates the preserved elements of each individuals. (modified after *Sinornithomimus dongi* (Kobayashi and Lü, 2003)).

The Bayanshiree Formation is mostly exposed at this locality, and the most complete section of the formation, which is up to 300 m thick, occur in nearby localities, Bayn Shire, Khara Khutul, and Khongil Tsav (Hicks et al., 1999). However, the contacts between the Bayanshiree Formation and other formations can rarely be seen around this region (Jerzykiewicz and Russell, 1991). The Bayanshiree Formation mainly consists of fine-grained, gray sandstones and gravels with isolated layers of clays and conglomerates in the lower part and multicolored clays and sandstones in the upper part. The age of the Bayanshiree Formation

has been determined to be the Cenomanian to lower Santonian because a basalt layer, which overlies the formation, was dated as 101-92 Ma. (Shuvalov and Nikolaeva, 1985; Harland et al., 1990).

The vertebrate assemblages of the Bayanshiree Formation are distinctive because of their variety of taxa and the abundance of turtles. Therizinosauroids, the primitive tyrannosaurid *Alectrosaurus*, and hadrosauroids have been reported from the formation (Perle, 1977; Maryánska and Osmólska, 1981; Hicks et al., 1999). However, no records of micro vertebrate fossil site have been noted.

Geological settings of Baishin Tsav

A recent geological study revealed four sedimentary units (associations) in the Upper Cretaceous successions at Baishin Tsav, Khoorai Tsav, Khavirgiin Zoo, Shar Tsav, and Shar Tsav Far-West within approximately 30 km x 40 km area (Fig. 4, Saneyoshi et al., pers. communication). The area is stratigraphically lower in the south and higher in the north.

The Unit 1 is the lower-most stratigraphic unit in the area and is exposed at Khoorai Tsav and Baishin Tsav, consisting of sandstones with reddish to grayish mudstones. The sandstones are mainly composed of course to medium sand with trough cross-stratification and current ripple lamination. The muddy part is massive with light red to light gray colored. Each sand and mud layer is 10-80 cm thick. A distinct fining upward sequences from sand to mud beds dominates this unit, suggesting meandering river systems.

The Unit 2 predominantly consists of very coarse to medium sandstones, deposited in a very shallow braided stream channel, approximately 2 km in estimated width. The Unit 3 crops out in the widest area from northeastern part of Baishin Tsav to Shar Tsav. This unit consists of the alternation of mud layer with a caliche, laminated mudstone, and rarely intercalated sandstones. The massive mudstones are typically reddish to light gray in colors. Caliche horizons crops out in whole part of the unit. Sand layers are up to 30 cm in thick. It indicates the cyclic weak flow, calm conditions and dried up on flood plain.

The Unit 4 forms the upper-most succession in the area, consisting of sandstones, laminated mudstones, and massive mudstones. This unit is characterized by thin synsedimentary tectonics and

convolution structures. The presence of unidirectional facies above and below lacustrine sediments support deltaic to lacustrine environments.

The BTs Ornith BB was discovered from a gray massive mudstone layer of the lower Unit 3, deposited at flood plain environments. The sedimentary sequences suggest that the bonebed was deposited in flood plain environments near river channels.

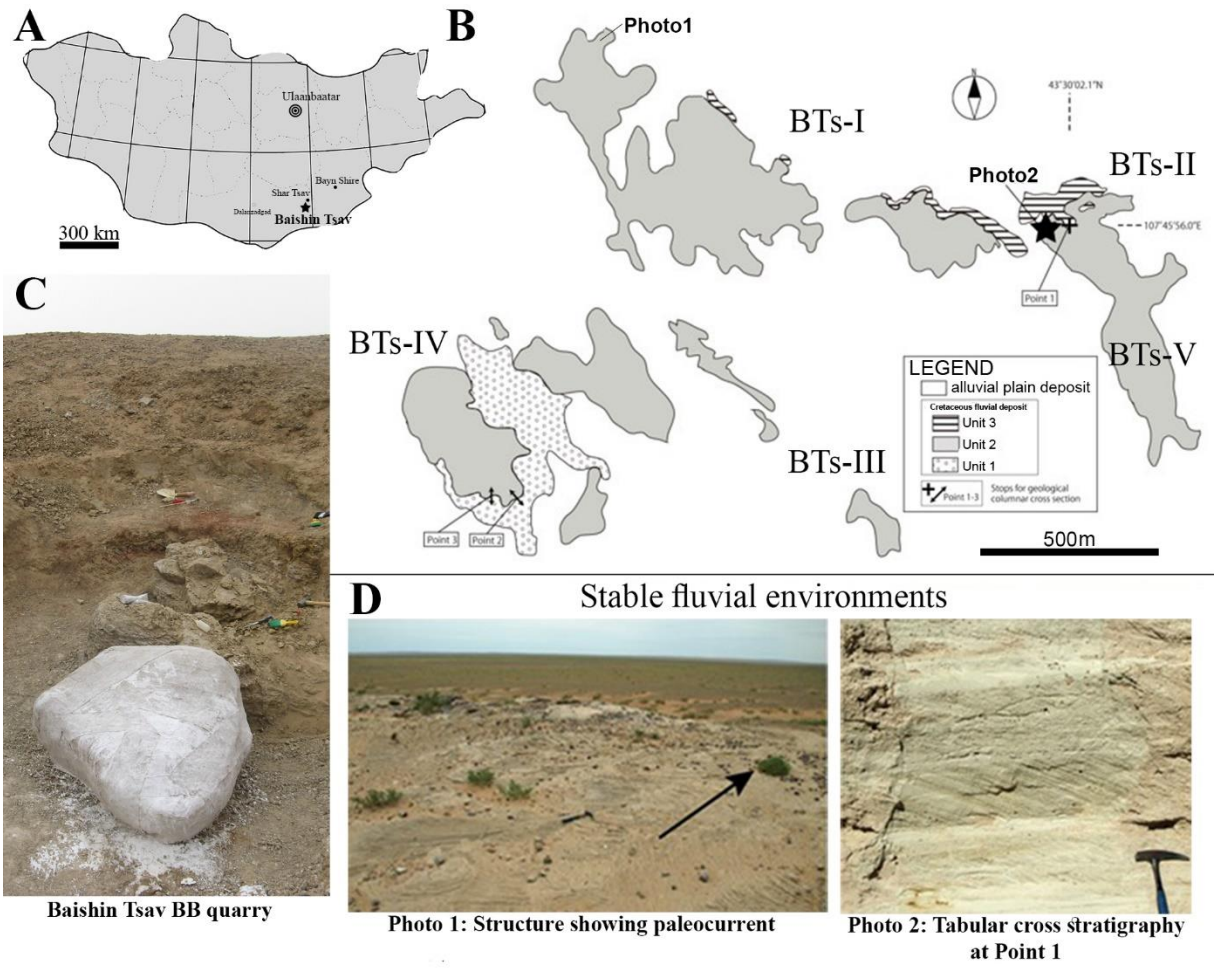

Figure 3. Quarry information of the BTs ornithomimosaur bonebed. (A), Map of Mongolia, indicating the Baishin Tsav locality with nearby locality, Shar Tsav, (B), Sub-localities of the Baishin Tsav locality, including a quarry location of ornithomimosaur bonebed (★), (C), a field view of the bonebed quarry, and (D), ancient paleoenvironmental aspects that are observed in the field.

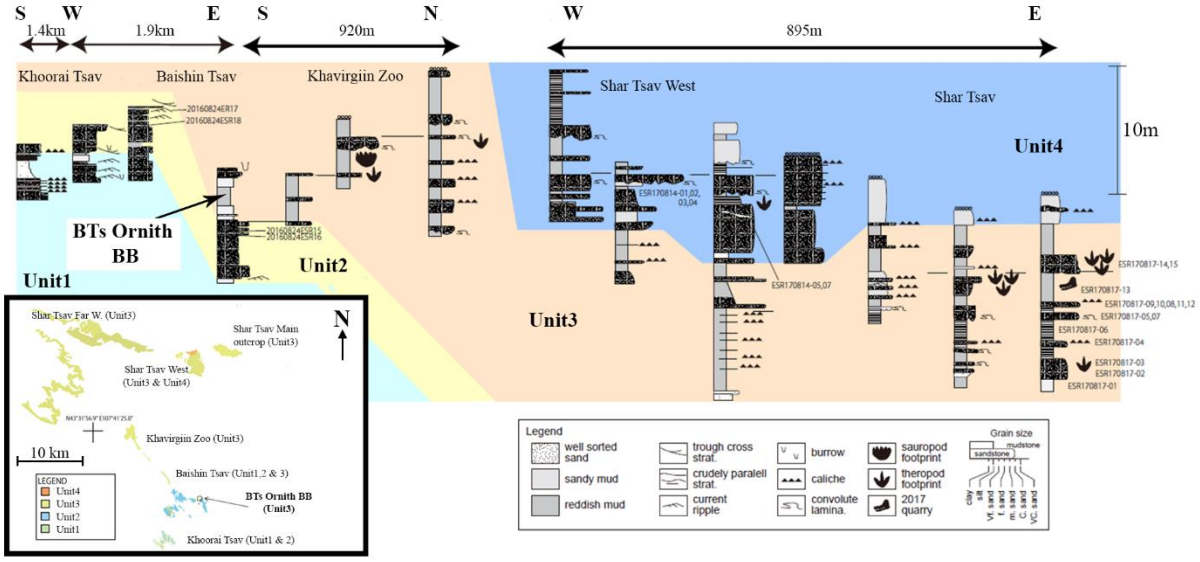

Figure-4. Stratigraphic position of the BTs Ornith BB at Baishin Tsav and a correlation with nearby localities. *Explanation:* Inset map shows a geographical distribution of outcrops Baishin Tsav locality within other localities.

MATERIALS AND METHODS

Data presented in this study were collected during a single summer fieldwork in 2010. Unfortunately, the quarry map was not performed, nor taphonomic surveys was made during the excavation. However, the research team draw a bone distribution map of the BTs Ornith BB specimens systematically while the specimens were under preparation in the laboratory. During last two summer field works, the team have revisited the BTs Ornith BB quarry and draw a stratigraphic map and collected its taphonomic data.

Among five different sizes of ornithomimosaurs in the BTs Ornith BB, the skeletal elements of each individual are preserved as following: MPC-D 100/139, a posterior cervicals, a complete series of dorsals, and sacrals, anterior half of caudals, a partial left and nearly complete right forelimbs, complete pelvic girdle, only missing a pubic boot, and a complete left and a partial right hind limbs; MPC-D 100/143, left and right articulated pubes; MPC-D 100/144, anterior cervicals, partially articulated dorsal and caudal vertebrae, complete sacrals, a sacral plate, left and right articulated pubes, a fragmentary ilium, ischium, and hind limb elements; MPC-D 100/145, right scapulocoracoid, right ulna and radius, and a

complete right manus; MPC-D 100/146, mid-dorsal vertebrae; and MPC-D 100/147, left ulna, and several single elements, such as a right scapulocoracoid, and a left metatarsal V (Figs. 2, 5).

All individual elements contained within the BTs Ornith BB specimens were measured in millimeters using digital calipers, and a measuring tape. The list of individual measurements is shown in Tables-A1 and A2.

Specimens were prepared from their plaster jackets using standard paleontological preparation techniques. To assess the relationship of BTs Ornith BB specimens described here to other ornithomimosaur taxa we scored them for a cladistics data matrix, with 48 characters (18 cranial and 30 postcranial), settled in Supplementary Data-S1, modified from Xu et al. (2011). The BTs Ornith BB specimens were employed as representatives of two individuals (MPC-D 100/139 and MPC-D 100/145). The individuals were coded the different for each specimen and therefore analyzed as two operational taxonomic units, because of the morphologic differences. The phylogenetic analysis performed with TNT 1.5 software version (Goloboff and Catalano, 2016) with a traditional Wagner search with 1000 replicates using Tree Bisection Reconnection branch swapping. In the analysis, fifteen ornithomimosaur taxa, including representatives of four bonebeds (*Archaeornithomimus, Sinornithomimus,* Dry Island bonebed specimens, and BTs bonebed specimens) were used, and *Allosaurus fragilis* is used as outgroup.

The right fibula of the first individual (MPC-D 100/139) of the BTs Ornith BB was histologically sampled with allowance from the Institute of Paleontology and Geology, MAS, and thin-sectioning and imaging performed at the Okayama University of Sciences Paleohistology Laboratory. The sectioned fibular shaft was cleaned by ethanol solution (99.5%) before coated with Devcon Epoxy resin in a plastic container to allow an initial transverse cut using a low-speed Refine Tec saw. Once cutting was done, a cutting side was polished the following grit size orders, G#400, G#1500, and G#6000, before a Plexiglas slide was mounted to the resin-coated bone surface using Devcon Epoxy, and the bone was again cut using a low-speed Refine Tec saw. The second cut using a Refine low-speed saw, adjusting a speed rate between 4 and 5, approximately 1 mm in thickness. Then, a thickness of the sectioned sampled specimen was measured in five points by Nikon Digi micro stand (MS-3G) before it was ground down 50 μm thickness

using a silicon carbide powder from G#110 to G#6000. Photographs of the thin-section were examined and analyzed using Adobe Photoshop CS6.

DESCRIPTION

General description

The assemblage composition of the BTs Ornith BB contains ornithomimosaur dominant specimens, which includes 226 (<99.87%) identifiable postcranial elements within four individuals out of 892 total elements, a single hadrosauroid astragalus, and many fish vertebrae (Fig. 5). Many of the elements from each individual skeleton are incomplete, except MPC-D 100/139, or some elements poorly preserved due to erosion (Table-S1).

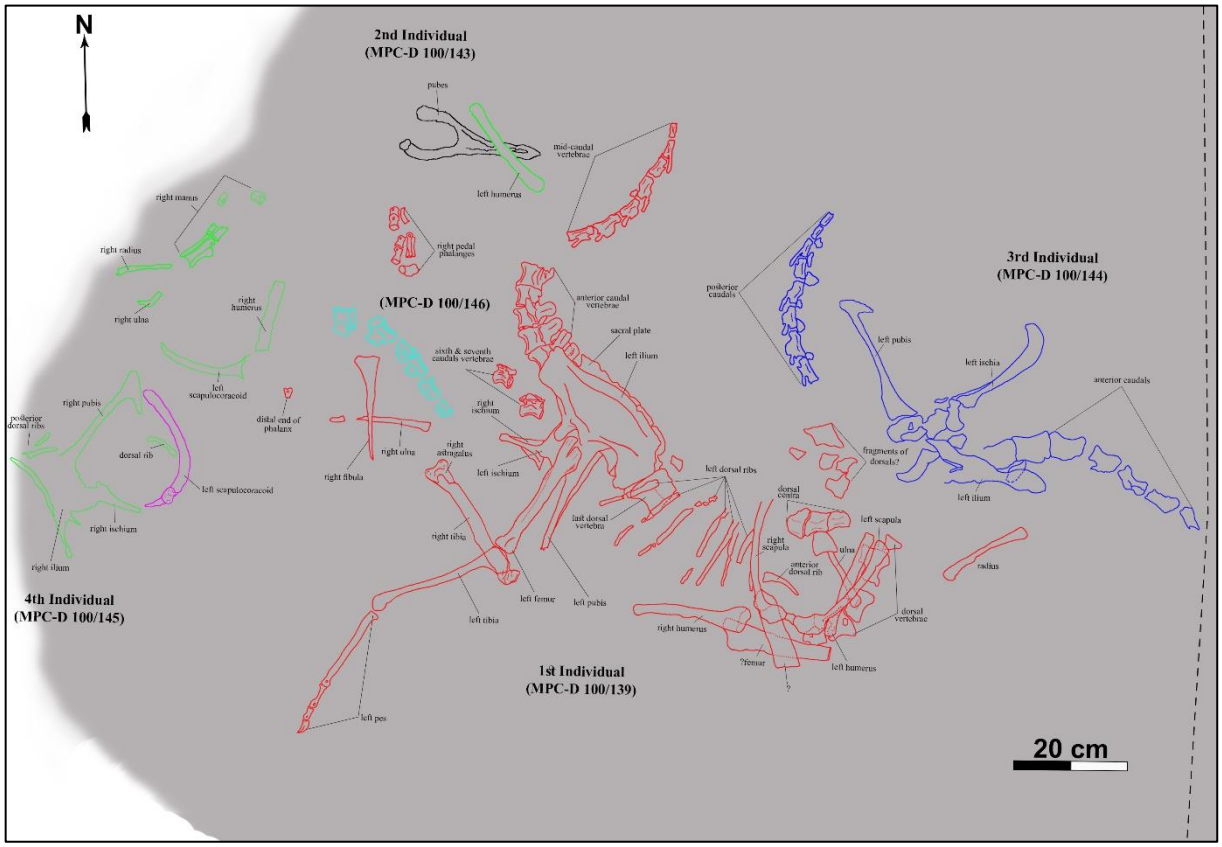

Figure 5. Bone distribution map of the BTs Ornith BB. *Explanation:* the dotted line shows the approximate border of the BTs Ornith BB quarry, and a gray-colored area shows edge of the sediment. *Abbreviations*: see the list of institutions on page vi.

First Individual (MPC-D 100/139)

MPC-D 100/139 is the most complete individual in the bonebed, missing only some elements of left forelimb, right hind limb, and a distal half of the tail vertebrae (Fig. 6). MPC-D 100/139 is catalogued as the first individual in this study on basis of its completeness. However, it is not the largest individual within the assemblage based on the comparisons of the pubis size of other individuals (Table-A2). The preserved elements of MPC-D 100/139 are mostly articulated, but some appendicular elements were displaced up to few centimeters from their original positions (Fig. 5).

A number of characters of this specimen are the combination of the primitive and derived characters of Ornithomimosauria. While the derived features of MPC-D 100/139 are subequal metacarpals, straight pubic shaft, the proximal end of metatarsal III covered by metatarsals II and IV anteriorly (arctometatarsalian condition), absence of the pedal digit I, and transversely flattened chevrons, the primitive features are the equally long tibia and femur, a thick metatarsal V, and ventrally curved pedal unguals (Makovicky et al., 2004; Kobayashi and Barsbold, 2005a; Kobayashi et al., 2009).

Based on comparison with the complete skeletons of *Gallimimus bullatus* (MPC-D 100/11), and MPC-D 100/121, it preserves fourth and posterior seventh to ninth cervicals (Fig. 6A). Additionally, posterior cervicals are partially preserved. The articular surfaces of all cervicals are concave. The anterior articular surface of the fourth centrum is wider than the high and is higher than the posterior articular surface. The posterior articular surface is slightly tilted anteriorly as in *Garudimimus brevipes*. The lateral surface of the centrum lacks a pneumatic fossa. The neural spine is low and rod-like, in contrast to *Garudimimus brevipes*, which has a high and round dorsal edge (Osmólska et al., 1972; Kobayashi and Barsbold, 2005a).

The postzygapophyses of the posterior cervicals are longer than the prezygapophyses, and the neural arch is X-shaped in dorsal view as in other ornithomimosaurs (Makovicky et al., 2004). The articular surfaces of the postzygapophyses are straight in posterior view, unlike *Gallimimus bullatus* and *Ornithomimus*, where postzygapophyses are curved slightly outward (Osmólska et al., 1972; Russell, 1972).

The dorsal vertebral series of MPC-D 100/139 includes 12 articulated dorsal vertebrae although parts of neural arches are missing (Fig. 6B). The anteroposterior length of the centrum is gradually longer posteriorly. Centra of the anterior dorsals are square-shaped, whereas those in the posterior dorsals are spool-like. The height and width of articular surfaces of anterior dorsal vertebrae are about same, while the height of the posterior dorsal vertebrae is greater than its width (Table-A1). The articular surface of the centrum is concave, platycoelous. Distinct parapophysis are preserved in each side close to the anterior end of all centrum sutures, and the position of the parapophysis is shifted to above suture in the posterior dorsals unlike *Gallimimus bullatus* (Osmólska et al., 1972). The first two dorsals bear a transitional characters between the cervical and dorsal vertebrae. The lateral surface of the first dorsal centrum persists a pneumatic foramen. The median keels form on the ventral surfaces of the first four dorsals, possibly fifth, as in *Harpymimus okladnikovi* but unlike other ornithomimosaurs such as *Garudimimus brevipes* (fourth and fifth dorsals), *Shenzhousaurus*, and *Ornithomimus* (fifth dorsal) (Kobayashi and Barsbold, 2005a).

MPC-D 100/139 has six sacral vertebrae as seen in *Garudimimus brevipes* (Kobayashi and Barsbold, 2005a). The anteroposterior length of sacrum is slightly shorter than the ilium (Fig. 6C, Table-A1). From the second to fifth sacrals are firmly fused each other. All neural spines of the sacral vertebrae are fused each other to form a single spinal plate as in other ornithomimosaurs, but the last sacral whose neural spine is separated from the spinal plate and distinctively higher than its height in lateral view. Anterior and posterior edges of the neural spines are visible. There are short, robust sacral ribs that are attached to the medial iliac blade. The first sacral has a concave articular surface and is similar to the last dorsal vertebra, in having a short prezygapophyses with nearly horizontal articular surface. There are depressions on the lateral surfaces of the second to fifth sacrals as seen in *Garudimimus brevipes* and *Ornithomimus* sp. (TMP 93.26.1) (Kobayashi and Barsbold, 2005a). The ventral surfaces of the anterior five sacrals are smooth. A pair of prominences are formed at the anterior and posterior ventral surface of sixth sacral. A similar pair of prominences is also seen in the anteroventral surface of *Garudimimus*

brevipes, but a posterior pair is absent in last sacral, differing from *Garudimimus brevipes* (Kobayashi and Barsbold, 2005a).

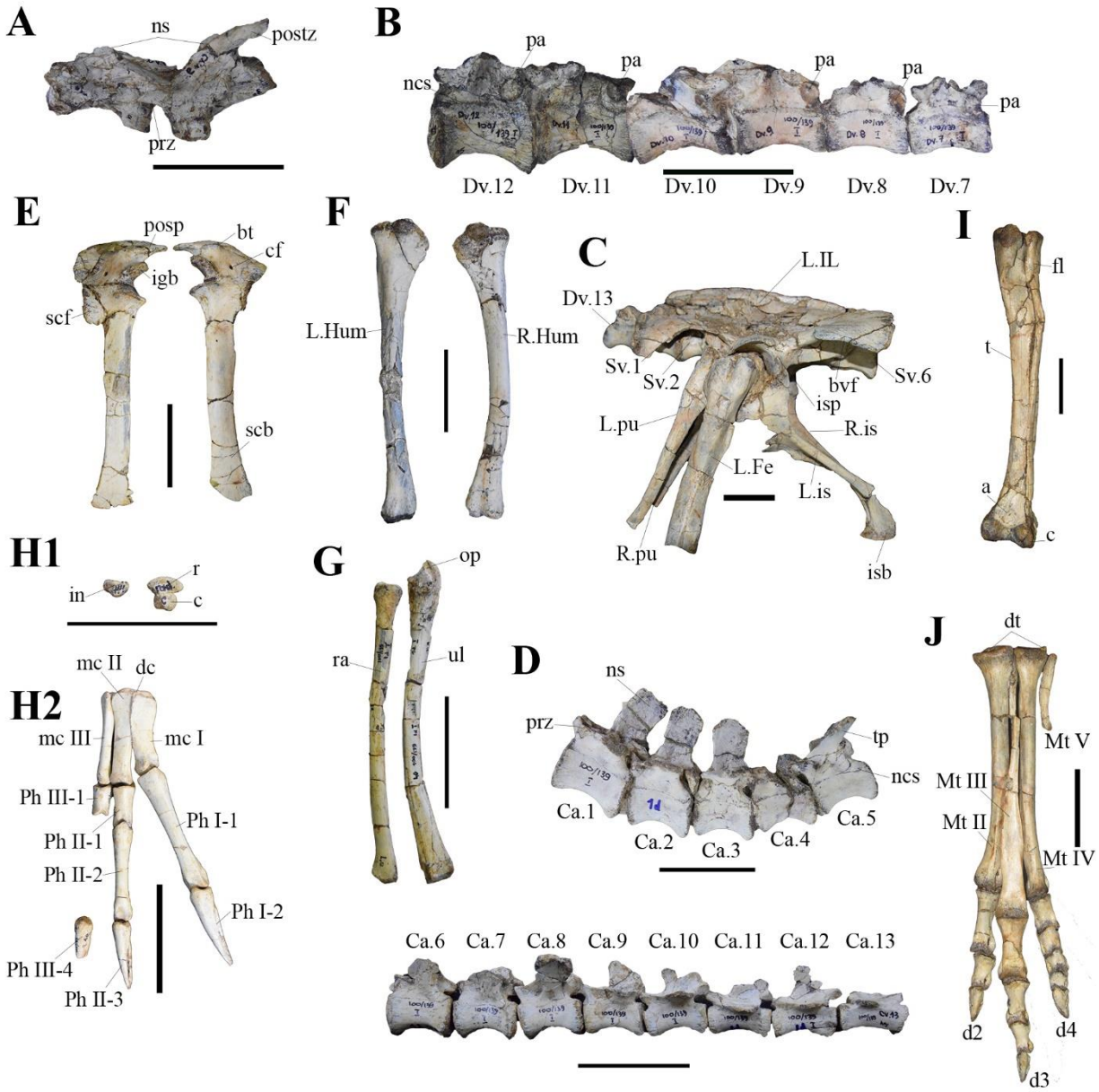

Figure 6. The preserved skeletal elements of the first individual (MPC-D 100/139). All scale bars = 5 cm. *Abbreviations*: see the list of abbreviations on page vi.

Anterior 13 caudal vertebrae are preserved in the specimen (Fig. 6D). The neural spine is the tallest at the first caudal and becomes gradually shorter posteriorly as in most ornithomimosaurs (Makovicky et al., 2004). The neural spine is positioned more posteriorly from the main axis. Both prezygapophyses and

postzygapophyses are short. The length of centra is about equal at least anterior 13 caudals, and the articular surfaces is higher than wide. As seen in caudal vertebrae of *Garudimimus brevipes*, MPC-D 100/139 has the following similar characters; posteriorly tilted neural spines with a grooved anterior and posterior edges of the anterior caudals, two depressions separated by a thin lamina at the bases of the neural spine and transverse process of at least first two caudals, a grooved dorsal edge of the neural spine at the first caudal, and a round dorsal edge of the neural spine at the third caudal, and a shallow sulcus at the ventral surfaces of the least anterior five caudals (Kobayashi and Barsbold, 2005a). The paired strong ridged prominences are present on the posteroventral surfaces of the centrum, and the posterior prominences are more pronounced than anterior ones, differing from *Garudimimus brevipes* which bears paired prominences on either side of the sulcus.

Forelimb

A nearly complete right forelimb, missing only phalanx III-2, and incomplete phalanges III-3 and III-4, and an incomplete left forelimb (Figs. 6E-6H_2). The scapula is thin and long, but shorter than the humerus (Table-A2). The posterior end of the scapular blade slightly widens and curved medially. The length ratio of scapula/humerus in MPC-D 100/139 is less than *Gallimimus bullatus* (85%) and *Sinornithomimus dongi* (96%) (Osmólska et al., 1972; Kobayashi and Lü, 2003). The acromion process is as strong as those in *Gallimimus bullatus* and *Struthiomimus altus* (Nicholls and Russell, 1985). A similar depression is present on the dorsal surface of the supraglenoid buttress as in *Gallimimus bullatus*, *Harpymimus okladnikovi*, *Sinornithomimus dongi*, and *Struthiomimus altus* (Osmólska et al., 1972; Russell, 1972; Kobayashi and Lü, 2003; Kobayashi and Barsbold, 2005b). The anterodorsal edge of the scapula forms a squared-ridge similar to *Gallimimus bullatus*, but different from *Sinornithomimus dongi* where it has a smoothly curved ridge along dorsal edge of the scapula.

Coracoid

The coracoid is slightly less than half of the scapular length (Fig. 6E, Table-A2). Positions of the prominent biceps tubercle and the coracoid foramen are similar to *Sinornithomimus dongi* (Kobayashi and Barsbold, 2005a). Unlike the posterior process of coracoid of *Sinornithomimus dongi*, the posterior process of MPC-D 100/139 is curved more anteroventrally, and its process is strongly pointed posteriorly.

Humerus

The humerus is long and slender and is slight twisted distal half medially (Fig. 6F). The proximal half of the shaft is slightly curved medially in anterior view. The ratio of width of the proximal end to total length is 0.19, in which is the same ratio as *Sinornithomimus dongi* (Kobayashi and Lü, 2003). The deltopectoral crest is smaller and weaker than that of *Anserimimus planinychus* and is positioned in the proximal one-fifth of the total humerus length. The lateral condyle is larger than the medial condyle. The entepicondyle is developed as weak as *Sinornithomimus dongi*. There is shallow depression in both dorsal and ventral surfaces of distal end for the reception of the proximal articular surface of the ulna.

Ulna and radius

The ulna is roughly three-quarter of the humerus and slightly longer than the radius (Fig. 6G). The shaft is convex towards the radius. The proximal end bears a well-developed olecranon process and is flatten transversely. The radius is straight and as slender as the ulna. The width of proximal end is slightly larger than the distal width.

Manus

The manus of MPC-D 100/139 is identified as Type-I morphotype in the bonebed. The right manus is more complete than the left side. Three proximal and two distal carpal elements are preserved in right manus of MPC-D 100/139 (Fig. 6H). The proximal carpals are supposed to be a radiale, intermedium, possibly pisiform on the basis of the manus figures of *Harpymimus okladnikovi* by Kobayashi and Barsbold

(2005b) and *Struthiomimus altus* by Nicholls and Russell (1985). All three proximal elements are isolated bones which are displaced from their original positions, while those of distal carpals are fused to the proximal articular surfaces of the metacarpals. The intermedium and radiale are contacted to each other in same degree, while the centrale is positioned in the distal to the distal tarsals. The pisiform is a triangle bone, and all surfaces are flat, except the articular surface of the ulna, which is slightly concave. The radiale is oval-shaped and is larger than the intermedium (Fig. $6H_1$). Two distal carpals are firmly fused each other to form a single bone and covers most of the area of the proximal articular surfaces of metacarpals I and II.

Three metacarpals are subequal in length as in derived ornithomimosaurs (Fig. $6H_2$). Metacarpal I is robust and shorter than the other two metacarpals, whereas metacarpals II and III are equal in length. The proximal articular surface of metacarpal I is subtriangular in proximal view. More than its half lateral surface contacts to the medial surface of metacarpal II, and its distal half is deviated medially. The distal articular surface of metacarpal I is rotated slightly clockwise. The distal end of metacarpal I has a ginglymoidal surface with distinct lateral and medial condyles for articulation with the first phalanx I-1 as in *Archaeornithomimus asiaticus* (AMNH 21889 and 6569) and those of basal ornithomimosaurs such as *Harpymimus okladnikovi* and *Pelecanimimus polyodon* (Perėz-Moreno et al., 1994; Kobayashi and Barsbold, 2005b). The lateral condyle is 1.5 times larger than its medial condyle (Table-A2). Metacarpal II is straight, and its proximal articular surface is subrectangular. The length of the proximal contact surface between metacarpals II and III is about one-third of the total length of metacarpal II like *Harpymimus okladnikovi*. In addition, there is no contact along the shafts of the metacarpals II and III, similar condition in *Gallimimus bullatus* and *Harpymimus okladnikovi* (Osmólska et al., 1972; Kobayashi and Barsbold, 2005b). However, the size of the area within these taxa varies. Metacarpal III is slender, and its anteroposterior length is greater than transverse width proximally. The articular surface of proximal end is half circular and covers the smallest area, comparing to other two metacarpals for articulation with the radius and ulna.

For the phalangeal series of the right manus, first two digits are complete, and the distal two phalanges as well as distal tip of ungual are missing in digit III (Fig. $6H_2$). The articular surfaces of all proximal phalanges have a concave single surface. The shafts of the penultimate phalanges of digits I and II are dorsally curved in medial view as in *Sinornithomimus dongi* (Kobayashi and Lü, 2003). Phalanx I-1 is the longest among manual phalanges as in other ornithomimosaurs. Phalanx II-1 is nearly three times shorter than phalanx I-1. Phalanges II-1 and III-1 are similar in shape but are different in their sizes, having faint lateral and medial ligament fossae, depressed ventral surface distally, and parallel lateral borders in dorsal view. Phalanx II-2 is somewhat similar to phalanx I-1; however, it has a dorsal lip at the proximal articular surface which differs from phalanx I-1. Length of phalanx II-2 is 80% of the total length of phalanx I-1 and more than two times longer than phalanx II-1. Ungual phalanges are generally similar in shape and straight less curved ventrally unlike *Gallimimus bullatus* and *Sinornithomimus dongi*, but similar to the manual unguals of *Archaeornithomimus asiaticus* (Smith and Galton, 1990). Ungual I is the largest within three unguals. The articular surfaces are concave and dorsal processes are pronounced in all unguals. The flexor tubercles are ridge-like and are distally positioned.

Pelvic girdle

Ilium

The ilium is longer than the sacrum (Fig. 6C, Table-A2). The dorsal edge of ilia meet each other along the neural plate and diverge laterally posteriorly. The height from the supracetabular crest to the dorsal edge is low unlike other ornithomimosaurs. A ventrally directed process on the anteroventral portion of the antilium is present as in other ornithomimosaurs. The preacetabular ridge is more strongly curved than *Gallimimus bullatus* and *Sinornithomimus dongi* (Osmólska et al., 1972; Kobayashi and Lü, 2003). Posteriorly, the height of the dorsal edge of ilium is decreased and intensively flares posterior blade outbound and forms a large brevis fossa unlike *Gallimimus bullatus*, but similar to *Garudimimus brevipes*. Unlike *Garudimimus brevipes*, a tip of the posterior blade is more curved posteroventrally in lateral view. The supracetabular crest is developed as strong as those in *Garudimimus brevipes* and *Sinornithomimus*

dongi and the lateral edge has a lateral expansion as in most ornithomimosaurs. The ischial peduncle has a broad flat surface anteriorly with a ventrally pointing apex in lateral view, which is slightly directed to laterally.

Pubis

The pubis is articulated with other pelvic elements, but missing its pubic apron and boot due to erosion (Fig. 6C). Unlike *Archaeornithomimus asiaticus* or *Garudimimus brevipes*, the pubis of MPC-D 100/139 has straight and slender shaft (Kobayashi and Barsbold, 2005a; Xu et al., 2011). Although its distal end is missing, the length of a preserved portion is reached the total length of the complete ischium, indicating that a complete pubis is longer than the ischium (Table-A2).

Ischium

The ischium is as straight and slender as the pubis (Fig. 6C). The length of ischium is shorter than the anteroposterior length of the ilium (Table-A2). The proximal portion of the ischium covers the most of posteroventral area of the acetabulum. The ischial apron is strongly developed between the medial sides of the ischial shafts, and the length of the apron is extended more than two-third of the total length of ischium. The distal ends of ischium are fused each other to form an anteroventrally curved ischial foot distally.

Hind limb

Femur

The length of femur is nearly equal to the tibia length, differing from the derived ornithomimosaurs (Fig. 6C, Table-A2). It has a wing-like lesser trochanter, which is slightly lower than the femur head and separated by a deep notch as in most ornithomimosaurs. Moreover, the anterior border of the lesser trochanter has an accessory trochanter. The posteromedial border of the femur shaft has the fourth trochanter, which is stronger than *Gallimimus bullatus*, *Garudimimus brevipes*, and *Sinornithomimus dongi* (Osmólska et al., 1972; Kobayashi and Lü, 2003; Kobayashi and Barsbold, 2005a). It is located about

one-thirds of the femur length from the proximal end. The distal condyles of the femur are separated by the intercondylar groove and are about same size in distal view. The intercondylar groove is deep and extends to the anterior surface between the lateral and distal condyles through the distal end of the femur. There is a strong ridge bears in lateral side of the lateral condyle as common as other ornithomimosaurs. The medial edge of the medial condyle is nearly straight as in *Garudimimus brevipes*, but is different from *Sinornithomimus dongi* where it has a round edge.

Tibiotarsus

Both sides of tibiotarsus are preserved in MPC-D 100/139, but the left tibiotarsus is better preserved than the right one (Fig. 6I). The cnemial crest of the tibia is well-developed, and its tip is curved laterally. The cnemial crest is robust as seen in *Garudimimus brevipes* but differs from *Sinornithomimus dongi*, where this process is more pointed and slender in proximal view. Moreover, the prominent process is developed at the anterior edge of the cnemial crest in lateral view, in which differs from *Garudimimus brevipes* and *Sinornithomimus dongi* with a smooth edge. At the posterior portion of the proximal end of tibia, it has distinct lateral and medial condyles, in which separated by a shallow sulcus. The posterior process of medial condyles is more pronounced and is positioned more posteriorly than the lateral one in proximal view. The slender fibula attached to the lateral side of the tibia. The proximal end is curved medially and contacts with the lateral condyle of the tibia proximally. The astragalus and the calcaneum are tightly contacted with distal end of the tibia and fibula. The astragalus has a long, anteroposteriorly thin, and triangular ascending process, which attaches roughly one-fourth of the anterior surface of the distal tibia. The ratio of astragalus to tibiotarsus length is 0.25, in which is similar to *Gallimimus bullatus* but is greater than *Sinornithomimus dongi*. The distal condyles of the astragalus are about equal size in distal view (Table-A2). The medial condyle is inclined laterally but a degree of the inclination is less than *Garudimimus brevipes* and *Sinornithomimus dongi* in distal view. A notch for a prominence of the calcaneum is developed at the anterolateral border of astragalus. The calcaneum is a thin and disc-like

bone, which firmly attaches to the distal end of fibula. The lateral surface is flat and the dorsal surface is concave for the reception of the fibula. The length of calcaneum is greater than its width (Table-A2).

Distal carpals

Two distal carpals are similar to other ornithomimosaurs, and the ratio of length and width is subequal (Fig. 6J, Table-A2). They are positioned at the proximal end of metatarsals and the contact between these bone is straight. The proximomedial ridge of distal tarsal III and the posterolateral ridge of distal tarsal IV are formed a notch, respectively. Distal tarsal III covers the posterolateral surface of metatarsal II and most of the proximal surface of metacarpal III, while distal tarsal IV covers posteromedial surface of metatarsal IV, and its medial edge is slightly covers the lateral edge of the articular surface of metatarsal III in proximally.

Pes

MPC-D 100/139 has a complete left pes, which shows a combination of primitive and derived features of ornithomimosaurs (Fig. 6J). Metatarsus of MPC-D 100/139 has four metatarsal (Mt II, Mt III, Mt IV, and Mt V), and metatarsal I is absent. Metatarsals II and IV are subequal in length and articulates each other by straight surface proximally to form the arctometatarsalian foot, which is one of the derived features for ornithomimosaurs and differs from *Garudimimus brevipes* (Kobayashi and Barsbold, 2005a). Metatarsal III is the longest of metatarsals, whereas two other metatarsals are subequal (Table-A2). The distal half of metatarsal III widens from the mid-shaft, and its lateral and medial borders are slightly cover the adjacent metatarsals anteriorly. The distal ends of metatarsals II and IV are diverged distally from metatarsal III. Metatarsal V is thick and rounded in cross-section as in *Garudimimus brevipes* and a new ornithomimid specimen reported by Kobayashi and his colleagues from the same formation (Kobayashi et al., 2009), but unlike that of derived ornithomimosaurs which bear a thin metatarsal V (Osmólska et al., 1972; Makovicky et al., 2004). It attaches to the posteroventral surface of the metatarsal IV. The

proximodistal length of metatarsal V is more than one-third of metatarsal III length. Its distal half bends dorsally in lateral view.

The pedal phalangeal formula is 0-3-4-5-0 as in other ornithomimosaurs, except *Beishanlong grandis*, *Deinocheirus mirificus*, and *Garudimimus brevipes* in which have digit I (Barsbold, 1981; Makovicky et al., 2009; Lee et al., 2014). Digit III is the longest, while other two digits are subequal in length (Fig. 6J, Table-A2). The proximal articular surfaces of all proximal phalanges and phalanges of the digit III form a single shallow concave surface as in the most ornithomimosaurs. Proximal articular surfaces of the remaining phalanges of digits II and IV are divided asymmetrically by low ridges. The length of distal phalanges is shorter than preceding phalanges. Ungual phalanges of MPC-D 100/139 are similar to the unguals of *Garudimimus brevipes* in having anteroposteriorly elongated, and ventrally curved unguals with a depression with a weak longitudinal ridge without tuber (Kobayashi and Barsbold, 2005a). However, the unguals differs from *Garudimimus brevipes* by less pronounced dorsal lips of unguals and a flexor tubercle of the ungual phalanx IV-5.

Second Individual (MPC-D 100/143)

Only articulated left and right pubes are preserved in MPC-D 100/143 and is catalogued as the second individual of the bonebed. The size of the pubis is about as same as the pubis length of MPC-D 100/144, but is 1.5 times larger than that of MPC-D 100/139 (Fig. 7, Table-A2). The pubis of MPC-D 100/143 is different from the third individual pubis (MPC-D 100/144) in having a stout and anteroventrally curved shaft in lateral view. The degree of the pubic boot seems to be directed anteroventrally instead of more anteriorly. Although the pubic boot is incomplete in this individual, there were at least some degrees of the anteroposterior extensions existed regarding to orientation. The pubic apron extends in two-thirds of the pubic length from the middle section between left and right shafts. In general, the features of the pubis of MPC-D 100/143 is very similar to that of *Garudimimus brevipes* in the robustness, a curvature of the pubic shaft, and orientation of the pubic boot (Kobayashi and Barsbold, 2005a).

Third Individual (MPC-D 100/144)

The third individual of the bonebed assemblage, MPC-D 100/144, is less complete than the first individual (MPC-D 100/139), but much of the skeletal elements are preserved than the rest of the individuals. The complete left and right pubes and disassociated vertebral columns are main preserved elements although it also includes incomplete pelvic and limb elements (Fig. 8, Table-A2).

Fragmentary posterior cervicals have some ornithomimosaurian features such as long postzygapophyses, concave articular surface of the centrum, and wider articular surface of the centrum than its height, and a short centrum of the last cervical. The anterior series of dorsals are poorly preserved than the posterior dorsals. The dorsal centra of MPC-D 100/144 have concave and dorsoventrally high articular surfaces. Interestingly, the anterior and posterior articular surfaces of the centra are anteriorly curved in lateral view, rather than perpendicular in most ornithomimosaurs (Makovicky et al., 2004). The prezygapophyses and postzygapophyses are short as typical of ornithomimosaurs. The neural spine of dorsal vertebrae is dorsoventrally longer than its central height and are gradually become high posteriorly as in other ornithomimosaurs. The anterior edge of neural spine is straight and nearly perpendicular from the main axis, while the posterior edge is straight, but its tip is tilted more posterodorsally. MPC-D 100/144 has six fused sacrals like *Garudimimus brevipes* and *Sinornithomimus dongi*, but unlike *Gallimimus bullatus* (Osmólska et al., 1972; Kobayashi and Lü, 2003; Kobayashi and Barsbold, 2005a). The centrum lengths of sacral vertebrae are subequal, except the last sacral which is longer than the preceding centra (Table-A1). The ventral surface of sacrals is flat and broad transversely, compare to that of dorsals and caudals. Anteroposteriorly elongate pleurocoels are present at least first three sacrals.

A series of caudal vertebral centrum (anterior and posterior, respectively) are preserved. The anterior five caudals have a pair of distinct prominence on the posteroventral surface like *Garudimimus brevipes* as well as the individual MPC-D 100/139 (Kobayashi and Barsbold, 2005a). The centra are amphicoelous. The anterior caudals have higher than wide articular surfaces, while the posterior caudals are reversed. Moreover, the prezygapophyses of posterior caudals are incomparably shorter than that of derived ornithomimosaurs (Osmólska et al., 1972; Russell, 1972).

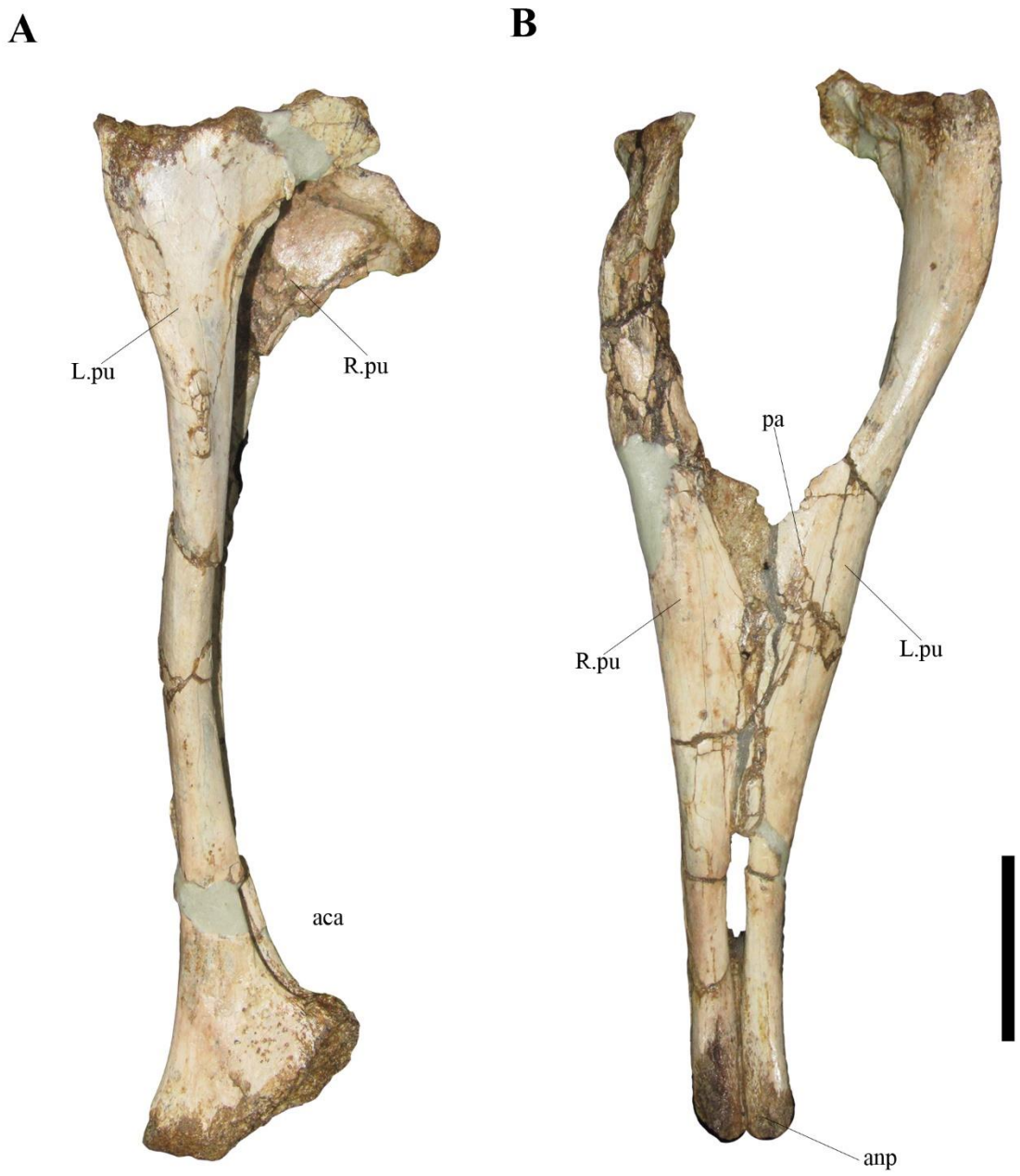

Figure-7. The pubes of the second individual, MPC-D 100/143. (A), left lateral, and (B), anterior views. Scale bar = 5 cm. *Abbreviations*: see the list of abbreviations on page vi.

Only lower portion of the left ilium and the anterior iliac blade of the right ilium are preserved (Fig. 8). The supracetabular crest is well-developed. The medial wall of the brevis fossa is visible from the lateral view. It has a straight pubic shaft and not curved distally, which is one of the derived features of

ornithomimosaurs (Fig. 8). The anterior process of the pubic boot is shorter than the posterior process, which is posteriorly more pointed end. Its ventral edge is a nearly flat, differing from North American taxa (Xu et al., 2011). In addition, the acute angle between the pubic shaft and posterior process of the pubic boot is not as wide as those in North American taxa. The left ischium is more complete than the right ones. The length of ischium is about two-thirds of the pubic length (Table-A2). The distal end of ischium curves anteroventrally like other ornithomimosaurs.

Fourth Individual (MPC-D 100/145)

Preserved skeletal elements of the fourth individual of the bonebed assemblage (MPC-D 100/145) are less complete than the first (MPC-D 100/139) and the third individual (MPC-D 100/144). Nevertheless, the elements of MPC-D 100/145, including left scapulocoracoid, both humeri, radii, and ulnae, a complete right manus, and pelvic girdle have taxonomically important features (Fig. 9). The general features of MPC-D 100/145 have similarities to an ornithomimid material from Shine Us Khudak locality (Bayanshiree Formation), reported by Kobayashi et al. (2009). The manus structure of MPC-D 100/145 belongs to Type-II morphotype in the bonebed. The left scapulocoracoid is present, but the acromion process of the coracoid and scapular prominence of scapula are incomplete (Fig. 9A). The scapula is shorter than the humerus and has a narrow scapular blade (Table-A2). Posteriorly, the scapular blade slightly widens and ends by round edge as in most ornithomimosaurs. The degree of the medial curvature of scapular blade is more curved than that of MPC-D 100/139 in dorsal view. The posterior process of coracoid is long, and its tip strongly bends to posteroventrally in lateral view. There is a deep notch in posterodorsal of the coracoid process. The glenoid buttress of coracoid is slightly offset laterally from the line of posterior process.

The humerus is longer than the scapula and is subequal when is measured with a combined length with the coracoid (Fig. 9B, Table-A2). The humeral head is rounded and much larger than the anterior and posterior tuberosities in proximal view. The deltopectoral crest is well-developed and it extends one-thirds of the proximal of the humerus.

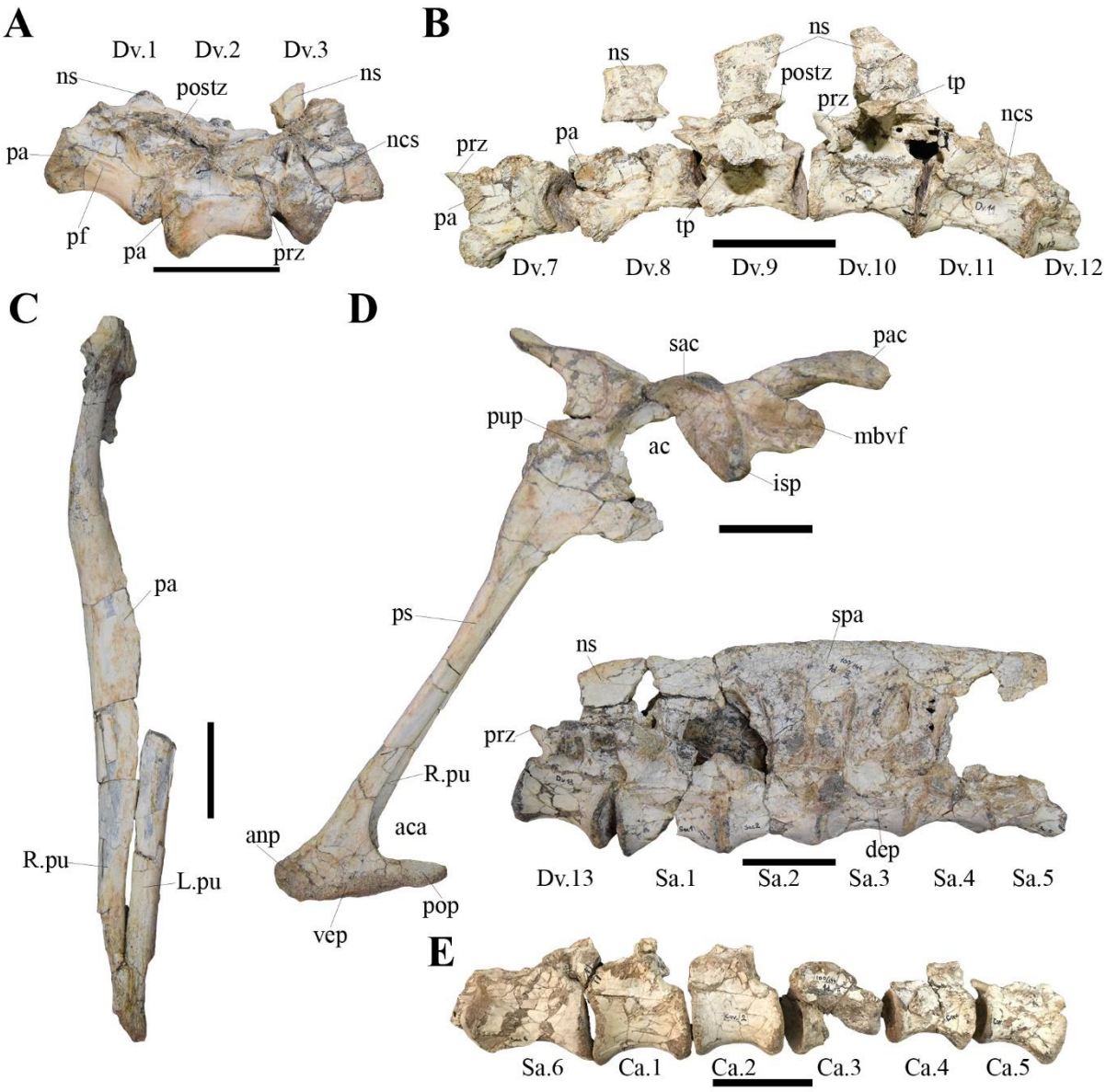

Figure-8. Preserved skeletal elements of the third individual (MPC-D 100/144). *Explanation:* (A), anterior dorsals, (B), posterior dorsals, (C), pubes in anterior view, (D), pelvis with articulated sacrals, and (E), anterior caudals in left lateral view. All scale bars = 5 cm. *Abbreviations*: see the list of abbreviations on page vi.

The humeral shaft is straight and sub-oval in cross-section. Distal condyles, ulnar condyle and radial condyle, are separated by a shallow depression, which runs anteroposteriorly. The ulnar condyle is larger than the radial condyle in distal view. There is a faintly developed ectepicondyle at the medial surface of the radial condyle. The entepicondyle is not developed. The ulna is longer than the radius (Fig. 9C). It bears

a well-developed olecranon process, and its shaft is nearly straight. The olecranon fossa is much pronounced than the coronoid process. The distal end of ulna is flattened as in other ornithomimosaurs. The radius is straight and sub-oval to rounded in cross-section at the mid-shaft. The length of radius is about 76% of the humerus length. The right manus is complete and a good preservational condition in MPC-D 100/145. Digit I is short, and digits II and III are subequal in length (Fig. 9D). Metacarpal I is the shortest and the most robust of metacarpals, whereas metacarpals II and III are subequal (Table-A2). The ratio length of metacarpal I to metacarpal II is 0.82, which is less than MPC-D 100/139 (0.86), but greater than *Sinornithomimus dongi* (0.75), (Kobayashi and Lü, 2003). The medial edge of metacarpal I is smoothly concave, and it contacts with the medial edge of metacarpal II about the proximal half of its lateral edge by straight line in dorsal view. Then, it diverges more distally. Its cross-section is subtriangular. The distal articular surface of metacarpal I is highly ginglymoidal (the medial condyle is distinctively larger than the lateral condyle), and rotated medially. Unlike metacarpal II of MPC-D 100/139, the distal half of metacarpal II is somehow diverged laterally from metacarpal I. The distal articular surface is rotated laterally. Metacarpal III is slender. The proximal articular surface is flat and triradiate, whereas the distal articular surface is rounded. Phalangeal shafts of all MPC-D 100/145 are straight, except the phalanx III-2 which forms dorsally curved shaft in lateral view. Phalanx I-1 is the longest element of the manus. There is a unique depression at the medial surface of proximal end of phalanx I-1.

Phalanges II-1 and III-1 are similar in shape but different in size. Like other ornithomimosaurs, all penultimate phalanges have ginglymoidal articulations. The length of phalanx II-1 is equal to the half-length of phalanx II-2. Phalanx II-2 is more slender than phalanx I-2, and it has a dorsal process at the proximal articular process as in phalanges III-2 and III-3. Like *Sinornithomimus dongi*, the lateral edges of phalanges II-1, III-1, and III-2 are parallel in dorsal view. The length of phalanx III-3 is slightly longer than a combined length of phalanges III-I and III-2 (Table-A2). The ligament fossae of distal phalanges I-1, II-2, and III-3 are deep and equally developed, while in phalanges II-1, III-1, and III-2 are faintly developed in both sides. All of the ungual phalanges are laterally compressed with deep lateral and medial grooves. All unguals are curved in lateral view as in *Gallimimus bullatus*, *Sinornithomimus dongi*, and a new

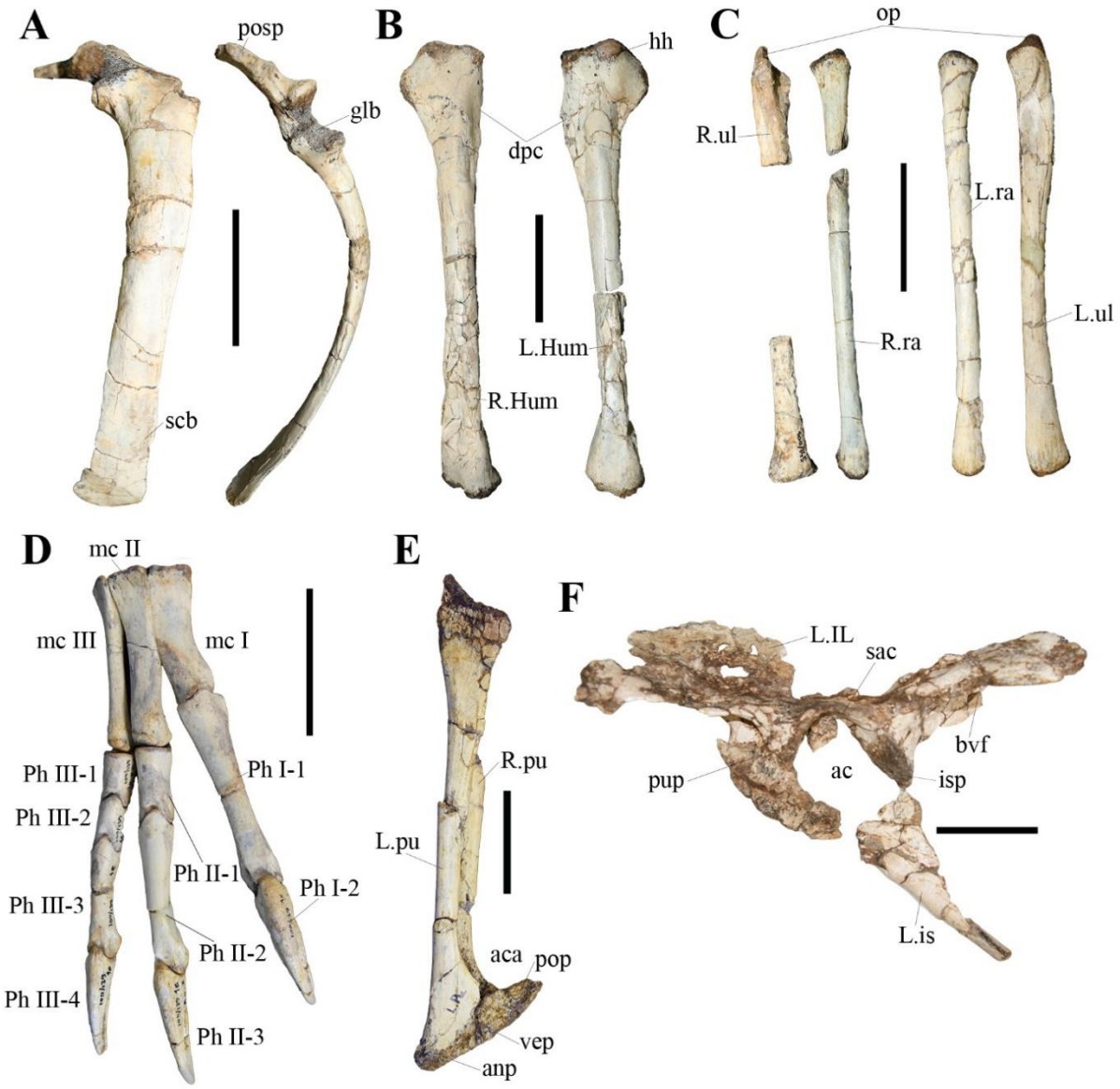

Figure-9. The preserved skeletal elements of the fourth individual (MPC-D 100/145). *Explanation:* (A), left scapulocoracoid in lateral and ventral views, (B), left and right humeri in anterior view, (C), left and right ulnae and radii in lateral views, (D), right manus in dorsal view, (E), pubes in left lateral view, and (F), partial left ilium and the proximal left ischium. All scale bars = 5 cm. *Abbreviations*: see the list of abbreviations on page vi.

ornithomimid specimen (051012 SUK-II TKH), (Osmólska et al., 1972; Kobayashi and Lü, 2003; Kobayashi et al., 2009). However, an ungual of the first digit is more strongly curved than the other two

unguals. In addition, these are oval-shaped in cross-sections and have the distally placed flexor tubercles for the tendons of M. flexor profundus as in *Gallimimus bullatus* and *Sinornithomimus dongi*.

The pubes are the best preserved element from the pelvis, although the badly weathered left ilium, and the proximal portion of ischium are also preserved in the individual (Figs. 9E, and 9F). The anteroposterior length of the ilium is shorter than the pubis length (Table-A2) like *Garudimimus brevipes* (Barsbold, 1981). The antilium has a ventrally projecting hook, although its tip is crashed. The ilium has a depression on the iliac blade dorsal to the acetabulum. The ischiac peduncle is wedge-shaped as in other ornithomimosaurs and facing anteroventrally. The brevis fossa, bounded by the brevis shelf laterally and medial crest medially, is as large as in other ornithomimosaurs but is shallow like *Garudimimus brevipes* (Kobayashi and Barsbold, 2005a). The medial crest is visible in lateral view. The supracetabular crest is not as strong as that in MPC-D 100/139, which could be because of the erosion. The pubic shaft is straight as in MPC-D 100/139 (Fig. 9E). The pubic boot has anterior and posterior processes. The anterior process is more round and shorter than the posterior one. The distal ends of pubis are fused each other to form a pubic boot. The ventral margin of the pubic boot is a nearly straight, differing from *Gallimimus bullatus* and North American taxa, but is similar to *Garudimimus brevipes* and *Sinornithomimus dongi* (Kobayashi and Lü, 2003; Kobayashi and Barsbold, 2005a; Xu et al., 2011).

Series of the dorsal vertebrae (MPC-D 100/146)

A series of partially articulated dorsal vertebrae are also preserved in the bonebed. These vertebrae are supposed to be a middle to posterior (the fifth to tenth dorsal vertebrae) portion of the dorsals based on a comparison with complete dorsal series of other ornithomimosaur specimens (Figs. 5 and 10). These dorsal vertebrae have some uniquely preserved morphologic features, in which are differentiated this specimen from the other individuals of the bonebed as well as known ornithomimosaurs from the formation. Whereas these dorsals share the following features with the other ornithomimosaurs, in having concave intervertebral articular surfaces of the centrum, a greater height than width of the articular surface of the centrum, and anteroposteriorly wide transverse processes (Makovicky et al., 2004). Both sides of the

neural spines bear expanded rugosities, in which are thought to be a metaplasia, as in other theropods such as *Garudimimus*, as well as *Allosaurus* (Wilson et al., 2016), (Fig. 10A). However, the metaplastic structure of MPC-D 100/146 dorsals is different from those of *Garudimimus* (Fig. 10A, D). The neural spines of dorsals are consistently the lowest among the Bayanshireenian ornithomimosaurs (Fig. 11). Although the eight and tenth dorsal vertebra of *Garudimimus* are even lower than those of MPC-D 100/146 on the graph (Fig. 11), it is possible that may effect of the preservational bias. The presence of a short neural spine (compared to its centrum height) and apically rounded neural spine is significant features of the dorsal vertebra. In addition, the fifth dorsal centrum of MPC-D 100/146 does not bear any ventral keel as seen in that of *Garudimimus* one (Kobayashi and Barsbold, 2005a). Moreover, a centrum shape of the fifth dorsal is curved ventrally in lateral view, differing from *Garudimimus* in having a square-shaped centrum (Fig. 10A, D). The features of dorsoventrally short, dorsally rounded tipped and anteroposteriorly cleft neural spine, and transversely wide spinopostzygapophyseal fossa of MPC-D 100/146 are unlike any Bayanshiree ornithomimosaurs (Fig. 10A).

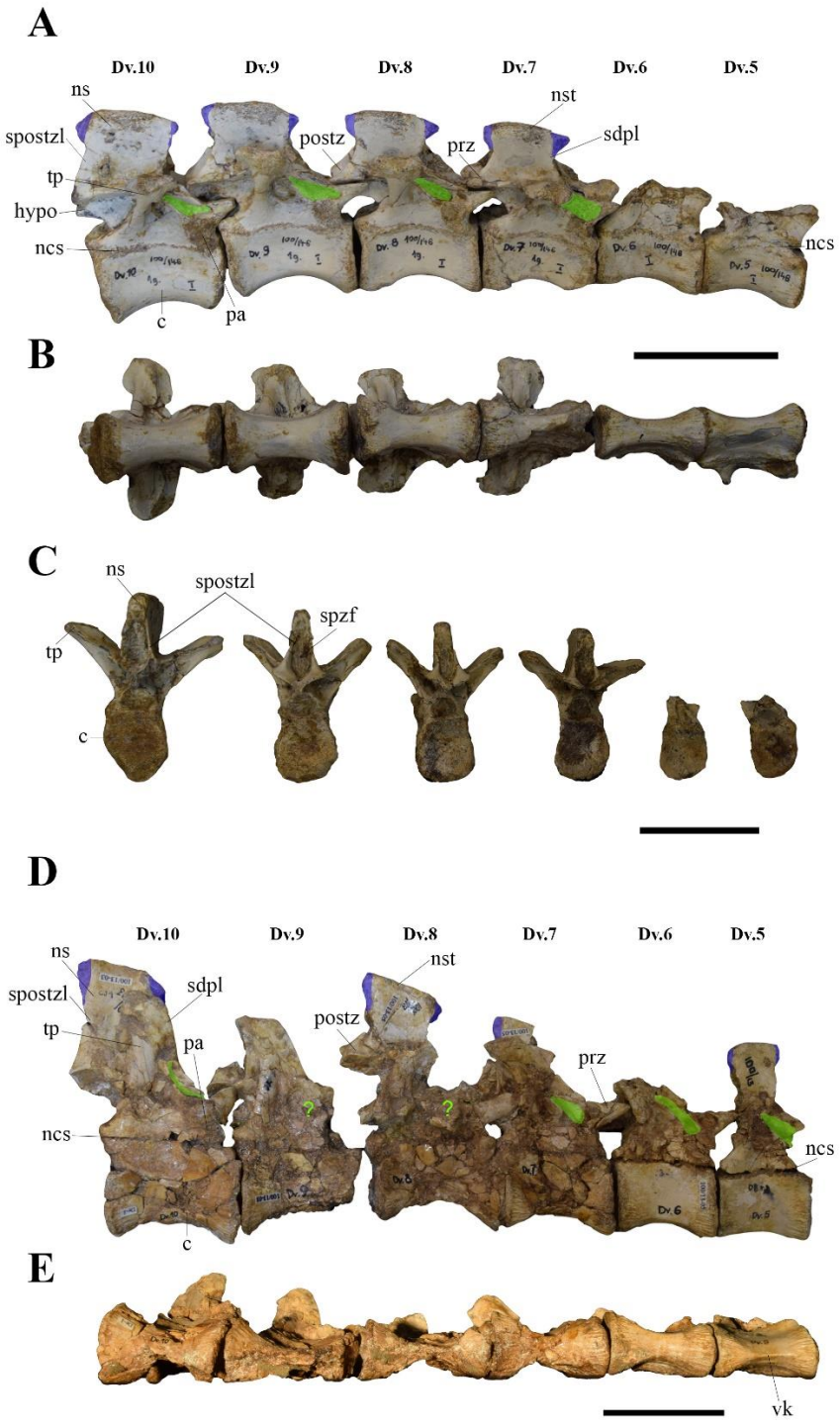

Figure-10. Comparison of the mid-dorsal vertebrae of MPC-D 100/146 (A-C) to *Garudimimus brevipes* (D-E). *Explanation:* (A and D), in right lateral, (B and E), in ventral, and (C), in posterior views. (Note that the expanded metaplastic rugosities of the neural spine and the positional variation of the parapophyseal centrodiapophyseal fossa are 40% green and purple transparencies, respectively. All scale bars = 5 cm. *Abbreviations*: see the list of abbreviations on page vi.

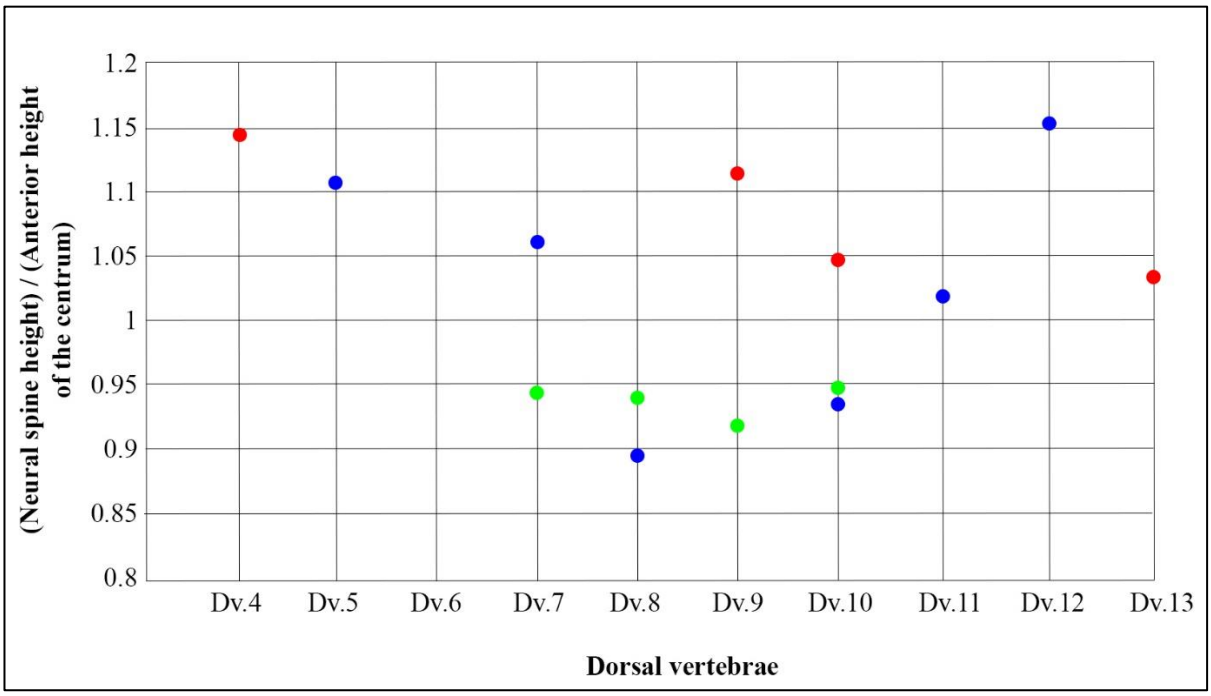

Figure-11. Graph of ratio of neural spine height to height of anterior articular surface of the centrum of Bayanshiree ornithomimosaurs. *Explanation:* (●), third individual, MPC-D 100/144, (●), a holotype of *Garudimimus brevipes*, and (●), dorsal vertebrae of MPC-D 100/146.

Single elements from the BTs Ornith BB

The left scapulocoracoid, left ulna, and metatarsal V are also contained in the bonebed assemblage, which are no notation to be belonged to the semi-articulated postcrania of any aforementioned individuals in basis of the distant distribution (Fig. 12).

The left scapulocoracoid was found in close to MPC-D 100/145 skeleton, but another left scapulocoracoid is also recovered from the close proximity to MPC-D 100/145 (Fig. 12A). Because of both scapulocoracoid are represent the left side, it indicates that they are belonged to two different individuals. The morphology of these two scapulocoracoids are very similar, in having a long posterior process of the coracoid, a slender and medially curved scapular blade with a round ending in distally, and a laterally facing infraglenoid buttress from line of the posterior process of the coracoid. The ulna is straight and has a well-developed olecranon process (Fig. 12B). The cross-section of the shaft is sub-oval. The length of ulna is 90% of total length of the first individual ulna (Table-A2). The proximal end of metatarsal V is thick and

oval, while its distal end is transversely flattened (Fig. 12C). The length of metatarsal (27.9 mm) is slightly longer than the half-length of metatarsal V of MPC-D 100/139 (Table-A2).

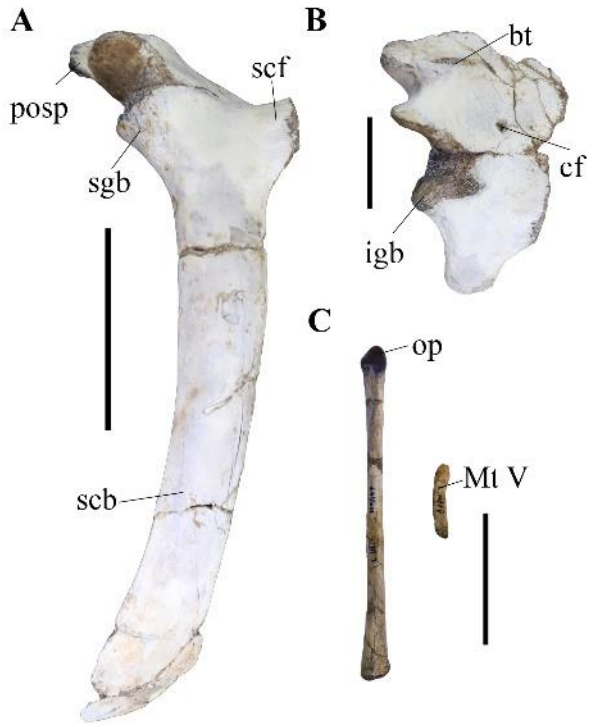

Figure-12. Single elements of the BTs Ornith BB. (A), the left scapulocoracoid, (B), the left ulna, (C), the left metatarsal V. All scale bars = 5 cm. *Abbreviations*: see the list of abbreviations on page vi.

Histology

In order to determine the age and growth stage of MPC-D 100/139, a transverse histological thin section was generated from the mid-shaft of the right fibula. The section was sampled about 14 cm from the proximal end, which is approximately 55% of the total length of the right fibula (Fig. 13A). The thin section is approximately 9.29 mm long anteroposteriorly and 4.23 mm wide mediolaterally. No any visible medullary cavity is developed in MPC-D 100/139 as seen in those of *Ornithomimus edmontonicus* (ROM 852) and an unnamed ornithomimosaur CMN 12068 (Cullen et al., 2014), but it differs from those of *Beishanlong grandis* (Makovicky et al., 2009), *Sinornithomimus dongi* (Varricchio et al., 2008), and an unnamed ornithomimosaur CMN 12069 (Cullen et al., 2014).

The sectioned fibula is almost entirely composed of woven and parallel-fibered bone, and longitudinally oriented vascular canals are dominant through innermost cortex to the outermost cortex,

although some circular, radial, and reticular vascularization occur in a middle section of the cortex (Fig. 13B). The secondary remodeling is intensive in the posteromedial cortex of the bone. The region is primarily occupied with secondary osteons that overlap to each other and only small amount of primary bone tissues present (Fig. 13B). The secondary osteons are generally larger than the primary osteons with the maximum diameter of 450 micrometers. The vascular canals of the secondary osteons are also generally larger than those of the primary osteons (maximum diameter = 15 micrometers). The osteocyte lacunae are oval to circular shaped and are arranged concentrically around the vascular canals. The osteocyte lacunae tend to be smaller and circular in the inner regions while they are larger and more oval in the outer regions of the secondary osteons. The lateral and the anterior cortex are fully composed of the primary bones and occupied with primary osteons. Majority of the vascular canals are longitudinally oriented although some circular, radial, and reticular canals are also present. The radial and reticular canals are limited to inner lateral cortex, and the outer lateral cortex is mainly occupied with the longitudinal canals. The vascular canals are randomly arranged in the inner cortex while they are arranged in circular rows in the outer cortex. The sizes of the longitudinal vascular canals are generally constant throughout the cortex (25 – 50 micrometers). Osteocyte lacunae of the primary osteons are oval-circular shaped. They are concentrically organized around the vascular canals but not as well organized as they are in secondary osteons.

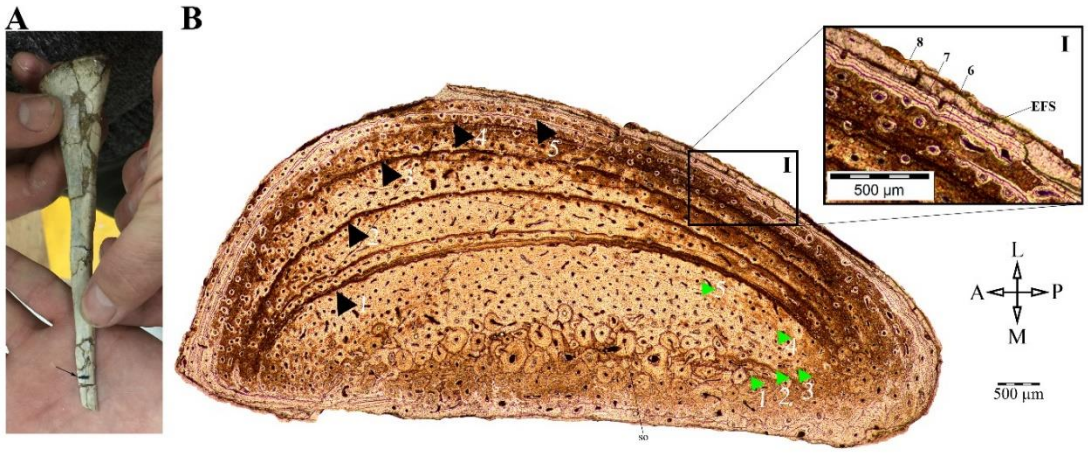

Figure-13. Details of histological section of the right fibular shaft of the first individual (MPC-D 100/139). *Explanation:* (A), sampled fibula, indicating the sectioned part of the shaft by a black arrow (Note that, human fingers are scale), (B), a full view of the sectioned element, showing the numbers of LAGs (black triangle), and the annuli (green triangle), (B-I), inset shows closely located last three LAGs (from 6 to 8) by referring EFS. *Abbreviations*: see the list of abbreviations on page vi.

At least eight lines of arrested growth (LAGs) and several annuli (up to five) are present (Fig. 13B). The annuli are visible in the anterior and posterior regions of the bone but are obscured in the lateral region, where the cortex is the thickest. Spacing between the LAGs gradually decreases towards the periosteal margin. Most of LAGs exhibit multiple lines in the fibula. The innermost LAG is composed of at least five distinct lines. The outermost line is separated from the other lines by one row of vascular canals in the lateral region, but it merges other lines at the anterior and the posterior regions. Those of the second and third LAGs are composed of two lines, respectively, whereas the fourth LAG has three lines. The fourth LAG bears a row of sparsely arranged longitudinal vascular canals between the innermost and the outer two lines in the lateral cortex. The fifth LAG is composed at least of two lines and is located adjacent to the fourth LAG. The sixth to eighth LAGs are located next to each other in the avascular periosteal region composed of lamellar bone (Fig. 13B-I). The periosteal region is likely to be the external fundamental system (EFS) (Cormack, 1987). In the outer cortex, the osteocyte lacunae tend to be small, circular, and sparse in inner adjacent to the LAGs. On the other hand, they are large, oval to spindle-shaped, and sometimes arranged in circumnarial rows in outer adjacent to the LAGs. The osteocyte lacunae in the EFS are small or oval to spindle-shaped and are arranged in circumnarial rows.

DISCUSSION

Taxonomic composition of the Baishin Tsav Ornithomimosaur Bonebed (BTs Ornith BB)

A total number of 226 elements were collected from the bonebed, including partially articulated or disassociated postcranial elements. Most of skeletal elements are identifiable and in good preservational condition, however some elements are badly weathered due to post-burial deposition. Based on the number of identified elements (n=226), 99.87% is assignable to ornithomimosaur (Table-A3). Within the BTs Ornith BB, two different ornithomimosaurs were identified in semi-articulated skeletons and isolated skeletal elements. The series of middle to posterior dorsal vertebrae, as cataloged as MPC-D 100/146, are potential to assign the third type of ornithomimosaur in terms of its unique shaped neural spine (Fig. 10). In

addition, a single hadrosauroid astragalus and many fish vertebrae were also recovered nearby the bonebed quarry. No invertebrate and plant fossils were recovered from the site.

Minimum Number of Individuals (MNI)

Based on the skeletal element list of the bonebed (Table-A3), the most abundant elements from the quarry are the axial and the forelimb elements, including dorsal vertebrae (14.22%), sacral vertebrae (7.11%), caudal vertebrae (16%), and manual phalanges (11.55%). The most common elements are vertebrae (n=86), followed by manual phalanges (n=26) and pedal phalanges (n=20). The next common elements were dorsal ribs (n=12), pubes (n=8), and metatarsals (n=8). The cervical vertebrae (n=6), femorae (n=2), tibiae (n=3), and fibulae (n=2) are relatively uncommon in the assemblage (Table-A3). The aggregation is identical that MNI is composed of at least four individuals based on the number of pubes, but it is possible that this number may increase up to n=7, on the basis of other isolated elements from the quarry such as the series of partially articulated dorsal vertebrae, scapulocoracoids, and small metatarsals V.

Phylogenetic analysis

The phylogenetic analysis of the BTs Ornith BB specimens resulted in five most parsimonious trees with 82 steps (consistency index = 0.610 and retention index = 0.719). The strict consensus tree originated a tree length of 89 steps with a consistency index of 0.562 and a retention index of 0.658 and shows BTs Ornith BB specimens are positioned within Ornithomimidae and a grouped together as a single clade (Fig. 14). The tree topology is similar to previously cladograms, purposed by Kobayashi and Lü (2003) and Cullen et al. (2013), except the position of *Sinornithomimus dongi*, in which forms a monophyly with BTs Ornith BB specimens. The clade of Ornithomimidae is supported by two unambiguous synapomorphies (absence of the first pedal digit and a level of tip of anterior extension of the pubic boot to anterior border of the pubic shaft). The result suggests three clades for Late Cretaceous ornithomimids (Chinese-Mongolian, Mongolian, and Chinese-North American) in derived ornithomimosaurs. The clade of

BTs Ornith BB specimens shares five unambiguous synapomorphies (presence of the depression on dorsal surface of supraglenoid buttress of scapula, less than 0.2 of the ratio of the humerus proximal width to total length, strong deltopectoral crest, slightly shorter metacarpal I than metacarpal II) and is a sister clade to *Sinornithomimus dongi* by sharing one character (infraglenoid buttress of the coracoid is offset laterally from line of posterior process). The clade of Mongolian taxa (*Anserimimus planinychus* and *Gallimimus bullatus*) shares two unambiguous synapomorphies (a long posterior process of coracoid and weak depression on dorsal surface of supraglenoid buttress of scapula). All North American taxa form a monophyly, including the Dry Island ornithomimid bonebed.

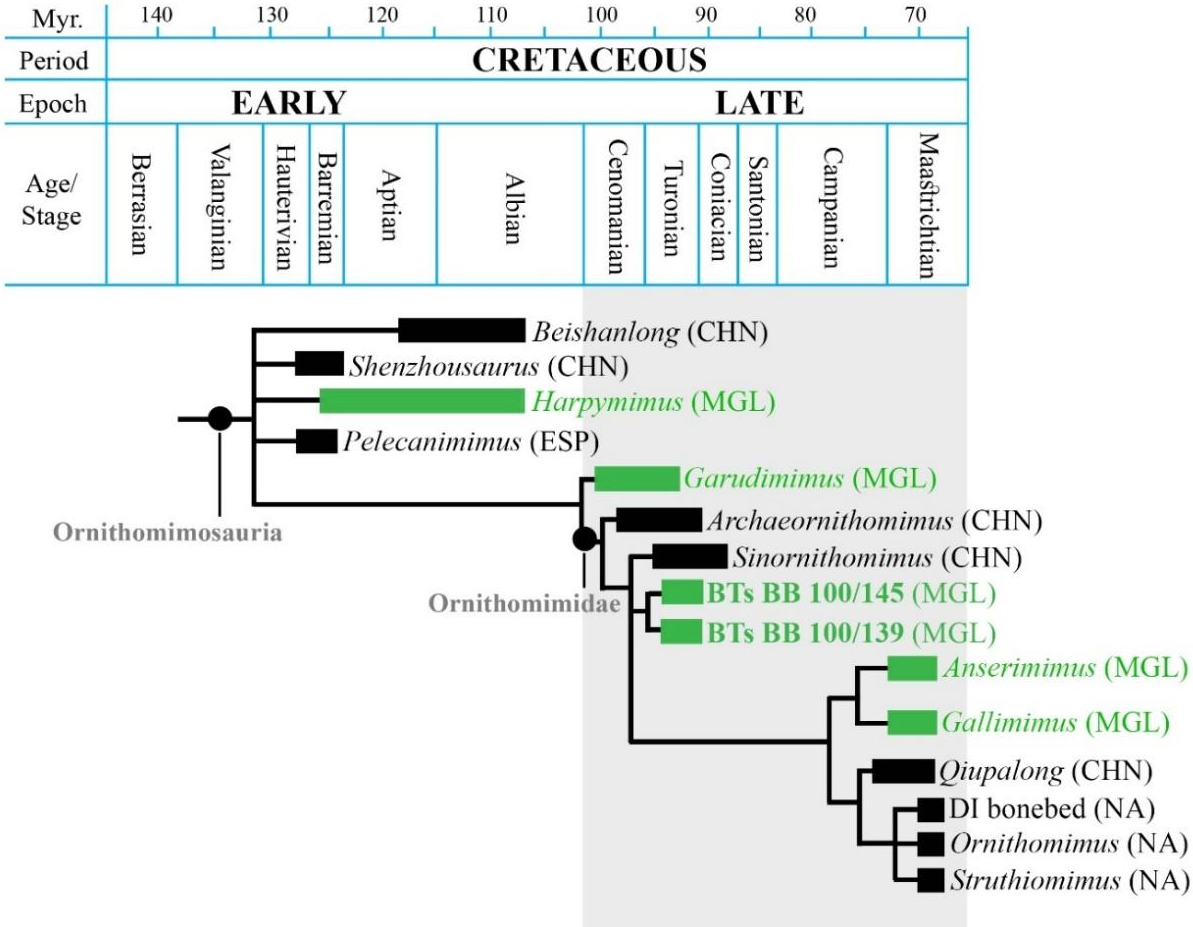

Figure-14. Time-calibrated strict consensus tree of BTs ornithomimosaur bonebed. *Explanation:* (CHN), China, (ESP), Spain, (MGL), Mongolia, and (NA), North America.

Minimum Number of Taxa

Although the characters presented in the description confirm that BTs Ornith BB specimens are placed within Ornithomimidae, a detail taxonomic determination between two distinct individuals from the bonebed was not resolved in this time without given that the skulls, which represent most of the important diagnostic characters, are missing from these specimens. Cullen et al (2013) is cited that the distal forelimb elements are taxonomically important utility in distinguishing different specimens. The forelimbs of both individuals are preserved from the BTs Ornith BB ornithomimosaur specimens, which are morphologically differentiated them in the aggregation, however, these characters are not adequately employed the character matrix used in present study (Fig. 15, Supplementary Data-S1).

In addition to the manus structure, BTs Ornith BB specimens show two morphotypes of dorsal vertebrae. The dorsal vertebrae of MPC-D 100/144 shows typical ornithomimosaur features, but MPC-D 100/146 has unique features such as the anteroposterior projections on the neural spine, a cup-shaped depression on the posterior surface of the neural spine, faint horizontal ridge on the lateral surface of the centrum, and a pair of tubercles at the posterior edge of the ventral surface of the centrum, suggesting that it differs from MPC-D 100/144 from the bonebed and as well as from *Garudimimus brevipes* of the same formation. *Garudimimus* has a similar structure in its neural spines of the dorsal vertebra, which is identified as metaplasia in previous study (Wilson et al., 2016). The anteroposterior projections of MPC-D 100/146 are clearly different from the metaplasia of *Garudimimus* but similar to the hook-like projections for ligament attachments as seen in some other coelurosaurs such as *Compsognathus, Ornitholestes, Huaxiagnathus, Scipionyx,* and *Sinosauropteryx* (Peyer, 2006). Two morphotypes in dorsal vertebrates confirm the presence of multiple taxa, at least two, in this bonebed.

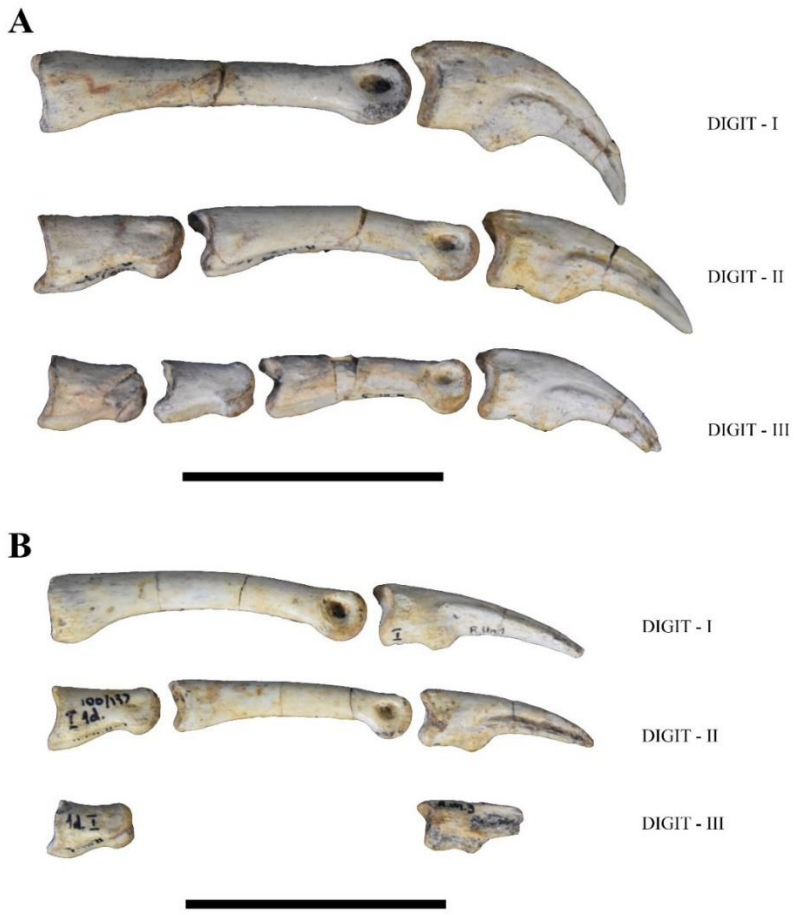

Figure-15. Comparison of manus of (A), MPC-D 100/139 and (B), MPC-D 100/145 in right lateral views. All scale bars = 5 cm.

Taphonomy

Although Behrensmeyer (1978) established six weathering stages (0-5) based on the physical alteration of modern bones, this study follows the taphonomic stages by Fiorillo (1988): Stage 0 as no sign of surface cracking or flaking; Stage 1 as cracking parallel to bone fibers; Stage 2 as start showing flaking along with cracking; and Stage 3 as loss of the outer bone layer. Within 226 elements from the BTs Ornith BB, over 90% (n=214) of the specimen show weathering stages of 0 and 1, suggesting these bones had been exposed for no more than two years in subaerial condition (Behrensmeyer, 1978; Fiorillo, 1988). The remaining specimens (5.31% (n=12)) show Stage 2.

Ontogenetic stage

Spacing between lines of arrested growth (LAG's) is often referred to qualitatively assess the relative growth rates and maturity in isolated bones of several theropod groups, namely *Tyrannosaurus* (Erickson et al., 2004; Horner and Padian, 2004), *Alioramus* (Brusatte et al., 2009), *Raptorex* (Fowler et al., 2011) as well as some ornithomimosaurs such as *Beishanlong*, *Sinornithomimus*, and a putative Alaskan ornithomimosaur (Varricchio et al., 2008; Makovicky et al., 2009; Watanabe et al., 2013). This interpretation assumes that a decrease in LAG spacing from the inner cortex to the periosteum corresponds with an individual approaching somatic maturity (Cullen et al., 2014). The thin-section of the right fibula of MPC-D 100/139 contains eight LAGs and the presence of EFS, suggesting that MPC-D 100/139 has reached its skeletal maturity (Fig. 13B) (Andrare et al., 2015) and demonstrating that MPC-D 100/139 is the smallest adult ornithomimosaur known to date at this moment. Under the assumption that LAGs and annuli are formed annually as they do in extant tetrapods (Peabody, 1961; Köhler et al., 2012), MPC-D 100/139 is estimated to have reached at least thirteen years old at the time of death. Despite its small size (femur length = 257.63 mm), its estimated age is equivalent with the giant ornithomimosaur *Beishanlong grandis* (a number of LAGs 13-14, femur length = 660 mm; (Makovicky et al., 2009)) and is much older than those of *Ornithomimus edmontonicus* (ROM 852, a number of LAGs = 5, femur length = 423 mm), unnamed ornithomimid specimens CMN 12068, (number of LAGs = 4, femur length = 417 mm), and CMN 12069, (a number of LAGs = 3, femur length = 390 mm), (Table-A4), (Cullen et al., 2014).

Domination of longitudinal vascular canals throughout the bone suggests slow growth rate of the animal (Chinsamy et al., 2012; Hübner, 2012). This is largely different from fibulae of other ornithomimosaurs which are dominated by radial and reticular vascular canals which suggests a fast growth rate (e.g., *Beishanlong grandis*, and *Ornithomimus edmontonicus* (ROM 852), (Makovicky et al., 2009; Cullen et al., 2014)). The accumulation percent of the cortical thickness based on the periosteal – LAGs – endosteal spacing suggests that the bone apposition rate was nearly constant until it reaches 90% of the cortical thickness (Fig. 16). The apposition rate is very different from those demonstrated by fibulae of Canadian ornithomimosaurs (*Ornithomimus edmontonicus*, ROM 852, unnamed ornithomimosaurs CMN

12068 and CMN 12069), which experience the highest rate in the early stage of their lives (Cullen et al., 2014).

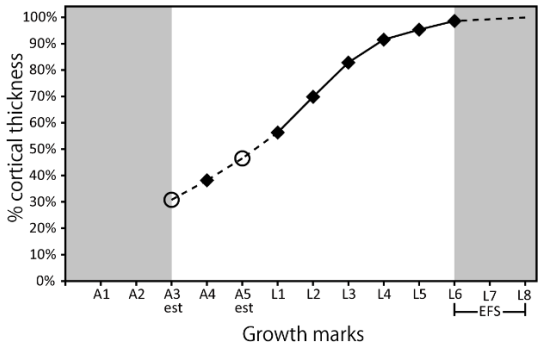

Figure-16. Graph of ratio of growth marks (LAGs and annuli) to the cortical thickness by percentage. *Abbreviations*: see the list of abbreviations on page vi.

Comparing to size distributions of the sampled fibula between the aforementioned ornithomimosaur specimens, the fibula of MPC-D 100/139 individual is the smallest (Table-A4). On the other hand, MPC-D 100/139 is the second smallest individual from the bonebed with the other individuals being up to 1.5 times larger than MPC-D 100/139 based on the pubis length (Table-A2). Moreover, the pubis of MPC-D 100/139 is much shorter than that of *Garudimimus brevipes* (pubis length = 390 mm) although its distal end is missing (Table-A2). The presence of two different body sizes in the bonebed suggests a sympatric niche-partitioning through grazing succession and browsing stratification (Elizabeth J. Kleynhans et al., 2011; Du Toit and Olff, 2014). Furthermore, smaller animals are known to consume diets of higher quality (Owen, 1842; Codron et al., 2007) due to their high nutritional demands in respect with body mass (Geist, 1974; Nagy et al., 1999). Therefore, the small body size and the constantly slow growth rate of MPC-D 100/139 are likely to have allowed it to occupy a different niche than the larger taxa. Together with the morphological differences (e.g., manual ungual shapes), and the body size differences are likely to have contributed to the large taxonomic diversity in the same region within a short period of time. Moreover, it can be said that a dwarfism was underwent within such a large taxonomic diversity, although this phenomenon is commonly represented within island dinosaur groups, such as ornithopods, sauropods, and a titanosaur, *Magyarosaurus* (Benton et al., 2006; Sander et al., 2006; Koen Stein et al., 2010). If above phenomenon of the Bayanshiree ornithomimosaur is an outstanding notion, a small body-

sized adult ornithomimosaur, MPC-D 100/139 is evident that a dwarf ornithomimosaur as well as the diminish ornithomimosaur from the early Late Cretaceous of Mongolia is known to report firstly.

Although it is difficult to give an exact determination of the exact cause of death of this bonebed assemblage, it is a noteworthy to present some possible hypotheses herein. Ornithomimosaurs were supposedly social animals that show evidence of gregarious behaviour (Kobayashi and Lü, 2003; Varricchio et al., 2008). Varricchio et al. (2008) is classified three environmental conditions for a cause of death for the *Sinornithomimus* bonebed, including miring, mass mortality, and drought conditions. Judging from the specimen accumulation, a quarry condition, and geological background of BTs Ornith BB, it is possible that a seasonal drought condition or rapid flooding condition may have been the cause of death because of the assemblage was recovered from near river channel of flood plain environments. The evidence of flood plain environments primarily consists of an overall arid to semi-arid paleoenvironment and the concentration of bone or individuals in a flood plain lake or depression. The bonebed aggregation of at least five individuals of two different ornithomimosaurs are likely they were formed mixed-species group and were packing together in time of death, which bears several advantageous factors for their group, such as foraging, antipredator advantage, and other social activities as in extant animals.

CHAPTER III

FIRST ORNITHOMIMID (THEROPODA, ORNITHOMIMOSAURIA) FROM THE UPPER CRETACEOUS, DJADOKHTA FORMATION OF TÖGRÖGIIN SHIREE, MONGOLIA

Manuscript Information Sheet

Tsogtbaatar Chinzorig, Yoshitsugu Kobayashi, Khishigjav Tsogtbaatar, Philip J. Currie, Mahito Watabe, Rinchen Barsbold

First ornithomimid (Theropoda, Ornithomimosauria) from the Upper Cretaceous Djadokhta Formation of Tögrögiin Shiree, Mongolia.

Scientific Reports

Status of Manuscript:

_x_ Prepared for submission to a peer-reviewed journal
_x_ Officially submitted to a peer-reviewed journal
_x_ Accepted by a peer-reviewed journal
_x_ Published in a peer reviewed journal

Published by Springer Nature

Contribution of Authors and Co-authors

Manuscript in Chapter III

Author: Tsogtbaatar Chinzorig

Contributions: conceived the study, catalogued and process the specimen, performed the analyses, prepared the figures, and wrote the manuscript.

Co-authors: Yoshitsugu Kobayashi, Philip J. Currie

Contributions: provided the useful comments and suggestions and improved to edit earlier drafts of the manuscript.

Co-authors: Khishigjav Tsogtbaatar, Mahito Watabe, and Rinchen Barsbold

Contributions: organized the joint expedition, allowed to access and study the specimen.

The citation of this research:

Tsogtbaatar Chinzorig, Yoshitsugu Kobayashi, Khishigjav Tsogtbaatar, Philip J. Currie, Mahito Watabe, Rinchen Barsbold, 2017. The first ornithomimid (Theropoda, Ornithomimosauria) from the Upper Cretaceous Djadokhta Formation of Tögrögiin Shiree, Mongolia. *Nature: Scientific Reports* 7: 5835, pp. 1-14 | http://www.nature.com/articles/s41598-017-05272-6

ABSTRACT

The Upper Cretaceous Djadokhta Formation has been intensively surveyed for its fossil vertebrate fauna for nearly a century. Amongst other theropods, dromaeosaurids and parvicursorines are common in the formation, but ornithomimosaurs are extremely rare. A new ornithomimosaur material was discovered from the Djadokhta Formation, represented by eolian deposits, of the Tögrögiin Shiree locality, Mongolia. This is only the third ornithomimosaur specimen reported from this formation, and includes the astragalus, the calcaneum, the third distal tarsal, and a complete pes. The new material is clearly belonged to Ornithomimidae by its arctometatarsalian foot condition and has the following unique characters; unevenly developed pair of concavities of the third distal tarsal, curved contacts between the proximal ends of second and fourth metatarsals, the elongate fourth digit, and a laterally inclined medial condyle on phalanx IV-1. These diagnostic characters of the Djadokhtan ornithomimosaur indicate that this is a new taxon. Our phylogenetic analysis supports three clades within derived ornithomimosaurs, and the new taxon is placed a member of the derived ornithomimosaurs. The present specimen is the first ornithomimid record from eolian Tögrögiin Shiree locality, and is indicative of their capability to adapt to arid environments.

Keywords

The Djadokhta Formation, eolian, Ornithomimidae, and Tögrögiin Shiree locality.

INTRODUCTION

Ornithomimosauria, one of the major arctometatarsalian groups of non-avian dinosaurs, is a clade of highly specialized theropod dinosaurs which are characterized by edentulous jaw, long fore limb with unusual metacarpal proportions, and a powerful hind limbs. Since its first description is published, the diversity of ornithomimosaurs increased dramatically (Ji et al., 2003; Kobayashi and Lü, 2003; Ksepka and Norell, 2004; Makovicky et al., 2004, 2009; Lee et al., 2014).

Ornithomimosaurs are mainly known from the Cretaceous beds of Asia and North America, ranging from ?Aptian-Albian to early Maastrichtian sediments (Makovicky et al., 2004; Weishampel et al., 2004a). The fossil occurrences of Asian ornithomimosaurs are rich in the Upper Cretaceous sediments, specifically from China and Mongolia (Makovicky et al., 2004). Mongolian ornithomimosaurs are represented by five definitive taxa, *Anserimimus, Deinocheirus* and *Gallimimus* are from the Nemegt Formation (early Maastrichtian), *Garudimimus* is from the Bayanshiree Formation (Cenomanian-Santonian), and *Harpymimus* is from the Khukhteeg Formation (late Albian) (Makovicky et al., 2004). Only two records of indeterminate ornithomimid specimens have been reported from the Campanian Djadokhta Formation at Ukhaa Tolgod (Makovicky and Norell, 1998; Ksepka and Norell, 2004).

The Djadokhta Formation has been intensively surveyed for its fossil vertebrate fauna for nearly a century (Berkey and Morris, 1927). Recent efforts continue to produce not only new specimens, but also new taxa (Tsogtbaatar et al., 2014; Tsuihiji et al., 2014). The Djadokhta Formation unconformably overlies the Bayanshiree Formation (Cenomanian-Turonian) and is disconformably overlain by the Baruungoyot Formation (Santonian-Campanian) (Gradzínski and Jerzykiewicz, 1974; Jerzykiewicz and Russell, 1991; Jerzykiewicz, 2000; Khand et al., 2000). Although a physical contact between the two formations has not been fully identified (Dingus et al., 2008), the Djadokhta Formation is stratigraphically lower than the Baruungoyot Formation (Gradziński et al., 1977; Jerzykiewicz and Russell, 1991; Dashzeveg et al., 2005) (Fig. 17A). The vertebrate assemblages of the Djadokhta Formation are rich in non-avian dinosaurs, such

as dromaeosaurids (Osborn, 1924), mononychids (Perle et al., 1993), troodontids (Tsuihiji et al., 2014) and oviraptorids, ornithomimids are extremely rare (Makovicky and Norell, 1998; Norell et al., 2001; Ksepka and Norell, 2004).

A new ornithomimosaur specimen was discovered from the Djadokhta Formation at Tögrögiin Shiree locality, about 50 km to the northwest of Bayn Dzak (Lefeld, 1971; Dashzeveg et al., 2005; Saneyoshi and Watabe, 2008) (Fig. 17B). The present specimen is the third ornithomimosaur record from this formation, and the first occurrence of Tögrögiin Shiree locality from Mongolia. This specimen is also the best preserved specimen of all of aforementioned three specimens known to date so far, and it provides new insight into ornithomimid dinosaur evolution and paleoenvironment.

Systematic paleontology

Dinosauria Owen, 1842 (Owen, 1842)

Theropoda Marsh, 1881 (Marsh, 1881)

Ornithomimosauria Barsbold, 1976 (Barsbold, 1976)

Ornithomimidae Marsh, 1890 (Marsh, 1890)

Aepyornithomimus tugrikinensis gen. et sp. nov.

Etymology. The generic name refers to the largest ratite bird *Aepyornis*~, which has similar pes structure; in Latin, ~*mimus* = 'as' or 'like'; the species name *tugrikinensis* refers to the locality where the specimen was found.

Holotype. MPC-D 100/130, articulated left pes preserved with an astragalus that is missing the ascending process, a complete calcaneum, and distal tarsal III (DT-III) (Figs. 18, 19, and 20). The original specimen is now housed in the Institute of Paleontology and Geology of the Mongolian Academy of Sciences (IPG-MAS).

Type locality and horizon: Central Sayr (44° 13' 54"N, 103° 16' 56"E) of Tögrögiin Shiree locality, Upper Cretaceous Djadokhta Formation (Campanian) (Fig. 17). This locality is interpreted as semi-arid eolian sediments (Currie and Padian, 1997) with up to 52 m of light gray, cross-bedded, structureless sands and sandstones (Dashzeveg et al., 2005).

Diagnosis. An ornithomimid dinosaur with the following unique characters; unevenly developed pair concavities on the posterior margin of the DT-III; robust distal articular caput of second metatarsal (Mt II) in dorsal view; proximoventrally rounded ridge of phalanx II-1 (II-1); the elongate fourth digit; laterally inclined medial condyle of phalanx IV-1 (IV-1); elongated pedal unguals.

A

Age		Formation	Mongolian ornithomimosaurs
Maa	65.5 – 70.6	Nemegt	*Anserimimus* *Deinocheirus* *Gallimimus*
Cmp	83.5	Baruungoyot Djadokhta	*Aepyornithomimus tugrikinensis* nov. gen. et nov. sp
Con-San	89.3		
Cen-Tur	99.6	Bayanshiree	*Garudimimus*
Alb-Cen	112	Baruunbayan	
Apt-Alb	125	Khukhteeg	*Harpymimus*

B

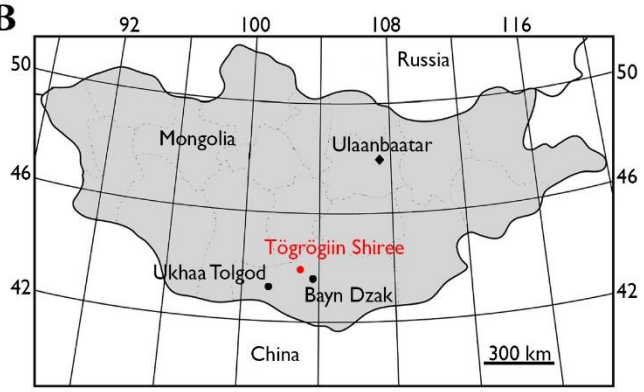

Figure-17. Location of *Aepyornithomimus tugrikinensis*. (A), Stratigraphic chart of ornithomimosaurs from Mongolia. (B), Location map. (◊), capital of Mongolia; (●), the position of type locality, Tögrögiin Shiree; (●), nearby other localities. Location map modified after Watabe et al. (2010).

MATERIAL AND METHODS

Specimen and Preparation

MPC-D 100/130 was not *in situ* in the field when it was first discovered. The main preparation work was done in the vertebrate preparation laboratory at Institute of Paleontology and Geology of Mongolia by using hand tools and Paraloid B72 and acetone. The solution used for this specimen was prepared as approximately 20 g of paraloid granules in 100 ml of acetone. During and after preparation, this solution was applied two or three times because of preservational condition of the specimen was very fragile.

Measurements

Original elements were measured in millimeters using digital calipers and a measuring tape (Table-1). Some data was collected from the literature when there was no chance for the first author to observe the original specimens directly. The photographs of specimens that are described in this study were taken using a Canon Eos Kiss X50 (4272x2848 pixel ratios, F-stop-f/8, exposure time-1.125 sec., ISO-800, focal length-55mm, and no flash) and a Nikon D80 (2592x3872 pixel ratios, F-stop-f/2.8) mounted on a tripod.

All figures, sketches, and tables are created in Adobe Photoshop CS6, Adobe Illustrator CS6, MS Word 2010 and MS Excel 2010 programs. Analytical part of this study was conducted by JMP.12 statistical software (SAS Institute Inc.), and online free statistical computing the R software (version 3.3.3), (R Core Team, 2016).

Phylogenetic analyses

Aepyornithomimus tugrikinensis characters were added to a recently published data set (Lee et al., 2014) on Ornithomimosauria. *Archaeornithomimus* was also coded. The data matrix was assembled in a NEXUS file, and is composed of 568 cranial and postcranial characters that are drawn from the recently published literature and from personal observations for 99 valid coelurosaurian taxa. Based on the preserved skeleton, *Aepyornithomimus tugrikinensis* could be scored for thirty characters (5.28%) of the 568 characters (Supplementary Data S1) and incorporated into the character-taxon matrix dataset after modified Choiniere et al. (2012) and Lee et al. (2014). *Allosaurus fragilis* was the outgroup taxon. All characters are considered unordered and were not weighted. Data matrix was analyzed using the software package TNT v. 1.1 (Goloboff et al., 2008). Most-parsimonious trees were obtained using following heuristic search parameters: the maximum number of the trees held in memory was increased to the maximum possible 10,000 trees; Driven Search, finding minimum length 1 times, and adjusting in the New Technology search method, was settled to using Sectorial Search, Ratchet, Drift, and Tree Fusing with default settings; followed by an additional round of tree bisection reconnection (TBR) of branch-swapping on MPTs. The analysis produced four most parsimonious trees, each with tree length of 2932 steps, a Consistency Index of 0.229, and a Retention Index of 0.591.

DESCRIPTION

Tarsus

Preserved tarsal bones include the astragalus, calcaneum and DT-III. Most of these elements are complete, although the ascending process of the astragalus is missing. The astragalus and calcaneum are not fused. The distal condyles of the astragalus are unevenly developed so that the medial condyle is more pronounced than the lateral one. It leans more anteromedially than in Early Cretaceous taxa (Makovicky et al., 2009) *Gallimimus*, *Qiupalong* and *Struthiomimus* (Osmólska et al., 1972; Russell, 1972; Xu et al., 2011) (Fig. 18C). A depression is present at the base of the ascending process in anterior view (Fig. 18A). The intercondylar sulcus is deeply concave as in *Garudimimus* and *Harpymimus*, but unlike more derived ornithomimosaurs in which it is shallow (Osmólska et al., 1972; Kobayashi and Barsbold, 2005a) (Fig. 18A, D). The outer margin of the lateral condyle is notched for receiving the medial tubercle of the calcaneum, as in other ornithomimosaurs (Fig. 18A, C). However, the notch of *Aepyornithomimus tugrikinensis* is not as deep as some taxa of derived ornithomimosaurs (Osmólska et al., 1972).

The calcaneum is a thin and disc-like bone (Fig. 18E, F). It extends anteroposteriorly to make an oval shape. It differs from most ornithomimosaurs by shape where is often represented as a round. A weakly developed tubercle is positioned at the center area (Fig. 18E). The facet at the proximal surface indicates that the fibula contacted the tarsus (Fig. 18E). The lateral surface is flat, but slightly concave as like those *Gallimimus* and *Garudimimus* (Fig. 18F).

One of the distal tarsals was preserved in the specimen. It supposed the distal tarsal III. It is a nearly complete, however part of the anteromedial edge is missing (Fig. 18G, H). DT-III is a thin proximodistally. Although the proximal end of Mt III is missing, DT-III would have been covered the proximal articular surface of Mt III completely or partially. It also partially covered the proximal end of Mt II as in other ornithomimosaurs. DT-III has developed a pair of uneven concavities on the posterior edge (Fig. 18G, H). The medial concavity is deeper than lateral one. The corresponding edge of DT-III is almost

straight in *Garudimimus*, but is convex in *Gallimimus* and the Bissekty ornithomimid (Barsbold and Perle, 1984; Barsbold, 1988; Claessens and Loewen, 2015; Serrano-Brañas et al., 2016). Moreover, the overall shape of DT-III is triangular with a straight medial edge in proximal view, whereas it is quadrangular with a convex medial edge in other ornithomimosaurs.

Metatarsals

Mt II, Mt III, and Mt IV are preserved. Metatarsals are generally complete, but are missing some parts of the distal end of Mt II, the proximal end of Mt III, and the medial condyle of Mt IV (Fig. 19). Mt I is not preserved and no any scars for Mt I are shown on the Mt II. The length ratios are as usual in ornithomimosaur, like Mt III is the longest, and Mt II is marginally shorter (98%) than Mt IV (Fig. 19A).

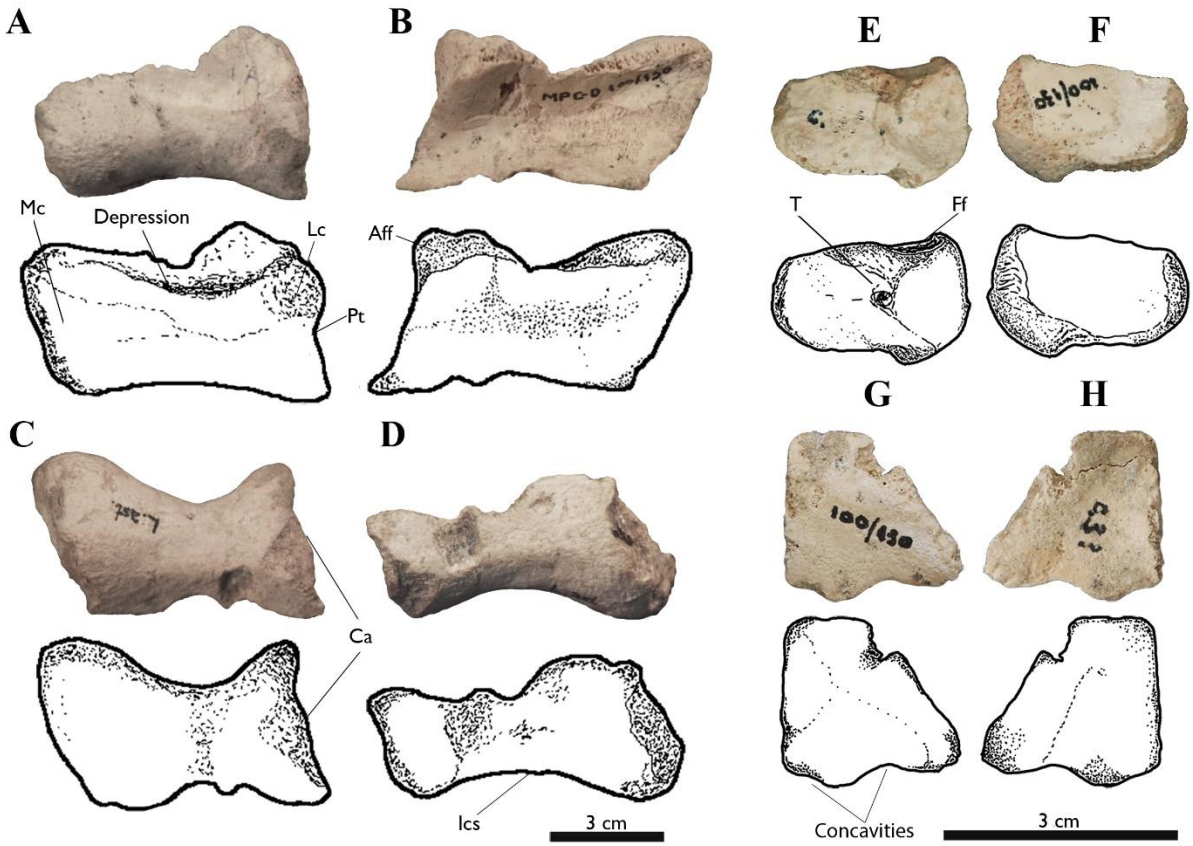

Figure-18. Ankle joint elements of *Aepyornithomimus tugrikinensis*. *Explanation:* (A-D), the astragalus, (E-F), the calcaneum, and (G-H), the third distal tarsal, including line drawings. (A), in anterior, (B, G), in proximal, (C, H), in distal, (D), in posterior, (E), in medial, and (F), in lateral views. *Abbreviations*: see the list of abbreviations on page vi.

The third digit of *Aepyornithomimus tugrikinensis* is shorter than those Late Cretaceous ornithomimosaurs when comparing to the total length of Mt III with the third digit length. However, this length is a comparable to *Deinocheirus* and *Garudimimus* (Kobayashi and Barsbold, 2005a; Lee et al., 2014). The metatarsals are more slender than Deinocheiridae; in this sense, the relatively slender metatarsals of *Aepyornithomimus tugrikinensis* are more resembled as derived ornithomimosaurs by its presence (Osmólska et al., 1972; Russell, 1972; Barsbold, 1988; Kobayashi and Lü, 2003).

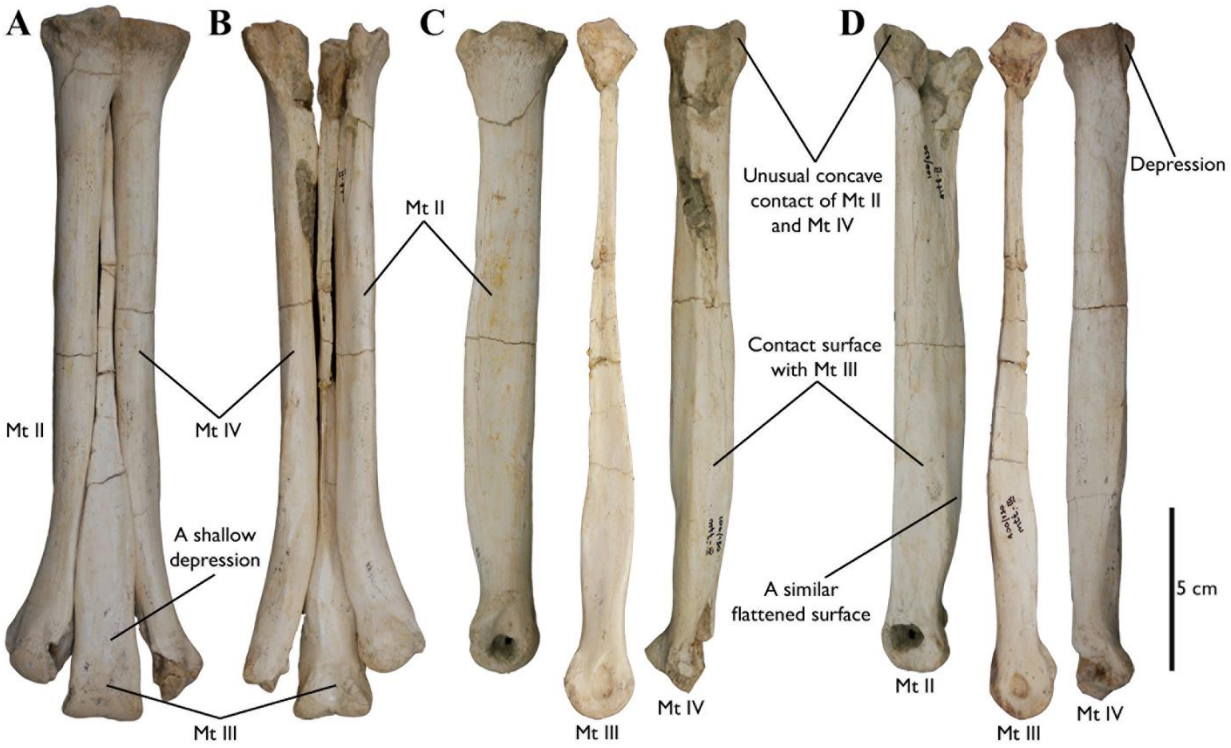

Figure-19. Metatarsals of *Aepyornithomimus tugrikinensis*. (A), in anterior, (B), in posterior, (C), in medial, and (D), in lateral views. *Abbreviations*: see the list of abbreviations on page vi.

The lengths of Mt II and Mt IV are subequal in *Aepyornithomimus tugrikinensis*, like *Anserimimus*, *Gallimimus*, and *Qiupalong* (Kobayashi and Barsbold, 2005b), whereas Mt IV is longer than Mt II in most ornithomimosaurs (Fig. 21). The outlines of the proximal articular surfaces of Mt II and Mt IV of *Aepyornithomimus tugrikinensis* resemble *Qiupalong* (Xu et al., 2011). In some taxa, these metatarsals tightly adhere to Mt III distally, whereas metatarsals of other taxa are distinctly divergent

(Makovicky et al., 2004). The distal articular surfaces are rounded as in other ornithomimosaurs (Makovicky et al., 2004). The collateral ligament fossae of Mt II and Mt IV are equally developed with the same depths.

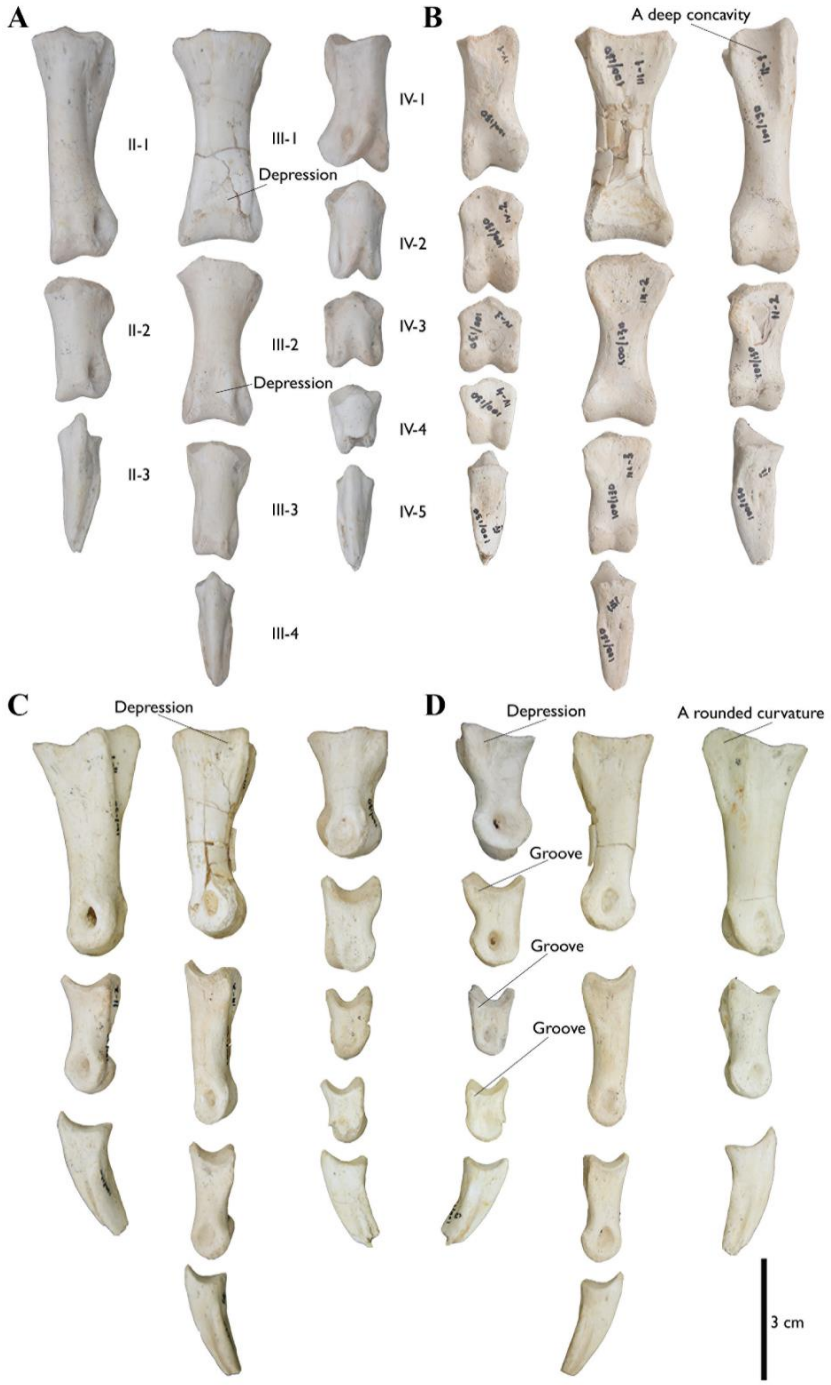

Figure-20. Phalanges of *Aepyornithomimus tugrikinensis*. (A), in dorsal, (B), in ventral, (C), in lateral, and (D), in medial views. *Abbreviations*: see the list of abbreviations on page vi.

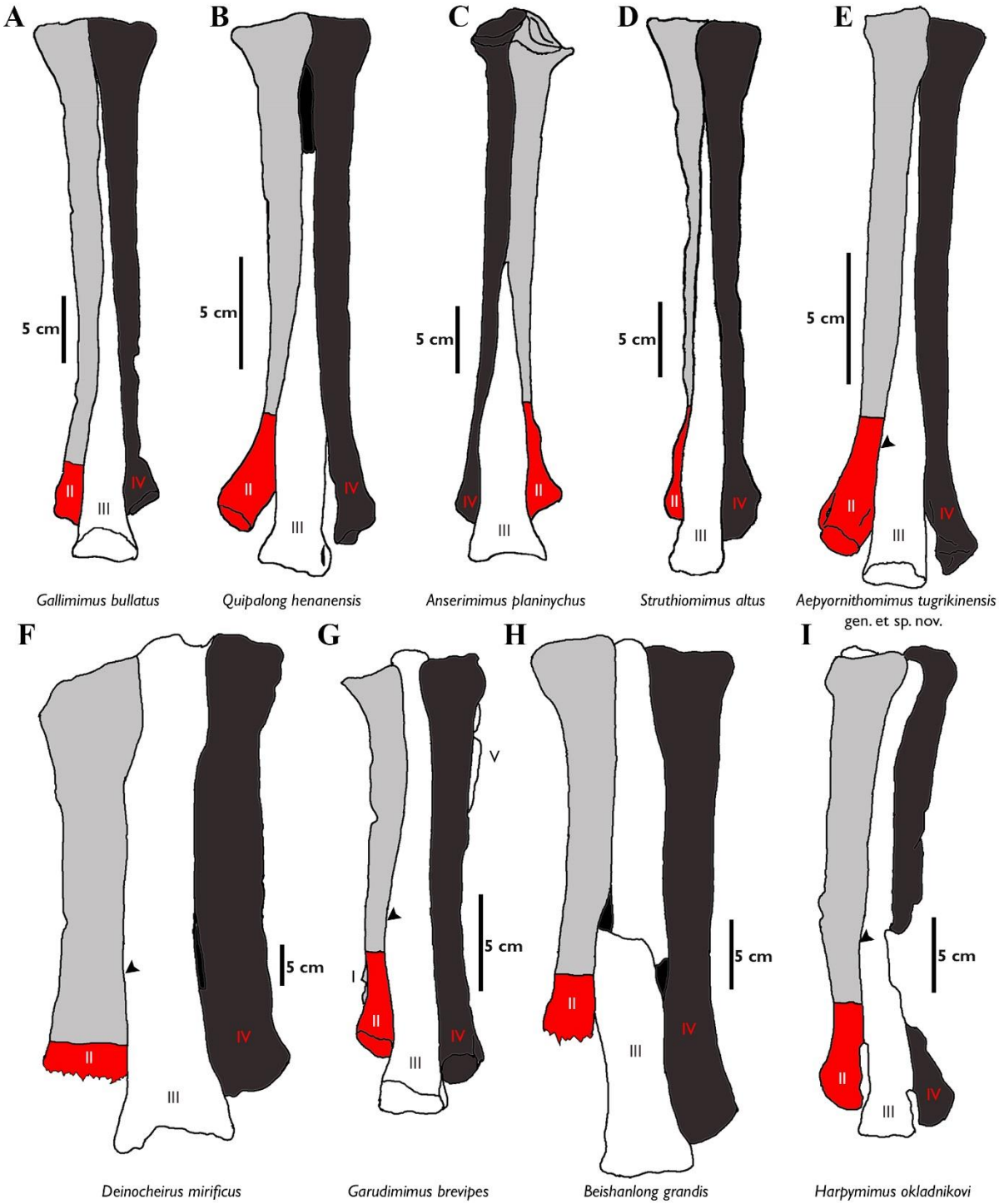

Figure-21. Comparisons of ornithomimosaur metatarsals. (A-E), "arctometatarsalian" condition, (F-I), "non-arctometatarsalian" condition. *Abbreviations*: see the list of abbreviations on page vi.

Mt II is nearly complete, but the lateral sides of both proximal and distal ends are crushed naturally (Fig. 19D). A morphologically interesting feature is present on the proximal end of metatarsus. The anterolateral surface of the proximal end of Mt II has a deep, rounded concavity for receiving the convex anteromedial surface of Mt IV; it forms an unusual curved contact in proximal view (Figs. 19D and 22A). This contact is straight in other ornithomimosaurs, such as *Anserimimus, Gallimimus, Ornithomimus,* and Ornithomimid indet. (MPC-D 100/14) (Barsbold, 1988; Makovicky et al., 2004; Kobayashi and Barsbold, 2006). The shaft of the diaphysis is straight and slender. The cross-section of Mt II is presumably subcircular. The width of the distal articular end is nearly the same as the width of the distal articulation of Mt III, which is unusual in ornithomimosaurs (Fig. 19A). The distal fifth of Mt II diverges medially from Mt III, but the degree of divergence is less than in *Anserimimus* and *Gallimimus* (Osmólska et al., 1972; Barsbold, 1988). Its divergence is relatively greater than in basal ornithomimosaurs (Barsbold and Perle, 1984; Kobayashi and Barsbold, 2005b, 2005a), although it is similar to the type specimen of *Qiupalong* (Xu et al., 2011). The lateral condyle of the Mt II is larger than the medial condyle, and these condyles are separated by a deep sulcus on the flexor side (Fig. 22B), which is even deeper than in *Anserimimus, Harpymimus,* and IVPP V12756 (Barsbold and Perle, 1984; Barsbold, 1988; Shapiro et al., 2003). The lateral collateral ligament fossa is somewhat weathered but visible.

Mt III is the longest metatarsal of other metatarsals (Fig. 19). Based on the configuration of the proximal contacts of Mt II and Mt IV, the proximal end of Mt III seems to be a triangular and tapering posteriorly (Fig. 22A). The proximal end is pinched as like *Gallimimus* and *Struthiomimus*. However, it differs from *Anserimimus,* in which the proximal half of the Mt III shaft is completely covered by other metatarsals (Fig. 22C). The anteromedial edge is straighter than the anterolateral edge (Fig. 19A). This feature is similar to one of diagnostic characters of *Rativates* (McFeeters et al., 2016). The cross-section of the distal half of Mt III is subrectangular. Mt III broadens distally and slightly covers the lateral and medial edges of Mt II and Mt IV, respectively (Holtz, T. R., 1994; Weishampel et al., 2004b). The anterolateral margin of MT III is more widely separated from Mt IV than it is from Mt II (Fig. 19A), whereas both

margins deviate equally in tyrannosaurids (Holtz, T. R., 2004). There is a shallow depression on the anterior surface of the distal half of Mt III (Fig. 19A).

The distal end of Mt III is similar to those ornithomimosaurs (Makovicky et al., 2004). However, the medial condyle is slightly larger than the lateral condyle (Osmólska et al., 1972; Shapiro et al., 2003; Kobayashi and Barsbold, 2005b, 2005a). The distal intercondylar groove is shallower than those of the Mt II and Mt IV. The articular caput of Mt III is as straight as *Rativates* on the flexor side (Fig. 22B) (McFeeters et al., 2016).

The nearly complete Mt IV is fractured in the proximomedial and distal parts (Fig. 19C and 19D). The medial and posterior surfaces of the proximal two-thirds of the shaft are flat (Fig. 19B and 19C). The shaft is oval to rectilinear in cross-section, and its width is less than its anteroposterior length. Although the fifth metatarsal is not preserved in *Aepyornithomimus tugrikinensis*, there is a deep depression to receive it on the proximolateral surface of Mt IV (Kobayashi and Barsbold, 2005a; Lee et al., 2014) (Fig. 19D).

Pedal phalanges

All pedal phalanges (II-1 to II-3, III-1 to III-4, and IV-1 to IV-5) are preserved (Fig. 20). The phalangeal formula is 0-3-4-5-0 as in other ornithomimosaurs, except for *Beishanlong* (Makovicky et al., 2009) and *Garudimimus* (Kobayashi and Barsbold, 2005a), both of which retained the first digit. Although the second and the fourth digits are shorter than the third digit as typical, the corresponding digits are relatively longer than in other ornithomimosaurs. The proximal halves of the ventral surfaces of all phalanges are flat, with the exception of II-1.

Articular surfaces of the most proximal phalanges (II-1, III-1, and IV-1) are shallow, undivided concavities. II-1 and III-1 are the most robust of the phalangeal series, although II-1 is slightly longer than III-1. The heights of the proximal ends of II-1 and IV-1 are greater than their widths, whereas the relationship is the opposite in III-1. There are shallow depressions on the lateral surfaces of II-1 and III-1, and a slightly stronger depression on the proximomedial surface of IV-1 near the proximoventral end (Figs. 20C-D and 22D-E). The proximoventral surface of II-1 has a deep concavity like other derived Asian

ornithomimosaurs, but unlike that of *Tototlmimus* (Serrano-Brañas et al., 2016). Also, the proximomedial boundary forms a rounded curvature (Fig. 20D). It is different than other ornithomimosaurs, especially *Garudimimus,* and *Tototlmimus*, where the corresponding boundary is rectilinear (Osmólska et al., 1972; Kobayashi and Barsbold, 2005b; Serrano-Brañas et al., 2016; Sues and Averianov, 2016a).

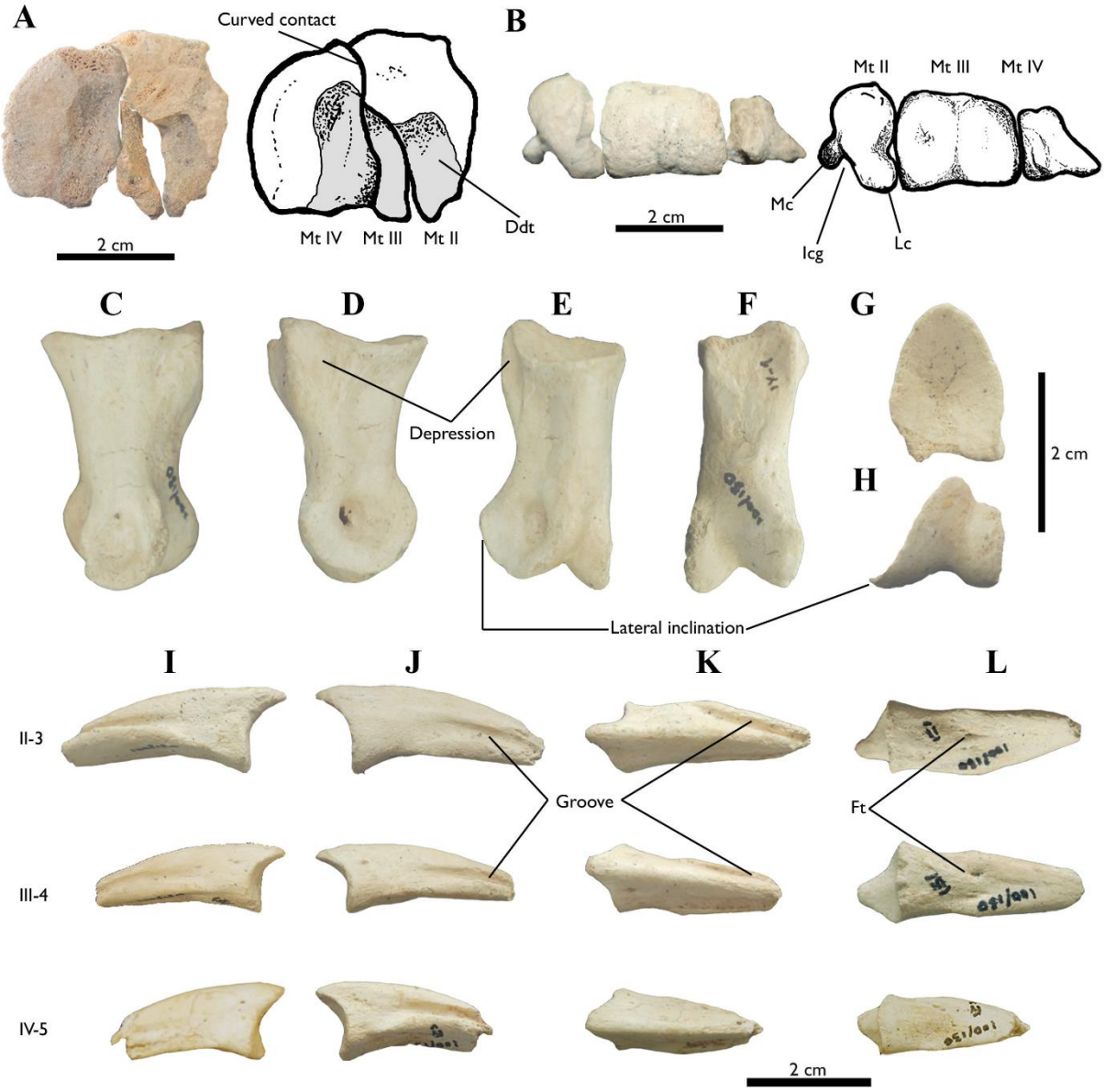

Figure-22. The articulated views of metatarsals, the first phalanx (IV-1) of digit IV, and the ungual phalanges of *Aepyornithomimus tugrikinensis*. (A), in proximal end, and (B), in distal end of metatarsals. (C-L), Phalanges IV-1, II-3, III-4, and IV-5 – (C, I), in lateral, (D, J), in medial, (E, K), in dorsal, (F, L), in ventral, (G), in proximal, and (H), in distal views. *Abbreviations*: see the list of abbreviations on page vi.

The proximal articular surface of II-2 is divided by a low vertical ridge for its weak ginglymoid joint with II-1. The lip-like proximodorsal process of II-2 overlaps its joint with II-1 (Fig. 20A). The length ratio of II-1 to II-2 is approximately 2:1. The length of II-2 is subequal to IV-1.

III-1 and III-2 are similar in appearance, although the lengths are different. The proximal articular surfaces of the third digit phalanges (III-1 to III-3) are undivided and nearly symmetrical, whereas there are strong, vertical ridges on the proximal articular surfaces of IV-2 to IV-4. The medial condyle of III-1 is slightly extended to distally. There are faint depressions on the dorsal surfaces of III-1 and III-2. The distal articular surface of III-3 is asymmetrical, and its lateral condyle is larger than the medial one in dorsal view. In addition, deep short grooves are presented along the proximomedial surfaces of IV-2 to IV-4, which are similar to those seen in III-1 and III-2 of *Garudimimus* (Kobayashi and Barsbold, 2005a), (Fig. 20D).

Successive phalanges of the fourth digit of *Aepyornithomimus tugrikinensis* become mediolaterally slender (Fig. 20, Table-1) (Osmólska et al., 1972; Russell, 1972; Kobayashi and Lü, 2003). Like phalanges of the second digit, those of the fourth digit have weakly ginglymoid joints. The lateral condyle of IV-1 is a relatively smaller (Fig. 22H). Its medial condyle is inclined more laterally than in any other ornithomimosaurs. The degree of inclination is about 35º, when it is measured from the base of the medial condyle of the IV-1 to the lateral. This degree is less in other ornithomimosaurs (e.g., *Deinocheirus* 21º, *Harpymimus* 17º, and *Struthiomimus* 25º). Phalanx IV-1 has a deep depression dorsal to the proximoventral ridge in medial view. Phalanx IV-3 is somewhat unlike other ornithomimosaurs in having a flattened flexor surface, a deeper proximal concavity, and a more elongate appearance in lateral and medial views. The medial collateral ligament pits of IV-1 to IV-4 are deeper than the corresponding lateral ones. However, the lateral ones are still deeper than their equivalents in *Deinocheirus* (Lee et al., 2014) and *Harpymimus* (Kobayashi and Barsbold, 2005b), (Fig. 20C-D).

Table 1. Left foot measurements of *Aepyornithomimus* (MPC-D 100/130) in mm.

Elements	Length	Proximal medial-lateral width	Proximal antero-posterior height	Distal medial-lateral width

Astragalus	51.8	-	-	-
Calcaneum	25.06	-	-	-
Metatarsal-II	201	19.19	36.7	21.61
Metatarsal-III	211	5.69	18.22+	25.15
Metatarsal-IV	207	19.23	25.26	16.64+
Phalanx II-1	59.08	17.87	24.07	17.07
Phalanx II-2	32.09	16.99	14.94	14.30
Phalanx II-3 ungual	36.35+	11.10	13.49	-
Phalanx III-1	52.11	24.84	21.34	21.54
Phalanx III-2	42.73	21.84	13.80	18.25
Phalanx III-3	29.48	16.80	11.94	12.12
Phalanx III-4 ungual	30.89+	10.86	10.88	-
Phalanx IV-1	32.88	15	20.89	18.16
Phalanx IV-2	24.34	15.58	15.67	14.04
Phalanx IV-3	19.80	15.32	11.76	14.66
Phalanx IV-4	17.68	13.56	10.95	10.62
Phalanx IV-5 ungual	27.74+	10.05	12.38	-

Note: (+) – Element incomplete and minimum value; (-) – element is not preserved.

All unguals are triangular in cross-section, but mediolaterally more slender than other ornithomimosaurs (Fig. 22I-L). The articular surfaces of ungual phalanges II-3 and IV-5 are asymmetric to match the distal ends of the penultimate phalanges. In contrast, the ungual phalanx III-4 is symmetrical to the dorsoventral axis. Flexor tubercles are weakly developed or almost not existed in all unguals, similar to *Qiupalong* (Xu et al., 2011) and *Tototlmimus* (Serrano-Brañas et al., 2016), but different from the Bissekty ornithomimid (Sues and Averianov, 2016a) (Fig. 22L). All unguals have shallow lateral and medial grooves, extending from the proximal articular edges to the distal tips (Fig. 22I, I, and 22J). In addition, sulci do not exist along the ventromedial and ventrolateral edges of any unguals known for *Struthiomimus* (Serrano-Brañas et al., 2016) and *Tototlmimus* (Serrano-Brañas et al., 2016). On the other hand, the general appearances of the shallow sulci and the proximodistally elongate unguals are similar to those of *Nqwebasaurus* (Choiniere et al., 2012). Ungual phalanx II-3 of *Aepyornithomimus tugrikinensis* is relatively larger than the other two unguals (Fig. 22I-L). Unguals of the second and the fourth digits are inclined somewhat outward from their inner parts as in most ornithomimosaurs. Similar to *Archaeornithomimus*, *Beishanlong* and *Qiupalong*, the ventral surfaces of the unguals are slightly curved ventrally in lateral view (Russell, 1972; Makovicky et al., 2004; Xu et al., 2011), but the condition of

unguals in *Ornithomimus* and *Tototlmimus* is a nearly straight which are differentiated *Aepyornithomimus tugrikinensis* from these taxa.

Phylogenetic analysis

In order to assess the phylogenetic position of *Aepyornithomimus tugrikinensis*, this taxon was added to a recently published modified dataset of coelurosaurians (Choiniere et al., 2012; Lee et al., 2014; Sues and Averianov, 2016a). Our analysis recovers four most parsimonious trees (MPTs), (Fig. A1). The strict consensus tree shows that basal ornithomimosaurs, from *Haplocheirus* to *Harpymimus*, are successive taxa, the monophyly of three clades of derived ornithomimosaurs (Deinocheiridae, *Archaeornithomimus* + Bissekty ornithomimid, and the clade of *Anserimimus*, *Aepyornithomimus tugrikinensis*, *Gallimimus*, *Struthiomimus*, and *Ornithomimus* (herein called "derived ornithomimids")), (Fig. 23). The relationships of Deinocheiridae, *Archaeornithomimus* + Bissekty ornithomimid, and "derived ornithomimids" remain an unresolved polytomy.

The clade of "derived ornithomimids" is well-supported by sharing the following unambiguous synapomorphic characters; the maxillary fenestra is recessed within a posteriorly shallow recessed maxillary fenestra **[17]**, a descending process of the squamosal is parallel to the shaft of the quadrate **[110]**, the quadrate is hollow **[112]**, scapula is longer than humerus **[361]**, absent or poorly developed medial tab on the proximal end of Mt I **[395]**, more or less symmetrical condyles of the Mt I **[396]**, the supraacetabular crest forms a hood over the femoral head **[448]**, the shaft of Mt IV is round or thicker than wide in cross-section **[558]**, and the pedal unguals have pronounced flexor fossae on the ventral surfaces of the proximal ends **[567]**.

There are two potential relationships among Deinocheiridae, *Archaeornithomimus* + Bissekty ornithomimid, and the clade of "derived ornithomimids" (Fig. A1). Two of four MPTs show two clades, Deinocheiridae and Ornithomimidae (*Archaeornithomimus*, Bissekty ornithomimid, and "derived ornithomimids"), as suggested by previous studies (Lee et al., 2014). The clade of Ornithomimidae shares following three unambiguous synapomorphies, absence of posterolateral crests on lateral surfaces of

cervical centra **[262]**, completely closed pubic apron **[463]**, and smooth and not ginglymoid distal end of Mt III **[553]** (Fig. A1a, b). The other two MPTs suggest Deinocheiridae and "derived ornithomimids", are monophyletic, supported by two synapomorphies; the parapophysis is distinctly below the transverse process in the most posterior dorsal vertebrae **[299]** and the ulnar shaft is straight **[375]** (Fig. A1c, d). The change in the phylogenetic position of *Archaeornithomimus* + the Bissekty ornithomimid is probably related to the fragmentary nature of these specimens.

The monophyletic "derived ornithomimids" suggests that *Aepyornithomimus tugrikinensis* belongs to Ornithomimidae, although interrelationships among these taxa are poorly resolved (Fig. 23). This clade is supported in all MPTs by sharing three unambiguous synapomorphies; absent or poorly developed medial tab on the proximal end of Mt I **[395]**, more or less symmetrical condyles of Mt I **[396]**, and the supraacetabular crest forms a hood over the femoral head **[448]**. *Anserimimus* is placed as the most basal taxon in this clade, and each MPT shows different phylogenetic positions for *Aepyornithomimus tugrikinensis*. MPTs 1, 2, and 4 support the monophyly of *Aepyornithomimus*, *Gallimimus*, *Ornithomimus*, and *Struthiomimus* with two unambiguous synapomorphies (scapula longer than humerus **[361]** and penultimate phalanx of the second digit longer than first phalanx **[411]**) although *Aepyornithomimus* does not preserve forelimbs.

In MPTs 1 and 4, *Aepyornithomimus tugrikinensis* is nested together with North American taxa (*Ornithomimus* and *Struthiomimus*) and shares the following synapomorphies; posterodorsal process of the lacrimal projects posterodorsally **[78]**, articular has elongate, slender medial, posteromedial, or mediodorsal process from retroarticular process **[208]**, and postzygapophyses of cervical vertebrae 2-4 are connected medially along their entire lengths by a dorsally concave intrazygapophyseal lamina for attachment of interspinous ligaments **[271]**, (Fig. A1a, d). These alternative positions of *Aepyornithomimus tugrikinensis* are due to its preservation in nature, and additional materials are required to determine the more obvious position of this taxon in the future.

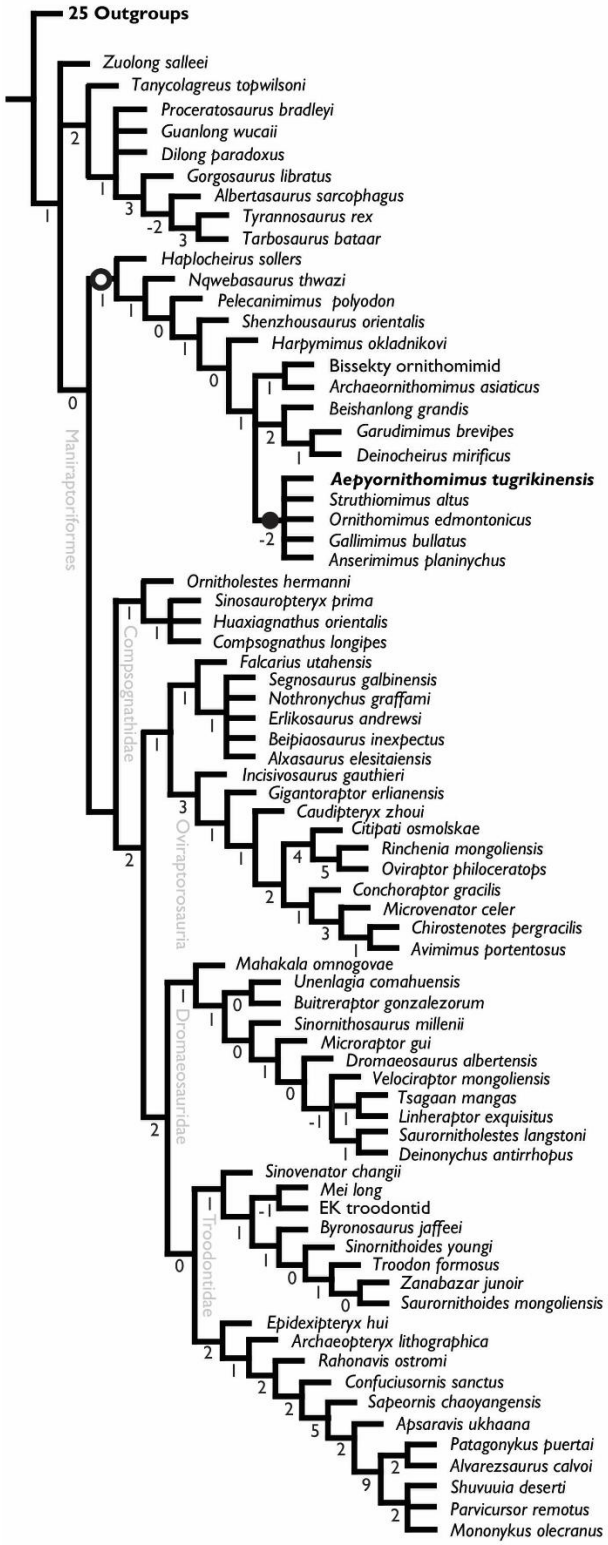

Figure-23. Strict consensus tree of the phylogenetic relationships of *Aepyornithomimus tugrikinensis* within the Coelurosauria. Explanation: (-I, -2….9), Bremer supports, (○), Ornithomimosauria, and (●), Ornithomimidae.

DISCUSSION

Aepyornithomimus tugrikinensis is the first ornithomimid ornithomimosaur identified from the Upper Cretaceous Djadokhta Formation of Tögrögiin Shiree in Mongolia and Late Cretaceous new member of this clade that has been named from Mongolia after nearly three decades (Jerzykiewicz and Russell, 1991; Weishampel et al., 2004b). Previously, only two ornithomimosaur materials have been reported from the Ukhaa Tolgod locality (Makovicky and Norell, 1998; Ksepka and Norell, 2004). Insufficient materials in nature, these specimens were unable to display any diagnostic characters for determining their taxonomic certainty. In addition, no any overlapped elements between *Aepyornithomimus tugrikinensis* and Ukhaa Tolgod materials that are not permit to compare them in this study.

Aepyornithomimus tugrikinensis has some unique features on the foot. For instance, it differs from *Beishanlong*, *Deinocheirus*, *Garudimimus*, and *Harpymimus* in having relatively slender arctometatarsalian metatarsals (Barsbold and Perle, 1984; Smith and Galton, 1990; Kobayashi and Barsbold, 2005a, 2005b; Makovicky et al., 2009; Lee et al., 2014), the unusual curved contact between the proximal ends of Mt II and Mt IV, and a robust distal articular caput of Mt II. In contrary to, all other Late Cretaceous ornithomimosaurs have a straight Mt II and Mt IV contact at the proximal end and a relatively small distal articular caput of Mt II (Barsbold and Osmólska, 1990).

The proportional differences of three metatarsal elements are compared among ornithomimosaur species by a ternary diagram (Fig. 24A and Table-2). Individual metatarsal measurements are averaged for each species. The diagram shows that basal ornithomimosaurs (*Nqwebasaurus* and *Harpymimus*), deinocheirids, and ornithomimids bear generally different metatarsal proportions. In addition, basal ornithomimosaurs have shorter Mt III, whereas deinocheirids have shorter Mt II. *Aepyornithomimus tugrikinensis* shares a similar metatarsal proportion with basal ornithomimosaurs. A discriminant analysis is used three categorized groups (basal ornithomimosaurs, Deinocheirids, and Ornithomimids). Mt II, Mt III, and Mt IV lengths as covariates that confirm the morphological separation among the three groups (Wilk's

lambda = 0.321, $F = 2.803$, $p = 0.03$). Twelve species out of sixteen species are correctly classified in the analysis. *Aepyornithomimus tugrikinensis* is classified into basal ornithomimosaurs with posterior probability of 0.858.

The mediolaterally slender phalanges of the fourth digit and the laterally inclined medial condyle of the IV-1 are unique characters of *Aepyornithomimus tugrikinensis*. In contrary to the derived ornithomimosaurs, the phalangeal lengths of the fourth digit are also long in basal ornithomimosaurs, like *Garudimimus* and *Harpymimus*. In spite of this, the elongate fourth digit of *Aepyornithomimus tugrikinensis* is distinct from those of derived ornithomimosaurs, such as *Anserimimus, Gallimimus, Ornithomimus,* and *Struthiomimus.* The phalanges of these taxa are highly abbreviated (Osmólska et al., 1972; Russell, 1972; Barsbold, 1988). The degree of inclination of the medial condyle of IV-1 is 35º which is greater than any ornithomimosaurs.

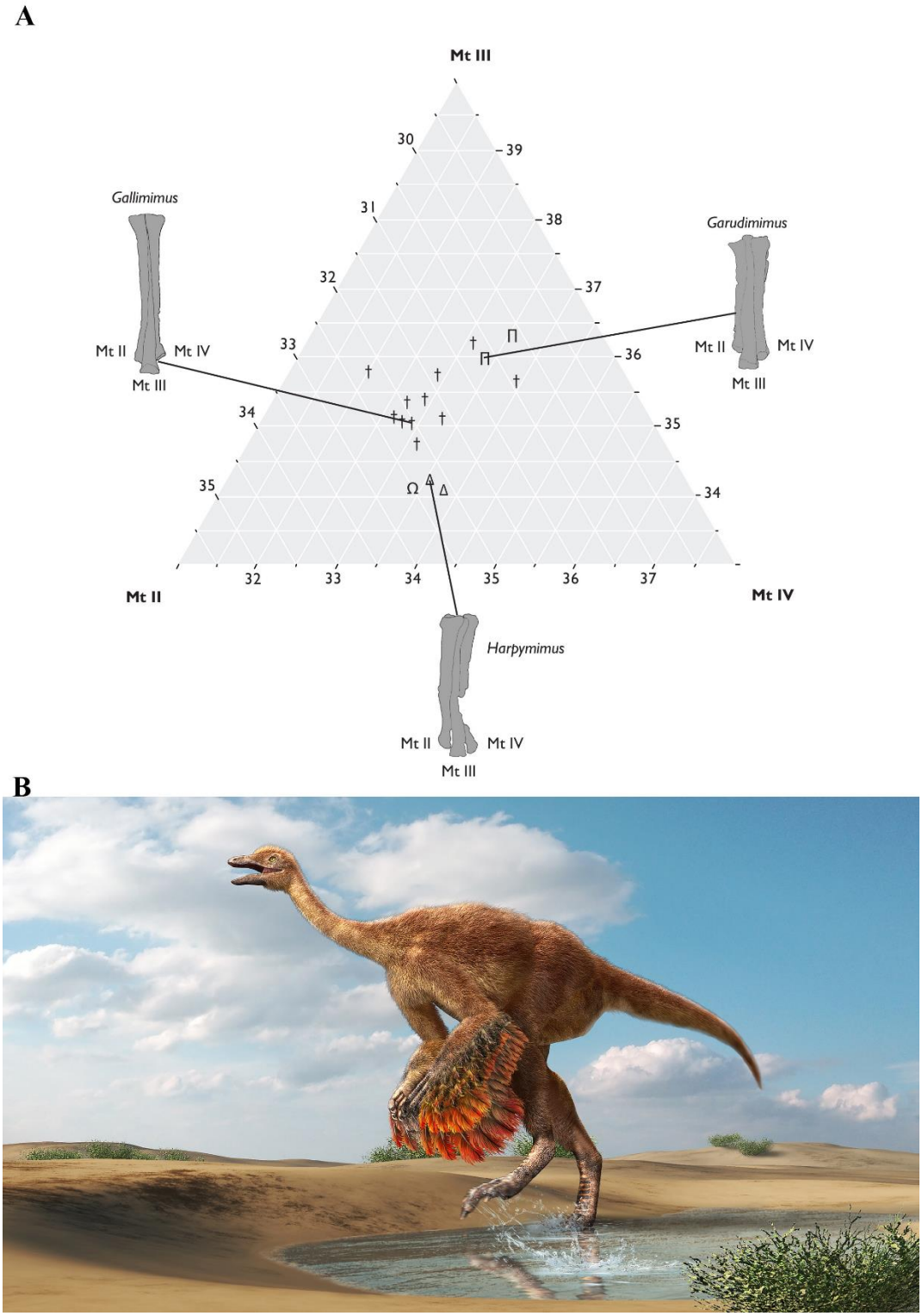

Figure-24. Comparative graph and restoration drawing of *Aepyornithomimus tugrikinensis*. (A), Different proportions of the three metatarsals is represented by ternary diagram (Table-2), (B), Illustration is drawn by Mr. Masato Hattori. *Explanation:* (Ω), *Aepyornithomimus tugrikinensis*, (Δ), basal ornithomimosaurs, (∏), deinocheirids, (†), ornithomimids. *Abbreviations*: see the list of abbreviations on page vi.

Table-2. The ratios of the fourth metatarsal length to the third metatarsal length and the second metatarsal length to the third metatarsal length. *Abbreviations*: see the list of abbreviations on page xvi.

Group	Taxa	Specimen #	Mt II Length	Mt III Length	Mt IV Length	Average of same taxa	Mt II length proportion	Mt III length proportion	Mt IV length proportion
Ornithomimids	*Aepyornithomimus tugrikinensis*	MPC-D 100/130	201	211	207	0.981042654	0.324	0.340	0.334
Ornithomimids	*Anserimimus planinychus*	MPC-D 100/300	270	300	268	0.893333333	0.322	0.357	0.319
Ornithomimids	*Archaeornithomimus asiaticus*	AMNH6565	258	282	262	0.929078014	0.321	0.351	0.326
Deinocheirids	*Deinocheirus mirificus*	MPC-D 100/127	497	600	553	0.921666667	0.301	0.363	0.335
Ornithomimids	*Dromiceiomimus brevitertius*	ROM797	253	298	273	0.916107383	0.307	0.361	0.331
Ornithomimids	*Dromiceiomimus*	ROM852	325	370	340	0.918918919	0.314	0.357	0.328
Ornithomimids	*Gallimimus bullatus*	MPC-D 100/10	144	157	148	0.938194444	0.320	0.350	0.329
Ornithomimids	*Gallimimus bullatus*	MPC-D 100/11	480	530	500				
Ornithomimids	*Gallimimus bullatus*	UALVP cast from Warsaw	435	470	440				
Ornithomimids	*Gallimimus bullatus*	MPC-D 100/52	256	283	263				
Ornithomimids	Ornithomimidae indet.	MPC-D 100/121	273	305	283	0.927868852	0.317	0.354	0.328
Ornithomimids	Ornithomimidae indet.	MPC-D 100/138	458	500	467	0.934	0.321	0.350	0.327
Deinocheirids	*Garudimimus brevipes*	MPC-D 100/13	195	229	212	0.925764192	0.306	0.360	0.333
Basal ornithomimosaurs	*Harpymimus okladnikovi*	MPC-D 100/29	292	310	304	0.980645161	0.322	0.342	0.335
Basal ornithomimosaurs	*Nqwebasaurus thwazi*	AM6040	118	125	124	0.992	0.321	0.340	0.337
Ornithomimids	*Ornithomimus edmontonicus*	ROM851	265	310	295	0.951612903	0.304	0.356	0.339
Ornithomimids	*Rativates evadens*	ROM1790	277	300	285	0.95	0.321	0.348	0.330
Ornithomimids	*Sinornithomimus dongi*	Alashan#3	100	111	105	0.945945946	0.316	0.351	0.332
Ornithomimids	*Struthiomimus altus*	AMNH5257	342	370	352	0.925675676	0.319	0.353	0.326
Ornithomimids	*Struthiomimus altus*	AMNH5339	328	370	333				

In addition, the length from the distal end of Mt III to its medial expansion is scored as 0.163 in *Aepyornithomimus tugrikinensis*, which is the lowest value for any ornithomimosaur taxa. This feature indicates *Aepyornithomimus tugrikinensis* is closer to derived ornithomimosaurs than to basal ornithomimosaurs, which confirms an intermediate step towards an arctometatarsalian condition of Ornithomimosauria as suggested by Currie (Currie, 2000) (Fig. 21E-G, and I, Table-3).

Table-3. The ratios of the length of the third metatarsal and the distal end to the medial expansion of the third metatarsals (in, mm). (Mt III), the third metatarsal length, (DE-ME), the length from the distal end to the medial expansion of the third metatarsal.

Taxa	Mt III (mm)	DE-ME (mm)	Ratio (%)
Harpymimus okladnikovi (MPC-D 100/29)	310	135	0.436
Deinocheirus mirificus (MPC-D 100/127)	600	240	0.4
Garudimimus brevipes (MPC-D 100/13)	229	81	0.354
indet. *Ornithomimius* (MPC-D 100/14)	271	78	0.288
Aepyornithomimus tugrikinensis (MPC-D 100/130)	211	34	0.163

Besides these characters, *Aepyornithomimus tugrikinensis* is differentiated all other ornithomimosaurs by following characters; unevenly developed pair of concavities present at posterior edge of the DT-III of *Aepyornithomimus tugrikinensis*. This morphology is different from any other ornithomimosaurs where posterior edge is either convex or concave (Barsbold, 1988; Kobayashi and Barsbold, 2005a; Claessens and Loewen, 2015; Serrano-Brañas et al., 2016); the proximoventral ridge of II-1 is round, II-3 is relatively larger than the other two unguals, and the pedal unguals are anteroposteriorly more slender and curve slightly downward.

The foot of *Aepyornithomimus tugrikinensis* is also compared with local fauna of the Djadokhta Formation which are persisted the same condition. The foot of *Aepyornithomimus tugrikinensis* is similar to *Avimimus portentosus* and *Kol ghuva* by the “arctometatarsalian” condition, and the subequal length of Mt II and Mt IV (Kurzanov, 1981; Watabe et al., 2006; Turner et al., 2009). However, some characters of both *Avimimus* and *Kol* are differentiated *Aepyornithomimus tugrikinensis*. Whereas a co-ossified tarsometatarsus, a short phalanx II-2 than the phalanx II-1, and the abbreviated phalanges of Digit IV are

characteristics of *Avimimus*, the alvarezsaurids *Kol* is differentiated by following features, such as almost no sign of the Mt III from the posterior view, and a presence of the first digit (Kurzanov, 1981, 1987).

Metatarsals are the most common recovered elements among troodontids from the Djadokhta Formation (Makovicky and Norell, 2004). The condition of the asymmetrical metatarsals of *Gobivenator mongoliensis* (Tsuihiji et al., 2014) is clearly distinguished from any ornithomimids. Whereas the lengths of Mt II and Mt IV of *Aepyornithomimus tugrikinensis* are subequal in length, Mt II of all known troodontids is mediolaterally compressed and markedly shorter than the more robust Mt IV (Wilson and Currie, 1985). The phalanges of Digit II are also highly modified in troodontids (Barsbold and Osmólska, 1990; Currie and Peng, 1993).

CHAPTER IV

A NEW ORNITHOMIMID (THEROPODA, ORNITHOMIMOSAURIA) FROM THE UPPER CRETACEOUS NEMEGT FORMATION OF BÜGIIN TSAV, MONGOLIA

Manuscript Information Sheet

Tsogtbaatar Chinzorig, Yoshitsugu Kobayashi

A new ornithomimid (Theropoda, Ornithomimosauria) from the Upper Cretaceous Nemegt Formation of Bügiin Tsav locality, Mongolia.

Status of Manuscript:

_x_ Prepared for submission to a peer-reviewed journal

___ Officially submitted to a peer-reviewed journal

___ Accepted by a peer-reviewed journal

___ Published in a peer reviewed journal

Published by _____

Contribution of Authors and Co-authors:

Manuscript in Chapter IV

Author: Tsogtbaatar Chinzorig

Contributions: conceived the study, catalogued and process the specimen, performed the analyses, prepared the figures, and wrote the manuscript.

Co-authors: Yoshitsugu Kobayashi

Contributions: provided the useful comments and suggestions and improved to edit earlier drafts of the manuscript.

ABSTRACT

A complete skeleton of an ornithomimid dinosaur, discovered from the Upper Cretaceous Nemegt Formation of Bügiin Tsav locality, southwestern part of the Gobi Desert, Mongolia, is described here. It is assigned to a new genus and species with the following unique features: the combination of features in manual unguals (a sharply recurved ungual I and straight unguals II and III), a hump-like tubercle on manual ungual I, reduced distal condyles of metacarpal I, a pronounced pubic boot anterior extension, and anteroposteriorly flat articular surfaces of anterior caudals. A phylogenetic analysis suggests that this new taxon belongs to the derived ornithomimosaurs and is positioned within the monophyly of the North American ornithomimids (*Ornithomimus edmontonicus*, *Rativates evadens*, and *Struthiomimus altus*), *Anserimimus planinychus*, and *Qiupalong henanensis*. It is the fourth definitive ornithomimosaur from the Nemegt Formation of Mongolia, demonstrating wider diversification in the latest Cretaceous in Asia than previously thought.

Keywords

Ornithomimid, Bügiin Tsav, the Nemegt Formation, manual ungual I, and arctometatarsalian foot.

INTRODUCTION

Ornithomimosauria are group of a medium-sized non-avian theropod dinosaurs characterized by a gracile build and elongated forelimbs and hind limbs (Russell, 1972; Makovicky et al., 2004). Fossil remains of ornithomimosaur dinosaurs have been unearthed from the Early Cretaceous through the Late Cretaceous, ranging from the Berriasian-Valanginian (*Nqwebasaurus thwazi*) to the late Maastrichtian (*Ornithomimus velox*) (Makovicky et al., 2004; Choiniere et al., 2012; Claessens and Loewen, 2015). Within Ornithomimidae, ten genera have been reported from the Late Cretaceous at present, including the North American taxa (*Ornithomimus*, *Rativates*, *Struthiomimus*, and *Tototlmimus*) and Asian taxa (*Aepyornithomimus*, *Anserimimus*, *Archaeornithomimus*, *Gallimimus*, *Qiupalong*, and *Sinornithomimus*) (Xu et al., 2011; McFeeters et al., 2016; Serrano-Brañas et al., 2016; Chinzorig et al., 2017b).

The Upper Cretaceous Nemegt Formation (upper Campanian-lower Maastrichtian) of the Nemegt Basin of Mongolia is one of the most fossiliferous land sediments in Asia (Gradziński, 1970; Osmólska, 1980a; Bronowicz, 2011; Currie, 2016). Skeletal remains of ornithomimid dinosaurs are relatively abundant among other dinosaurs in this formation (Osmólska et al., 1972; Barsbold, 1988; Hurum and Sabath, 2003; Makovicky et al., 2004; Kobayashi and Barsbold, 2006; Bronowicz, 2011; Lee et al., 2014). Since the first ornithomimid materials, which are composed of three nearly complete skeletons, collected by the Polish-Mongolian Palaeontological Expedition and Mongolian Paleontological Expedition between 1965 and 1967, and were described as a new genus and species, *Gallimimus bullatus* (Osmólska et al., 1972). Since then, two more definitive ornithomimosaurs, *Anserimimus planinychus* and *Deinocheirus mirificus*, have been described from the Nemegt Formation up to now and are housed in Institute of Paleontology and Geology, Mongolian Academy of Sciences (Barsbold, 1988; Lee et al., 2014). Although all of these ornithomimosaurs are described from the Nemegt Formation, the phylogenetic relationships of *Anserimimus planinychus* and *Gallimimus bullatus* are belonged to a derived ornithomimosaur clade,

Ornithomimidae, while *Deinocheirus mirificus* is positioned outside of the Ornithomimidae and forms its own clade, called Deinocheiridae.

In the summer of 1995, the Japan-Mongolian Joint Paleontological Expedition (HMNS-MPC) with researchers from the Hayashibara Museum of Natural Sciences (now belongs to Okayama University of Sciences) and the Institute of Paleontology and Geology found a nearly complete articulated ornithomimid skeleton with a skull (MPC-D 100/121) from the Upper Cretaceous Nemegt Formation of Bügiin Tsav, in the northwestern part of the Nemegt Basin, Mongolia, Here we describe this specimen, which provides us a great deal of anatomical information and disparities of ornithomimosaurs and helps us to resolve the interrelationships within ornithomimosaurs for better understandings of the derived ornithomimosaurs evolution.

GEOLOGY

The Bügiin Tsav is one of the fossiliferous localities of Mongolia and is situated in the northwestern region of the Nemegt Basin (Osmólska, 1980a; Currie, 2016) (Fig. 25). The Upper Cretaceous Nemegt Formation is the youngest strata of the Nemegt Basin, which is widely regarded as the Campanian to lower Maastrichtian or Maastrichtian (e.g., (Khand et al., 2000) and conformably overlies the Baruun Goyot Formation (Gradziński et al., 1969, 1977; Jerzykiewicz and Russell, 1991; Eberth, 2018). The Nemegt Formation crops out at this locality (e.g., Gradziński et al., 1977), consisting mainly of a meandering river system deposits (e.g., (Gradziński, 1970; Weishampel et al., 2008).

The rock unit of the Nemegt Formation was firstly studied by the Russian paleontologist Efremov at the type section of the Nemegt locality where is located about 140 km away from Bügiin Tsav in the southeast direction (Gradziński et al., 1977) (Fig. 25). In general, Upper Cretaceous sediments in the whole area of the Nemegt Basin are divided into two sections: the Lower and Upper Nemegt beds based on the differences of lithology and fauna (Gradziński et al., 1969). Recent studies on the Nemegt Formation at Bügiin Tsav classified into two sections (upper and lower) in the exposed outcrop (Eberth, 2018). The middle Nemegt Formation includes grey-to-brown lenticular paleochannel sandstones, alluvial sheet sandstones, and planar laminated red-brown to grey-green mudstones and fine-grained sandstones of paludal and lacustrine origin, whereas the upper Nemegt Formation is 25 m thick and is dominated by coarse-grained, light-grey to-tan colored siltstones, sandstones, and granular beds (Eberth, 2018). Paleoenvironmental zones were suggested by Eberth (2018) for the Nemegt Formation, exposed at four major localities of the Nemegt Basin. At the Bügiin Tsav locality, zones 6 and 7, which are deposited in fluvial to mixed fluvial, lacustrine, or paludal environment, are recognized.

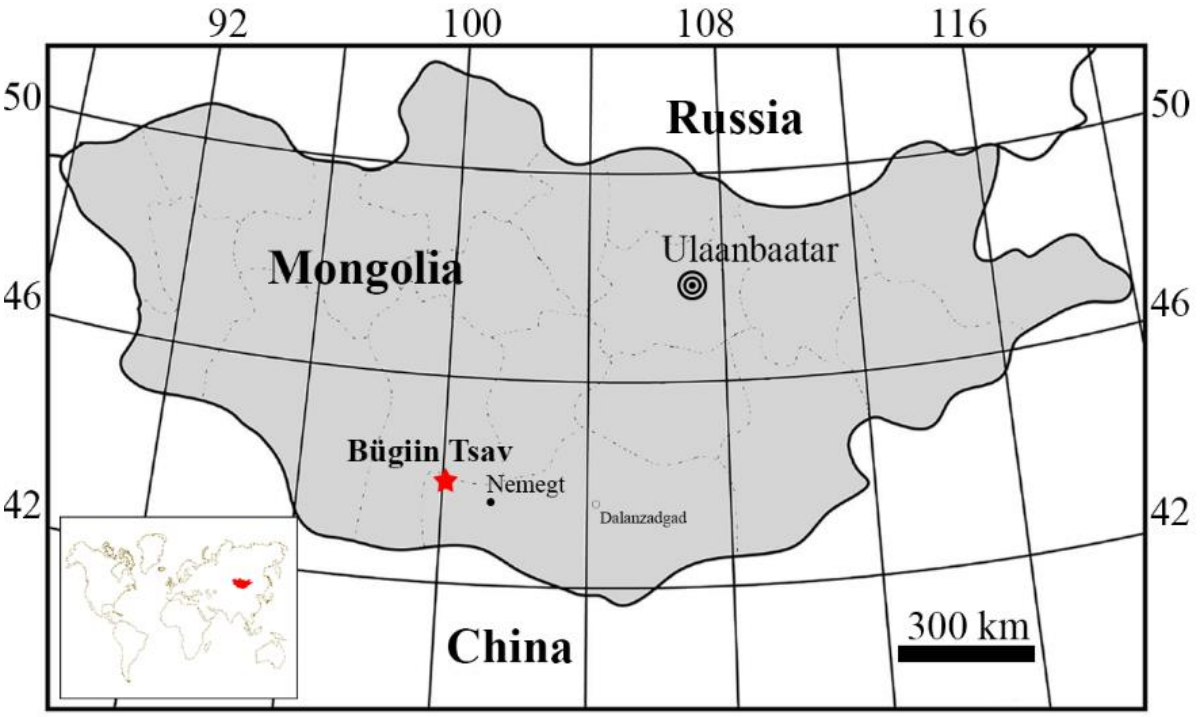

Figure-25. Location map of MPC-D 100/121.

MATERIAL AND METHODS

Materials

MPC-D 100/121 preserves a nearly complete skeleton including a skull (damaged in some elements of braincase and ventral region of the skull due to weathering), a left lower jaw, vertebral column (associated cervical vertebral series, including fragmentary atlas and axis, Cv.4, and the posterior cervicals (Cv.6 to Cv.9)), the dorsal vertebra, including Dv.4, and the posterior articulated dorsal vertebrae (Dv.5 to Dv.12), a complete articulated sacral vertebra (Sv.1-Sv.6) and caudal vertebrae (Ca.1-Ca.35)), dorsal ribs, chevrons, pectoral girdle (only distal scapular blade of left scapula), forelimbs (distal half of both humeri, complete radii and ulnae, and manus), pelvis (all pelvic girdle elements, except anterior iliac blades), and hind limb (both hind limb elements, only missing right metatarsal V and a tip of left metatarsal V).

Methods

In order to resolve the relationships between MPC-D 100/121 and other dinosaurs, we performed a phylogenetic analysis using coelurosaurian taxa with a modified data matrix of Lee et al. (2014), incorporating additions by Sues and Averianov (2016b) and McFeeters et al. (2016) (Supplementary Data-S2A). A matrix of 104 terminal taxa and 568 cranial and postcranial characters was constructed (Supplementary Data-S2B) and analyzed using the software program TNT ver.1.5 (Goloboff et al., 2016). *Herrerasaurus ischigualastensis* was chosen as an outgroup, and the characters were weighted equally followed by 1000 replicate random addition traditional search with TBR (tree bisection and reconnection branch) swapping, holding 10 trees at each replicate. The analysis produced 580 most parsimonious trees with a tree length of 2942 steps, a consistency index of 0.227, and a retention index of 0.616. The strict consensus tree was obtained of 3032 steps with a consistency index of 0.221 and a retention index of 0.601.

In order to obtain alternative relationships of MPC-D 100/121 within other ornithomimosaurs, we performed additional phylogenetic analysis with another data matrix, which consists of 18 terminal taxa and 41 characters with a modification from Kobayashi and Lü (2003), Makovicky et al. (2004), and Serrano-Brañas et al. (2016), (Supplementary Data-S3A). All characters were equally weighted and unordered, and codings follow Serrano-Brańas et al. (2016). Only one outgroup taxon, *Allosaurus fragilis*, was chosen from the original matrix, instead of two outgroup taxa, *Allosaurus* and three tyrannosaurids, and 17 ornithomimosaur taxa were used in this analysis (Supplementary Data-S3B), including six ornithomimosaur taxa (*Aepyornithomimus tugrikinensis, Beishanlong grandis, Deinocheirus mirificus*, *Qiupalong henanensis*, *Rativates evadens*, and *Shenzhousaurus orientalis*). Analysis was performed using the software program TNT ver.1.5 (Goloboff and Catalano, 2016), and run in a new technology search, with a combined analysis of Sectorial Search, Ratchet, Drift, and Tree Fusing.

Systematic Paleontology

Locality and age: Bügiin Tsav locality – Nemegt Formation, Upper Cretaceous, Gobi Desert, Mongolia (Fig. 25).

Diagnosis: An ornithomimid ornithomimosaur with the combination of the following characters: a sharply recurved manual ungual I and straight manual unguals II and III, a hump-like tubercle on manual ungual I, reduced distal condyles of metacarpal I, anteriorly pronounced pubic boot extension, and anteroposteriorly flat articular surfaces of anterior caudals.

DESCRIPTION

Skull

The holotype skull is crushed transversely and is missing the left side of the premaxilla, maxilla, lacrimal, and jugal and the right lower jaw (Fig. 26). All preserved skull elements are somewhat displaced from their original positions, except for the frontals, parietals, and left lower jaw. Some of braincase elements, such as opisthotic, basioccipital, basisphenoid, squamosal, and supraoccipital bones are crushed or not preserved due to erosion. The description of the skull elements is based on the observation of the right side of the skull and the left side of the lower jaw.

Skull openings

The length of the skull is less than half of the length of the cervical series. The orbit is longer than high and is twice as long as the antorbital fenestra. The anterior border of the antorbital fenestra is straight and vertical as in *Garudimimus brevipes*, *Ornithomimus* sp. (TMP 95.110.1), and *Sinornithomimus dongi* (Kobayashi and Lü, 2003; Kobayashi and Barsbold, 2005a).

Premaxilla

The left premaxilla is preserved, missing its anterior tip (Fig. 27). It is long and slender and has the thin and posteriorly narrowing maxillary process. A dorsal edge of the maxillary process contacts the lateral margin of the anterior nasal and terminates posterior to the anterior border of the antorbital fossa, similar to *Garudimimus brevipes* and *Sinornithomimus dongi*, but unlike *Harpymimus okladnikovi* and *Shenzhousaurus orientalis* (Ji et al., 2003; Kobayashi and Lü, 2003; Kobayashi and Barsbold, 2005a, 2005b). Series of small foramina along the ventral edge of the nasal process as known in other ornithomimosaurs.

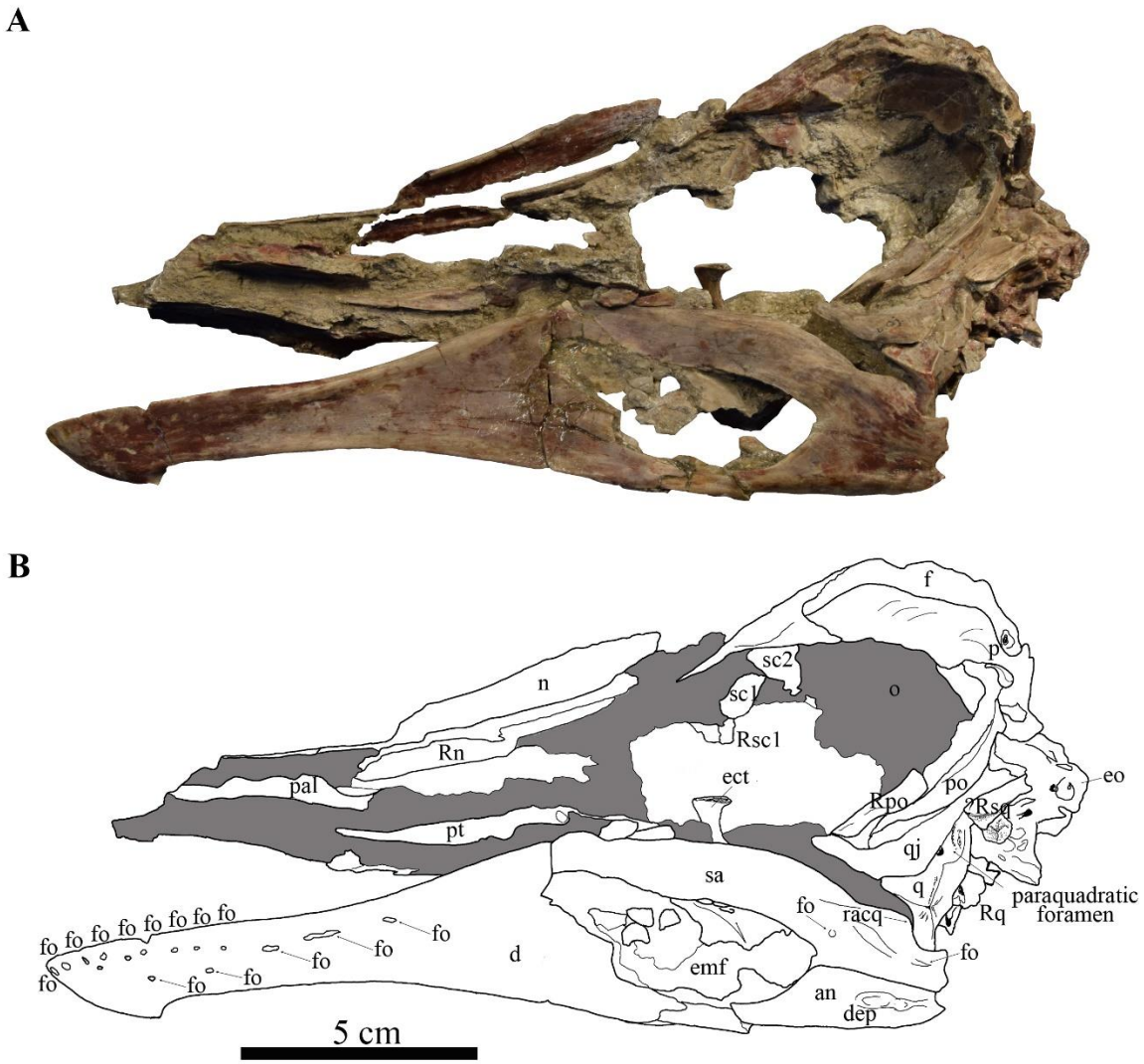

Figure-26. Left lateral view of the skull (MPC-D 100/121). (A), a photo, and (B), drawing with skeletal names. *Abbreviations*: see the list of abbreviations on page vi.

In lateral view, the ventral border of the premaxilla is straight and lacks the ventral expansion, which is also similar feature in *Gallimimus bullatus*, but not in *Harpymimus okladnikovi* or *Garudimimus brevipes* (Kobayashi and Barsbold, 2005a, 2005b). The lateral exposure of the premaxilla-maxilla suture is perpendicular to the ventral border of the upper jaw like *Garudimimus brevipes* and *Sinornithomimus dongi*, but lacking the short posterior process which differs from North American taxa (*Ornithomimus sp.* (TMP 95.110.1) and *Struthiomimus sp.* (TMP 90.26.1)) (Kobayashi and Lü, 2003; Kobayashi and Barsbold, 2005a).

Maxilla

The maxilla has a broad dorsal process and a long ventral process (Fig 27). The dorsal border of the dorsal process contacts the ventral edge of the premaxilla anteriorly and the lateroventral edge of the nasal posteriorly. The ventral process widens posteriorly and meets the anterior tip of the jugal. There are a few foramina around a midpoint of the main body posterior to the premaxilla-maxillary suture along the ventral margin of the maxilla, which differs from *Gallimimus bullatus* and *Sinornithomimus dongi* (Kobayashi and Lü, 2003; Kobayashi and Barsbold, 2005a). Within the antorbital fossa, there is one accessory fenestra, the maxillary fenestra, which is different from *Garudimimus brevipes* and *Sinornithomimus dongi* (Kobayashi and Lü, 2003; Kobayashi and Barsbold, 2005a). The convex ventral margin of the main body of the maxilla expands anteroventrally as strong as in *Gallimimus bullatus* and *Sinornithomimus dongi*. This expansion may meets the dorsomedially directed dorsal margin of the dentary to form a cutting edge as in *Sinornithomimus dongi*.

Nasal

Both nasals are incomplete (Fig. 28A). The posterior ends of the nasals are well-preserved, whereas the anterior half of the left nasal and the anterior tip of the right nasal are missing. The nasal is anteroposteriorly long and transversely narrow as in most of ornithomimosaurs (Makovicky et al., 2004).

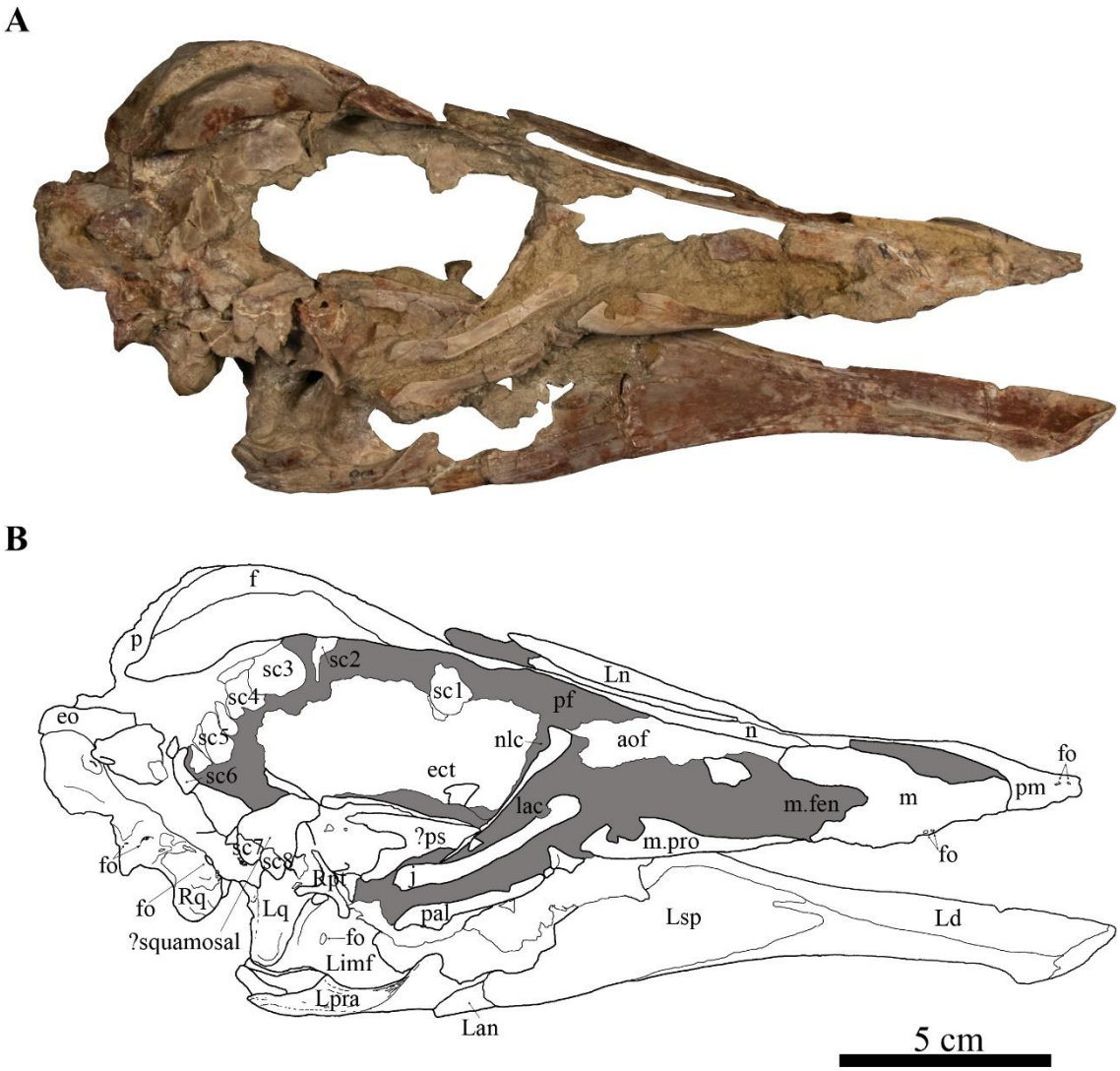

Figure-27. Right lateral view of the skull (MPC-D 100/121). (A), a photo, and (B), drawing with skeletal names. *Abbreviations*: see the list of abbreviations on page vi.

It broadens posteriorly, with the maximum breadth at the level of the anterior edge of the lacrimal and narrows lateromedially towards the contact with the anterior margin of the frontal as seen in *Garudimimus brevipes*. The posterior end of the nasal lies the posterior end of the prefrontal as in *Harpymimus okladnikovi* and *Struthiomimus altus*. The nasals contact each other along a straight sagittal suture. The dorsal surface of the nasal has foramina along outer margin of the main body as in other ornithomimosaurs (Russell, 1972; Makovicky et al., 2004).

Frontal

The frontals are well-preserved and intact bones (Figs. 26-28). In dorsal view, the frontals are triangular-shaped as in other ornithomimosaurs (Makovicky et al., 2004). The anteroposterior length of the frontal is greater than its maximum width close to the posterior edge along the frontal-parietal suture (Table-4). The planar anterior end of the frontals is sloped anteriorly to insinuate the posterior ends of the nasals. Posteriorly, the frontals form a dome on each side separated by a midline depression like *Gallimimus bullatus* and *Sinornithomimus dongi*, but unlike *Garudimimus brevipes* which has a single dome (Osmólska et al., 1972; Kobayashi and Lü, 2003; Kobayashi and Barsbold, 2005a). The lateral slope of the dome abruptly down right behind the frontal whereas this slope is more gently in *Sinornithomimus dongi* and forms part of the anterior portion of the supratemporal fossa (Kobayashi and Lü, 2003).

Postorbital

Both left and right postorbitals are complete (Fig. 26). The postorbital is dorsoventrally elongate and nearly straight, differing from other ornithomimosaur postorbitals with an anterodorsally curvature of the element (Makovicky et al., 2004). The dorsal end is slightly expanded anteroposteriorly unlike *Garudimimus brevipes*. Ventrally, it narrows more anteriorly. which resembles to *Sinornithomimus dongi* and *Struthiomimus altus*, but unlike *Gallimimus bullatus* which has a dorsoventrally short postorbital (Osmólska et al., 1972; Russell, 1972; Kobayashi and Lü, 2003).

Parietal

The parietals are poorly preserved on the posterior portion of the skull table (Fig. 28A). Based on the preserved part of the right parietal, it is anteroposteriorly small as compare to the frontal length, unlike *Sinornithomimus dongi* with the anteroposteriorly elongated parietal (Kobayashi and Lü, 2003).

Lacrimal

Only the right lacrimal is faintly preserved at between the orbit and the antorbital fossa (Fig 27). It is a thin bone with long anterior and ventral processes and a short posterior process as in *Sinornithomimus dongi*. The ventral process narrows and is insinuated beneath the ventral side of the parasphenoid.

Jugal

The right jugal is well-preserved (Fig 27). The jugal is anteroposteriorly long with slightly expanded and rounded anterior and posterior ends unlike that of *Sinornithomimus dongi* with a pointed end anteriorly. The anterior end of the jugal is not bifurcated for its contacts with the maxilla and lacrimal as in *Sinornithomimus dongi*, but unlike *Struthiomimus* sp. (TMP 90.26.1) and *Ornithomimus* sp. (TMP 95.110.1). In addition, its posterior end is not bifurcated unlike *Garudimimus brevipes*, which has two anteriorly projecting processes (Kobayashi and Barsbold, 2005a). Along with the shaft of the jugal, there is a shallow depression extending parallel to the dorsal and ventral edges.

Quadratojugal

The left quadratojugal is well-preserved than other side and is positioned at the lateral side of the accessory condyle of the quadrate (Fig. 26). The quadratojugal is stout and L-shaped with dorsal and anterior processes as in most ornithomimosaurs (Makovicky et al., 2004), but unlike *Gallimimus bullatus* (Osmólska et al., 1972). The dorsal process is much longer than the anterior process and is not bifurcated at the tip. The ventral half of the process forms gradual concave anterior border for the posteroventral corner of the infratemporal fenestra. The posteroventral border of the element ends by a thin lamina and forms a square corner.

Quadrate

The quadrate is slender dorsally and tapers ventrally. It is slightly twisted at its shaft in posterior view (Figs. 26, and 29). The presence of the quadrate fossa is not clear. Ventrally, the lateral and medial mandibular condyles is separated by a weak sulcus. The medial mandibular condyle is more pronounced

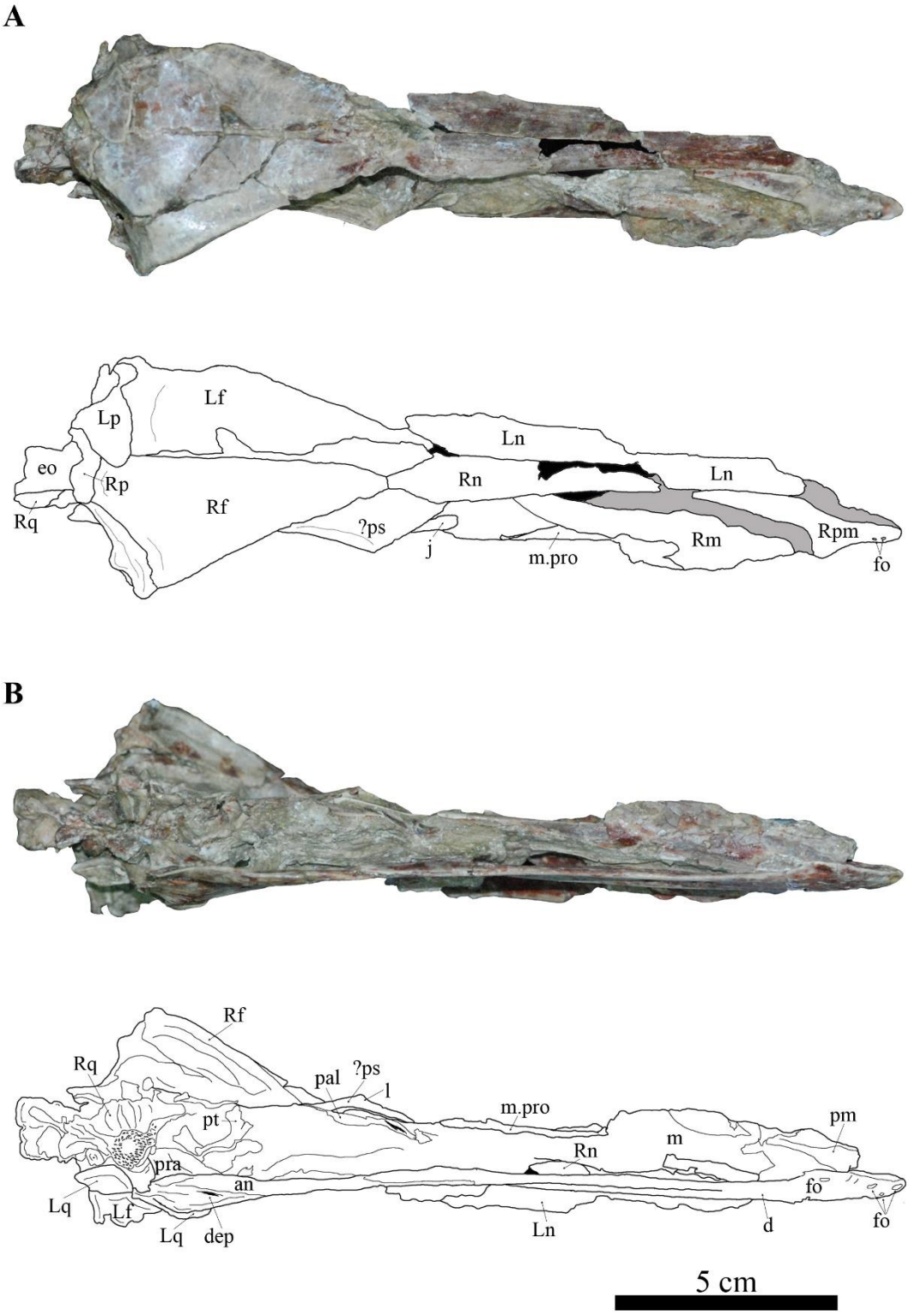

Figure-28. Dorsal (A), and ventral (B) views of the skull (MPC-D 100/121).
Abbreviations: see the list of abbreviations on page vi.

Table-4. Measurements (in mm) of the skull and the lower jaw of MPC-D 100/121.

Skeletal elements	Specified measured areas	Measurements
Skull	anteroposterior length from the occipital condyle to the premaxilla	235.1+
	length between the quadrate and the premaxilla	200.56+
	width between the left and right frontals	62.43+
	total height between the uppermost and lowermost extremity, including the mandible	104.37
Frontal (right)	maximum length anteroposteriorly	78.18
	maximum width transversely between orbital slots	34.95
Quadrate (left)	height	48.26
	maximum width of the distal condyles transversely	12.25
Quadratojugal (left)	length along the anterior process	27.82
Postorbital (left)	total length anteroposteriorly	43.78
Jugal (right)	total length anteroposteriorly	44.36
Orbit (right)	total length anteroposteriorly	73.11
	total height dorsoventrally	34.15
Scleral ring, #sc1	total length/width (right)	9.88/12.38
Scleral ring, #sc2	total length/width (left)	11.44/9.87
Scleral ring, #sc3	total length/width (right)	13.57/10.01
Scleral ring, #sc4	total length/width (right)	11.47/11.30
Scleral ring, #sc5	total length/width (right)	7.11+/10.21
Scleral ring, #sc6	total length/width (right)	7.57+/8.45
Antorbital fenestra (right)	total length anteroposteriorly	35.26
	total height dorsoventrally	11.44
Naris (left)	total length anteroposteriorly	117.94
Maxilla (right)	total length	93.69+
Mandible (left)	total length between the anterior end of the dentary and the posterior surangular	199.83
	maximum height	40.82
Dentary (left)	total length	144.54
	maximum height	35.66
Surangular (left)	total length	88.96
	maximum height	14.38
Angular (left)	total length	61.36
	maximum height	13.41
External mandibular fenestra (left)	total length	60.65
	maximum height	20.21

than the lateral condyle in the posterior view, unlike the equally sized mandibular condyles of *Garudimimus brevipes* (Kobayashi and Barsbold, 2005a). Lateral to the lateral condyle there is an accessory condyle and is more dorsally positioned than the mandibular condyles. As shown in *Sinornithomimus dongi*, the accessory condyle is contoured to the dorsally expanded region of the

surangular. Moreover, there is another accessory condyle is located on the dorsal to the medial condyle, which is unique to this taxon. In posterior view, there is a slight concavity for the paraquadratic foramen as in other ornithomimosaurs.

Parasphenoid

The laterally flattened parasphenoid is exposed in the right lateral side of the skull (Fig. 27). It has the bulbous structure as in ornithomimosaurs and troodontids. It is wide posteriorly and has anterior parasphenoid rostrum as in *Gallimimus bullatus*, *Garudimimus brevipes*, and *Sinornithomimus dongi* (Osmólska et al., 1972; Kobayashi and Lü, 2003; Kobayashi and Barsbold, 2005a). In lateral view, the dorsal edge of this element is straight, and its ventral edge becomes convex anteriorly as in *Gallimimus bullatus*, *Garudimimus brevipes*, and two other troodontids (*Saurornithoides* and *Troodon*).
It has a horizontal dorsal edge at the same level as the dorsal border of the bulbous portion as seen in *Sinornithomimus dongi* (Kobayashi and Lü, 2003). The anterior process narrows gradually as in *Garudimimus brevipes* and *Gallimimus bullatus* as well as those reported troodontids, *Saurornithoides* and *Troodon*, but unlike *Sinornithomimus dongi* (Osmólska et al., 1972; Currie, 1985; Kobayashi and Barsbold, 2005a).

Palatine, pterygoid, ectopterygoid, and sclerotic ring

The left pterygoid is anteroposteriorly elongate and is positioned parallel to the ventral side of palatine (Fig. 26). The vomeral process of the palatine is thinner than the maxillary process unlike *Garudimimus brevipes* (Kobayashi and Barsbold, 2005a). It has a deep groove at the posterior half of the ventral portion, extending to the posterior end. The right pterygoid is preserved as attached to the posteroventral portion of the parasphenoid (Fig. 27) and has equally developed three processes, forming triradiate bone like *Gallimimus bullatus* and *Garudimimus brevipes* (Osmólska et al., 1972; Kobayashi and Barsbold, 2005a). The ectopterygoid is a hook-like bone, positioned next to the surangular. The dorsal edge of the element is broadened anteroposteriorly, and its dorsal extremity is flat in lateral view. It has no

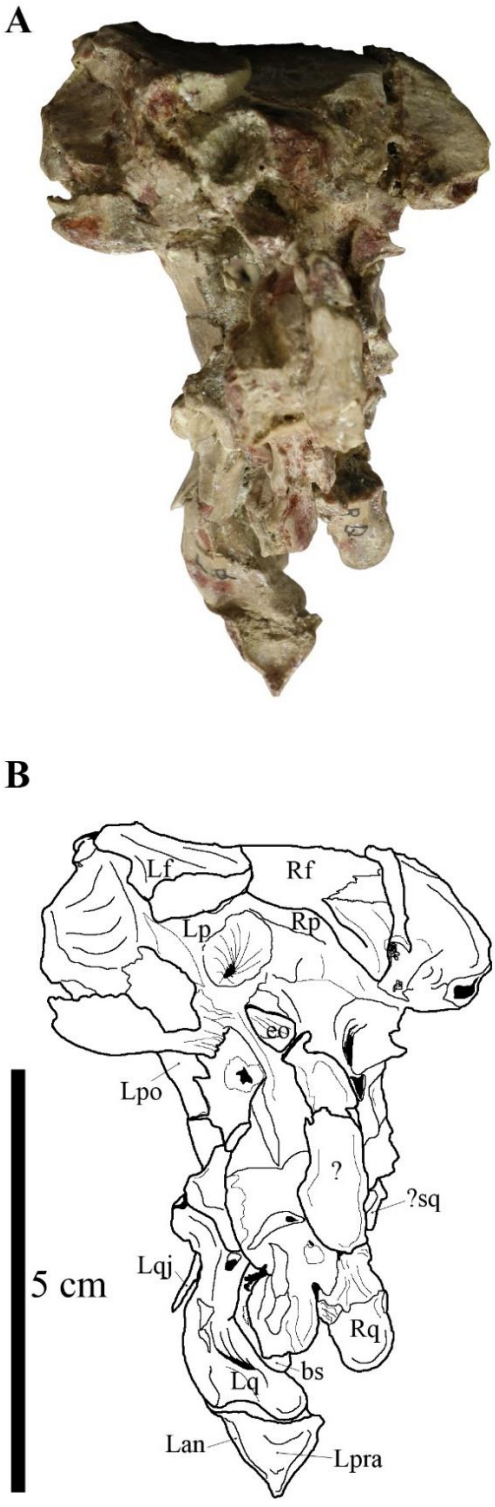

Figure-29. Posterior view of the skull (MPC-D 100/121). (A), a photo, and (B), drawing with skeletal names. *Abbreviations*: see the list of abbreviations on page vi.

contact with the lacrimal like *Garudimimus brevipes* but unlike *Oviraptor* (Elzanowski, 1999). Both sides of the skull preserve articulated scleral plates (Fig. 26 and 27). The right scleral plates are much complete than the left scleral plates and preserves 8 scleral plates. The diameters of the circle inside and outside of the scleral ring is 49 mm and 72.1 mm, respectively. The breadth of each well-preserved scleral plate is roughly 11 mm.

Mandible

Although only left lower jaw is preserved, it is one of the well-preserved skull elements without any crush and deformation (Figs. 26 and 27). In general, the mandible is a delicate structure and consists of very thin bones. Moreover, it is slender and shallow anteriorly, but its posterior portion is more than twice deeper than its anterior height. The rostrum is not as broad as that in *Gallimimus bullatus*. The ratio of mandible maximum height to its length is 0.2, which is the highest among ornithomimosaurs (e.g. *Ornithomimus edmontonicus* (TMP 95.110.1), (0.120), *Ornithomimus edmontonicus* (ROM 851), (0.132), *Struthiomimus altus* (TMP 90.26.1), (0.139), *Garudimimus brevipes* (MPC-D 100/13), (0.146), *Harpymimus okladnikovi* (MPC-D 100/29), (0.153), *Deinocheirus mirificus* (MPC-D 100/127), (0.171), and *Gallimimus bullatus* (MPC-D 100/11) (0.18)).

Dentary

The edentulous dentary is complete and well-preserved (Fig. 26). The dentary is the longest of the mandibular elements, and its length is more than four times longer its greatest height. The anterior part of the dentary has a straight edge and does not show a ventral deflection unlike *Garudimimus brevipes* and *Gallimimus bullatus*, but resembles to those in *Sinornithomimus dongi* and some North American taxa, including *Struthiomimus* sp. (TMP 90.26.1) (Russell, 1972; Kobayashi and Lü, 2003; Kobayashi and Barsbold, 2005a). The dorsal border of the dentary is sharp for "cutting-edge" in the anterior two-thirds of the element and is rounded in the posterior third which is similar to *Sinornithomimus dongi*. A series of foramina is present on the lateral surface of the dentary along the ventrally reflected region and symphysis

like other ornithomimosaurs such as *Pelecanimimus polyodon*, *Ornithomimus edmontonicus* (TMP 95.110.1), and *Struthiomimus* sp. (TMP 90.26.1), but unlike *Sinornithomimus dongi* (Kobayashi and Lü, 2003). The medial surface has a Meckelian groove, which is covered by the splenial posteriorly. This groove narrows anteriorly and extends farther anteriorly as in *Garudimimus brevipes* but differs from *Gallimimus bullatus*. As seen in *Gallimimus bullatus* and *Garudimimus brevipes*, the medial surface of the dentary forms a shovel-like shelf dorsal to the symphysis. The dentary has three posterior processes, which are two at the posterodorsal and posteroventral corners of the dentary and the third at the anterior edge of the external mandibular fenestra. The posterodorsal process is short and fits onto the lateral side of the surangular as in *Struthiomimus* sp. (TMP 90.26.1). The dentary-surangular suture is bifurcated but less distinct than *Garudimimus brevipes* with a W-shaped suture. The ventral process at the posterior end extends more posterior than the dorsal process and laterally overlaps the anterior process of the angular with a W-shaped suture. The contact is positioned middle of the external mandibular fenestra; in contrast, the contact in *Sinornithomimus dongi* is rostral to the middle of the fenestra, that in *Struthiomimus* sp. (TMP 90.26.1) is posterior to the mid-length of the fenestra (Kobayashi and Barsbold, 2005a). The ratio of the anteroposterior length of the fenestra to total mandibular length is 0.300, which is the largest in ornithomimosaurs (*Ornithomimus* sp. (TMP 95.110.1) 0.125, *Harpymimus okladnikovi* 0.127, *Garudimimus brevipes* 0.176, and *Sinornithomimus dongi* 0.146). The anteroposterior length is nearly twice as long as its maximum height. The process at the anterior edge of the external mandibular fenestra is dorsoventrally taller than that of *Garudimimus brevipes* (Kobayashi and Barsbold, 2005a).

Splenial

The splenial covers the entire Meckelian groove and extends medially almost posterior half of the dentary (Fig. 27). The anterior tip of the element is bifurcated and forms the upper and lower processes. The lower process is more pronounced than the upper one and is positioned more anteriorly, unlike *Garudimimus brevipes* whose upper process is more pronounced than the lower one. Its deepest level

reaches at the posterior end of the cutting edge of the mandible and gradual narrows anteriorly. The posterior edge of the element is slightly concave and tilted anteriorly in medial view.

Surangular

The surangular is the second longest mandibular element, and its total length is longer than half of the dentary length (Fig. 26). The dorsal process of the element is convex in lateral view and has an anteroposteriorly oriented ridge anterior to the retroarticular process for the reception of the accessory condyle of the quadrate. There are two surangular foramina exist on the lateral surface. The positions of the surangular foramina are different from other ornithomimosaurs, where are pronounced these foramina. Both foramina is located on the posterior half of the surangular, differing from *Garudimimus brevipes* which has only one anteriorly positioned foramen. The posterior surangular foramen is also represented in *Harpymimus okladnikovi* (Kobayashi and Barsbold, 2005b). The suture with the angular originates at the posterior end of the mandibular fenestra and extends to the posterior end of the retroarticular process as in *Garudimimus brevipes*, *Ornithomimus* sp. (TMP 95.110.1), *Sinornithomimus dongi*, and *Struthiomimus* sp. (TMP 90.26.1). There is a minute excavation formed at just above the suture of the mandibular fenestra unlike other ornithomimosaurs. The retroarticular process in the mandible is as strong as *Gallimimus bullatus* (Osmólska et al., 1972). The surangular participates in only the anterior half of the lateral surface of the retroarticular process, which points slightly upward at its posterior tip as in *Garudimimus brevipes*, *Ornithomimus* sp. (TMP 95.110.1), and *Struthiomimus* sp. (TMP 90.26.1). The contact surface with the articular has posteriorly projected two process.

Angular

The angular is half length of the surangular and borders posteroventral of the external mandibular fenestra by a concave edge (Figs. 26 and 27). The contact with the surangular is straight as in *Gallimimus bullatus* and *Garudimimus brevipes*, but unlike *Struthiomimus* sp. (TMP 90.26.1). The anterior process is long and contacts the posteroventral process of the dentary. In lateroventral side of the angular, there is an

anteroposteriorly extending deep groove at half-way to the posterior edge, in which may be unique feature of this taxon. The posterior end of the angular contacts with the articular by upward projecting process.

Prearticular

The prearticular is long anteroposteriorly, but is much shorter than that of *Gallimimus bullatus* (Hurum, 2001) (Fig. 27). The anterior end of the element bends upward and lies posteroventral border of the external mandibular fenestra. A strong ridge along the medial surface extends from the anterior tip of the element to the posterior end ventrally.

Postcranial skeleton

Vertebral column

The vertebral column in MPC-D 100/121 preserving of 56 vertebrae, including 7 cervicals, 8 dorsals, 6 sacrals, and 35 caudals (Figs. 30, 31, 33, and 34). Nearly all vertebral series are exposed in the specimen except some of the cervicals and the anterior dorsals. Vertebral centra are platycoelus, except amphiplatyan in the anterior first to sixth caudals. The neural arches are not fused to the centra except the cervicals and posterior caudals as in *Gallimimus bullatus* (Osmólska et al., 1972).

Cervical vertebrae

Seven cervical vertebrae are preserved, missing the third, fifth, and tenth cervicals in the cervical series. The prezygapophyses of all postaxial cervicals extend anteriorly further than the anterior surface of the centrum and have slightly convex articular surfaces. The centra of the postaxial cervicals are longer than high and elongated anteroposteriorly from the ninth cervical. The anterior ends of the centra are flattened dorsoventrally, while the posterior ends are flattened laterally like *Gallimimus bullatus*. In addition, the centra are platycoelous with the posterior articular surfaces are more concave than the anterior ones. As in other ornithomimosaurs, the epipophyses are faintly developed as insignificant elevations on all cervicals.

The anterior portion of the left and right atlas (Figs. 30A-a, and 30A-c) and the anterior half of the axis (Fig. 30B) are preserved. The atlas and axis are long and wide as in *Gallimimus bullatus* (Osmólska et al., 1972) (Fig. 30).

The fourth cervical vertebra has long and slender prezygapophyses, but a short and transversely broad postzygapophyses in dorsal view (Fig. 30). The articular surfaces of pre- and postzygapophyses are rounded, and postzygapophyses are larger than prezygapophyses. The postzygapophyses do not reach beyond the posterior edges of the centrum as seen in *Gallimimus bullatus*. The anteroposterior length of each neural arch is much longer than that of the axis and becomes longer posteriorly (Table-5).

The neural spines are positioned about the center of the neural arch unlike *Sinornithomimus dongi*, but are similar to *Gallimimus bullatus* and *Ornithomimus* sp. (TMP 95.110.1) (Osmólska et al., 1972). The neural spines are low, rounded dorsally and a rod-like in lateral view. In dorsal view, the posterior border of the neural arch is straight in the fourth and sixth cervicals because of a lamina, connecting postzygapophyses as in *Sinornithomimus dongi*. The concave anterior and posterior intervertebral articular surfaces of the fourth cervical are exposed and are strongly inclined anterodorsally and anteroventrally respectively. The ventral surface of the centrum is slightly concave in lateral view, and the anterior end is transversely wider than its posterior end for the reception of the cervical rib.

The posterior cervical vertebra (from sixth to nine) are distinguished from the anterior cervical vertebra in having long and slender postzygapophyses that are reached to far onto succeeding vertebra (Fig. 30). Comparing to the anterior cervical vertebra, the neural spines form long, low and flat sharp ridges and are positioned at the center above the centrum. In general, the zygapophyses are X-shaped in dorsal view. The posterior edge of the diapophysis has a strong excavation in posterior cervicals. The bases of the postzygapophyses extends posterolaterally, and the articular surfaces are directed laterally as in *Gallimimus bullatus*, *Ornithomimus* sp. (TMP 95.110.1), and *Sinornithomimus dongi*, but unlike *Harpymimus okladnikovi* (where they are almost parallel) (Kobayashi and Lü, 2003; Kobayashi and Barsbold, 2005b). The articular surfaces of the prezygapophyses and postzygapophyses are equally developed and are

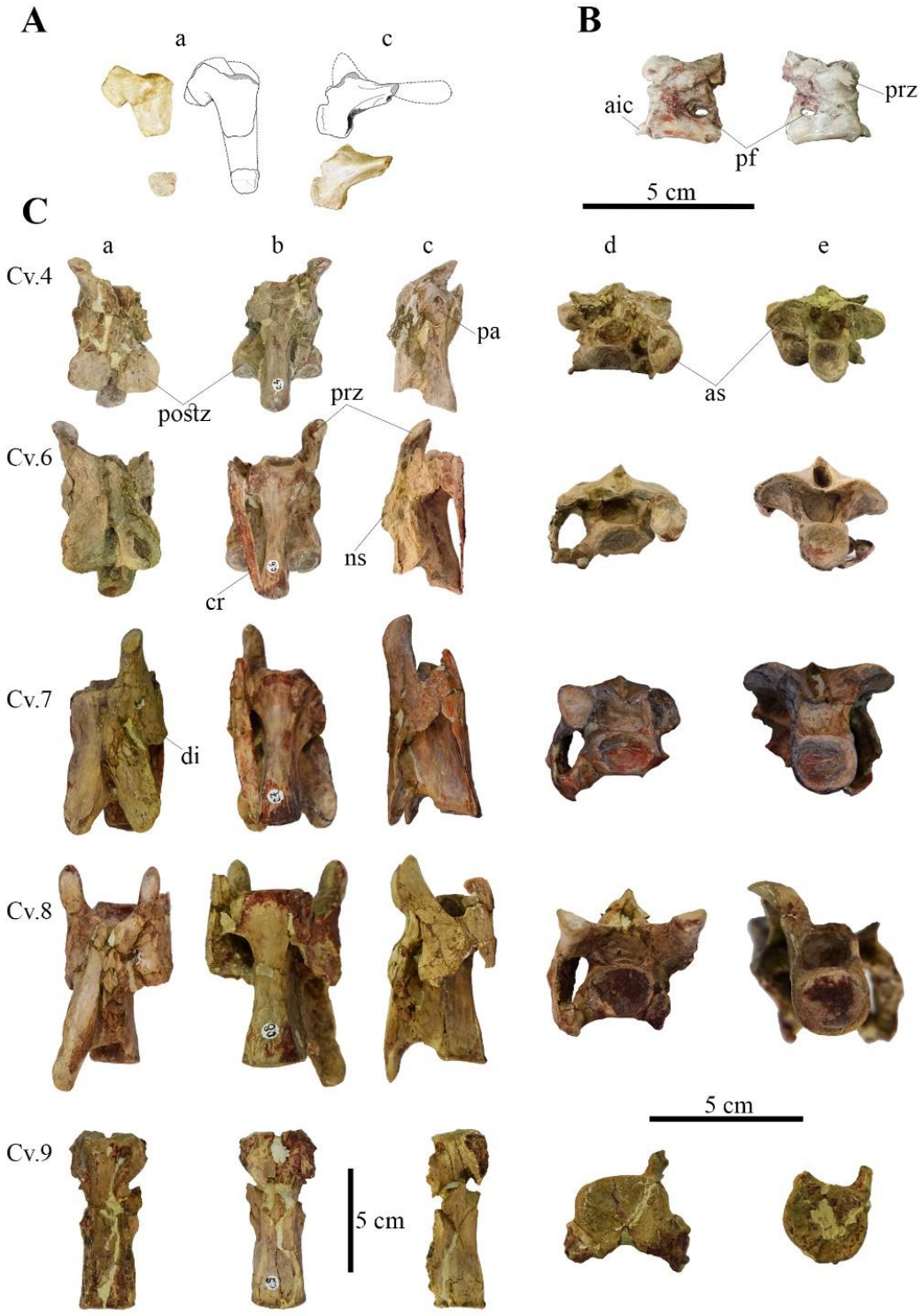

Figure-30. Cervical vertebrae of MPC-D 100/121. (A), atlas, (B), axis, and (C), cervical vertebrae. Explanation: (a), dorsal, (b), ventral, (c), right lateral, (d), anterior, and (e), posterior views. *Abbreviations*: see the list of abbreviations on page vi.

oval-shaped more posterior cervicals, where the sixth and seventh cervicals have rounded prezygapophyseal articulations and transversely wide postzygapophyseal articulations. The posterior cervicals have spool-shaped centra. The articular surfaces of the centra of the sixth and seventh cervicals are inclined anterodorsally and anteroventrally, while the corresponding regions of the eighth and ninth cervicals are nearly perpendicular to the main axes of the centra in lateral view like *Gallimimus bullatus*. The lateral side of the seventh cervical vertebra has a central pneumatic fossa on the center region of the centrum shaft while this fossa is exhibited in the eight cervical vertebra of *Sinornithomimus dongi*. Strong ridges are extended both sides of the eighth and ninth cervicals lateroventrally.

Dorsal vertebrae

Eight dorsal vertebrae are consecutively preserved in the specimen, except the anteriormost four dorsals (Fig. 31). The neurocentral sutures are visible and are not completely fused, suggesting that the animal was not fully matured at the time of death. Neural spines are preserved in nearly all dorsals, except those of the sixth and eight ones. The dorsal edges of the neural spines are straight, and the posterodorsal corner of the neural spine tips are slightly widened posteriorly in lateral view unlike *Gallimimus bullatus* (Osmólska et al., 1972). The distinct interspinous ligament scars developed at the posterior tip of the posterior dorsals like the twelfth dorsal of *Garudimimus brevipes*, in which forms a deep, narrow groove along the neural spine (Kobayashi and Barsbold, 2005a). All neural spines become progressively taller in more posterior dorsals as in other ornithomimosaurs (Table-5). In lateral view, all neural spines are slightly inclined posteriorly, except the twelfth dorsal in which it forms straight in the main axes. The posterior edges of the neural spines of all dorsals form curved margins, specifically eleventh and twelfth dorsals are strongly excavated in lateral view unlike *Gallimimus bullatus* and *Garudimimus brevipes*. The anterior and posterior sides of each neural spine bears a strong hyposphene-hypantrum articulations. The prezygapophyses and postzygapophyses are short and have circular articular surfaces like other ornithomimosaurs. They are positioned nearly horizontally. The transverse processes of all dorsals are

gradually lifted posteriorly. They are also angled posteriorly up to the ninth dorsal, but they become close to perpendicular to the sagittal plane from the tenth to twelfth dorsals as in other ornithomimosaurs.

Table-5. Measurements (in mm) of the vertebral column of MPC-D 100/121. Note: (-), missing part of the element; (?), measuring part is existed, but impossible to measure due to hidden location in the specimen, (+), existed element, but incomplete.

No.	Centrum length	Centrum height (anterior)	Centrum width (anterior)	Centrum height (posterior)	Centrum width (posterior)	Neural spine height	Neural spine tip length (ant-post.)
Cv.4	48	6.90	13	9.50	9	-	-
Cv.6	58	6.50	15.50	11	12	-	-
Cv.7	66	8.50	17.50	18.50	15.50	-	-
Cv.8	71	11.50	18.50	14.50	17.10	-	-
Cv.9	75.50	13+	20.50	18.50	20	-	-
Dv.5	-	-	-	28.60	23.18+	30.88	19.31
Dv.6	51.90	34.17	24.55	33.36	27.55+	31.40	23.51
Dv.7	52.69	34.25	27.15	36.21	28.80	38.08	24.95
Dv.8	-	37.46	29.21	38.97	33.82	-	-
Dv.9	57.91	40.41	32.97	44.04	39.09	-	-
Dv.10	58.49	48	32	49.37	36.16	47.45	35.01
Dv.11	59.89	48.26	36.27	47.73	39.92	51.25	33.15
Dv.12	60.54	48.40	39.33	45.69	43.98	60.54	35.11
Sv.1	66.51	46.41	43.76	38.36	47.50	75.16	-
Sv.2	68.25	37.41	46.97	?	?	?	?
Sv.3	70.23	?	?	?	?	?	?
Sv.4	77.01	?	?	?	?	?	?
Sv.5	79.16	?	?	?	40.37	?	?
Sv.6	81.04	?	37.59	48.19	43.69	?	58.67
Ca.1	65.30	51.16	43.58	47.38	39.43	67.17	21.62
Ca.2	56.11	49.09	41.62	44.31	38.60	59.39	24.86
Ca.3	55.27	46.26	39.43	39.75	35.78	55.62	25.44
Ca.4	52.82	41.13	36.02	38.81	32.88	52.11	24.73
Ca.5	52.23	37.52	33.04	34.73	30.51	46.85	24.16
Ca.6	52.37	34.92	31.10	32.93	28.93	43.09	22.19
Ca.7	50.32	32.69	29.54	30.10	28.02	38.90	21.52
Ca.8	49.01	30.38	28.38	29.66	26.80	36.99	24.08
Ca.9	48.67	29.17	27.34	28.03	26.19	32.46	27.03
Ca.10	47.96	27.57	26.38	27.48	25.07	29.54	26.54
Ca.11	48.54	26.50	25.23	25.28	25.74	27.08	31.09
Ca.12	48.99	26.16	25.92	24.22	26.63	27.80	32.23
Ca.13	50.71	24.06	27.28	22.75	28.40	31.82	24.11+
Ca.14	49.26	22.27	28.71	21.49	29.37	26.53	38.63
Ca.15	53.40	20.57	30.09	20.12	30.91	19.38	42.49
Ca.16	51.83	19.82	30.79	-	30.31	-	43.91
Ca.17	56.33	-	29.80	-	28.81	-	44.65

Ca.18	57.17	-	29.43	-	27.16	-	48.97
Ca.19	60.15	-	26.03	-	25.35	-	48.64
Ca.20	60.52	-	25.12	-	23.36	-	52.30
Ca.21	60.98	-	22.79	-	21.86	-	51.62
Ca.22	59.57	-	21.48	-	19.88	-	-
Ca.23	58.76	-	20.45	-	17.85	-	-
Ca.24	55.76	-	17.45	-	16.95	-	-
Ca.25	51.44	-	16.29	-	15.46	-	-
Ca.26	46.31	-	14.88	-	14.60	-	-
Ca.27	41.73	10.68	13.84	9.15	13.95	7.86	27.01
Ca.28	36.96	10.22	12.97	9.28	12.39	-	-
Ca.29	20.87+	8.69	10.74	-	-	-	-
Ca.30	28.88	7.79	9.84	8.28	9.70	-	-
Ca.31	25.84	8.70	9.51	7.16	8.55	5.98	-
Ca.32	22.94	7.78	8.59	6.25	7.81	5.66	-
Ca.33	20.21	6.78	7.86	6.19	6.97	-	-
Ca.34	17.93	5.85	6.58	4.64	5.47	4.13	-
Ca.35	15.66	5.02	5.44	3.97	4.51	-	-

The centra of the dorsal vertebrae are spool-shaped and become long and tall posteriorly (Table-5). The intervertebral articular surfaces are oval (higher than wide) and amphicoelous and are perpendicular to the main axes of the centrum like *Garudimimus brevipes* (Kobayashi and Barsbold, 2005a). The parapophyses are oval in lateral view. They are developed at the anteroventral transverse process and higher than the neurocentral suture of the both lateral sides. The pleurocoels are extensive, but shallow as in *Gallimimus bullatus* (Osmólska et al., 1972). On the ventral surface of the fifth dorsal centrum, there is no any median keel preserved or faintly preserved, in which is differentiated from *Harpymimus okladnikovi* (in the first five dorsals), *Shenzhousaurus orientalis* (in fifth dorsal vertebra), and *Garudimimus brevipes* (in the fourth and fifth dorsal vertebrae) (Ji et al., 2003; Kobayashi and Barsbold, 2005a, 2005b). The ventral surface of the centrum from the sixth to ninth dorsals is flat, while the remaining dorsals have rounded ventral surfaces. The posteroventral surfaces of the sixth to ninth dorsal centra have a paired weak prominences as in *Ornithomimus* sp. (TMP 93.62.1) (Makovicky, 1995). The infraprezygapophyseal, infradiapophyseal, and infrapostzygapophyseal fossae are evenly divided by laminae, however the infraprediapophyseal lamina is weaker than the postzygapophyseal lamina and become weak in posterior dorsal vertebrae as in

Garudimimus brevipes and *Sinornithomimus dongi* (Kobayashi and Lü, 2003; Kobayashi and Barsbold, 2005a).

Sacral vertebrae

Sacrum is composed of six vertebrae which are progressively longer posteriorly and are tightly attached to the ilia (Fig. 32; Table-5). A number of the sacral vertebrae is as same as other ornithomimosaurs, *Gallimimus bullatus*, *Garudimimus brevipes* and *Sinornithomimus dongi* (Osmólska et al., 1972; Kobayashi and Lü, 2003). The centra of the vertebrae are spool-shaped and ventrally flattened. The contacts between the first and second as well as the third and fourth sacral vertebral centra are fused, but other intervertebral articular surfaces remain unfused, similar to *Sinornithomimus dongi* (Kobayashi and Lü, 2003).

The first and last sacrals have similar articular surfaces of *Gallimimus bullatus* in which are formed a rectangular surface for the first sacral, and a round for the last sacral. The second and third sacrals are positioned between the pubic and ischiac peduncles like *Gallimimus bullatus*, but unlike *Garudimimus brevipes* (they are positioned between the third and fourth sacrals). The neural spines of the first to fifth sacrals are fused to form a single thin plate which ends the posterodorsally inclined neural spine. The last sacral has a dorsally around neural spine, similar to the last sacral of *Gallimimus bullatus*. Although the anterior dorsal half of the plate is fairly seen above the upper margin of the iliac blade in lateral view, the posterior half is more exposed together with the neural spine of last sacral. There is a strong ridge at the posteroventral ridge of the last sacrals. The transverse processes of the sacrals are heavily damaged.

Caudal vertebrae

A number of caudal vertebrae varies within ornithomimosaurs, for instance, *Gallimimus bullatus* (ZPal.No.Mg.D-I/1) with 36 caudals and the holotype specimen of *Gallimimus bullatus* (MPC-D 100/11) with 38-39 caudals. The caudal vertebrae with 35 caudal vertebrae in this specimen are articulated

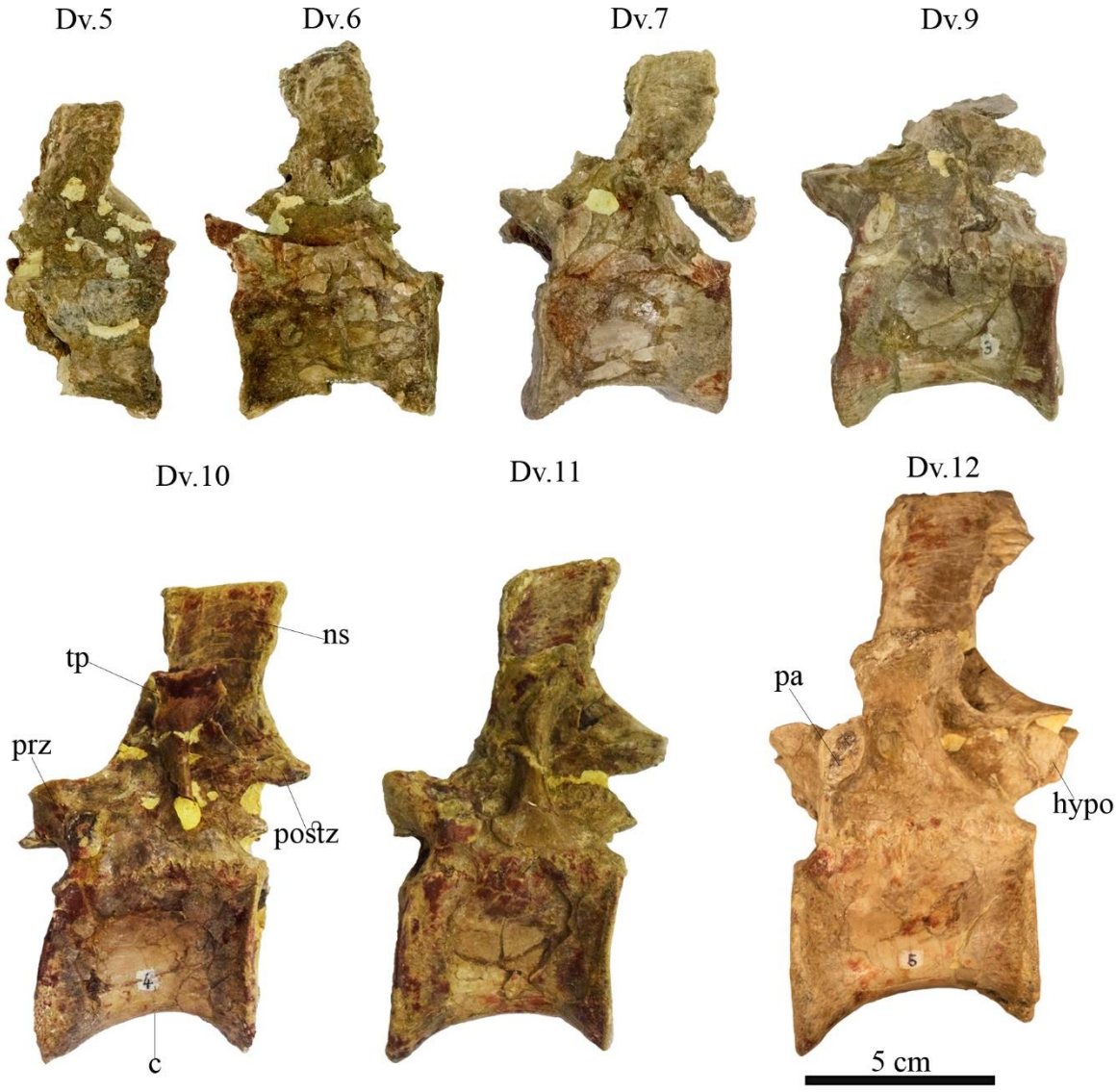

Figure-31. Dorsal vertebrae of MPC-D 100/121 in left lateral view. *Abbreviations*: see the list of abbreviations on page vi.

and the most complete in the vertebral series (Figs. 33-35). The neural spine is the tallest at the first caudal vertebra become progressively shortened posteriorly. From the 18th caudal, caudals form as horizontal striations at the anterior and posterior edges of the centrum for the attachment of the ligaments but these striations diminish posteriorly. The main axis of the neural spines are tilted, whereas posterior ones are positioned in perpendicular to its centrum. The anterior and the posterior edges of the neural spines are

grooved as in *Garudimimus brevipes*. As known in *Garudimimus brevipes*, two depressions, separated by a thin lamina, are present at the bases of the neural spine and transverse process of the first caudal. The anterior depression is triangular-shaped and is deeper than the posterior one. In the more posterior caudals, these depressions become weak and diminished. The prezygapophyses and the postzygapophysis are short and their articular surfaces are slightly angled from the horizontal. A shape of the zygapophyses is circular in the anterior caudals. From the caudal 10 or 11, the prezygapophyses become longer and they are reached a half the length of centrum of the proceeding caudal at the behind the transition point, and then they are extended to three-quarters of the preceding centrum. The postzygapophyses are generally short along the whole length of the tail and being thin and spine-like in the posterior caudals. The transverse processes of the anterior caudals are long and slightly directed posteriorly. The transition point between anterior and posterior caudals occurs between caudal 15 and caudal 16 as in *Gallimimus bullatus*.

The anterior caudals persist neurocentral sutures, whereas the posterior caudals are diminished. The anterior five or six caudals are amphiplatyan (both articular surfaces are flat), while rest of the caudals are procoelic (both articular sides are concave). The centra are taller than wide. The lateral surfaces of the centra lack pneumatic feature. Centra of the anterior caudals are subcircular while they become distinctly subrectangular and transversely elongated from the caudal 13 before the transition point unlike *Gallimimus bullatus*. The articular facets for the chevrons are situated on the edges of all centra, except the anterior edge of the first caudal.

Chevrons

Twenty-five chevrons are preserved. The anterior chevrons are Y-shaped, whereas the posterior chevrons are boat shaped in lateral view as in *Gallimimus bullatus*. The first chevron is positioned at the first caudal. The anterior chevrons are anteroposteriorly narrow and bent gently posteriorly. From the 14th and 15th chevron, the chevrons become anteroposteriorly elongate and are tightly adhered to the centra.

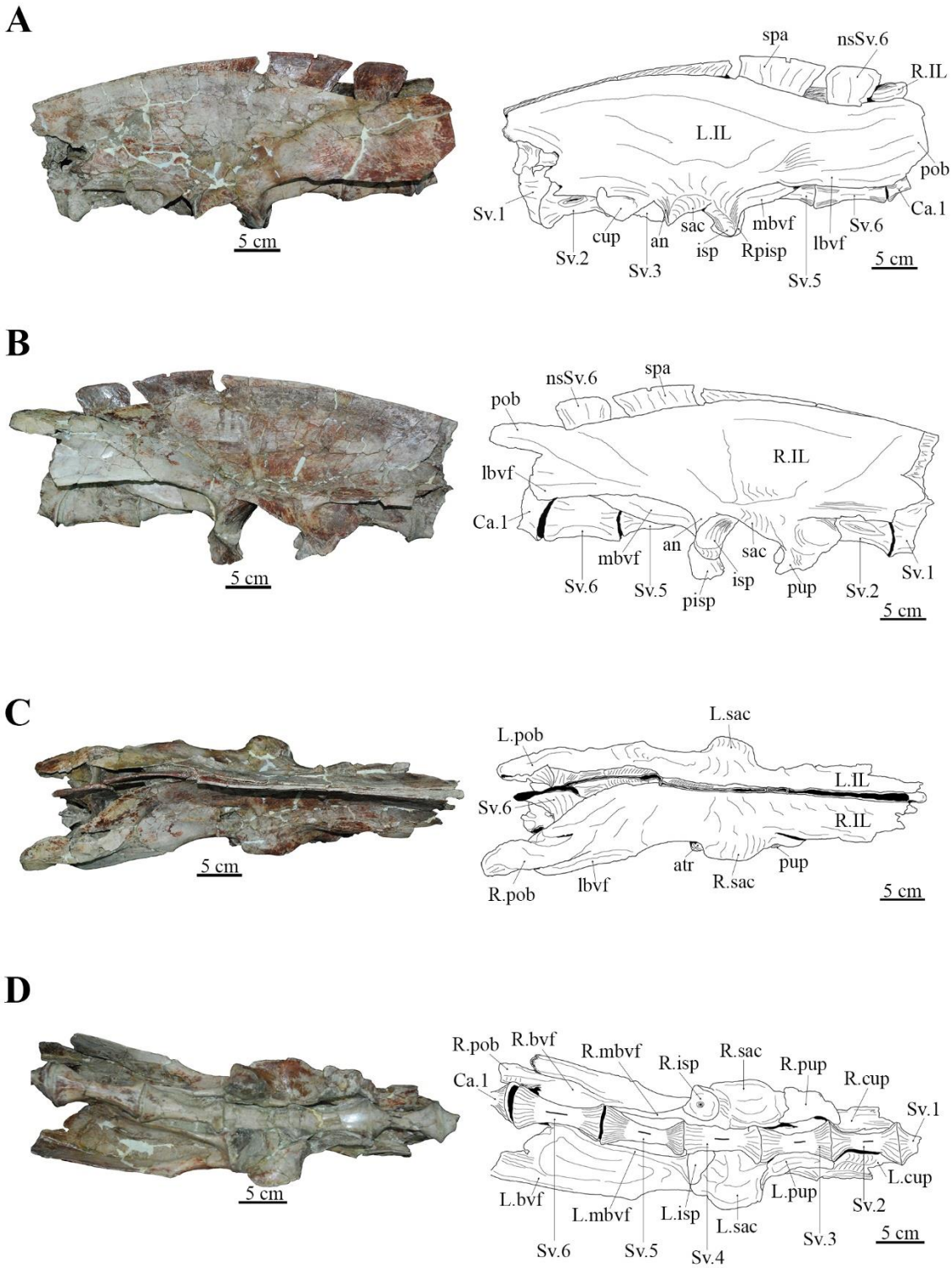

Figure-32. Ilia with sacral vertebrae of MPC-D 100/121. *Explanation:* left lateral (A), right lateral (B), dorsal (C), and ventral (D). *Abbreviations*: see the list of abbreviations on page vi.

Dorsal ribs

Some of the posterior cervical ribs are preserved with articulation with the cervicals (Fig. 30 C-b and c). The shafts of the cervical ribs are slender and slightly rounded in cross-section. The anterior end of the rib is located more anteriorly than the anterior articular surface of the centrum while the posterior end is about the same level of the posterior edge of the centrum.

Left and right dorsal ribs are inconstantly preserved in the specimen (Fig. 36). The dorsal ribs expose broad and flat dorsal ends with a widely spaced the capitulum and tuberculum, separated each other by a shallow notch. As in other ornithomimosaurs, the capitulum becomes strong, and the tuberculum become weak posteriorly. The shafts of the dorsal ribs gradually curve gently posteriorly. There are sharp rib flanges, extending anterior and posterior sides of the dorsal half. The posterior flange of the anteriormost dorsal ribs is more pronounced than those of the posterior ones. The distal ends of the ribs are slightly widened anteroposteriorly and abruptly ended. None of the pectoral girdle elements are preserved in the specimen, except the distal half of the left scapular blade, attach to one of the dorsal rib (Fig. 37A). The distal blade of the scapula is thin and slightly curved downward posteriorly in lateral view.

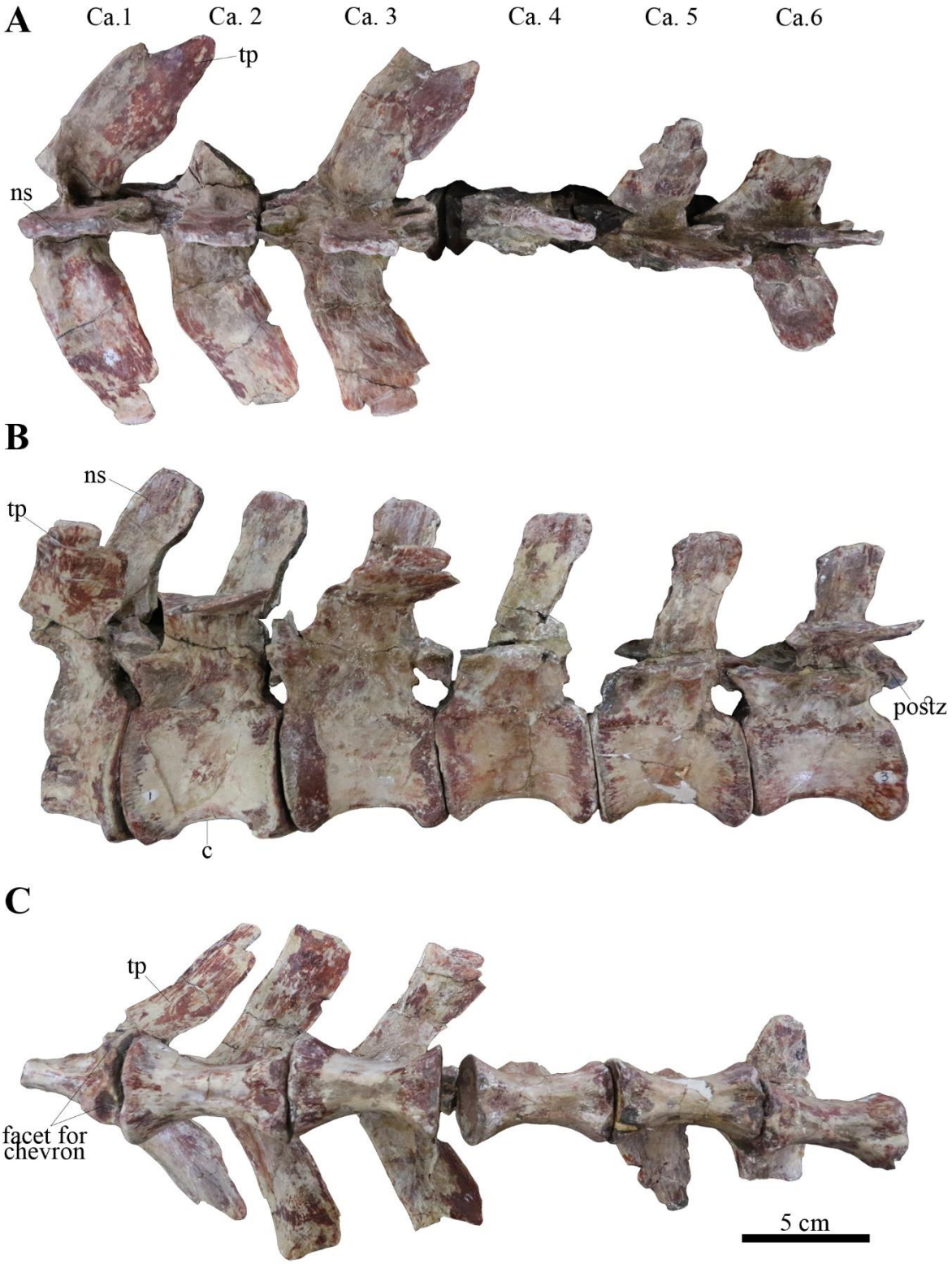

Figure-33. Anterior caudal vertebrae (Ca.1 – Ca.6) of MPC-D 100/121. *Explanation:* dorsal (A), left lateral (B), and ventral (C). *Abbreviations*: see the list of abbreviations on page vi.

Forelimbs

Humerus

Only distal half of the left and right humeri are preserved (Fig. 37B). The ulnar condyle is larger than the radiale condyle like *Sinornithomimus dongi* and *Struthiomimus altus* (UCMZ (VP) 1980.1), but unlike *Gallimimus bullatus* (Osmólska et al., 1972; Nicholls and Russell, 1985; Kobayashi and Lü, 2003). An entepicondyle is present at the lateral to the ulnar condyle, which is as strong as *Anserimimus planinychus*, but differs from that in *Sinornithomimus dongi* where it is weakly developed (Barsbold, 1988; Kobayashi and Lü, 2003).

Ulna and radius

Both radii and ulnae are complete (Fig. 38). The radius is positioned on the ventral side of the ulna proximally and is slightly shorter than the ulna (Table-3). The proximal half of the ulna is weakly curved towards the radius. The olecranon process is prominent and forms bowl-shape laterally. The shaft is subtriangular in cross-section. The distal ulna is flattened into a slight transverse expansion with the crescent shape. The distal condyles are more pronounced than *Sinornithomimus dongi*. The radius is straighter than the ulna except for the slightly medially curved proximal end and is thinner than the ulna. The anterior surface of the shaft of the radius is somewhat flattened. The articular surface of the proximal end of the radius is suboval and slight concave in proximal view. The distal articular surface is flattened anteroposteriorly. A short ridge extends upwards along the lateral edge of the distal end like *Gallimimus bullatus*. Likewise *Gallimimus bullatus*, the anterolateral edge of the distal end is developed in the form of a short, longitudinal ridge (Osmólska et al., 1972).

Manus

The manus is tridactyl with all digits are subequal in length. The total length of the manus along metacarpal II and digit II is 294 mm, which is longer than the ulna unlike in *Gallimimus bullatus*, but is the

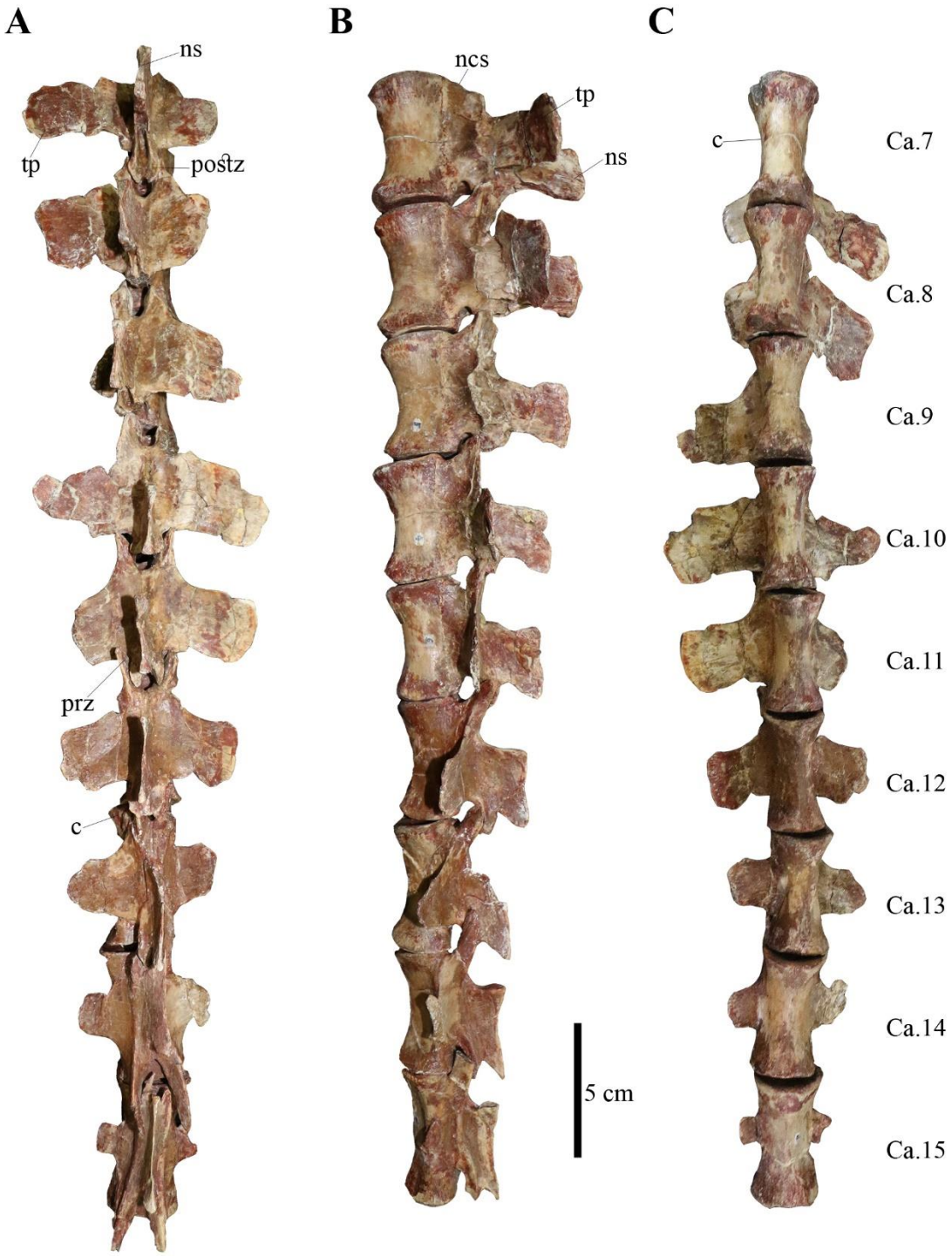

Figure-34. Anterior caudal vertebrae (Ca.7 – Ca.15) of MPC-D 100/121. *Explanation:* dorsal (A), left lateral (B), and ventral (C). *Abbreviations*: see the list of abbreviations on page vi.

same ratio as *Harpymimus okladnikovi* and *Sinornithomimus dongi* (Osmólska et al., 1972; Kobayashi and Lü, 2003; Kobayashi and Barsbold, 2005b).

Carpals

Three elements of the carpals, intermedium, distal carpals two and three, are preserved (Figs. 38 and 39). Proximally, there is one round bone is preserved on the distal end of the ulna. By judging this bone's identification, this bone is thought to be the Based on the position and shape, the intermedium is similar to that *Struthiomimus altus* and *Sinornithomimus dongi* (Nicholls and Russell, 1985; Kobayashi and Lü, 2003). The distal carpals two and three are attached to the proximal surfaces of mainly third metacarpals and some on the second metacarpal (Fig. 15A, B, and D). The arrangement and shape of the first and second distal carpals are similar to that described in *Harpymimus okladnikovi*, but the first carpal is relatively smaller than in *Harpymimus okladnikovi* (Kobayashi and Barsbold, 2005b).

Metacarpals

Metacarpals are weakly arched transversely, being strongly adherent each other proximally, but diverging slightly distally (Fig. 39). The ratio of metacarpals I, II, and III is 0.95:1:0.96 (Table-6), and this is a derived condition among ornithomimosaurs in having subequal metacarpals by Kobayashi and Lü (2003). Metacarpal II attaches along two thirds of the lateral edge of metacarpal I, and its distal third is slightly deviated from metacarpal II like *Gallimimus bullatus*, but unlike *Sinornithomimus dongi* (Osmólska et al., 1972; Kobayashi and Lü, 2003; Chinzorig et al., 2018). The surface of the attachment is concave (Osmólska et al., 1972; Chinzorig et al., 2018). The distal articular surfaces are ball-shaped, constituting ball and socket articulation between the metacarpal and the first manual phalanx, which is characteristic to Ornithomimidae (Kobayashi and Lü, 2003).

The shaft of metacarpal I is broad transversely and triangular in cross-section as in most ornithomimosaurs. The proximal articular surface is smooth, flat, and triangular, having a dorsal apex,

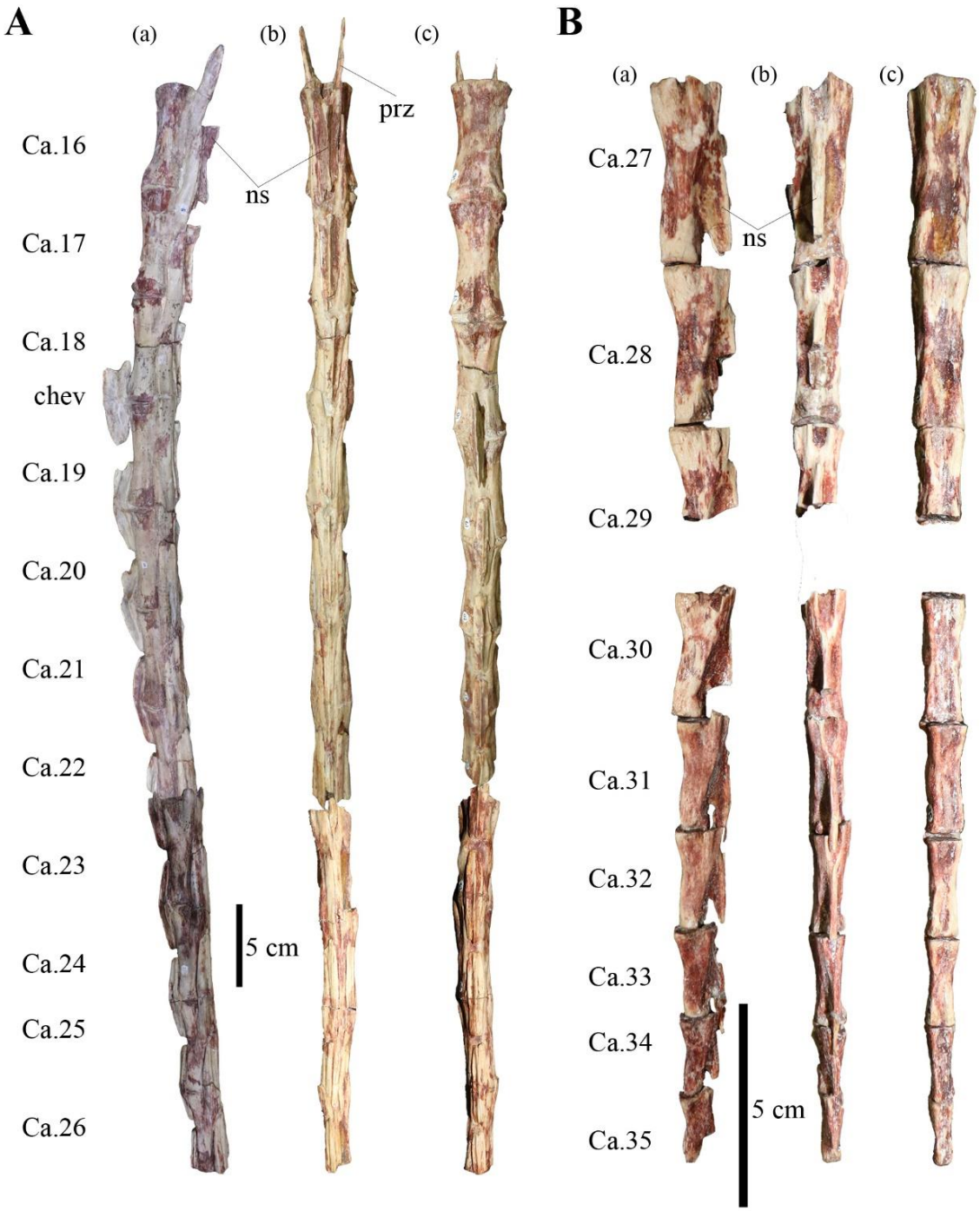

Figure-35. Posterior caudal vertebrae (Ca.16 – Ca.35) of MPC-D 100/121. *Explanation:* (A), Ca.16 – Ca.26, (B), Ca.27 – Ca.35, and (a), left lateral, (b), dorsal, and (c), ventral. *Abbreviations*: see the list of abbreviations on page vi.

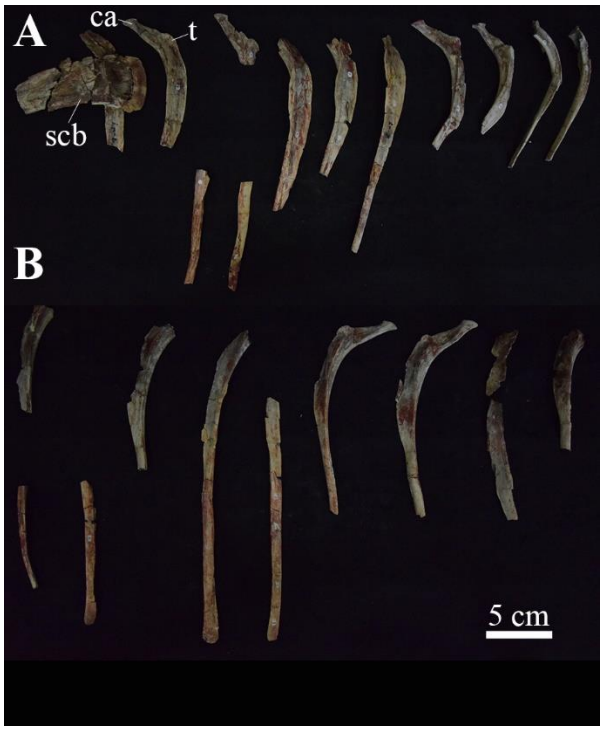

Figure-36. Left (A) and right (B) dorsal ribs of MPC-D 100/121 in lateral view. *Abbreviations*: see the list of abbreviations on page vi.

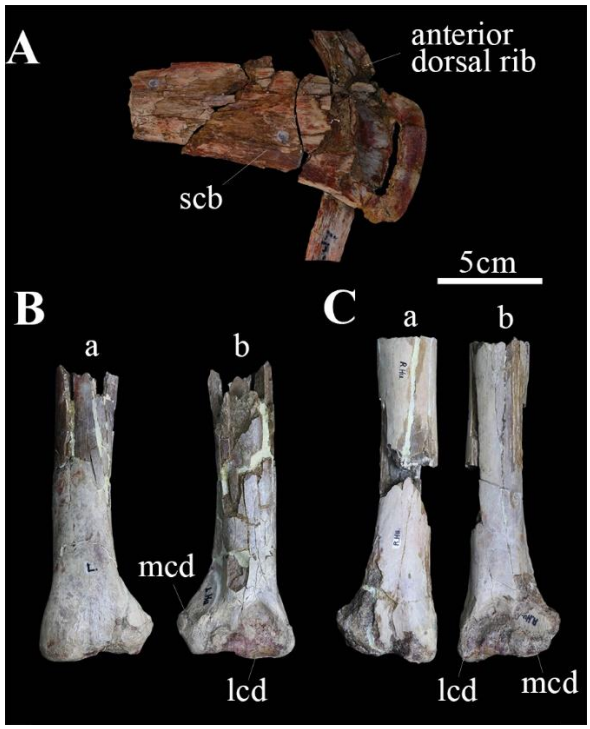

Figure-37. Partial left scapula (A) in lateral, and distal ends of the left (B) and right (C) humeri of MPC-D 100/121. *Explanation:* dorsal (a), and ventral (b) views. *Abbreviations*: see the list of abbreviations on page vi.

while the distal articular surface is asymmetric, differing from *Gallimimus bullatus* with a subrectangular articular surface.

The lateral and medial condyles are equally developed in distal view (Chinzorig et al., 2018). The intercondylar groove is much deeper than remaining two metacarpals as in most ornithomimosaurs. The lateral fovea ligamentosa is much stronger than the medial one like *Gallimimus bullatus*. Metacarpal II adheres closely to metacarpal III along the lateral side, differing from *Gallimimus bullatus*, which has a space between metacarpal II and III along its shaft (Osmólska et al., 1972). The shaft of metacarpal II is dorsoventrally flattened and subrectangular in cross-section. The distal articular surface is symmetrical. The lateral fovea ligamentosa is larger than the medial one, but the medial is much deeper than the lateral one. Metacarpal III is the most slender in the metacarpus. Its proximal end is triangular, and the shaft is straight and circular in cross-section as in other ornithomimosaurs.

Figure-38. Right ulna and radius of MPC-D 100/121. *Abbreviations*: see the list of abbreviations on page vi.

The distal articular surface is strongly pressed lateromedially. The condyles are equally developed, but they are much slender than metacarpal II condyles in distal view. The lateral and medial edges of the distal articular surface are notched as in *Anserimimus planinychus*, but unlike *Gallimimus bullatus* and *Deinocheirus mirificus* (Chinzorig et al., 2018).

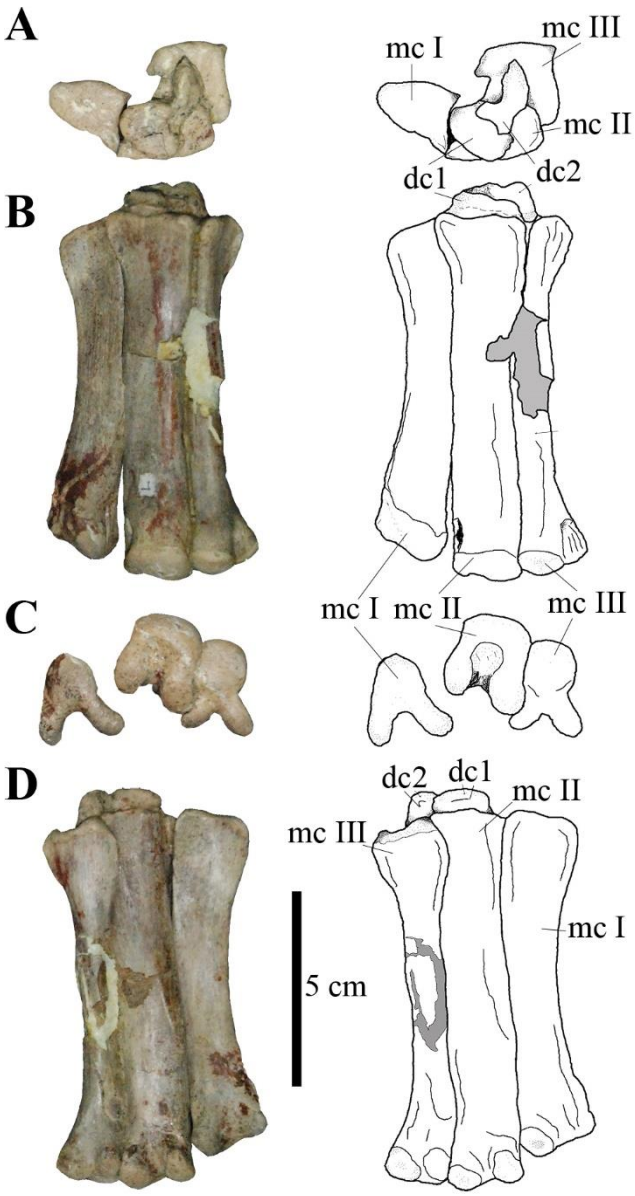

Figure-39. Left metacarpals of MPC-D 100/121.
Explanation: (A), proximal, (B), anterior, (C), distal, and (D), posterior. *Abbreviations*: see the list of abbreviations on page vi.

Digits

All manual elements of both sides are well-preserved except tips of some unguals (Fig. 40). Manual phalangeal formula is 2-3-4-0-0. The first digit is strongly divergent medially, while digit III is somewhat divergent laterally, relation to the articular surfaces of the first and third metacarpals like *Gallimimus bullatus*. The proximal articular surfaces of all first phalanges are concave and no ridge is

formed, whereas all remaining phalanges are somewhat ridged distinctly and the dorsal processes are more pronounced with a ginglymoid articulation. In lateral view, the proximal articular surfaces of these phalanges are vertically straight, whereas remaining phalanges are curved lateromedially and can be seen their sagittal ridge in lateral view. In addition, the proximodorsal ridge of phalanx I-1 is slightly concave unlike *Sinornithomimus dongi*. It has a ball and socket metacarpal-phalangeal articulation, regarding to their metacarpal joints (Kobayashi and Lü, 2003). There are two prominent ridges developed in both sides of the articular surfaces along proximoventral of first phalanges. On the other hand, the corresponding surfaces of the penultimate phalanges are flat. The shafts of all phalanges are straight in lateral view, differing from *Sinornithomimus dongi* with dorsally curved penultimate phalanges of digits I and II. Phalanx I-1 is the longest among the manual elements as in other ornithomimosaurs and is longer than the sum of phalanges III-1 and III-2 (Barsbold and Osmólska, 1990; Perėz-Moreno et al., 1994; Kobayashi and Lü, 2003) (Table-3). Phalanx I-1 is more than twice as long as phalanx II-1 and more than three times as long as phalanx III-1 unlike *Sinornithomimus dongi* (3.8 times and 5.5 times, respectively), but similar to the ratios in *Gallimimus bullatus* (Osmólska et al., 1972; Kobayashi and Lü, 2003). Phalanx II-2 is more than twice as long as phalanx II-1.

Table-6. Measurements (in mm) of the pectoral girdle and forelimb elements of MPC-D 100/121. Note that: (+), existed element, but incomplete.

Skeletal elements	Specified measured areas	Measurements
Humerus (right)	length of the distal end, anteroposteriorly	55.60
	width of the distal end, transversely	25.33
Ulna (left)	total length	231.23
	length of the proximal end, anteroposteriorly	36.05
	width of the proximal end, transversely	32.12
	length of the distal end, anteroposteriorly	18.54
	width of the distal end, transversely	28.86
	least shaft diameter	48.50
Radius (left)	total length	212.28
	length of the proximal end, anteroposteriorly	25.10
	width of the proximal end, transversely	18.20
	length of the distal end, anteroposteriorly	23.38
	width of the distal end, transversely	13.48
	least shaft diameter	43.01

Manus (right)	total length along the metacarpal II and the digit II								294
Manual digit I	total length								157.56
Manual digit II	total length								194.96
Manual digit III	total length								211.97
Metacarpal I (right)	total length								86.68
	width of the proximal articular surface								19.30
	height of the proximal articular surface								13.52
	width of the distal articular surface								19.43
	height of the distal articular surface								21.23
Metacarpal II (right)	total length								91.51
	width of the proximal articular surface								19.28
	height of the proximal articular surface								19.28
	width of the distal articular surface								17.70
	height of the distal articular surface								20.88
Metacarpal III (right)	total length								87.89
	width of the proximal articular surface								15.33
	height of the proximal articular surface								21.98
	width of the distal articular surface								16.20
	height of the distal articular surface								20.37
Phalanges (left)	Ph. I-1	Ph. I-2	Ph. II-1	Ph. II-2	Ph. II-3	Ph. III-1	Ph. III-2	Ph. III-3	Ph. III-4
total length	104.6	52.96	42.88	93.54	58.54+	33.62	32.30	74.97	71.08+
width of the proximal articular surface	20.06	13.89	19.23	18.34	14.55	16.29	15.65	14.52	13.47
height of the proximal articular surface	19.94	20.20	24.61	19.32	20.08	24.48	19.29	17.26	18.28

This feature differs from *Gallimimus bullatus* (less than two times, 1.8) but similar *Sinornithomimus dongi*. Phalanx III-3 is longer than the combined length of phalanx III-1 and III-2. Its ratio is 0.88 (phalanx III-1 length + phalanx III-2 length/ phalanx III-3 length), which falls within the range of the other ornithomimosaurs (*Sinornithomimus dongi*, 0.66, *Harpymimus okladnikovi*, 0.84, *Gallimimus bullatus*, 0.92, *Deinocheirus mirificus*, 1.06, and *Anserimimus planinychus*, 1.14). The ligament fossae are strongly developed in both lateral and medial surfaces of phalanges I-1, II-2, and III-3, but the lateral ligament fossa of phalanx I-1 is stronger than the other ligament fossae. Those of phalanges II-1, III-1, and III-2 are faint. Ungual phalanges are laterally compressed with lateral and medial grooves. The first ungual is robust and strongly curved like *Gallimimus bullatus*, while other two unguals are slender and less curved (Chinzorig et al., 2018). There is a small hump-like structure on the dorsal edge of ungual I within proximal

half about the same level of the flexor tubercle, which is a unique feature for ornithomimosaurs (Fig. 40). Ungual I is shorter than unguals II and III. The articular surfaces of all unguals are higher than wide, having a weak sagittal ridge. Their articular surfaces are developed in the form of a narrow triangle unlike *Anserimimus planinychus* (Barsbold, 1988). The flexor tubercles for the tendons of M. flexor profundus are placed distally about one-third to the proximal ends. The flexor tubercle of ungual I is bowl-shaped, while the flexor tubercle of other two unguals is ridge-like.

Ilium

Other than the left and right antilium, the ilia are complete and articulate with a sacral (Fig. 32). Although the ilium is incomplete, it is much longer than its pubis (Table-7) like *Gallimimus bullatus*. It is also three times as long as the iliac height above the center of supraacetabulum, which differs from *Sinornithomimus dongi* (Kobayashi and Lü, 2003). Posteriorly, the height of the ilium gradually decreases and slightly flares posteriorly, with a rectangular posterior edge as in most ornithomimosaurs (Makovicky et al., 2004). The dorsal edges of the ilia are thin transversely and firmly attach to the sacral plate as in other ornithomimids (Makovicky et al., 2004) and some oviraptorosaurs (Barsbold et al., 2000; Lü et al., 2002) and diverges posteriorly. The lateral edge of the supraacetabular crest has a strong lateral expansion as in *Gallimimus bullatus*, *Sinornithomimus dongi*, and *Struthiomimus* sp. (TMP 90.26.1) (Osmólska et al., 1972; Kobayashi and Lü, 2003). The supraacetabular ridge on the lateral iliac blade is less pronounced than tyrannosaurids (Maleev, 1955). The base of the iliac blade has depression above the supraacetabular crest in dorsolateral view. A small prominent process is developed along the lateral edge of the lateral wall of the brevis fossa in dorsal view, which is similar structure to *Garudimimus brevipes*, but unlike *Gallimimus bullatus* and *Sinornithomimus dongi*. The edges of lateral wall of the cuppedicus fossa and brevis fossa are nearly straight in lateral view. The lateral wall of the cuppedicus fossa is different from *Gallimimus bullatus*, which has a dorsally concaved edge. The medial wall of the brevis fossa is visible in lateral. The brevis fossa is as large as in other ornithomimosaurs but deeper than *Garudimimus brevipes*. The pubic peduncle is much larger than the ischiac peduncle (Table-7). The ischiac peduncle has wedge-shaped

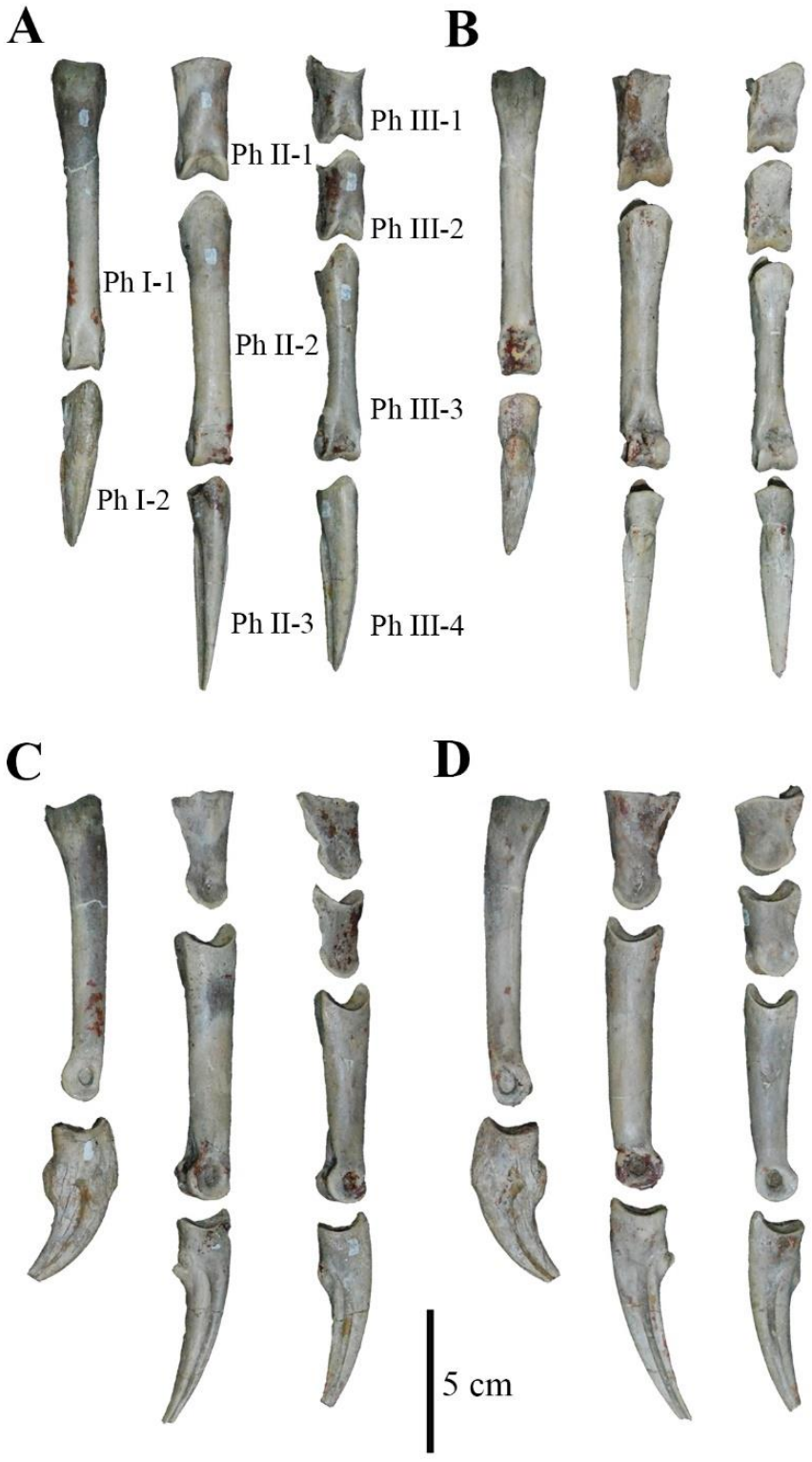

Figure-40. Left manual phalanges of MPC-D 100/121. *Explanation:* (A), anterior, (B), posterior, (C), medial, and (D), lateral. *Abbreviations*: see the list of abbreviations on page vi.

articular surface and ventrally pointing apex in lateral view. As known in *Sinornithomimus dongi*, the ventral end of the ischiac peduncle is anteroposteriorly flattened for a peg-and-socket articulation.

Table-7. Measurements (in mm) of the pelvic girdle of MPC-D 100/121. Note: (+), existed element, but incomplete.

Skeletal elements	Specified measured areas	Measurements
Ilium	anteroposterior length	450+
	height between the highest point of the ilium and supracetabular crest	148.91
	length/height of the acetabulum	95.27/75.47
	length of the brevis fossa, anteroposteriorly	208.55
Pubis	total length	434
	length of the pubic boot	160.58
	length along the pubic boot, ventrally	187.50
	length/width of the pubic peduncle	82/34.83
Ischium	total length	326
	length of the ischial foot	75.49
	length/width of the ischiac peduncle	30.56/30.64

Pubis

The pubis is the second longest element in the pelvis (Fig. 41). The surface for attachment with the ischium is short while that for the pubic peduncle of the ilium is much more extensive as in ornithomimosaurs (Table-4). In addition, the pubic contribution to the boundary of the acetabulum is lesser than other two bones surrounding the acetabulum as in other ornithomimids. The posteroventral margin of the proximal end of the pubis is weakly concave and sharp. There is a distinct scar preserved on the proximal half of the pubic shaft in lateral, which is probably muscle attachment of *m. ambiens* as is interpreted in a holotype of *Gallimimus bullatus* (Osmólska et al., 1972). The pubis has a straight shaft with an anteroposteriorly expanded pubic boot in lateral view. The posterior process of the pubic boot is slightly longer than its anterior process.

Ischium

Both ischia are nearly complete, but the obturator process is damaged (Fig. 42). The ischium is as slender as the pubis and roughly two-thirds of the pubic length (Table-7). The proximal end of the ischium

has very short iliac and pubic peduncles, forming a weakly concave acetabular rim. The sutural surface of the iliac peduncle is excavated as in *Sinornithomimus dongi* to receive the ischial peduncle of the ilium.

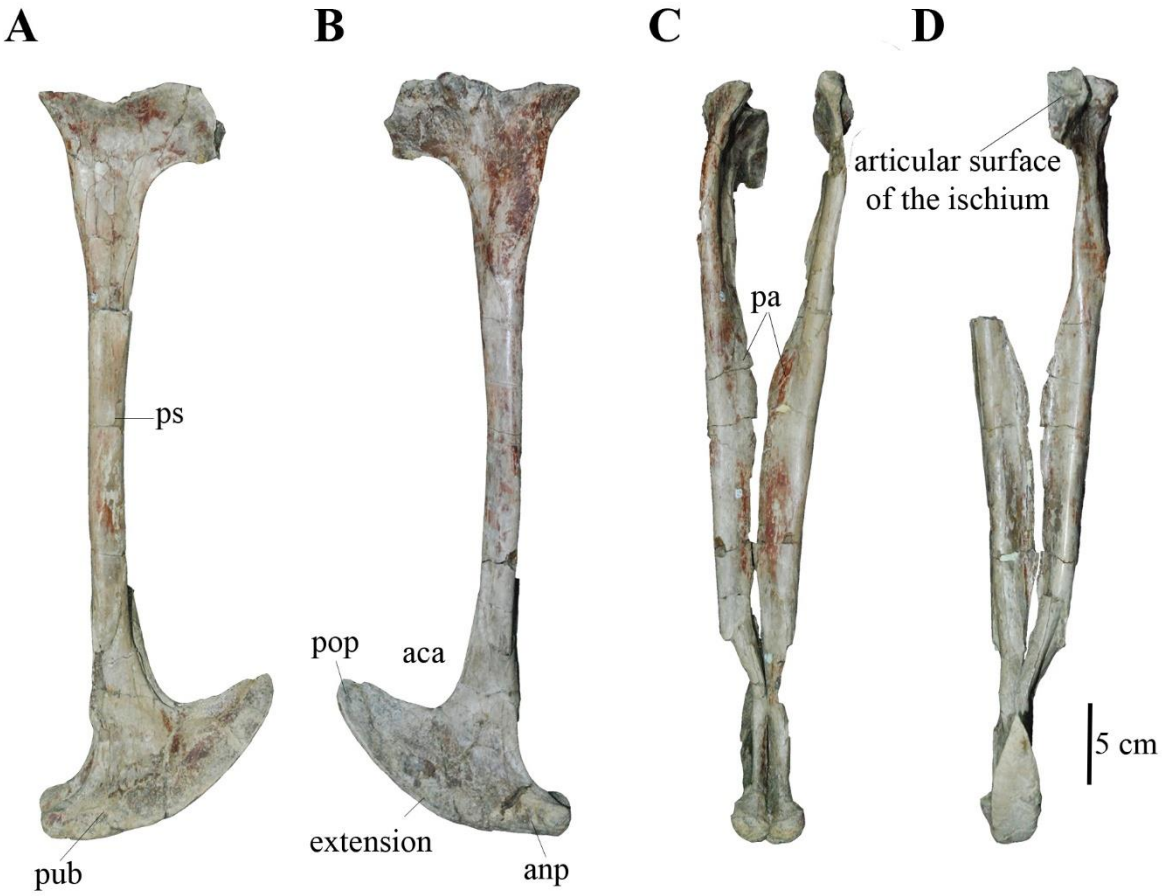

Figure-41. Left and right pubi of MPC-D 100/121. *Explanation:* (A), left lateral, (B), right lateral, (C), anterior and (D), posterior. *Abbreviations*: see the list of abbreviations on page vi.

The ischial shaft is nearly straight and has an apron, extending more than two-thirds of the element. Left and right ischial aprons are fused each other at the mid-section and are folded anteriorly. The ischial foot is extended anteroposteriorly and has dorsally projecting process anteriorly and a straight ridge posteriorly (Fig. 42A and B). The ventral expansion of the ischial foot is rounded in lateral view. Ventrally, it thins anteriorly but widens posteriorly, to form oval structure. A faintly developed sulcus in the ventral ischial foot is present.

Femur

Both femora are well-preserved (Fig. 43). The femur is almost straight, long and slender, and its shaft sub-circular and flattened laterally. It is as long as the tibia (Table-8) although it is usually shorter femur than the tibia in other ornithomimosaurs (Table-9). The femur head is transversely wider than its anteroposterior length unlike *Garudimimus brevipes*, but as in other ornithomimosaurs. The anterior and posterior surfaces have unevenly developed tubercles. The lesser trochanter is situated in slightly lower than the femur head and distinctly separated from the head by narrow sulcus. The anterior border of the lesser trochanter has a strong accessory trochanter as in most ornithomimosaurs (Makovicky et al., 2004). On the proximo-posterior surface of the greater trochanter, there is a small protuberance developed as bending at medially, which is also seen in *Sinornithomimus dongi*, but it is larger than MPC-D 100/121.

Table-8. Measurements (in mm) of the hind limb elements of MPC-D 100/121. Note: (?), measuring part is existed, but impossible to measure due to hidden location in the specimen, (+), existed element, but incomplete.

Skeletal elements	Specified measured areas	Measurements
Femur	total length	445
	widths of the proximal end/distal end, transversely	85.30/70.75
	lengths of the proximal end/distal end, anteroposteriorly	44.12/73.95
	least shaft diameter	128
Tibia	total length	447
	total length with astragalus	463
	widths of the proximal end/distal end, transversely	56.30/70.82
	lengths of the proximal end/distal end, anteroposteriorly	99.44/39.85
	least shaft diameter	109.50
Fibula	total length	418.50
	widths of the proximal end/distal end, transversely	15.84/5.01
	lengths of the proximal end/distal end, anteroposteriorly	72.25/16.52
	least shaft diameter	33.50
Astragalus	length of the ascending process	113
	width, transversely/ with the calcaneum	65.67/69.60
	length of the lateral condyle	38.56
	length of the medial condyle	40.10
Calcaneum	length	34.03

	height										27.03	
Pes	total length along metatarsal III, and digit III										495.24	
Metatarsal II	total length										277.54	
	width/height of the proximal end										30.35/55.86	
Metatarsal III	total length										309.36	
	width/height of the proximal end										8.45/?	
Metatarsal IV	total length										290.21	
	width/height of the proximal end										34.33/48.69	
Metatarsal V	total length										56.78+	
	width/height of the proximal end										8.09/10.05	
Digit II	total length										138.92	
Digit III	total length										187.27	
Digit IV	total length										131.59	
Phalanges (left)	Ph. II-1	Ph. II-2	Ph. II-3	Ph. III-1	Ph. III-2	Ph. III-3	Ph. III-4	Ph. IV-1	Ph. IV-2	Ph. IV-3	Ph. IV-4	Ph. IV-5
total length	65.85	28.99	44.08	62.72	46.93	35.22	42.40	36.53	21.35	15.57	14.81	43.33
width of the proximal articular surface	25.59	21.97	18.14	35.76	29.22	24.33	17.95	25.46	22.81	19.92	18.09	17.55
anteroposterior length of the proximal articular surface	32.46	23.97	20.62	31.31	21.77	19.67	18.89	27.72	24.26	22.02	19.76	19.84

The fourth trochanter is positioned at about one third of the femur length from the proximal end. The ratio of the anteroposterior length to the lateromedial width of the distal end of the femur is about one (Table-8). The lateral condyle is slightly larger than the medial condyle, and these condyles are separated each other by a shallow groove through the distal articular surface (Fig. 43F). The intercondylar fossa at the distal end is deep. The popliteal groove is strong and extends along the lateral condyle. The lateral and medial surfaces of the condyles are convex as in *Sinornithomimus dongi* and *Gallimimus bullatus*, but unlike *Garudimimus brevipes* that has straight surfaces in distal view. There is a deep depression on the anterior surface of the medial condyle, which is bordered a sharp crest medially. The corresponding depression is also known in *Gallimimus bullatus*, but it is less pronounced or almost nothing in *Garudimimus brevipes*

and *Sinornithomimus dongi* (Osmólska et al., 1972; Kobayashi and Lü, 2003; Kobayashi and Barsbold, 2005a).

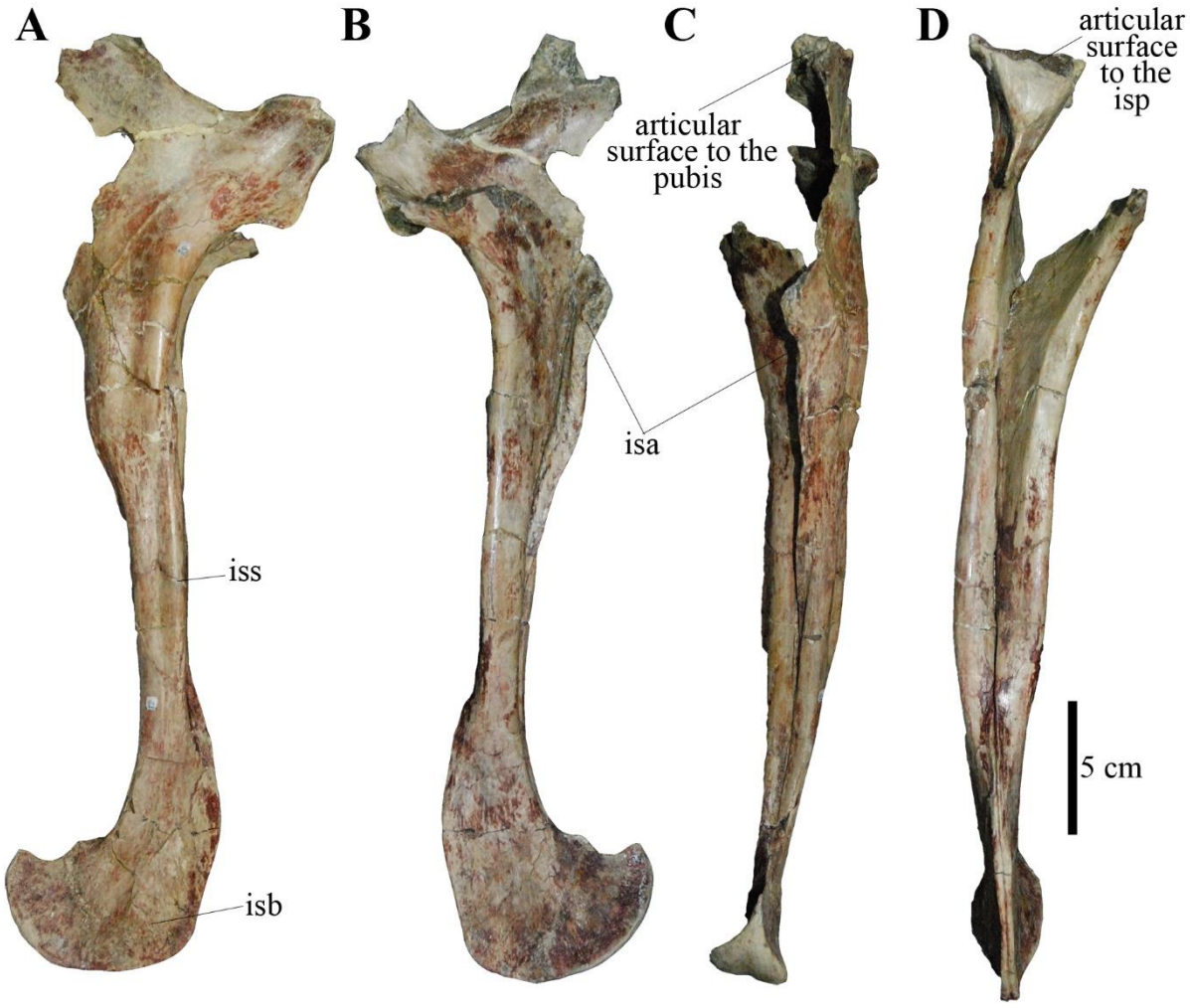

Figure-42. Left and right ischia of MPC-D 100/121. *Explanation:* (A), left lateral, (B), right lateral, (C), anterior, and (D), posterior. *Abbreviations*: see the list of abbreviations on page vi.

Table-9. Ratios of selected anatomical elements between MPC-D 100/121 and other ornithomimosaurs. *Abbreviations*: see the lists of abbreviations on page vi and institution on page xvi.

Species	OrL/SkL to SkL	MandH /MandL	emfH/emfL	TbL/FeL	MtIIIL/FeL
MPC-D 100/121	0.309788136	0.2	0.4817330	1.004494382	0.695191011
Gallimimus bullatus MPC-D 100/10	0.330769231			1.135416667	0.817708333

Gallimimus bullatus MPC-D 100/11	0.267857143			1.045112782	0.796992481
Gallimimus bullatus MPC-D 100/12	0.235294118			1.016	0.72
Garudimimus brevipes MPC-D 100/13	0.245634921	0.14634146		1.045822102	0.617250674
Gallimimus sp. MPC-D 100/52					
Gallimimus sp. MPC-D 100/133					
Gallimimus sp. MPC-D 100/138				1.090163934	0.819672131
Gallimimus bullatus Zpal MgD-I/1	0.291666667	0.16774193			
Gallimimus bullatus Zpal MgD-I/180					
Gallimimus bullatus Zpal MgD-I/94		0.19607843		1.081481481	0.814814815
Anserimimus planinychus MPC-D 100/300				1.034482759	0.689655172
Deinocheirus mirificus MPC-D 100/127	0.11328125	0.17128205	0.3558558	0.991304348	0.569565217
Harpymimus okladnikovi MPC-D 100/29	0.205725191	0.15384615			
Ornithomimus edmontonicus ROM 851	0.26212766	0.13227513		1.091954023	0.712643678
Ornithomimus edmontonicus TMP 95.110.1	0.265822785	0.12019230		1.094117647	0.781176471
Sinornithomimus dongi IVPP V11797-10	0.290005461			1.037151703	0.659442724
Struthiomimus altus TMP 90.26.1	0.322274882	0.13917525		1.083511777	0.802997859

Tibia

The tibia is straight (Fig. 44) and has two well-developed proximal condyles, which are separated by a deep narrow groove like other ornithomimosaurs (Makovicky et al., 2004). The medial condyle is larger than the lateral one in proximal view. The cnemial process is long and pointed as in most ornithomimosaurs, and its anterolateral border does not formed any prominence as seen in *Garudimimus*

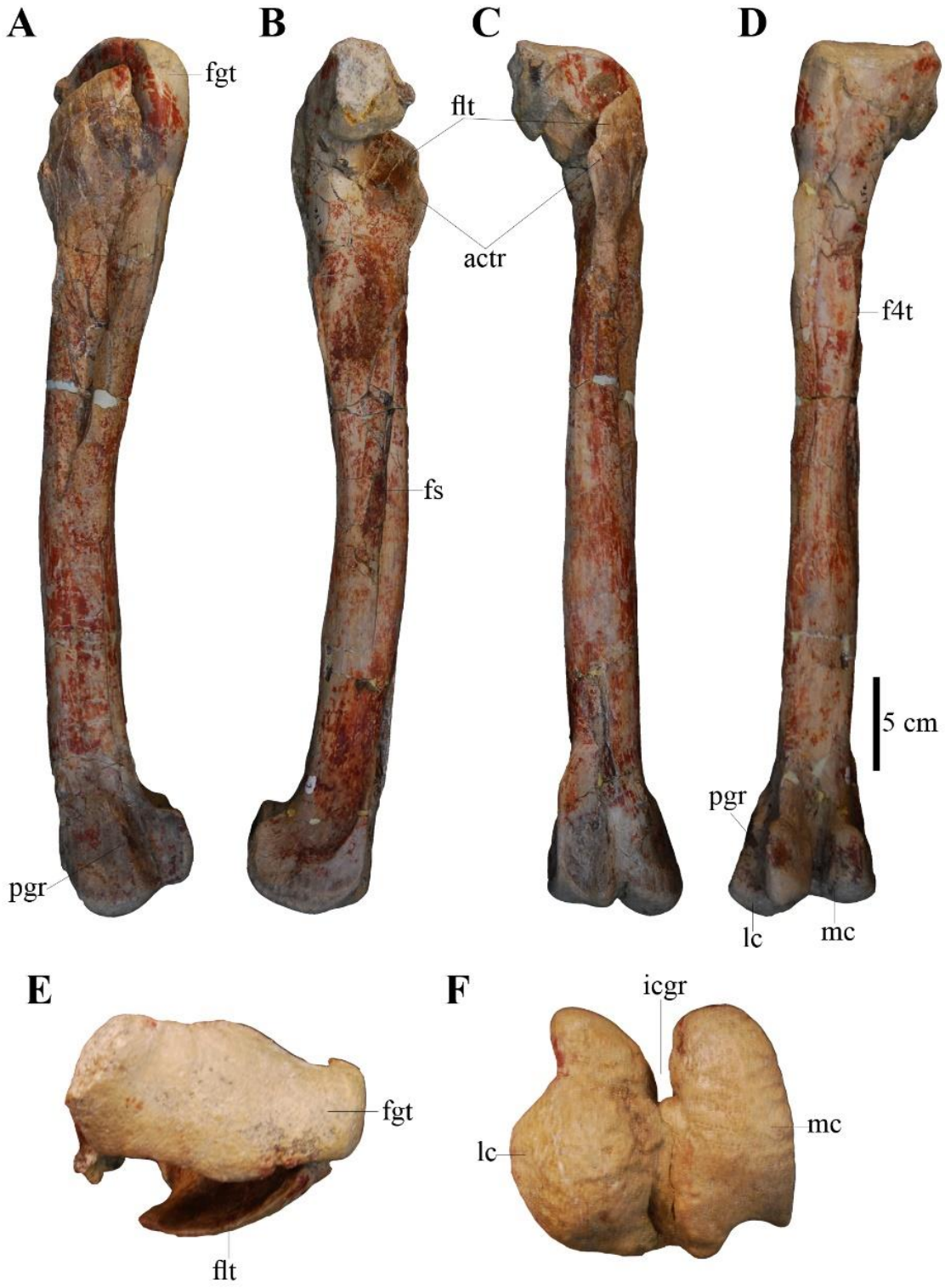

Figure-43. Left femur of MPC-D 100/121. *Explanation:* (A), lateral, (B), medial, (C), anterior, (D), posterior, (E), proximal, and (F), distal views. *Abbreviations*: see the list of abbreviations on page vi.

brevipes and *Sinornithomimus dongi* (Kobayashi and Lü, 2003; Kobayashi and Barsbold, 2005a). The cross-section of the tibia is roughly circle. The fibular crest is as strong as other ornithomimosaurs. Instead of this prominence, strong ridge is formed dorsoventrally. This ridge is gradually merged the shaft to the ventrally unlike some of undescribed specimens (pers.observ. of Yagaan Khovil ornithomimid). The lateral and posterior surfaces of the distal end are flat. The anteromedial and posterolateral corners of the distal end have small-scaled, but strong ridges, in which posterolateral ridge is also explained in *Harpymimus okladnikovi* (Kobayashi and Barsbold, 2005b).

Fibula

Other than the proximolateral of the right fibula, both fibulae are complete and preserve as attaching to each of their tibia (Fig. 44A, D and E). The fibula is thin flat bone as in other ornithomimosaurs. The length of the fibula is slightly shorter than the tibia length (Table-8). The proximal end is anteroposteriorly extended, but transversely flattened. The posterior border of the proximal end narrows posteriorly like *Gallimimus bullatus*, but unlike *Garudimimus brevipes* and *Sinornithomimus dongi*. The posterior border of the proximal end has a similar ridge as known in *Garudimimus brevipes*, but unlike *Sinornithomimus dongi*. Like other ornithomimosaurs, the fibular fossa is developed in the medial one third of the fibula to the proximal end. The shaft is thin and transversely flat. The distal end of the fibula thins and contacts to the proximal end of the calcaneum notch by a rounded extremity.

Tarsals

Both sides of the astragalus and calcaneum are nearly complete, except a tip of the ascending process of the right astragalus. All tarsal bones are firmly attached to the tibia. The ascending process is about one fourth of the tibia length (Table-8), may probably equivalent to the ratio of *Gallimimus bullatus*. The ascending process of the astragalus is triangular in anterior view and its tip leans laterally to the fibula. The base of the astragalus has a transversely extended strong depression. The medial condyle is larger than the lateral condyle in distal view as in *Gallimimus bullatus*, *Sinornithomimus dongi*, and *Aepyornithomimus*

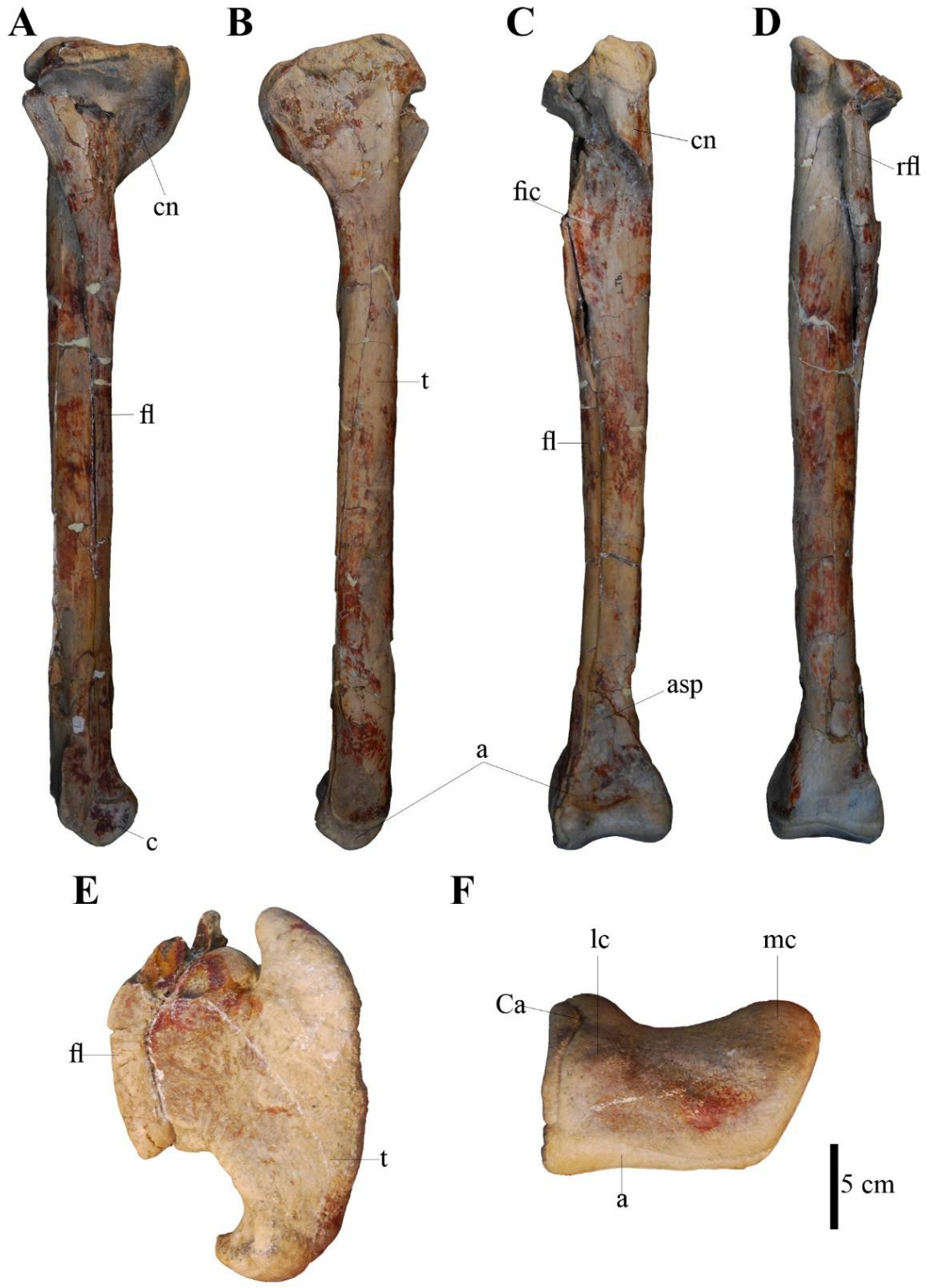

Figure-44. Right tibia and fibula of MPC-D 100/121. *Explanation:* (A), lateral, (B), medial, (C), anterior, (D), posterior, (E), proximal, and (F), distal views. *Abbreviations*: see the list of abbreviations on page vi.

tugrikinensis (Osmólska et al., 1972; Kobayashi and Lü, 2003; Chinzorig et al., 2017b). However, it is less leant to the medially, compare to the lateral condyle, than that of *Aepyornithomimus tugrikinensis*. There are two distinct notches developed on the anterolateral edge of the lateral condyle for the reception of the medial protuberances of the calcaneum, which is different from other ornithomimosaurs. The calcaneum is thin, with a flat lateral surface (Fig. 44F). Its upper border bears a notch for the articulation with the fibula. The anteromedial edge forms two distinct protuberances, which fit into a corresponding notches on the astragalus. Distal tarsals III and IV are complete in both sides of the pes, attaching tightly to the metatarsus (Fig. 45A, B, and F) and cover metatarsal III complete and the posterior half of metatarsal II and III in distal view. Distal tarsals III and IV are similar in shape to those in *Archaeornithomimus asiaticus* and *Gallimimus bullatus* (Gilmore, 1933; Osmólska et al., 1972; Smith and Galton, 1990) but differ from *Aepyornithomimus tugrikinensis* and *Garudimimus brevipes* (Kobayashi and Barsbold, 2005a; Chinzorig et al., 2017b).

Pes

Metatarsals

MPC-D 100/121 has four metatarsals (Mt II, Mt III, Mt IV, and Mt V). Both left and right metatarsals are well-preserved, except the fifth metatarsal of right side and preserve each other in articulated condition, together with distal tarsals (Fig. 45). In generally, all metatarsals are slender and tend to be elongated proximodistally. The proximal articular surface of metatarsals II and IV are about equally participated the articulation with crus in distal view. Metatarsal III is the longest, whereas metatarsals II and IV are subequal in length (Table-8). The height of the proximal articular surfaces of metatarsals are greater than their width (Table-8). The proximoventral of metatarsals have a short flat surface like *Gallimimus bullatus* (Osmólska et al., 1972). Metatarsal III is broad in its distal half, partly covers the sides of adjoining metatarsals II and IV by its concave surface. In its mid-length narrows abruptly and wedges between metatarsals II and IV at the proximal end. Metatarsals II and IV cover metatarsal III proximally by a straight contact surface in proximal view, therefore metatarsal III is not visible anteriorly. The lateral

surface of metatarsal II and the medial surface of metatarsal III are concave for the proximal end of metatarsal III. The length of metatarsal III is 69% that of the femur length, which is same ratio as in *Sinornithomimus dongi* (69%), but less than *Gallimimus bullatus* (80%) and *Dromiceiomimus brevitertius* (86%) (Osmólska et al., 1972; Barsbold and Osmólska, 1990). The proximolateral surface of metatarsal IV has a distinct, but limited depression which is a contact surface for metatarsal V. There is a long splint groove extends along lateroventral border of metatarsal IV, extending about three fourth to the proximal end. Metatarsal V is transversely thin and proximodistally elongate. The proximal end is thicker than its distal end transversely (Table-8). The dorsal border of metatarsal V is straight, while the ventral border is slightly widened and curved in lateral view. The articular condyles of metatarsals are unevenly developed in distal view. For example, the lateral condyle of metatarsal II and the medial condyle of metatarsal IV are larger than their medial and lateral condyles. The condyles of metatarsal III are nearly symmetric, but the medial condyle is slight greater than the lateral condyle. Unlike *Harpymimus okladnikovi* and *Garudimimus brevipes*, the lateral ligament fossae are as deep as *Sinornithomimus dongi*, except those on the medial ligament fossa of metatarsal II and the lateral ligament fossa of metatarsal IV, which are shallow.

Pedal phalanges

All pedal phalanges are well preserved in both sides of the pes (Fig. 46), and the pedal phalangeal formula is 0-3-4-5-0 as in other ornithomimosaurs, except *Beishanlong grandis*, *Garudimimus brevipes*, and *Nqwebasaurus thwazi* which digit I is present (Barsbold, 1981; Makovicky et al., 2009; Choiniere et al., 2012). Digit III is the longest, and digits II and IV are subequal (Table-8). The most proximal phalanges have a single concave proximal articular surface, whose anteroposterior length is close to its width, except in phalanx III-1 (wider than long), as in other ornithomimosaurs (Makovicky et al., 2004). Other than these phalanges, all remaining phalanges have a weakly pronounced sagittal groove in the proximal articular surfaces. The proximoventral surface of phalanx I-1 has two ridges, which are separated by a deep concavity in proximal view unlike that of *Tototlmimus packardensis* (Serrano-Brañas et al., 2016). Phalanx I-1 has deep collateral ligament fossae, and its distal condyles are asymmetrical as in most

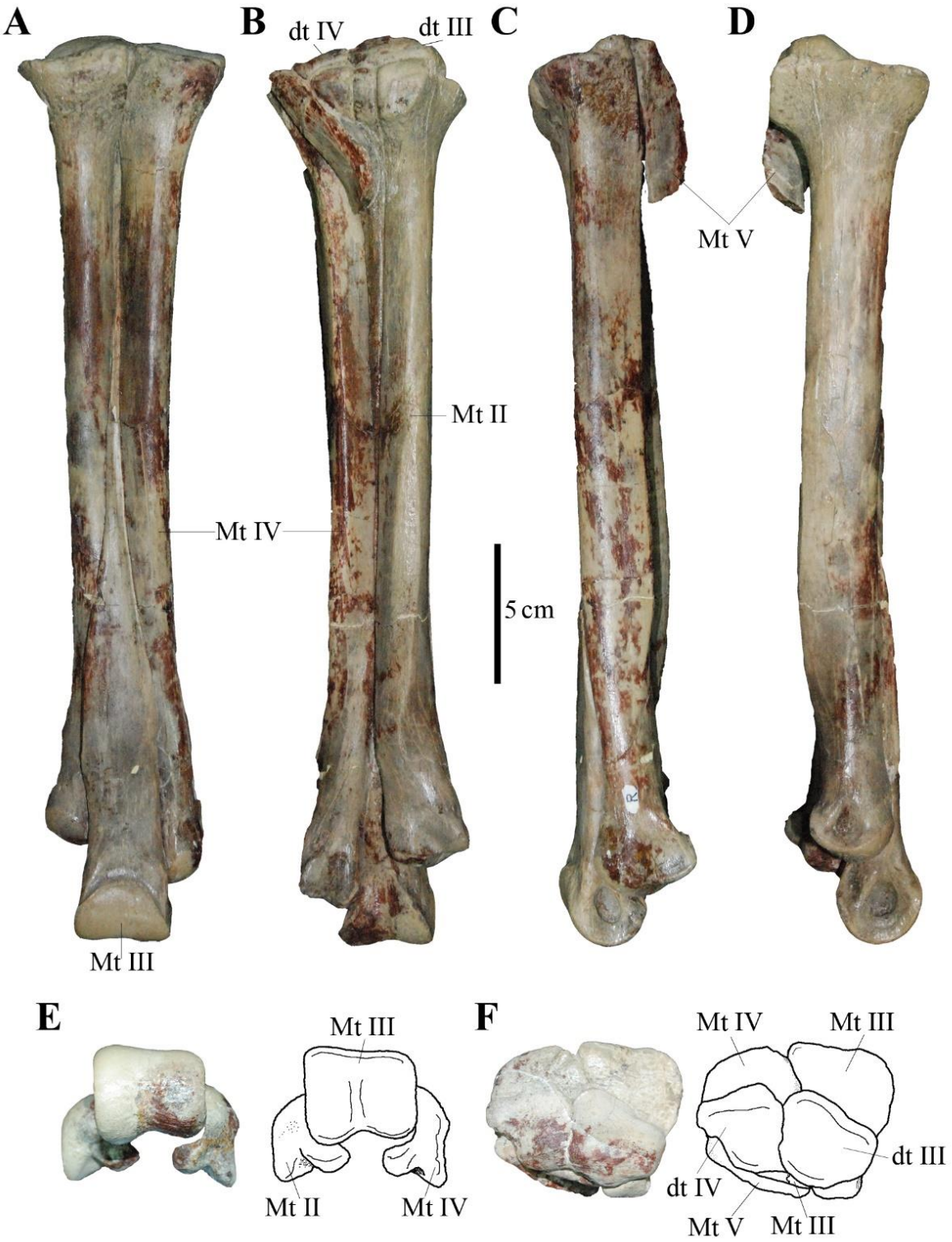

Figure-45. Left metatarsals of MPC-D 100/121. *Explanation:* (A), anterior, (B), posterior, (C), lateral, (D), medial, (E), distal, and (F), proximal views. *Abbreviations*: see the list of abbreviations on page vi.

ornithomimosaurs. There is a shallow dorsal depression on phalanges II-1, and III-1 to III-3. The proximomedial border of phalanx II-1 forms a curvature as seen also in *Aepyornithomimus tugrikinensis* (Chinzorig et al., 2017b) but unlike those of *Garudimimus brevipes* and *Tototlmimus packardensis* where is the corresponding border rectilinear. Phalanx II-1 is slightly longer than phalanx III-1 and is the longest of among the pedal phalanges. This phalanx is similar to phalanx IV-1 in having unevenly developed distal condyles, but is much longer than phalanx IV-1 (phalanx II-1 is nearly two times long). The phalanges of digit III lack ginglymoid articulation, except for the ungual-penultimate articulation. The proximolateral surfaces of phalanges III-1 and III-2 are smooth as in *Harpymimus okladnikovi*, no any grooves as known in *Garudimimus brevipes* (Kobayashi and Barsbold, 2005a). Phalanges of digit IV become shorter distally. Phalanges IV-2 to IV-4 are similar to phalanx IV-1 except that in each of these the proximal surface, which are divided by a sagittal groove. The lateral collateral ligament fossae of phalanges IV-1 to IV-4 are shallower than the medial fossae. The lateral condyle of phalanx IV-1 is relatively smaller than the medial condyle. Its degree of inclination is much lesser than the one in *Aepyornithomimus tugrikinensis*, but similar to most ornithomimosaurs (Makovicky et al., 2004). Ungual phalanges are complete in both sides (Fig. 46). As in other derived ornithomimosaurs, ventral surfaces are flat, and the articular surfaces of each unguals has a depression with a weak sagittal ridge without any tuber. The dorsal lip is well exposed in the proximodorsal articular surfaces. Ungual III is symmetrical, while unguals II and IV are asymmetrical in dorsal view and are somewhat declined outwards in respect to the longitudinal axis of the corresponding digits. As in *Gallimimus bullatus* and *Struthiomimus altus*, the ventral surface of the unguals has a semicircular depression at the mid-length, which is bordered by the sharp edges along their sides. Thus, these edges are abruptly end before reaching backwards about the proximal fourth of the ungual, which results in a small spur on either side of the ungual in dorsal and ventral views. A deep grooves extends each side of the ungual from the dorsal to the spur to a tip of the ungual.

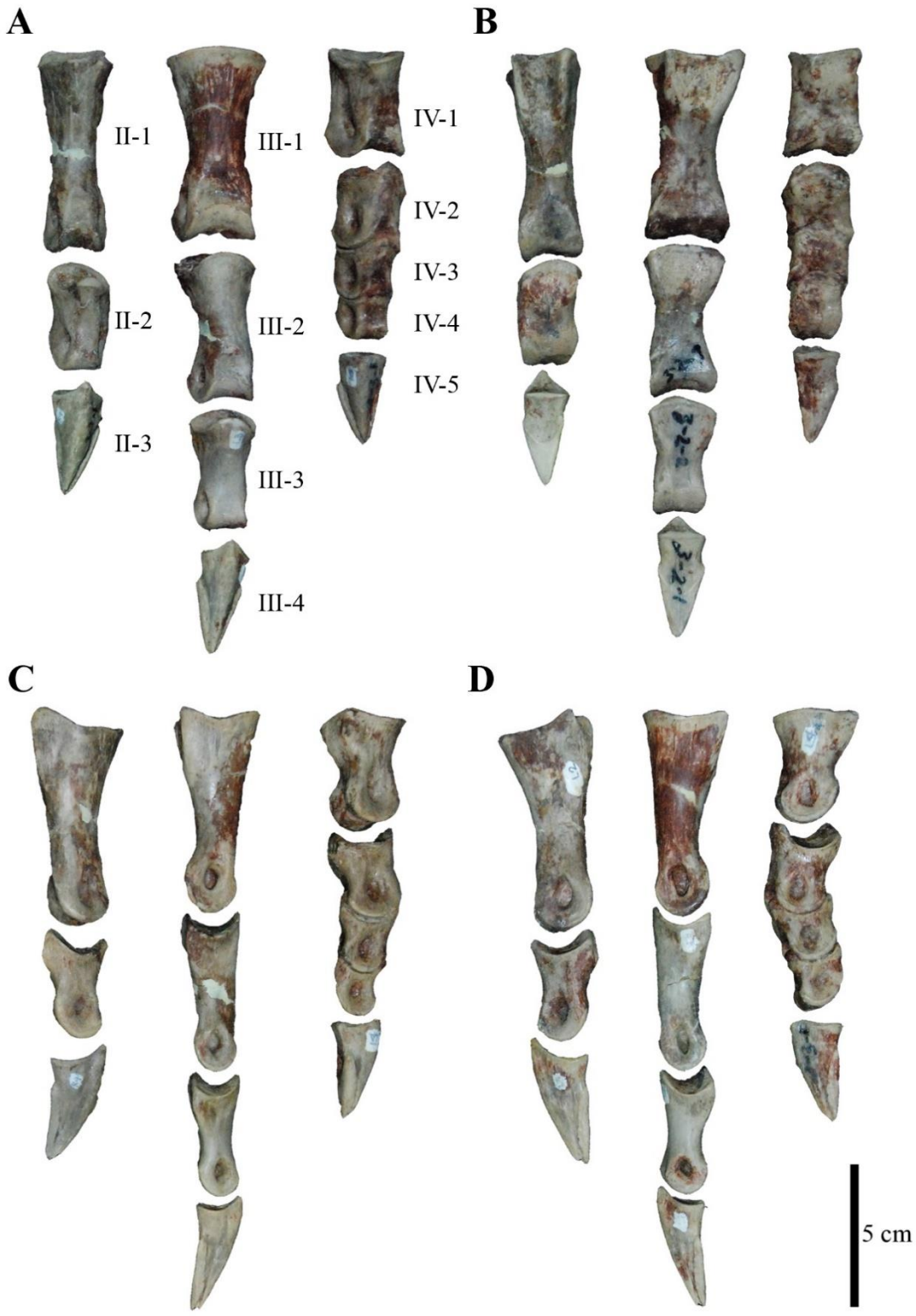

Figure-46. Left pedal phalanges of MPC-D 100/121. *Explanation:* (A), dorsal, (B), ventral, (C), medial, and (D), lateral views. *Abbreviations*: see the list of abbreviations on page vi.

DISCUSSION

Ornithomimid features of MPC-D 100/121

All articulated materials were recovered from the single horizon of area, about 3 m x 2 m, at the quarry (Fig. A2). The combination of characters in skull, forelimb, and hind limb elements show that it belongs to Ornithomimidae such as the presences of a lightly built skull with long, shallow snout, edentulous jaw, a lack of pleurocoels in the presacral vertebrae, a tridactyl manus with subequal second and third digits, subequal metacarpals, a combined length of the first and second phalanges of the third manual digit is not greater than the third phalanx length of the same digit, tibia-astragalus longer than femur, a metatarsus at least two-thirds of the tibiotarsus length, arctometatarsalian pes, and a lack of the first pedal digit (Osmólska et al., 1972; Russell, 1972; Holtz, T. R., 1994). In addition, the presence of ball and socket articulation between metacarpal and phalanges as seen in *Gallimimus bullatus* and *Struthiomimus altus*, MPC-D 100/121 suggest that it belongs to Ornithomimidae (Kobayashi and Lü, 2003). Although some diagnostic characters, which equally represent in both *Gallimimus bullatus* and *Struthiomimus altus*, are not preserved in the specimen, specifically vertebral column and forelimb elements, due to missing in nature, it can be compared to other diagnostic characters of *Gallimimus bullatus* and *Struthiomimus altus*, such as a long snout, anteriorly shovel-like lower jaw, greater posterior width of anteriormost fifteen caudal centra than half of central length, and transition point between caudals 15 and 16. However, the new specimen exhibits several similar features in its cranial and postcranial elements that resemble other ornithomimosaur taxa, it differs from the known taxa in its unique characters. Comparisons with known taxa either of Asia and North America suggest that MPC-D 100/121 does not correspond to any of them by its unique morphology.

Morphological comparisons to other ornithomimosaurs

The general morphology of the skull of MPC-D 100/121 is similar to other ornithomimosaurs, in having lightly built structures. Although some parts of the skull, including the braincase, maxilla, and

premaxilla, have characters, which can recognizable for comparing to other taxa. In dorsal view, the distinct difference preserves in the anterior part of the snout, although the most anterior tip is missing, which tends to be more narrowing anteriorly. This feature is similar to North American taxa with an anteriorly acute premaxilla such as *Struthiomimus altus*, while the anterior end of the rostrum of those in Asian forms are generally characterized by U-shaped such as *Gallimimus bullatus* (Osmólska et al., 1972; Kobayashi and Lü, 2003). The presence of the maxillary neurovascular foramina is preserved along the ventral margin of MPC-D 100/121. These foramina are commonly reported in North American forms, as well as Asian primitive forms, *Garudimimus brevipes* and *Shenzhousaurus orientalis*, however, these foramina have not been reported in Asian derived forms, such as *Gallimimus bullatus* and *Sinornithomimus dongi* (Osmólska et al., 1972; Kobayashi and Lü, 2003). Some of the elements of MPC-D 100/121 skull have different features when compare to other ornithomimosaurs. The ratio of maximum height to total length of MPC-D 100/121 mandible is compared in Table-6. The height of MPC-D 100/121 mandible is greater than any other ornithomimosaurs, but juvenile *Gallimimus bullatus* (ZPAL MgD-I/94) is positioned in close to MPC-D 100/121, which it is probably ontogenetic difference (Osmólska et al., 1972), (Fig. 47A). Also, another ratio is also seen in between skull length and orbit length in ornithomimosaurs in Table-6. The length ratio of orbit to skull is greater in MPC-D 100/121 than *Gallimimus bullatus*, as well as in most ornithomimosaurs, but similar *Struthiomimus altus* (TMP 90.26.1), (Fig. 47B). However, juvenile *Gallimimus bullatus* has a larger orbit than MPC-D 100/121. In addition, the external mandibular fenestra of MPC-D 100/121 is larger than any other ornithomimosaurs. The ratios of external mandibular fenestra height to its length in some ornithomimosaurs are *Gallimimus* sp. (MPC-D 100/133) (0.34), *Deinocheirus mirificus* (MPC-D 100/127) (0.36), and MPC-D 100/121 (0.48). Moreover, the posteroventrally projecting strong process is developed in the ventral border of MPC-D 100/121 mandible tip. A similar process is commonly developed in North American taxa such as *Ornithomimus edmontonicus* (TMP 95.110.1) and *Struthiomimus altus* (TMP 90.26.1), but the corresponding process is not formed or less commonly developed in Asian taxa, including *Gallimimus bullatus*, *Sinornithomimus dongi*, and *Garudimimus brevipes* (Osmólska et al., 1972; Kobayashi and Lü, 2003; Kobayashi and Barsbold, 2005a). Although

morphology of this process in MPC-D 100/121 is comparable to those North American taxa, the ventral deflection of the mandible is strong in North American taxa, while MPC-D 100/121 has straight or less deflection. MPC-D 100/121 metacarpals are generally similar structure of those in derived ornithomimosaurs, having subequal length of metacarpals with closely appressed proximally each other. However, it has some differences in comparison to other ornithomimosaurs previously described. Subequal length of the metacarpals of MPC-D 100/121 is comparable to the metacarpals of *Gallimimus bullatus* and *Struthiomimus altus*, in having a short metacarpal I and a subequal metacarpals II and III, although they have many variation in their metacarpal configurations. Metacarpals of MPC-D 100/121 are not similar to those in *Ornithomimus edmontonicus*, *Ornithomimus velox*, and *Anserimimus planinychus* which having a long metacarpal I than remaining two metacarpals (Barsbold, 1988; Claessens and Loewen, 2015). In addition, both MPC-D 100/121 and *Anserimimus planinychus* have similar notch on the lateral outline of the distal articular surface of metacarpal III, however, a long metacarpal I and ungual shapes of *Anserimimus planinychus* differentiate them each other (Chinzorig et al., 2018). A sharply recurved ungual I and straight or slightly curved manual unguals II and III are the unique features for MPC-D 100/121. Such a combination of the manual unguals has not been yet reported in ornithomimosaurs at least in Asia (Makovicky et al., 2004). Moreover, one partially preserved new ornithomimid specimen materials (ZPAL MgD-I/65), which is reported from Tsagan Khushuu locality, the Upper Cretaceous Nemegt Formation by Bronowicz, are morphologically similar to MPC-D 100/121 based on their feature of the distal articular surface of metacarpal II, a shaft curvature of manual phalanges in lateral view, slightly curved unguals, and a medially inclined pedal ungual IV-5 (Bronowicz, 2011). Although Bronowicz (2011) concluded it as aff. *Anserimimus planinychus* based on insufficient materials and also suggested its morphological differences and represented this new ornithomimid material as a potential new taxon.

Most of major features of Bronowicz's ornithomimid materials are characteristically more similar to MPC-D 100/121 than the holotype of *Anserimimus planinychus* (Barsbold, 1988). On the other hand, the presence of MPC-D 100/121 hand structure, including a configuration of metacarpals and combination of

manual unguals, resembles that of North American taxa such as *Struthiomimus altus* (TMP 90.26.1 and UCMZ(VP) 1980.1), (Nicholls and Russell, 1985).

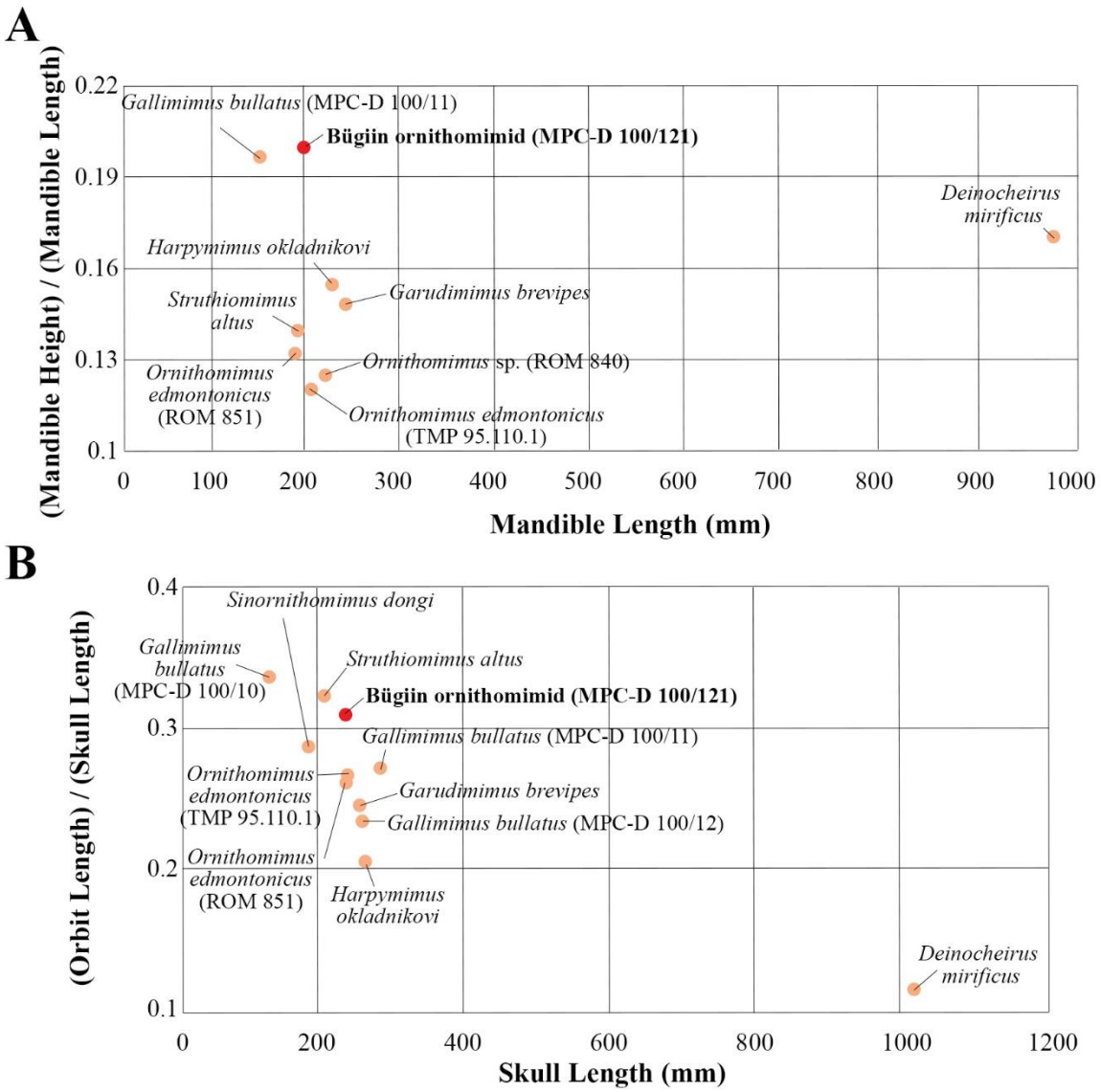

Figure-47. Ratios of skull elements within ornithomimosaurs. (A), Graphs of the mandible length to ratio of mandible length to mandible height; (B), the skull length to ratio of orbit length to skull length. *Abbreviations*: see the list of institutions on page xvi.

Comparing to North American taxa, for example *Ornithomimus edmontonicus* (ROM 851), the anterior extension of the pubic boot in MPC-D 100/121 is much shorter, but is more pronounced than *Gallimimus bullatus* (MPC-D 100/11), *Garudimimus brevipes* (MPC-D 100/13), and probably *Shenzhousaurus orientalis* (NGMC 97-4-002), (Xu et al., 2011). It has a greater acute angle between the dorsal edge of the pubic boot and the shaft as in *Qiupalong henanensis* and North American taxa (Ji et al., 2003; Xu et al., 2011) but similar to *Gallimimus bullatus* and *Garudimimus brevipes* (Osmólska et al., 1972; Kobayashi and Barsbold, 2005a). In addition, the tip of the anterior extension is rounded, and the posterior extension is pointed posteriorly and fused to form a single posterior extension like a condition of *Anserimimus planinychus* (Barsbold, 1988), rather than rounded ends as seen in other ornithomimosaurs (Xu et al., 2011). The degree of ventral expansion of the pubic boot is also different. The ventral expansion is more expanded in MPC-D 100/121 in lateral view. Although this feature is similar to most North American taxa, such as *Dromiceiomimus brevitertius* (ROM 797), *Ornithomimus edmontonicus* (AMNH 5201 and CMN 8652), and *Struthiomimus altus* (AMNH 5339 and UCMZ 1980.1), as well as some of Asian taxa, *Gallimimus bullatus* (MPC-D 100/11), *Qiupalong henanensis* (41HIII-0106), it is different than *Anserimimus planinychus* and *Garudimimus brevipes* (Xu et al., 2011; McFeeters et al., 2017). In general, most of North American taxa have greater extension of the anterior process of the pubic boot, whereas the Asian taxa have a less extension, *Gallimimus bullatus*, *Garudimimus brevipes*, and *Qiupalong henanensis*. The Early Late Cretaceous Chinese taxon, *Archaeornithomimus asiaticus*, has more pronounced anterior extension, however, its outline of the anterior extension and a curved shaft are different from MPC-D 100/121 (Smith and Galton, 1990).

Some of hind limb elements of MPC-D 100/121 are compared to other ornithomimosaurs. Although the ratio of tibia length to femur length of MPC-D 100/121 and *Deinocheirus mirificus* are sub-equal, MPC-D 100/121 has shorter tibia than other ornithomimosaurs (Fig. 48). Because of differences in the ratios of tibia length, MPC-D 100/121 is not belong to *Gallimimus bullatus*.

Metatarsal + pedal phalanges

Features of MPC-D 100/121 pes are generally similar to those of ornithomimids. The structure of pedal unguals is similar in *Gallimimus bullatus* and *Struthiomimus altus*, however, it is different from that of *Aepyornithomimus tugrikinensis* and *Ornithomimus edmontonicus*

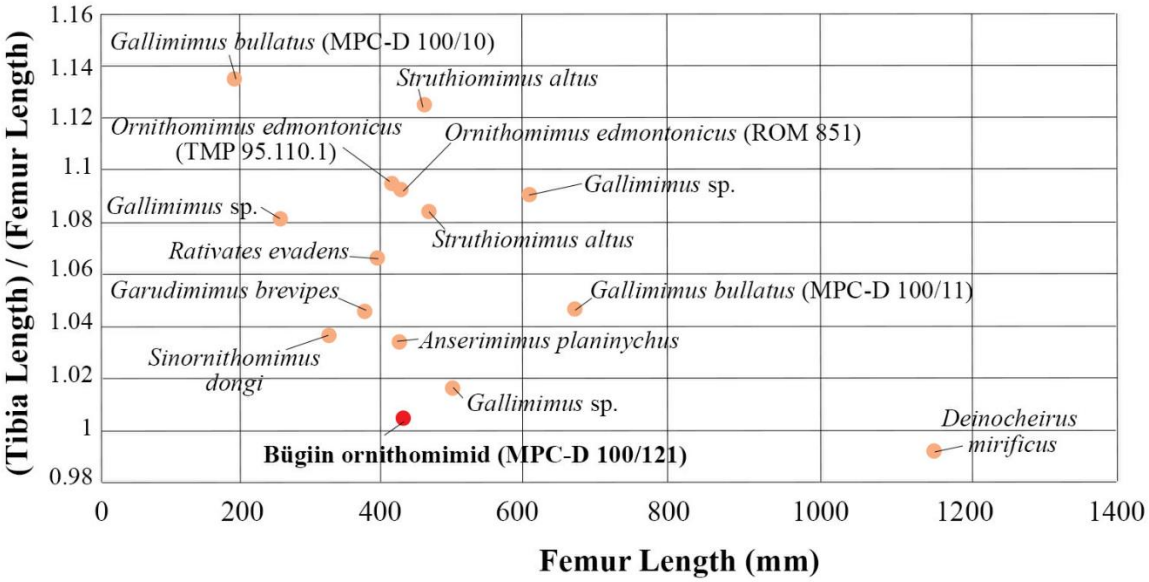

Figure-48. Graph of the femur length to ratio of tibia length to femur length within ornithomimosaurs. *Abbreviations*: see the list of institutions on page xvi.

where having anteroposteriorly elongated pedal unguals (Osmólska et al., 1972; Nicholls and Russell, 1980; Chinzorig et al., 2017b).

Phylogenetic position of MPC-D 100/121

The result of a phylogenetic analysis based on a data matrix in this study, MPC-D 100/121 is positioned in a monophyly of the derived ornithomimids, including *Anserimimus planinychus*, *Ornithomimus edmontonicus*, *Qiupalong henanensis*, *Rativates evadens*, and *Struthiomimus altus* (Fig. 49). This clade is placed more derived than *Gallimimus bullatus* and *Sinornithomimus dongi*. The tree topology of Ornithomimosauria is similar to the one proposed by McFeeters et al. (2016). The monophyly of Ornithomimidae has been previously supported by a number of characters (Barsbold and Osmólska, 1990). The present phylogenetic analysis supports the clade of Ornithomimidae with three unambiguous

synapomorphic characters (absence of posterolateral crests on lateral surfaces of cervical centra, proximally well-separated fibular crest, and smooth distal end of metatarsal III without ginglymus).

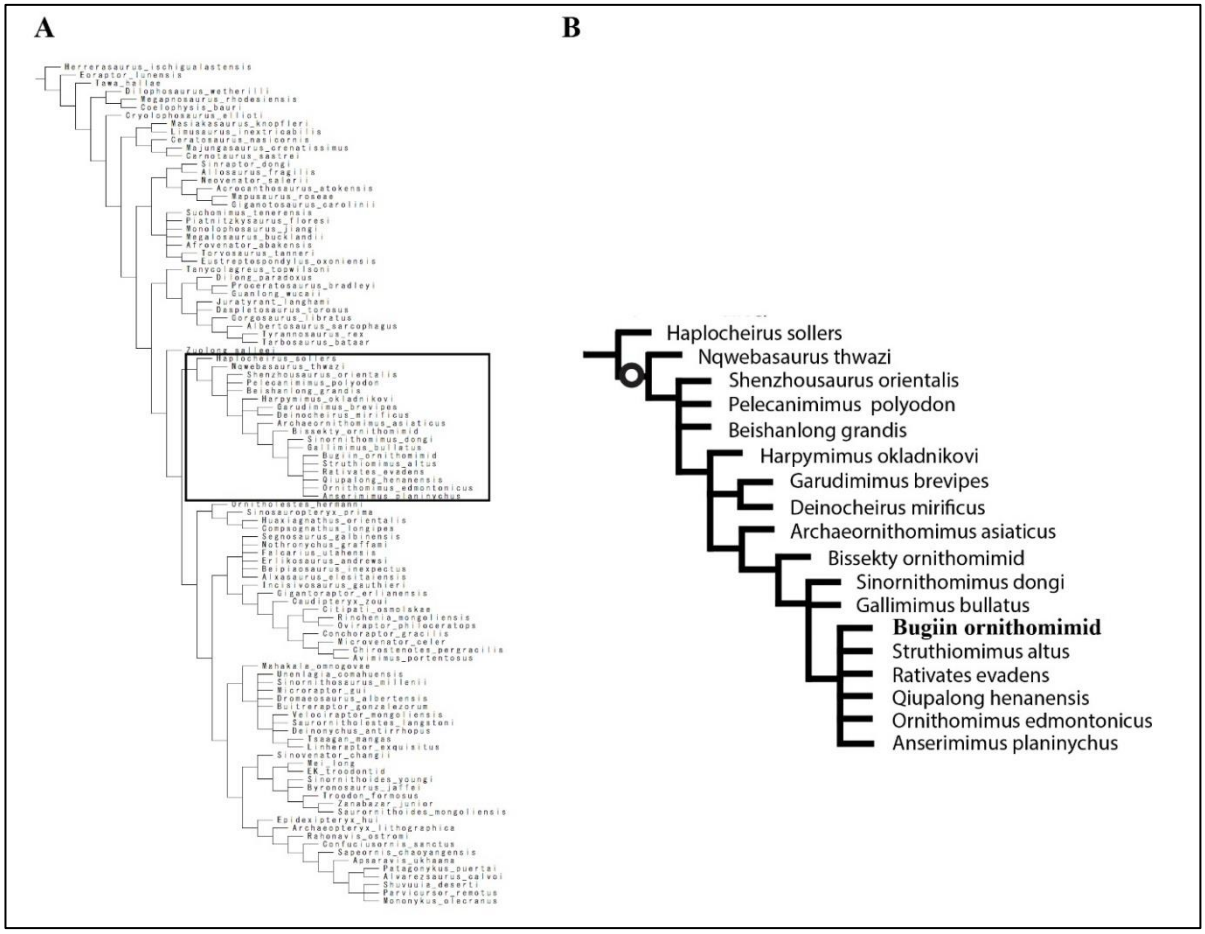

Figure-49. Strict consensus tree of MPC-D 100/121 after modified data matrices of Lee et al. (2014), Sues and Averianov, (2016), and McFeeters et al. (2016). (A), a complete tree, (B), extracted tree of only Ornithomimosauria.

Our result of the second phylogenetic analysis resulted in eight most parsimonious trees of 70 steps, with a C.I. = 0.586 and a R.I. = 0.730. The topology of strict consensus tree is similar to the one proposed by Serrano-Brańas et al. (2016) (Fig. 50). Two unambiguous synapomorphies (absence of promaxillary teeth and dorsally and ventrally subparallel borders of dentary) support the monophyly of *Garudimimus* and Ornithomimidae. Kobayashi and Barsbold (2005a) previously suggested that a different food processing function may evolved from *Garudimimus* due to loss of dentary teeth, cutting edge of

dentary and long maxillary process. The present analysis is also confirm this hypothesis by different characters, absence of premaxillary teeth and dorsoventrally subparallel bordered dentary.

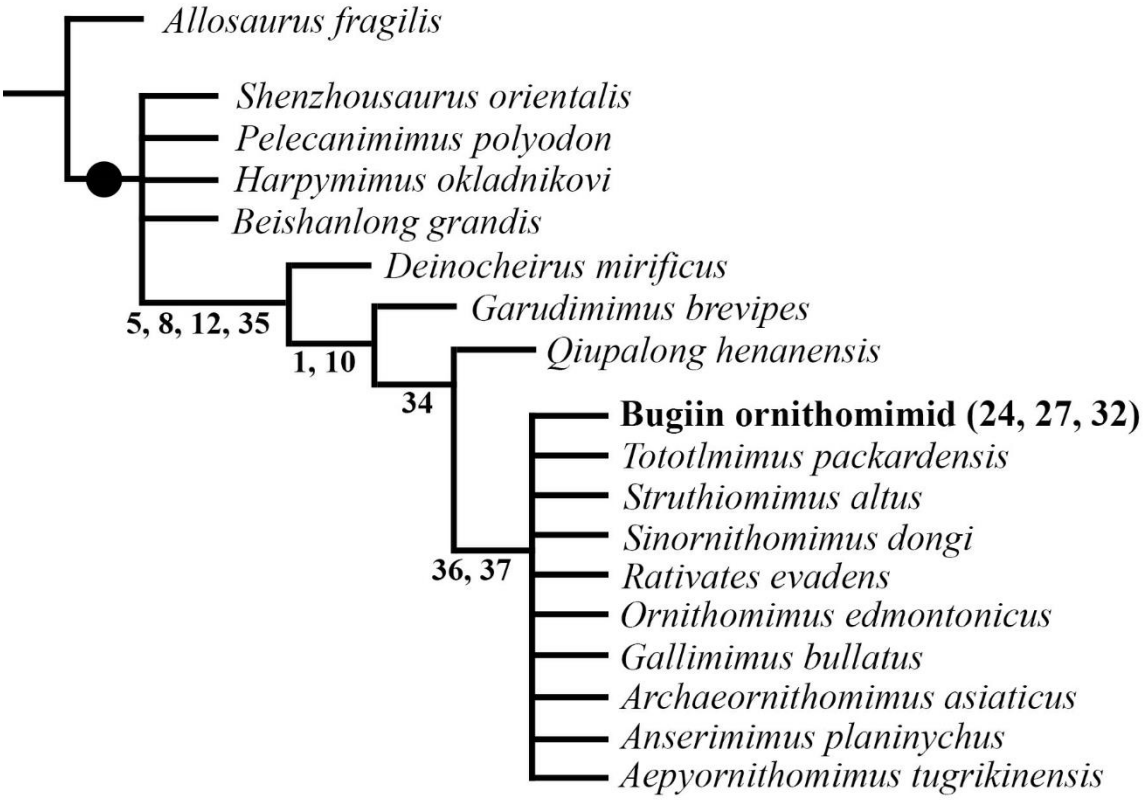

Figure-50. Strict consensus tree of MPC-D 100/121 within ornithomimosaur taxa after modified Kobayashi and Lü, (2003) and Xu et al. (2011). Note that: (•), refers to Ornithomimosauria, and numbers are synapomorphic characters.

Ornithomimidae is a sister taxon to *Garudimimus brevipes* and supports a single unambiguous synapomorphy (absence of pedal digit-I). In addition, the monophyly of the derived ornithomimosaurs which includes MPC-D 100/121 and other ornithomimids, except *Qiupalong*, shares two unambiguous synapomorphies; a length of pedal phalanx II-2 is less than 60% of pedal phalanx II-2 and a straight pedal unguals. Both characters are related to foot, which may indicate that the locomotion proficiency of derived ornithomimosaurs was a different than the basal forms. Nevertheless, MPC-D 100/121 represents a different taxon because it possesses unique characteristics and separates it from the North American taxa and other Nemegt ornithomimosaurs: acute anterior tip of premaxilla, a combination of manual unguals (a

sharply recurved ungual I and straight unguals II and III), a hump-like tuber on manual ungual I, reduced distal condyles of metacarpal I, more pronounced anterior extension of pubic boot, anteroposteriorly flat articular surfaces of anterior caudals, and anteroposteriorly short pedal unguals.

Several previous studies have discussed about the functional analysis of the forelimb of ornithomimosaurs based on the different hand structures (Ostrom, 1969; Osmólska et al., 1972; Nicholls and Russell, 1985). Osmólska et al (1972) suggested a possibility of the maximum flexion and extension of the *Gallimimus bullatus* hand where the movements were very limited and mentioned that the hand of *Deinocheirus mirificus* exhibits a similar adaption, but its hand used for the different purposes, such as a tearing the prey asunder. Contrary to *Deinocheirus mirificus*, a short manus of *Gallimimus bullatus* was not presumably used for carrying food to the mouth, but more probably for raking and digging light substrates on the ground in order to reach the food (Osmólska et al., 1972; Russell, 1972). Moreover, Nicholls and Russell are described two types of manus joint structures, the ball and socket and the ginglymoid (Nicholls and Russell, 1985). The ball and socket type joint is allowing more considerable flexion, extension, and rotational movements than the ginglymoid type of the hand. As like *Struthiomimus altus* (UCMZ(VP) 1980.1), a hand configuration of MPC-D 100/121 is similar, in having a nearly equal length of three digits which are oriented the extreme divergence between digit I and the tightly adhered digits II and III. Such an alignment of the manual digits, as previously interpreted by Nicholls and Russell (1985), displays as all the digits move posteriorly towards the midline of the hand, showing tentatively narrowing the hand when flexed. Although all three digits lie closely together, the hand is not a capable of fully grasping function in the hand. However, the digits of MPC-D 100/121 might have a different function from *Anserimimus planinychus*, *Deinocheirus mirificus*, and *Gallimimus bullatus*, regarding to their ungual forms (Chinzorig et al., 2018). The manual digits of MPC-D 100/121 form a function of very effective hooking, clamping, and may be some scratching performances in order to access to food, which suggest that a condition of the manual digits of MPC-D 100/121 might allow similar functions of those in *Anserimimus planinychus*, *Gallimimus bullatus*, *Deinocheirus mirificus*, and *Struthiomimus altus* and may probably have a multiplex hand function in it.

CHAPTER V

ORNITHOMIMOSAURS FROM THE NEMEGT FORMATION OF MONGOLIA: MANUS MORPHOLOGICAL VARIATION AND DIVERSITY

Manuscript Information Sheet

Tsogtbaatar Chinzorig, Yoshitsugu Kobayashi, Khishigjav Tsogtbaatar, Philip J. Currie, Ryuji Takasaki, Tomonori Tanaka, Masaya Iijima, Rinchen Barsbold.

Ornithomimosaurs from the Nemegt Formation of Mongolia: manus morphological variation and diversity.

Status of Manuscript:

_x_ Prepared for submission to a peer-reviewed journal

_x_ Officially submitted to a peer-reviewed journal

_x_ Accepted by a peer-reviewed journal

_x_ Published in a peer reviewed journal

Palaeogeography, Palaeoclimatology, Palaeoecology

Published by Elsevier

Contribution of Authors and Co-authors:

Manuscript in Chapter IV

Author: Tsogtbaatar Chinzorig

Contributions: conceived the study, catalogued and process the specimen, performed the analyses, prepared the figures, and wrote the manuscript.

Co-authors: Yoshitsugu Kobayashi and Philip J. Currie

Contributions: provided the useful comments and suggestions and improved to edit earlier drafts of the manuscript.

Co-authors: Masaya Iijima, Ryuji Takasaki, and Tomonori Tanaka

Contributions: provided important discussions and ideas, helped to accomplish statistical analyses, and prepared the graphs of the manuscript.

The citation of this research:

Chinzorig, T., Y. Kobayashi, K. Tsogtbaatar, P. J. Currie, T. Ryuji, T. Tanaka, M. Iijima, and R. Barsbold. 2018. Ornithomimosaurs from the Nemegt Formation of Mongolia: manus morphological variation and diversity. Palaeogeography, Palaeoclimatology, Palaeoecology, 494: 91–100.

ABSTRACT

The Upper Cretaceous Nemegt Formation of Mongolia is rich in well-preserved dinosaurs and Ornithomimosauria is one of the most common taxa in the formation. Three ornithomimosaur taxa, *Anserimimus planinychus, Deinocheirus mirificus*, and *Gallimimus bullatus*, have been discovered from the formation so far. However, the recently discovered specimens suggest there is even greater morphological variation of ornithomimosaurs in the Nemegt Formation than are presently recognized. This study focuses on the structures of manual elements among Nemegt ornithomimosaurs and reveals their remarkable diversity. The manual structures of seven individuals, including three known taxa and four new individuals, are morphologically distinct from each other. Numerical analyses on metacarpals, phalanges, and unguals also support high morphological diversity of the Nemegt ornithomimosaurs. The large diversity of manual morphology may be related to large variety of palaeoecological niches were prevailed in the Nemegt ecosystem.

Highlights

- Morphologically different ornithomimosaur mani are discovered from Mongolia.
- Nemegt ornithomimosaurs are highly diversified by their manus variation.
- Various paleoecological niches are presumably occupied in the Nemegt Formation.
- The different manual unguals may be used for different functions related to feeding.

Keywords

Metacarpal, function, mechanical advantage, and ungual.

INTRODUCTION

The Upper Cretaceous Nemegt Formation (upper Campanian – lower Maastrichtian) of Mongolia is one of the most fossiliferous formations in the world (Gradziński, 1970; Osmólska, 1980; Currie, 2016). Ornithomimosaurs are one of the most diverse theropod dinosaur groups and their remains are abundant within the formation (Hurum and Sabath, 2003; Makovicky et al., 2004). They are generally characterized by their medium to large body size, proportionately small skulls with large orbits, elongate forelimbs with weakly developed mani, and cursorially adapted powerful hind limbs (Osborn, 1917; Norell et al., 2001; Makovicky et al., 2004; Lee et al., 2014). To date, four definitive ornithomimosaurs have been described from the Nemegt Formation of Mongolia; namely, *Anserimimus planinychus* from Bügiin Tsav, *Deinocheirus mirificus* from Altan Uul III and IV, and from Bügiin Tsav, *Gallimimus bullatus* from most of localities of the Nemegt Formation, and a new ornithomimid (aff. *Anserimimus planinychus* Barsbold, 1988) from Tsagaan Khushuu (Kobayashi and Barsbold, 2006; Bronowicz, 2011), (Fig. 51). *Deinocheirus mirificus* belongs to the clade Deinocheiridae (Lee et al., 2014), and the other three are positioned within the cursorial clade Ornithomimidae (Makovicky et al., 2004).

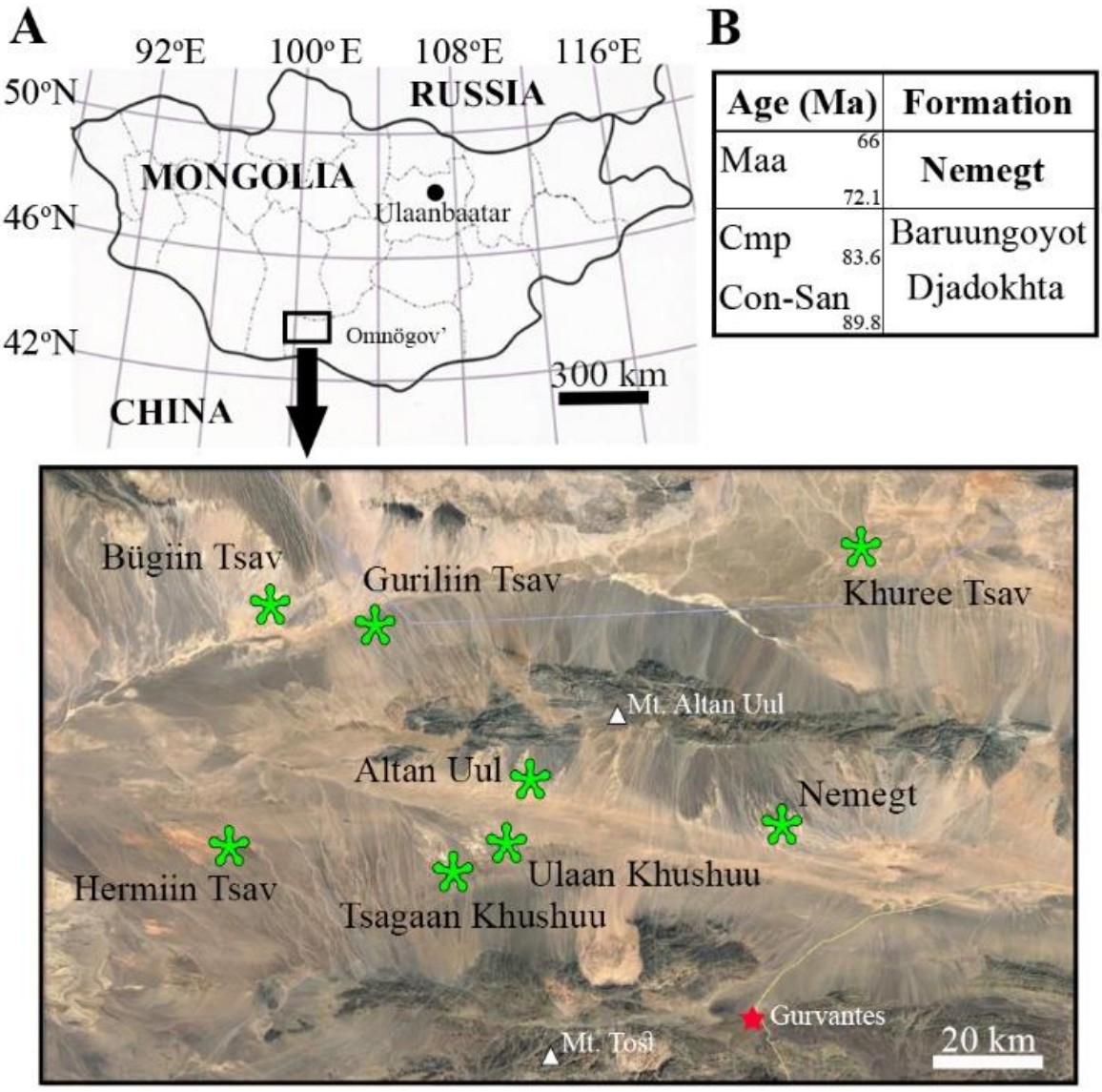

Figure-51. Position of the Nemegt Formation localities in the southwestern Gobi Desert. (A), Geographical map of the Nemegt Formation localities of the Gobi Desert, Mongolia, (B), Stratigraphic chart showing the Nemegt Formation (Cohen et al., 2017).

Although body designs of the cursorial ornithomimids are extremely similar, there are distinct differences in the hand structure (Kobayashi and Barsbold, 2006). In fact, the forelimb structures of ornithomimosaurs, specifically for derived ornithomimosaurs, are important for phylogenetic analysis (Kobayashi and Barsbold, 2006). Members of this group show high morphological variation in their manual structures, the phalangeal proportions and the shapes of their unguals, including curvature and robustness. These variations may be related to functional diversity (Osmólska et al., 1972; Nicholls and

Russell, 1981,1985; Makovicky et al., 2004; Kobayashi and Barsbold, 2005; Choiniere et al., 2012; Lee et al., 2014; Claessens and Loewen, 2015).

In the last few decades, intensive fieldwork at the Nemegt Formation localities have collected hundreds of isolated bones and several semi-articulated or articulated specimens of ornithomimosaurs. Additional species may be present in the Nemegt Formation based on the hand structure (e.g., the ornithomimid from Ulaan Khushuu locality, Kobayashi et al., 2010). Although previous studies have compared the structures and relative length proportions of ornithomimosaur hand elements, statistical analysis has not been conducted yet (Kobayashi and Barsbold, 2006). Here, morpho-functional differences among Nemegt ornithomimosaurs are demonstrated by qualitative morphological comparisons and by quantitative statistical analyses.

The purposes of this study are: 1) to describe manual elements of new specimens from the Nemegt Formation and compare them statistically; 2) to demonstrate the morphological disparity of Nemegt ornithomimosaurs within Ornithomimosauria.

MATERIALS AND METHODS

Specimen sampling

Measurements and the photographic dataset includes 26 specimens, containing 13 species, including 1 unnamed, but described specimen (Bissekty ornithomimid) and 7 undescribed specimens of ornithomimosaurs (Table-A6). Multiple specimens are used for *Gallimimus bullatus* (2), *Ornithomimus edmontonicus* (2), *Sinornithomimus dongi* (2), and *Struthiomimus altus* (3). The three named taxa from the Nemegt Formation are *Anserimimus planinychus* (MPC-D 100/300), *Deinocheirus mirificus* (MPC-D 100/18), and *Gallimimus bullatus* (MPC-D 100/11 and MPC-D 100/12). Among seven undescribed specimens, four are from the Nemegt Formation (MPC-D 100/121, MPC-D 100/133, MPC-D 100/134, and MPC-D 100/142) and three are from the Bayanshiree Formation (MPC-D 100/14, MPC-D 100/132, and MPC-D 100/202). The Bayanshiree Formation (Cenomanian-Turonian), exposed at the eastern Gobi Desert, is composed of fluvial deposits of a semi-arid environment (Martinson, 1982; Jerzykiewicz and

Russell, 1991) and is rich in dinosaur remains, including ornithomimosaurs (*Garudimimus brevipes* and undescribed taxa) (Kobayashi and Barsbold, 2005b; Kobayashi et al., 2009; Chinzorig et al., 2017).

Measurements were collected from all metacarpals and manual phalanges of each specimen using a digital caliper and a measuring tape, or from the literature. All figured photographs were taken with a Nikon digital camera, and figures were processed using the image editing software, Adobe Photoshop CS6 and Adobe Illustrator CS6.

Comparison of length proportions among metacarpals and phalanges

Measurements of available individuals were used for the comparison. To visualize the diversity of metacarpal proportions, the length ratios of metacarpals I through III (mcI, mcII, and mcIII) were plotted on a scatter-plot. A principal components analysis (PCA) of manual phalanges, excluding unguals (PhI-1, PhII-1, PhII-2, PhIII-1, PhIII-2, and PhIII-3) was conducted with log10-transformed measurements using R software (R Core Team, 2016), (Table 10).

Table-10. Summary of principal component analysis of log10-transformed phalangeal measurements.

	PC1	**PC2**	**PC3**	**PC4**
% explained	96.600	2.419	0.565	0.230
% after PC1		71.147	16.618	6.765
Eigenvector coefficient				
log10(PIx. I-1)	-0.412	0.161	-0.464	0.148
log10(PIx. II-1)	-0.403	0.592	0.210	0.575
log10(PIx. II-2)	-0.412	-0.302	0.048	-0.133
log10(PIx. III-1)	-0.410	0.338	-0.269	-0.703
log10(PIx. III-2)	-0.410	-0.164	0.763	-0.188
log10(PIx. III-3)	-0.402	-0.625	-0.289	0.316

Comparison of manual ungual shapes

Because ungual I exhibits a different shape from unguals II and III in some specimens, two analyses were performed (unguals II or III and ungual I). To quantify manual ungual shapes, two-

dimensional geometric morphometrics were performed with 4 landmarks and 12 sliding semi-landmarks that were digitized from lateral view using tpsDig v. 2.17 (Rohlf, 2013a). Four landmarks were chosen; the pointed tip of the ungual, dorsal and ventral extremities of the proximal articular surface, and at ventral extremity of the flexor tubercle. The coordinate data were subjected to generalized Procrustes analysis (Gower, 1975; Rohlf and Slice, 1990) and relative warp analysis in tpsRelw v. 1.53 (Rohlf, 2013b).

Mechanical advantage of unguals

Unguals were simplified as third-class levers because the flexor force is applied at a point between a fulcrum (midpoint of the proximal articular surface) and resistance point (ungual tip). The mechanical advantage of the ungual can be calculated as:

$$MA=\sin(\theta + \delta)\, d / a \quad (1)$$

In the equation (1), ***a*** is the output lever length from the point of the fulcrum to the resistance, ***d*** is the length from the point of the fulcrum to the flexor tubercle, ***θ*** is the angle of the input force vector to the line of output lever, and ***δ*** is the angle between the line from the point of the fulcrum to the flexor tubercle and the line of output lever (Ostrom, 1966) (Fig. 52). Therefore, MA is the ratio of input lever length to output lever length. The flexor force is hypothesized to be applied perpendicular to the articular surface of the unguals.

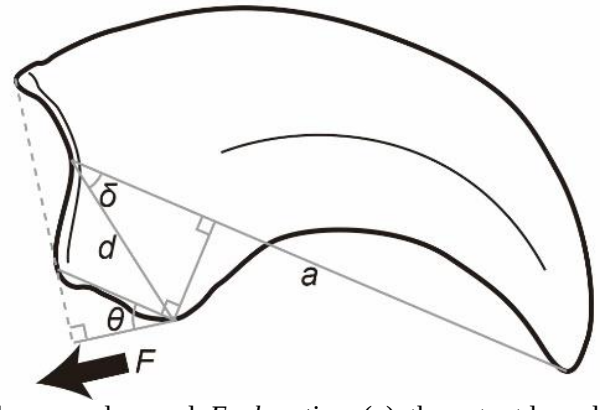

Figure-52. Schematic of the manual ungual. *Explanation:* (*a*), the output lever length from the point of the fulcrum to the resistance, (*d*), the length from the point of the fulcrum to the flexor tubercle, (*θ*), the angle of the input force vector to the line of the output lever, and (*δ*), and the angle between *d* and the line of the output lever.

Morphological disparity

To explore the contribution of the Nemegt ornithomimosaurs to the overall manual morpho-functional disparity of Ornithomimosauria, a partial disparity (Foote, 1993) of metacarpals, phalanges excluding unguals, and unguals were compared between two subgroups (Nemegt and non-Nemegt forms). Measurements of metacarpals and phalanges were log10-transformed, and a PCA was conducted. For metacarpals, a squared distance from the overall shape centroid was obtained by summing the squared PC2 and PC3 scores for each individual. This squared distance was summed over all individuals and divided by n–1 to obtain a partial disparity for each subgroup. Similarly, PC2 through PC6 scores for phalanges and partial warp scores from the geometric morphometrics of ungual shapes (Zelditch et al., 2004) were used to calculate the phalangeal and ungual partial disparities for the subgroups. Additionally, partial disparities of ungual function were measured using the mechanical advantage values.

GEOLOGICAL SETTING AND OCCURRENCES

The Upper Cretaceous Nemegt Formation (upper Campanian – lower Maastrichtian) is distributed at Altan Uul, Bügiin Tsav, Guriliin Tsav, Hermiin Tsav, Khuree Tsav, Nemegt, Tsagaan Khushuu, and Ulaan Khushuu localities (Gradziński et al., 1969, 1977; Efremov, 1954; Martinson, 1982; Jerzykiewicz and Russell, 1991; Eberth, 2018; Fanti et al., 2018), (Fig. 51). All of the ornithomimosaur specimens described herein were collected from three different localities of the Nemegt Formation in the Nemegt Basin: Tsagaan Khushuu (MPC-D 100/11), Altan Uul (MPC-D 100/18 and MPC-D 100/142), and Bügiin Tsav (MPC-D 100/133, MPC-D 100/134, MPC-D 100/121, and MPC-D 100/300).

The Nemegt Formation consists of a stacked succession of light grey-colored fining-upward alluvial deposits, including channel lag, channel fill, and sheet flood deposits (Gradziński et al., 1977; Eberth et al., 2009; Eberth, 2018; Fanti et al., 2018). It conformably overlies the Baruungoyot Formation (upper Campanian) through the interfingering interval of the Baruungoyot and Nemegt sedimentary facies (at least 23 m thick) (Eberth et al., 2009; Eberth, 2018; Fanti et al., 2018). The interfingering interval

suggests that the transition between the Baruungoyot (eolian) and the Nemegt (dominantly fluvial) environment was gradual (Gradziński and Jerzykiewicz, 1974; Eberth et al., 2009; Fanti et al., 2012, 2018; Eberth, 2018). Eberth, 2017, this volume demonstrated that the Nemegt Formation consists of three stratigraphic zones: Zone 5 (fluvial, seasonally wet-dry), Zone 6 (mixed fluvial lacustrine and paludal, mesic to seasonally wet-dry), and Zone 7 (fluvial and mesic) in ascending order. Bügiin Tsav is stratigraphically located in zones 6 and 7. The Nemegt Formation at Altan Uul crops out at four sub-localities (Altan Uul I, II, III, and IV). Altan Uul II (MPC-D 100/142) exposes zones 6 and 7, whereas Altan Uul III (MPC-D 100/18) shows mainly Zone 5. Tsagaan Khushuu has exposures of the upper Nemegt Formation and the Paleogene Naran-Bulak Formation, bounded by an unconformity. Therefore, all ornithomimosaur specimen in this study except MPC-D 100/18 were recovered from zones 6 and 7 although another specimen of *Deinocheirus* is known from Bügiin Tsav as well (Lee et al., 2014; Eberth, 2018).

DESCRIPTION

Metacarpals

Metacarpals (mcI, mcII, and mcIII) of ornithomimosaurs generally have the following features: metacarpal II longer than metacarpals I and III; robust metacarpal I; slender metacarpal III; proximally weakly arched metacarpals; a slightly concave or flat proximal articular surfaces of metacarpals; and proximally closely adherent to each other (Fig. 53). However, many other features such as the length ratios of metacarpals, the contact surfaces between metacarpals, the deviation and the rotation of the distal ends of metacarpals, and morphologies of the proximal and distal ends of metacarpals are different from each other.

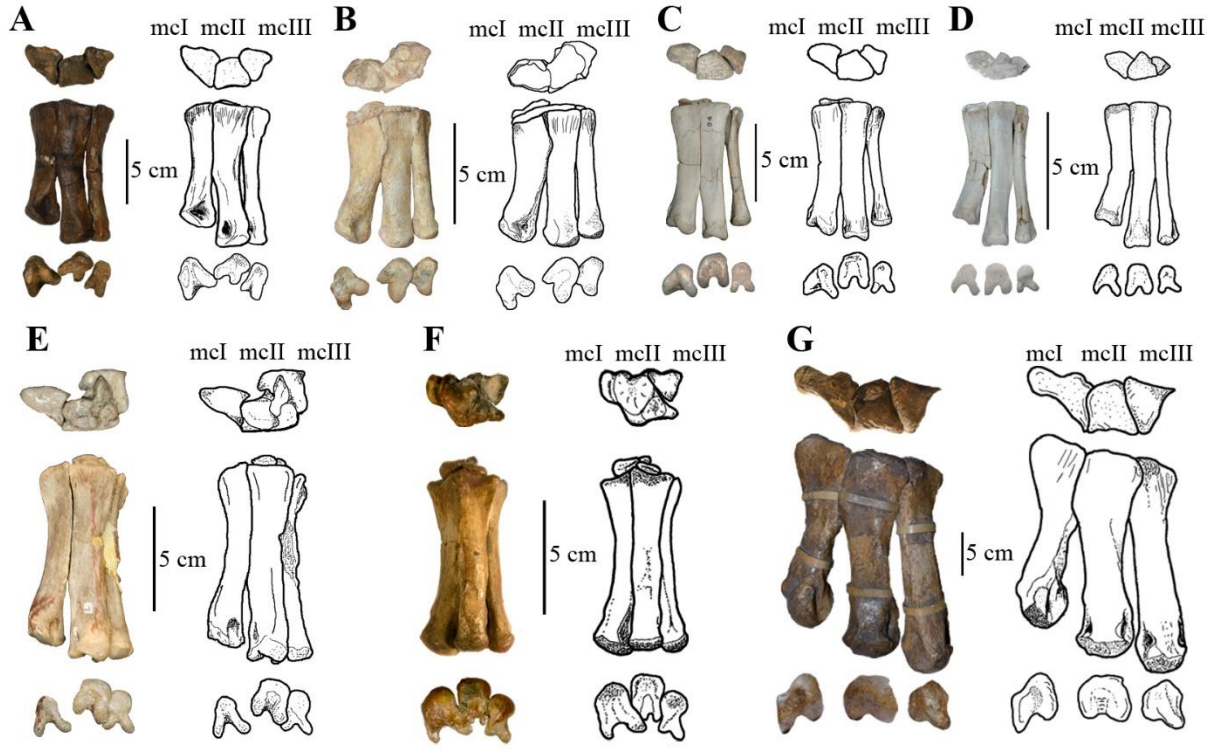

Figure-53. Metacarpals of the Nemegt ornithomimosaurs. (A), *Gallimimus bullatus* (MPC-D 100/11), (B), specimen MPC-D 100/142, (C), specimen MPC-D 100/134, (D), specimen MPC-D 100/133, (E), specimen MPC-D 100/121, (F), *Anserimimus planinychus* (MPC-D 100/300), and (G), *Deinocheirus mirificus* (MPC-D 100/18). *Explanation:* proximal, dorsal, and distal views (from top to bottom), (A-C, E), left metacarpals, (D, F, G), right metacarpals (reverse views). *Abbreviations*: see the list of abbreviations on page vi.

Length ratios of each metacarpal over the sum of all metacarpal lengths are plotted on a ternary diagram (Fig. 54A). Whereas *Deinocheirus mirificus* and MPC-D 100/133 have low ratios of metacarpal I, a high ratio is seen in *Anserimimus planinychus* and MPC-D 100/134 (Table-A6). Ratios of metacarpal III are similar in all of the Nemegt ornithomimosaurs except for the high ratio in *Deinocheirus mirificus* and the low ratio in MPC-D 100/134.

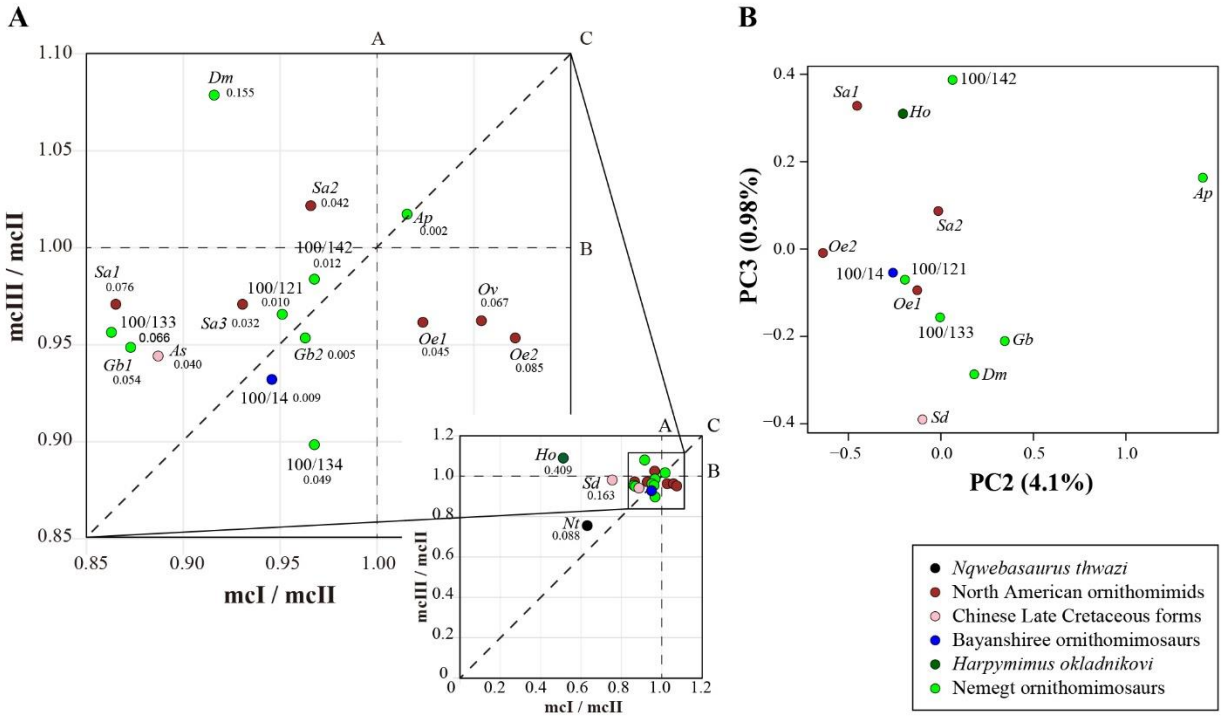

Figure-54. The length ratios of metacarpals and phalanges. (A), scatter plot of metacarpal I / II and metacarpal III/II length ratios. Dashed line A is where lengths of mc I and II are equal and dashed line B is when lengths of mc II and III are the same. Dashed line C is where mc I and III are equal. Numbers next to symbols for taxa represents distances from the dashed line C; (B), Principal components analysis of log10-transformed phalangeal measurements (excluding unguals). All other individuals are with specimen numbers of MPC-D. *Abbreviations*: see the list of abbreviations on page vi.

The contact surfaces between metacarpals are also different among Nemegt ornithomimosaurs (Fig. 53). While the contact surface between metacarpals I and II is less than a half the entire length of entire metacarpal I in *Deinocheirus mirificus*, it is approximately half the length in *Gallimimus bullatus*, MPC-D 100/133, and MPC-D 100/142 (Fig. 53A, B, D). In MPC-D 100/121 and MPC-D 100/134, this contact extends two-thirds the length of metacarpal I, whereas metacarpal I of *Anserimimus planinychus* is

attached along the entire metacarpal II (Fig. 53F). While metacarpals II and III are closely adherent each other in *Anserimimus planinychus*, *Gallimimus bullatus*, and MPC-D 100/121, only one third of the overall length of metacarpals II of *Deinocheirus mirificus* and MPC-D 100/142 articulate with metacarpal III (Fig. 53B, C, G).

Metacarpal I is strongly divergent medially compared with the lateral divergence of metacarpal III in all ornithomimosaurs. Whereas a large medial divergence of metacarpal I is found in *Deinocheirus mirificus*, *Gallimimus bullatus*, MPC-D 100/133, and MPC-D 100/142 (Fig. 53A, C, D, G), less medial divergence is observed in MPC-D 100/121 and MPC-D 100/134 (Fig. 53C, E). Metacarpal I of *Anserimimus planinychus* is also less medially divergent, but metacarpals I and II are contacted each other all their surfaces (Fig. 53F).

The proximal end of metacarpal II is usually trapezoidal in most ornithomimosaurs in proximal view. However, the proximal end of metacarpal II in MPC-D 100/133 is slightly triangular in cross section (Fig. 53D). Moreover, the proximodorsal edges of all metacarpals are straight in most Nemegt ornithomimosaurs in lateral view, except for *Anserimimus planinychus* whose proximodorsal edges are concave (Fig. 53F). In addition, the proximomedial corner of metacarpal I is also different from others, forming a squared corner. The proximal articular surface of metacarpal I of *Deinocheirus mirificus* extends largely medially unlike any of the other Nemegt ornithomimosaurs, and forms a round edge (Fig. 53G).

While distal articular surfaces of left metacarpal I of *Gallimimus bullatus* and MPC-D 100/142 are largely rotated medially, metacarpals II and III are rotated laterally (Fig. 53A, B). The degree of rotation of metacarpal I differs in other Nemegt ornithomimosaurs. For instance, metacarpals I of *Anserimimus planinychus* (right), *Deinocheirus mirificus* (right) and MPC-D 100/134 (left) are rotated medially, whereas metacarpals I of MPC-D 100/121 (left) and MPC-D 100/133 (left) lack of rotation (Fig. 53). However, metacarpals II and III are almost straight in all these ornithomimosaurs (Fig. 53C-G). The distal condyles of metacarpal I are unevenly developed, and the lateral condyle usually larger than the medial one. However, both condyles of MPC-D 100/121 and MPC-D 100/133 are equally developed in distal view (Fig. 53D, E). The intercondylar grooves of metacarpal I are deeper than other metacarpals in all

ornithomimosaurs. The lateral edge of distal metacarpal III is concave in *Anserimimus planinychus,* MPC-D 100/121, and MPC-D 100/134, whereas the concavity is shallow in *Deinocheirus mirificus, Gallimimus bullatus,* and MPC-D 100/142. Unlike any other Nemegt ornithomimosaurs, both metacarpals II and III of *Deinocheirus mirificus* have a narrow transverse ridges on the dorsal surfaces of the distal ends, and ligament fossae that are visible in dorsal view (Fig. 53G).

Digits

Ornithomimosaur digits (d1, d2, and d3) are generally characterized by their sub-equal in lengths, ginglymoid interphalangeal articulations of all phalanges except those of the first phalanges of the three digits (II-1, III-1, and IV-1), and elongated unguals (Makovicky et al., 2004).

Digits of the Nemegt ornithomimosaurs differ from each other by their robustness and length ratios. All phalanges of digits are generally robust and proximodistally straight in *Deinocheirus mirificus, Gallimimus bullatus,* and MPC-D 100/142 (Fig. 55A-C), whereas phalanges of *Anserimimus planinychus,* MPC-D 100/121, MPC-D 100/133, and MPC-D 100/134 are elongated and curved proximodistally (Fig. 55D-G).

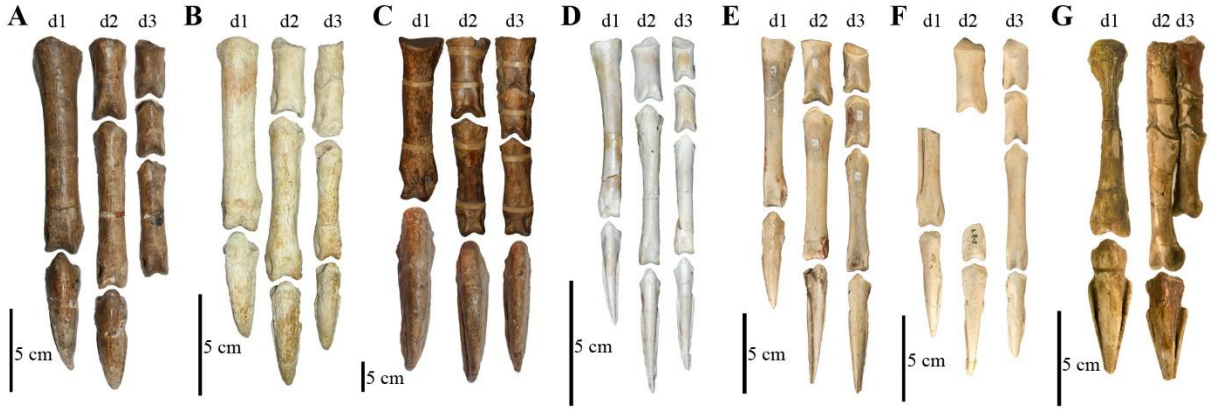

Figure-55. Phalanges of the Nemegt ornithomimosaurs in dorsal view. *Explanation:* (A), *Gallimimus bullatus* (MPC-D 100/11), (B), specimen MPC-D 100/142, (C), *Deinocheirus mirificus* (MPC-D 100/18), (D), specimen MPC-D 100/133, (E), specimen MPC-D 100/121, (F), specimen MPC-D 100/134, and (G), *Anserimimus planinychus* (MPC-D 100/300). *Abbreviations*: see the list of abbreviations on page vi.

The ratio of phalanx I-1 length to its proximal width ranges between 3.94 and 7.63. A high ratio is present in MPC-D 100/121 (7.63) and MPC-D 100/133 (5.68), because these specimens each have a long slender phalanx I-1 (Fig. 54D, E). On the other hand, a low ratio is seen in *Deinocheirus mirificus* (3.94), and *Gallimimus bullatus* (4.24), as these specimens each have a massive phalanx I-1 (Fig. 55A, C). The length ratios of phalanges II-2 to II-1 range between 1.39 and 2.73 (Table-A6). The ratio is approximately two in *Gallimimus bullatus* (2.11) and MPC-D 100/142 (2.04). Two specimens (MPC-D 100/121 and MPC-D 100/133) show high ratios (2.56 and 2.73, respectively), because of the elongated phalanx II-2. It is a low in *Deinocheirus mirificus* (1.52), which has a short phalanx II-2, and *Anserimimus planinychus* (1.39), which has an elongate phalanx II-1.

Unguals

Unguals of ornithomimosaurs generally have the following variable features; degree of curvature and elongation, depths of grooves, outline and degree of concavity on the articular surface, and position of the flexor tubercle.

Morphologies of ungual I vary within Nemegt ornithomimosaurs (Fig. 56). Based on the shape of ungual I, four different types of unguals are recognized in ornithomimosaurs. The first manual unguals of *Gallimimus bullatus*, MPC-D 100/121, and MPC-D 100/142 are robust, strongly curved, have shallow grooves and distally positioned flexor tubercles (Figs. 55A, B, E; and 56A, C, F). In contrast, MPC-D 100/133, and MPC-D 100/134 are less strongly curved, have shallower grooves, and have elongate first unguals with distally positioned flexor tubercles (Figs. 55D, E; and 56B, C). While *Deinocheirus mirificus* has a strongly curved, mediolaterally compressed, shallowly grooved ungual I with a proximally positioned flexor tubercle, *Anserimimus planinychus* has a straight, and dorsoventrally flattened ungual I with a distally positioned flexor tubercle and strong grooves (Figs. 55G; and 56A, G). The shapes of unguals II and III are similar to each other in ornithomimosaurs. MPC-D 100/121, MPC-D 100/133, and MPC-D 100/134 have elongate, less curved unguals II and III with distally positioned flexor tubercles in lateral view.

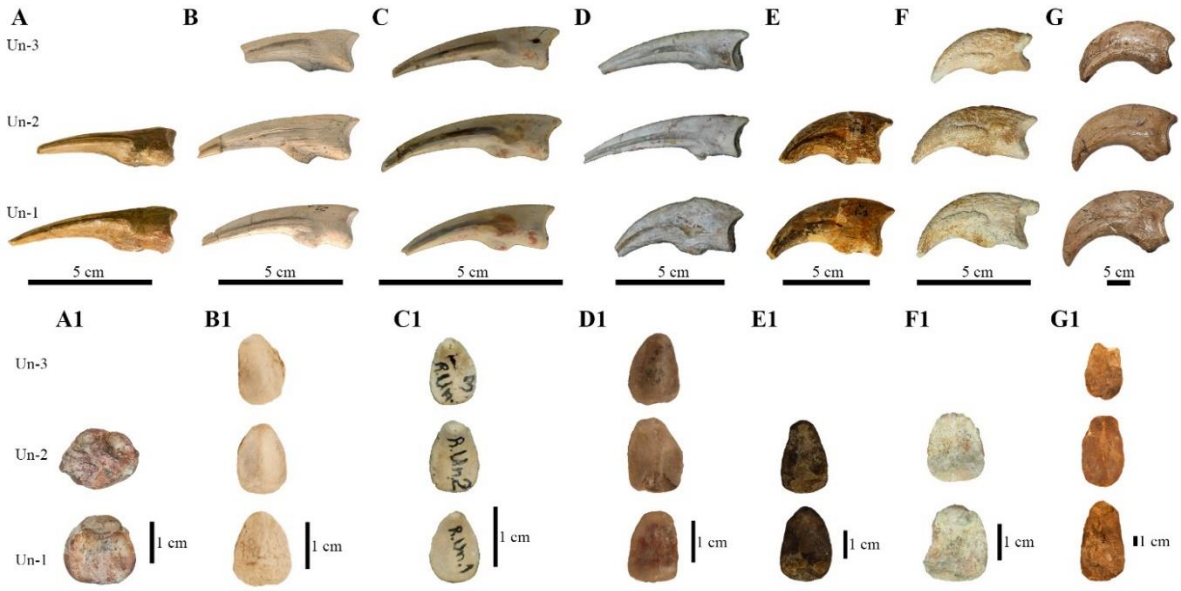

Figure-56. Unguals of the Nemegt ornithomimosaurs. (A, A1), *Anserimimus planinychus* (MPC-D 100/300), (B, B1), specimen MPC-D 100/134, (C, C1), specimen MPC-D 100/133, (D, D1), specimen MPC-D 100/134, (E, E1), *Gallimimus bullatus* (MPC-D 100/11), (F, F1), specimen MPC-D 100/142, and (G, G1), *Deinocheirus mirificus* (MPC-D 100/18). *Explanation:* (A-G), lateral view and (A1-G1), proximal view. *Abbreviations*: see the list of abbreviations on page vi.

However, those of *Deinocheirus mirificus*, *Gallimimus bullatus,* and MPC-D 100/142 are robust, strongly curved, and bear shallow grooves (Fig. 56). Specimen MPC-D 100/121 is different from any Nemegt ornithomimosaur in having a strongly curved ungual I and elongated unguals II and III (Fig. 56D). Ungual I of MPC-D 100/121 is similar to those of *Gallimimus bullatus* and MPC-D 100/142, but its unguals II and III are elongate and resemble unguals II and III of MPC-D 100/133 and MPC-D 100/134 (Fig. 56D). While articular surfaces of Nemegt ornithomimosaur unguals are generally oval (taller than wide) with weakly developed sagittal ridges along the midline (Fig. 56B1-G1), the unguals of *Anserimimus planinychus* have round articular surfaces and the articular surfaces are wider than high (Fig. 56A1). The height/width ratio of ungual I of *Anserimimus planinychus* is the lowest (0.93), and the length/height ratio among other ornithomimosaurs is the highest (4.01) as previously suggested by Kobayashi and Barsbold, (2006), (Fig. 56A1-G1, Table-A6).

Quantitative comparisons and analyses

Metacarpal and phalangeal variations among ornithomimosaurs

A scatter-plot (Fig. 54A) shows two basal ornithomimosaur taxa (*Nqwebasaurus thwazi* and *Harpymimus okladnikovi*) and *Sinornithomimus dongi* are unique in that each has a relatively short metacarpal I. Other taxa, including the Nemegt ornithomimosaurs, are represented as a large cluster. Among the type specimens of the Nemegt forms, *Anserimimus planinychus* (*Ap*) has metacarpals I and III, which are sub-equal in length and are longer than metacarpal II. *Deinocheirus mirificus* (*Dm*) has a long metacarpal III and the highest ratio of mc III/mcII among the Nemegt ornithomimosaurs. *Gallimimus bullatus* (*Gb*1) forms a cluster with MPC-D 100/133 by having metacarpal III shorter than metacarpal II but longer than metacarpal I. Metacarpal II of the paratype specimen of *Gallimimus bullatus* (*Gb*2) is the longest among metacarpals, and metacarpals I and III are nearly equal in length. MPC-D 100/121 and MPC-D 100/142 are placed close to the *Gallimimus bullatus* paratype, but metacarpal III is slightly longer than metacarpal I. MPC-D 100/134 is unique among the Nemegt ornithomimosaurs because its metacarpal I is significantly longer than metacarpal III.

PCA for the phalangeal dataset shows the morphological diversity of phalanges of the Nemegt ornithomimosaurs (Fig. 54B). The summary of PCA of log-10 transformed phalangeal measurements can be found in Table-10. PC1 (94.4%) is attributed to the size variation, while PC2 (4.01%) and PC3 (0.98%) are largely attributed to the non-size variations. PC2 and PC3 explain 72.7% and 17.4 % of the non-size variation, respectively. The eigenvector coefficients of six variables suggest that individuals with high PC2 scores have a relatively long phalanx II-1 and III-1 and short phalanx II-2, III-2, and III-3, while those with high PC3 scores have a short phalanx I-1 and II-2 and long phalanx II-1 and III-2. The bivariate plot of PC2 and PC3 scores shows that *Anserimimus planinychus* plots far apart from others on the positive extremity of the PC2 axis, indicating its uniqueness in manual digit proportions among ornithomimosaurs. Other Nemegt ornithomimosaurs are greatly dispersed in the morphospace on both PC2 and PC3 axes.

Manual ungual morpho-functional variation among ornithomimosaurs

Geometric morphometrics of unguals II or III demonstrate that more than 80% of the total shape variation is explained by the first two relative warps (RWs) (Fig. 57). RW1 (64.5%) is related to the lengths and depths of unguals, while RW2 (17.9%) reflects the curvatures of unguals and the positions of the flexor tubercles. Nemegt ornithomimosaurs occupy nearly the entire morphological breadth of the RW1 axis. Individuals with slender unguals are placed on the positive side of RW1, while those with deep unguals are positioned on the negative side. Nemegt forms are also diverse on RW2, where individuals with similar RW1 scores (e.g., *Deinocheirus mirificus* and *Gallimimus bullatus*) are distantly placed from each other on RW2, indicative of their differences in ungual curvature and the positions of the flexor tubercles. The geometric morphometrics of ungual I also showed that most of the shape variations are related to the lengths and depths of unguals (RW1: 63.6%), and curvatures and the positions of the flexor tubercles (RW2: 18.9%) (Fig. A3).

The RW1 scores and the mechanical advantage (MA) of unguals II or III are significantly correlated (adjusted $R = 0.727$, $p < 0.001$, $n = 19$) (Fig. 58). *Deinocheirus mirificus*, *Gallimimus bullatus*, and MPC-D 100/142 are similar in having low RW1 scores and high MA. Among Nemegt forms, four specimens (*Anserimimus planinychus*, MPC-D 100/121, MPC-D 100/133, and MPC-D 100/134) are placed close to each other with high RW1 scores and low MA. All of the Nemegt ornithomimosaurs are plotted within 95% prediction intervals. It is noteworthy that MPC-D 100/142 is placed close to the lower limit of the 95% prediction interval. RW2 scores are not correlated with MA (adjusted $R = -0.051$, $p = 0.734$, $n = 18$).

Manual morpho-functional disparity of Nemegt ornithomimosaurs

The partial disparity (PD) of Nemegt ornithomimosaurs contributes to 14.7% of the overall morphological disparity of ornithomimosaur metacarpal lengths (Table-11). However, when two morphologically distinct basal taxa (*Nqwebasaurus thwazi* and *Harpymimus okladnikovi*) were excluded, Nemegt forms contribute 32.4% of the total disparity among the derived ornithomimosaurs. The Nemegt

forms contribute to approximately half of the total PD of the lengths of phalanges excluding unguals (68.7%) and ungual shapes (49.9%), and mechanical advantage of unguals (56.0%).

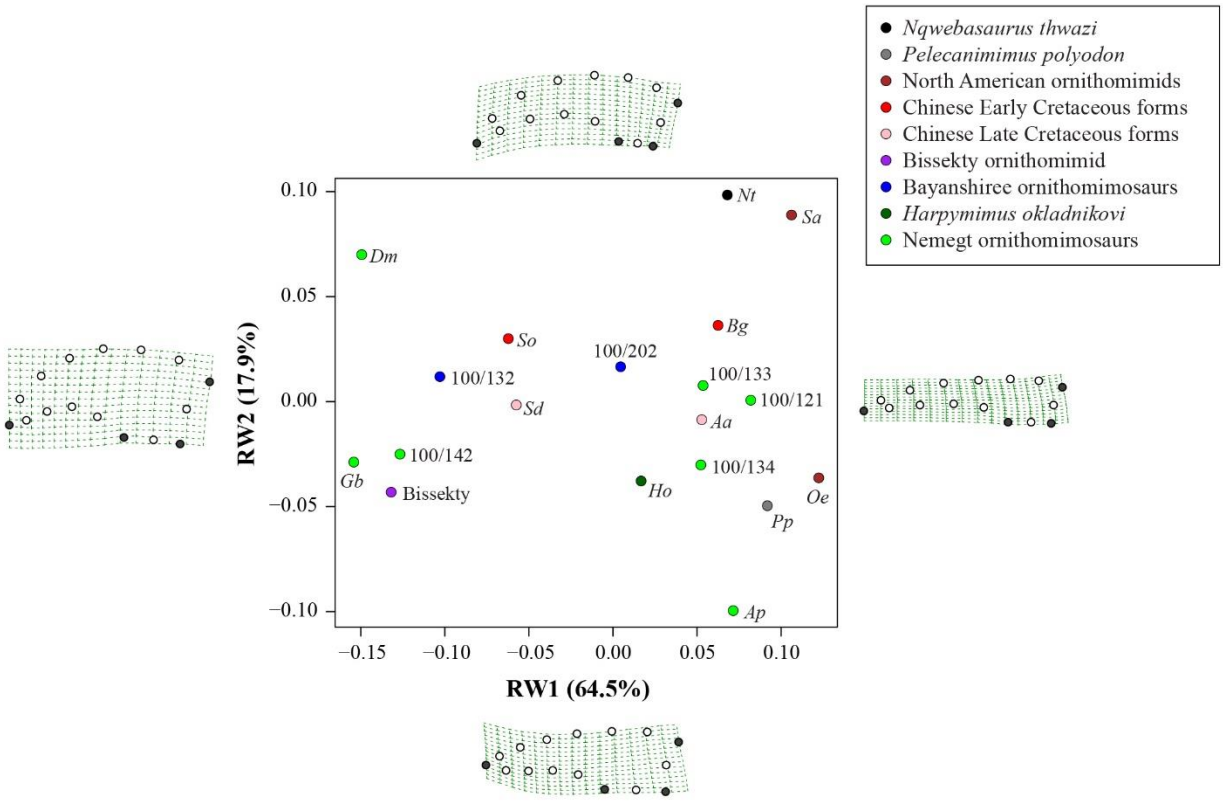

Figure-57. Geometric morphometrics of unguals II (or III). All other individuals are with specimen numbers of MPC-D. *Abbreviations*: see the list of abbreviations on page vi.

Table-11. Partial disparity (PD) and its percentage of overall morpho-functional disparity for Nemegt and non-Nemegt ornithomimosaurs. MA, mechanical advantage. Note that: a number in parenthesis is sample size for each subgroup.

Classification of forms	Metacarpal lengths	Phalangeal lengths (without unguals)	2nd or 3rd ungual shape	2nd or 3rd ungual MA
Nemegt forms PD	0.019 (7)	0.247 (7)	0.006 (7)	0.079 (7)
Non-Nemegt forms PD	0.13 (8)	0.19 (5)	0.006 (12)	0.062 (12)
Nemegt forms %	12.5	56.5	49.9	56.0
Non-Nemegt forms PD (excluding *Nqwebasaurus* and *Harpymimus*)	0.031 (6)	–	–	–
Nemegt forms % (excluding *Nqwebasaurus* and *Harpymimus*)	37.7	–	–	–

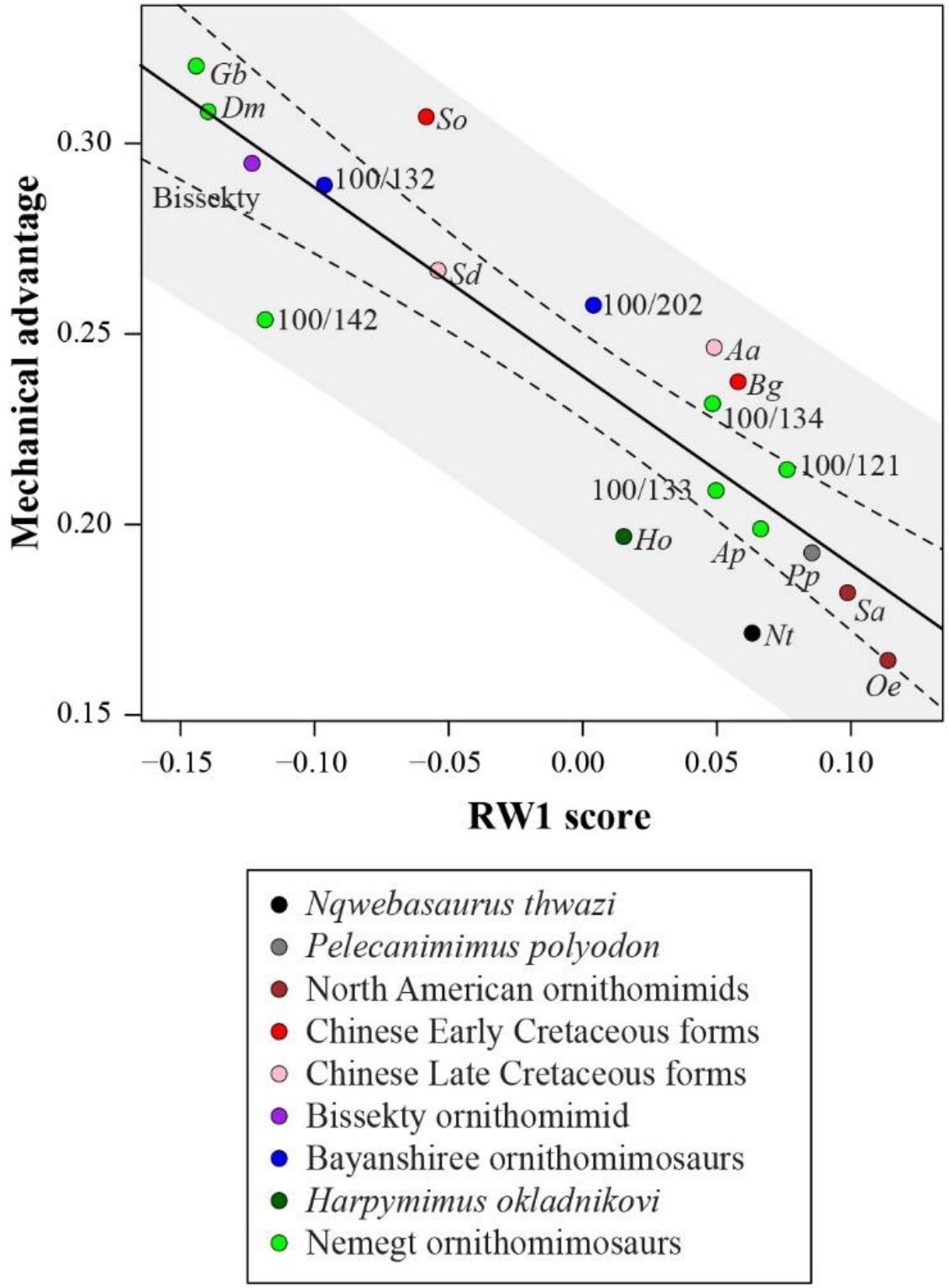

Figure-58. Relationship of ungual II or III shapes (RW1 scores) and mechanical advantage obtained from the geometric morphometrics. An ordinary least squares line is fit on the plots. *Abbreviations*: see the list of abbreviations on page vi.

DISCUSSION

Manual morphological variations and functional implications

The comparisons of Nemegt ornithomimosaur hands revealed that manual structures of three known taxa and four new individuals are distinct from each other. Morphological diversity of ornithomimosaur hands is discussed here, along with their possible functional implications.

The cluster of derived ornithomimosaurs in the scatter-plot diagram reflects the character used in the phylogenetic analysis (showing "sub-equal metacarpals" [Makovicky et al., 2004]) (Fig. 54A). At the same time, this diagram shows variations in the relative metacarpal lengths of Nemegt ornithomimosaurs within the cluster and can be categorized into five types: (1) *Anserimimus planinychus*, (2) *Deinocheirus mirificus*, (3) the holotype of *Gallimimus bullatus* and MPC-D 100/133, (4) the paratype of *Gallimimus bullatus*, MPC-D 100/121, and MPC-D 100/142, and (5) MPC-D 100/134. *Anserimimus planinychus* (type 1) shares with all specimens of *Ornithomimus* a long metacarpal I and with *Deinocheirus mirificus* and one of the specimens of *Struthiomimus altus* a long metacarpal III; however, the combination of short metacarpals I and III is unique among all ornithomimosaurs. Among derived ornithomimosaurs, *Deinocheirus mirificus* (Type 2) has the highest length ratio of mc II/mc III and the greatest difference in length between mcI and mcIII. The holotype of *Gallimimus bullatus* represents type 3 and has shorter metacarpals I and III than metacarpal II where metacarpal I is slightly shorter than metacarpal III as in the holotype of *Struthiomimus altus* (*Sa1*) and *Archaeornithomimus asiaticus* (*Aa*). The paratype of *Gallimimus bullatus*, type 4, is similar to type 3 in the length ratio of mc III/mc II but different because metacarpals I and III are nearly equal as seen in *Anserimimus planinychus*. Lastly, MPC-D 100/134 (type 5) is unique among the Nemegt ornithomimosaurs because it has metacarpal I longer than metacarpal III. This condition is present in *Ornithomimus edmontonicus* (*Oe1* and *Oe2*) and *Ornithomimus velox* (*Ov*) but MPC-D 100/134 (type 5) differs from *Ornithomimus* in having short metacarpal I. The distribution of these

five types on the scatter-plot diagram indicates that the Nemegt ornithomimosaurs had more variations and a wider range of metacarpal morphology than North American taxa.

For phalanges, the high PC2 score of *Anserimimus planinychus* demonstrates that this taxon is distinct in having relatively elongated proximal phalanges (PhII-1 and PhIII-1) and reduced distal phalanges (PhII-2, PhIII-2, PhIII-3) among the Nemegt ornithomimosaurs (Fig. 55G, Table-A6). The elongation of phalanx I-1 in each of *Deinocheirus mirificus*, *Gallimimus bullatus*, and MPC-D 100/133 is demonstrated by low PC3 scores, which might be correlated with their short first metacarpals. Short metacarpals with longer digits would allow the tip of the digit to move longer distances with the same extension/flexion angles. Therefore, the first digits of these taxa might be utilized for any work that requires longer reach and wider range of movements.

The geometric morphometric analyses show that Nemegt ornithomimosaurs exhibit large variation in ungual shapes by occupying a broad range of RW1 scores for both unguals I and II or III. MPC-D 100/121 is unique within the Nemegt ornithomimosaurs in having a robust ungual I (low RW1 score) and slender unguals II and III (high RW1 score) (Figs. 57, 59, and S3, Table-A6). This resembles the basal ornithomimosaur *Harpymimus okladnikovi* (Fig. 55E). Meanwhile, the general configuration of the manus is similar to that of *Struthiomimus altus* (Nicholls and Russell, 1985). The slightly divergent metacarpal I and sub-equal metacarpals II and III in MPC-D 100/121 also resemble the derived ornithomimosaur MPC-D 100/14 (Kobayashi and Barsbold, 2005). The divergences between digit I and digits II and III in each of these two specimens is wide when the manus is extended, whereas they become parallel when the manus is fully flexed. Likewise, extension and flexion movements may be determined in MPC-D 100/121 based on its manual structure. Moreover, hooking and clamping functions can be proposed in both *Struthiomimus altus*, *Gallimimus bullatus*, and the derived ornithomimosaur MPC-D 100/14 (Nicholls and Russell, 1985; Kobayashi and Barsbold, 2005), which suggests that the manual condition of MPC-D 100/121 might allow similar functions.

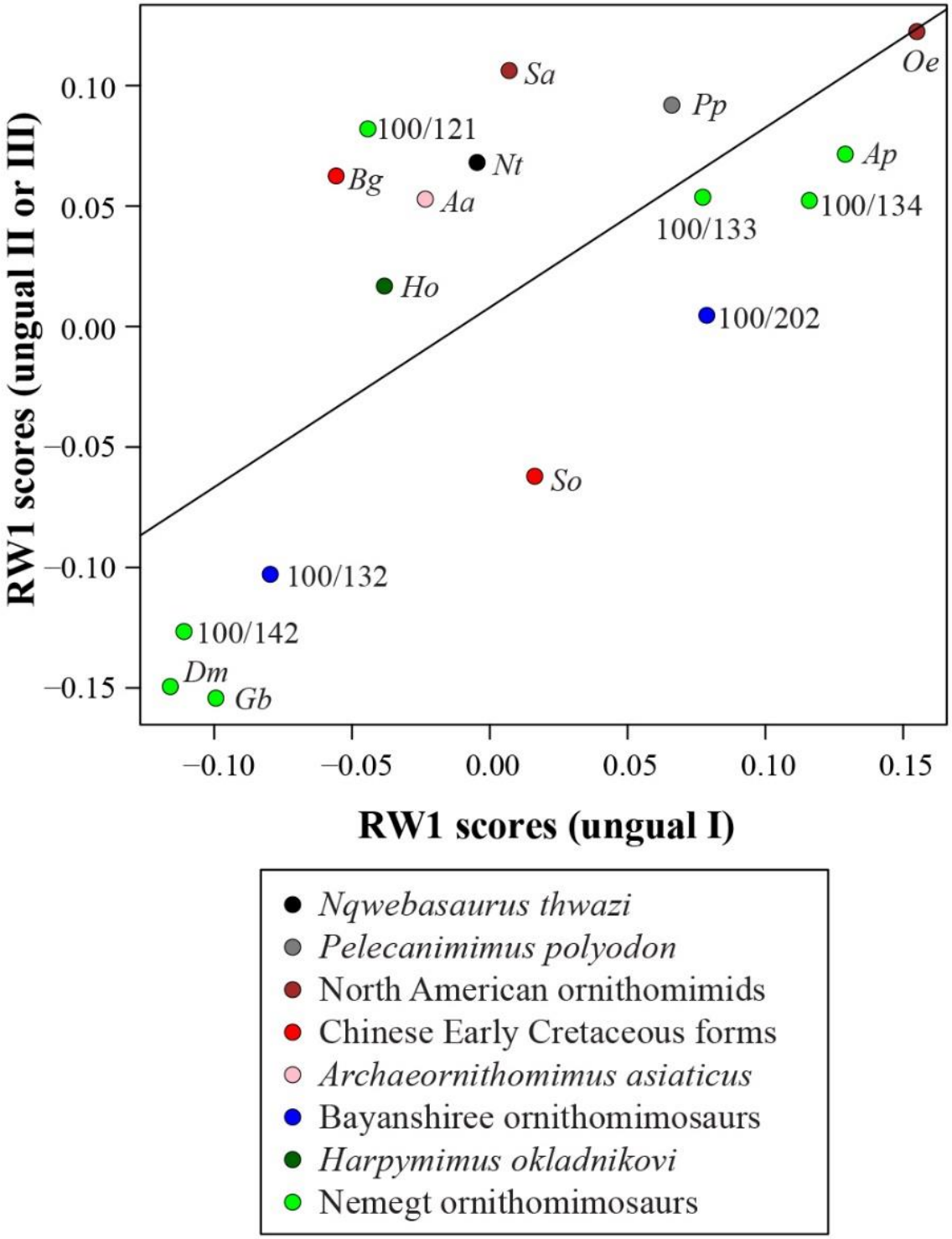

Figure-59. Correlation of RW1 scores (ungual I) versus RW1 scores (unguals II or III). *Abbreviations*: see the list of abbreviations on page vi.

The correlations between RW1 scores (ungual massiveness) and MA values (efficiency of output force relative to input force) of unguals I and II or III may suggest that the variations of ungual morphologies are the result of functional convergences, but are not phylogenetically relevant as previously suggested in Kobayashi and Barsbold (2006). Meanwhile, some specimens have exceptionally high/low MA values relative to their RW1 scores (Figs. 58 and S4). MPC-D 100/142 is one of those exceptions: although RW1 scores of its unguals I and II are comparable to those of *Deinocheirus mirificus* and *Gallimimus bullatus*, the unguals show low RW1 scores (95% prediction intervals in ungual I and 95% confidence intervals in ungual II). The difference likely reflects the weak development of the flexor tubercles of MPC-D 100/142 (Fig. 56F). On the contrary, the well-developed flexor tubercle of ungual II of MPC-D 100/134 (Fig. 56B) is likely to have contributed to its high MA despite its slender outline (outside of 95% confidence intervals). Ungual II of MPC-D 100/121 also has a similarly developed flexor tubercle and shows a high MA value relative to its RW1 score, although it is positioned within the 95% confidence interval (Fig. A4). Although robustness and slenderness of the ungual is the primary factor of determining MA, the results suggest that degree of development of the flexor tubercle also affects MA value. Because the flexor tubercle is the attachment point of the flexor digitorom longus (Burch, 2014), a well-developed flexor tubercle increases not only output/input force efficiency, but also provides a larger muscle attachment surface. Therefore, the unguals with high MA values are likely to be utilized for producing large forces compared to the unguals with low MA values.

Barsbold (1988) proposed that the "nonprehensile" manus of *Anserimimus* was not well adapted for obtaining foods or direct attacks on its prey. Instead, the hoof-like manual unguals of *Anserimimus planinychus* were better adapted to scraping off relatively light and loose objects (Barsbold, 1988), which is concordant with the low MA values of unguals I and II (Figs. 58 and S4). The two taxa with high MA values of the unguals, *Deinocheirus mirificus* and *Gallimimus bullatus*, have been interpreted to have limited ranges of motion. Functional interpretations in these two taxa are tearing and gathering for *Deinocheirus mirificus* and digging and "raking" for *Gallimimus bullatus* and *Deinocheirus mirificus*, but the interpreted functions are expected to require high MA values in order to accomplish some functions.

The blunt tips of the pedal unguals and preserved stomach contents (fish remains) of *Deinocheirus mirificus* suggest that it frequented freshwater habitats (Lee et al., 2014). The long forearms with giant unguals of *Deinocheirus mirificus* have been interpreted as useful for digging and gathering herbaceous plants. It is presumed that high MA values of unguals in *Deinocheirus mirificus* might reflect its ability to pull out substantial quantities of herbaceous plants from the water and to decrease water resistance. Although the manus configuration of MPC-D 100/142 is similar to that of *Deinocheirus mirificus*, rotational abilities of distal metacarpals, the length of metacarpal III, and a low MA are different (Fig. 53B, G). These suggest that MPC-D 100/142 might have had a different mode of life from *Deinocheirus mirificus*.

CHAPTER VI

PHYLOGENY OF ORNITHOMIMOSAURIA

Phylogenetic analysis is tested in this chapter in order to determine synapomorphies of Ornithomimosauria and to resolve phylogenetic relationships of members of Ornithomimosauria. In order to resolve the relationships between the members of Ornithomimosauria, we performed a phylogenetic analysis using a character list of Kobayashi and Lü (2003), (Supplementary Data S4A). A matrix of 21 terminal taxa and 17 cranial and 21 postcranial characters was constructed (Supplementary Data-S4B) and the data matrix was analyzed using the software program TNT ver.1.5 (Goloboff et al., 2016). *Allosaurus fragilis* was chosen as outgroup, and the characters were weighted equally followed by 100 replicate random addition traditional search with TBR (tree bisection and reconnection branch), holding 10 trees at each replicate and a memory of 1000. The analysis produced 20 most parsimonious trees with a tree length of 86 steps, a consistency index of 0.477, and a retention index of 0.654. The strict consensus tree was obtained of 106 steps with a consistency index of 0.387 and a retention index of 0.500.

The result of a phylogenetic analysis recovered by this study shows that the basal taxa, *Pelecanimimus polyodon, Harpymimus okladnikovi, Garudimimus brevipes,* and a clade of *Deinocheirus mirificus* and *Shenzhousaurus orientalis* are well-supported (Fig. 60). The monophyly of Ornithomimidae has been supported previously by a number of characters (Barsbold and Osmólska, 1990; Kobayashi and Lu, 2003). A clade of Ornithomimidae supports six unambiguous synapomorphies in the present analysis. In the cladogram, *Aepyornithomimus tugrikinensis,* Bügiin ornithomimid, and BTs ornithomimosaur bonebed specimens are positioned within Ornithomimidae. Our phylogenetic analysis suggests two clades Late Cretaceous ornithomimids (Mongolian and North American clades) in the Ornithomimidae. Although similar result is also reported in the study of Kobayashi and Lu (2003), the involvement of taxa are different. While a clade of BTs ornithomimosaur bonebed specimens shares five unambiguous synapomorphies (offset laterally from line of the posterior process of the infraglenoid buttress of the coracoid is (23), strong deltopectoral crest of the humerus (25), larger ulnar condyle of the humerus than the radial condyle (26), medially rotated distal condyle of the metacarpal I (29), and distinct condyles with ginglymoid articulation of the distal end of metacarpal I (30)), a North American clade shares only one unambiguous synapomorphic character, the ventral border of pubic boot is strongly convex with ventral

expansion (35). *Aepyornithomimus tugrikinensis,* and Bügiin ornithomimid are nested in the cladogram as a monophyly. Bügiin ornithomimid supports five unambiguous synapomorphies, such as presented series of foramina along the ventral border of lateral surface of maxilla (5), anteroposterior lengths of cervical neural spines is more than one-third of neural arch lengths (19), medially rotated distal condyle of the metacarpal I (29), and the ventral border of pubic boot is strongly convex with ventral expansion (35).

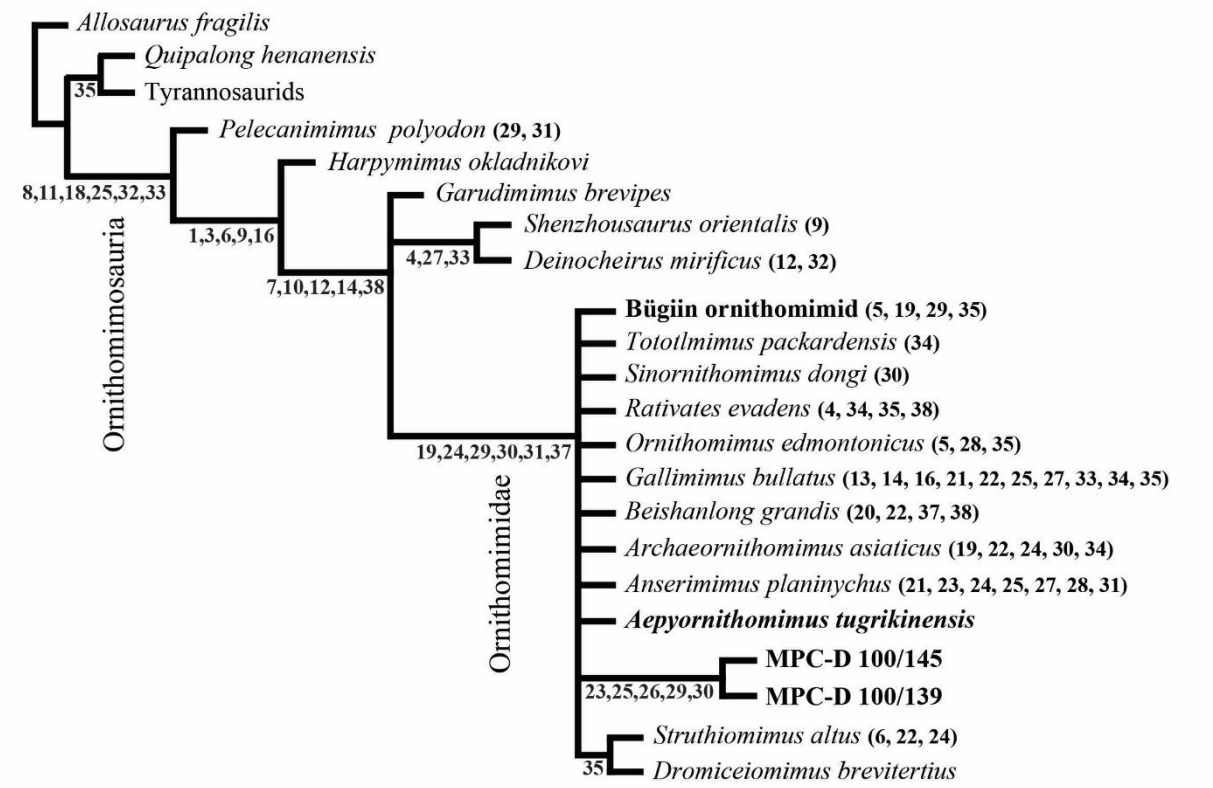

Figure-60. Strict consensus tree of members of Ornithomimosauria after modified Kobayashi and Lü, (2003). Note that: numbers are synapomorphic characters.

CHAPTER VII

PALEOBIOGEOGRAPHY AND PALEOECOLOGY

Paleobiogeography

The complex paleobiogeographic history of ornithomimosaur dinosaurs in the Late Cretaceous is poorly understood, with evolutionary trend gaps. While the records of poorly documented possible ornithomimosaur specimens are reported from the early Late Cretaceous of North America and the well-known Campanian-Maastrichtian taxa are recorded abundantly in North America (Gilmore, 1920; Ostrom, 1970), the "Middle" to Late Cretaceous ornithomimosaur records are contrary to poorly documented from Asia, in which is left unfilled evolutionary gap, instead (Osmólska, 1980a; Currie, 2000; Makovicky et al., 2004). On the other hand, the presence of known vertebrate records both in Mongolia and North America indicates that a high degree of endemism persisted in these regions during Cretaceous time, which has been considered as one of substantial intercontinental interchange (Jerzykiewicz and Russell, 1991).

The recent increasing number of fossil discoveries suggests that ornithomimosaurs were highly diversified during the Late Cretaceous of central Asia and western North America (Makovicky et al., 2004). To date, twenty-two valid species within twenty-one genera have been assigned to Ornithomimosauria (Makovicky et al., 2004, 2009; Buffetaut et al., 2009; Choiniere et al., 2012; Lee et al., 2014; McFeeters et al., 2016; Brownstein, 2017; Chinzorig et al., 2017b; Sereno, 2017; Ian Macdonald and Currie, 2018). Among all of the known taxa, fourteen of them are known from the Late Cretaceous and their fossil occurrences are commonly recovered from the Upper Cretaceous sediments of Asia and North America. North American derived ornithomimosaurs (*Dromiceiomimus, Ornithomimus, Rativates,* and *Struthiomimus*) have been restricted between the lower Campanian and the upper Maastrichtian, indicative of a diversity of ornithomimosaurs in this time bin. In contrast, derived ornithomimosaurs (*Anserimimus, Deinocheirus,* and *Gallimimus*) in Mongolia seem to be more diversely found in the Upper Cretaceous sediments, ranging from the Bayanshiree Formation (Cenomanian-Turonian) to the Nemegt Formation (upper Campanian-lower Maastrichtian), (Currie, 2000). However, ornithomimosaurs from the Campanian is extremely rare in Mongolia (Makovicky et al., 2004). Although Kobayashi and Lü (2003) and subsequent authors using a modified version of the phylogenetic analysis suggested that Asian ornithomimids are basal taxa of the clade, which supports that an Asian origin of ornithomimosaurs (Xu et

al., 2011; Cullen et al., 2013; Lee et al., 2014). However, it becomes questionable arguments by other workers, particularly when it comes to more basal members discovered in Europe and Africa (Perėz-Moreno et al., 1994; Choiniere et al., 2012). Moreover, some workers have suggested that the unique Mongolian taxon, *Anserimimus*, is more closely related to the North American taxon, *Ornithomimus*, requiring either separate migrations from Asia for the ancestors of *Ornithomimus* and *Struthiomimus*, or a migration of the ancestor of *Anserimimus* back to Asia from Laramidia.

A complex paleobiogeographic aspect involving multiple dispersals between the Asia and North America continents that has been supported for several Late Cretaceous dinosaur clades, including hadrosauroids, dromaeosaurids (Evans et al., 2013; Tsogtbaatar et al., 2014). Makovicky et al. (2004) proposed that the derived monophyletic clade (*Struthiomimus* and *Ornithomimus*) from North America accounted for at least one dispersal event from Asia to North America across Beringia. Alternatively, one more dispersal event probably occurred into North America or a back to Asia if *Ornithomimus* and *Struthiomimus* are not immediate sister taxa (Makovicky et al., 2004). In addition, one widely accepted palaeobiogeographic analyses of ornithomimosaurs is suggested by Kobayashi and Barsbold (2004) that supported an Asian origin for Ornithomimidae and had occurred a single dispersal events of ornithomimids from Asia into North America during, or prior to, the Campanian.

The following hypothesis proved that King and Jones hypothesis (1997), in which they proposed as North American ornithomimids first appeared in Appalachia, and then spread out from there in the Laramidia during the mid-Campanian. Based on patterns of the most parsimonious trees of the phylogeny of *Aepyornithomimus tugrikinensis*, dispersal event of Ornithomimidae was probably occurred in two directions (from Asia to North America and back to Asia from North America) across Beringia in during Late Cretaceous (Fig. A1A, B). Tree topologies suggest two possibilities. The second and the third patterns show a monophyly of North American taxa (*Ornithomimus* and *Struthiomimus*), suggesting a single dispersal by the Campanian (Fig. A1B, C). Two dispersal events with two scenarios are implied by the first and the fourth patterns because *Aepyornithomimus tugrikinensis* is nested together with North American taxa (*Ornithomimus* and *Struthiomimus*), and *Struthiomimus* is a sister taxon to *Aepyornithomimus*

tugrikinensis (Fig. A1A, D). One scenario is that the first dispersal event was occurred from Asia to North America during Campanian time, and the second dispersal event was returned from North America to Asia by the lineage of *Aepyornithomimus tugrikinensis*. The other scenario is two independent dispersals (*Ornithomimus* and *Struthiomimus*) from Asia to North America during the Campanian.

Paleoenvironment and Paleoecology

Environmental factors clearly controlled the distribution of terrestrial vertebrate assemblages during late Mesozoic time (Jerzykiewicz and Russell, 1991). Faunal and floral fossil records are poorly documented in the adjacent formations by some circumstances due to taphonomic bias. In general, while the geography of the Cretaceous was generating changing the environments and climates, other changes have also been affected in the fauna and flora, for example fossil records of plants (Norman, 2000). While the Early Cretaceous seems to have a little changes in the dominant plant types (conifers, cycads, ginkgos, extinct gymnosperm trees, and ferns), the "middle" Cretaceous marked an important event. Most dramatically, the flowering plants (angiosperms) that are so widespread in this time (Norman, 2000; Okada, 2000).

Many controversial opinions have been published regarding the depositional environments of the Upper Cretaceous (Jerzykiewicz and Russell, 1991; Jerzykiewicz, 2000; Okada, 2000). Sochava (1975) regards that alluvial cycles are reflected in the Bayanshiree, Baruun Goyot, and Nemegt formations. Wind-blown and associated facies of subaerial deposition, interfingering with water-laid interdune/ephemeral facies, have been documented from the Upper Cretaceous Djadokhta Formation and Baruun Goyot formations (Berkey and Morris, 1927; Lefeld, 1971; Gradziński and Jerzykiewicz, 1974b; Fastovsky et al., 1997). During the Late Cretaceous, the vertebrates of Mongolia lived in different climatic conditions than the contemporaneous continental North American faunas (Tverdokhlebov and Tsybin, 1974; Osmólska, 1980b). The non-marine Cretaceous fossil fauna and flora are abundant, represented by amphibians, fresh-water bivalves, plants, spor-pollen assemblages, ostracods, charophytes, insects, fishes, reptilian and

mammals (Okada, 2000). These faunas and floras serve as one of the most important bases for the stratigraphic classification and correlation.

On the basis of biogeochemical studies of palaeohydrochemistry of Cretaceous continental water, Kolesnikov (1982) established that at the beginning of the Early Cretaceous the limnic basins existed in humid subtropical climate condition with average annual air temperature of 17˚C to 20˚C. By the end of the Early Cretaceous the aridization of subtropical climate was observed and the seasonal contrast was increasing. At the end of Early Cretaceous, the aridity persisted and mineralization of large water reservoir increased up to 6.1-10.4%. During the Late Cretaceous, the climate was arid and the maximum rise in temperature was at the Baruungoyotan time, and the salinity of basins reached 11.5-12.2%. At the final stage of the Late Cretaceous Nemegtan time (Maastrichtian) the climate condition was gradually continued and degree of mineralization went down and reached 9.8-11.3%. The Late Cretaceous paleoenvironments of the major dinosaur-bearing formations of the Gobi Desert are divided into the following four main successions (Bayanshiree, Djadokhta and Baruun Goyot, and Nemegt formations).

While perennial, widespread lacustrine sedimentation were predominated in during end of the Early Cretaceous and early Late Cretaceous time (the Bayanshiree Formation), the Campanian Djadokhtan time and subsequent units were mainly semi-arid to arid conditions, characterized by eolian-influenced environments with a lacking permanent fluvial drainage system (Jerzykiewicz and Russell, 1991). Furthermore, the paleoenvironment conditions and vertebrate remains found within the Djadokhta and Baruun Goyot formations are basically similar and resemble each other more closely than do either older Bayanshireenian or younger Nemegtan assemblages (Jerzykiewicz and Russell, 1991). Whereas the Djadokhtan time has been documented as primarily arid with minor ‘wet’ facies, which was influenced by large lakes (Osmólska, 1980b), the Maastrichtian Nemegtan time has been interpreted as a mostly fluvial environment with most fossils from channel fill, point bar, and occasional overbank deposits laid down under more humid condition (Gradzínski and Jerzykiewicz, 1974). Nonetheless, part of the Nemegtan time is time equivalent to the Baruungoyotan time with regards to presence of a more specifically to dry, eolian deposits of this formation. Some of dinosaur groups such as troodontids, dromaeosaurids, oviraptorids,

hadrosaurids, and birds are well-known in both Djadokhta and Nemegt formations, suggesting that members of these dinosaur groups were adapted for both arid and wet environments (Osmólska, 1980b; Dashzeveg et al., 2005; Tsogtbaatar et al., 2014; Tsuihiji et al., 2014; Funston et al., 2018). Although a partially or single independent skeletal elements, for instance pedal phalanges and unguals, of ornithomimosaur have been previously collected from the Baruun Goyot Formation (Chinzorig pers. observation), none of them have not yet been officially reported yet until this time (Jerzykiewicz and Russell, 1991; Makovicky et al., 2004).

In the Djadokhtan time, its depositional environments is mainly represent eolian xeric environments (Eberth, 1993; Fastovsky et al., 1997; Dashzeveg et al., 2005). Even it is mostly interpreted that arid environments were mainly prevailed during this time, an abundance of invertebrate and vertebrate fossils have been found and described from the beds, including *Protoceratops, Shuvuuia, Velociraptor,* ostracods, lizards, multituberculate mammals, an enantiornithine birds, and a hundreds of the known dinosaur eggs and eggnest (Mikhailov, 1991), as well as floral families (Okada, 2000). *Aepyornithomimus tugrikinensis* is possibly the first evidence of an ornithomimosaur taxon that could have tolerated more diverse climatic conditions that were shifting from humid to more arid conditions. Later on, the climate changed during Late Campanian times to a more humid, which favored flora and fauna immigrating from neighboring areas surrounding today's Mongolia (Jerzykiewicz et al., 1993). It is possible that *Aepyornithomimus tugrikinensis* is a transitional form between the basal and derived ornithomimosaurs. Strong similarities in vertebrate fauna and lithology are persisted at Bayn Dzak and Tögrögiin Shiree localities of Mongolia, and a locality of the northeastern Chinese, known as Bayan Mandahu (the Wulansuhai Formation), (Berkey and Morris, 1927; Currie and Eberth, 1993; Jerzykiewicz et al., 1993). Itterbeeck and colleagues (2005) restudied the stratigraphy and sedimentology of the Iren Dabasu Formation at Iren Dabasu, which hosts one of the derived ornithomimosaurs, *Archaeornithomimus* (Smith and Galton, 1990). Although this formation was originally considered as Cenomanian-Turonian (Currie and Eberth, 1993), Itterbeeck et al. (2005) concluded that the Iren Dabasu Formation should probably be assigned as late Campanian-early Maastrichtian in age which means it is equivalent to the Nemegt

Formation based on the micro-fauna. This line of evidence suggests that *Aepyornithomimus tugrikinensis* could be stratigraphically the oldest known ornithomimid occurrence in the Late Cretaceous of Asia, and the easternmost occurrence of ornithomimid dinosaurs from the Campanian in the northern hemisphere. Nevertheless, *Aepyornithomimus tugrikinensis* is replaced a missing gap of Asian ornithomimosaur evolution from the Campanian Djadokhta Formation, as well as the new taxon increased vertebrate fauna of Tögrögiin Shiree locality.

In the Nemegtan time, three species of ornithomimosaurs are recognized: the rare *Anserimimus planinychus*, the gigantic *Deinocheirus mirificus*, and the most common ornithomimid *Gallimimus bullatus*, all from the Nemegt Formation (Makovicky et al., 2004; Lee et al., 2014). Although the hands of *Garudimimus brevipes*, *Qiupalong henanensis*, *Rativates evadens*, and *Tototlmimus packardensis* are missing, data covers most of the major ornithomimosaur taxa distributed in Asia, North America, Europe and Africa, with time ranges from the Berriasian to the Maastrichtian (Makovicky et al., 2004; Choiniere et al., 2012). The considering the fact that the formation occupies only a small part of the spatial and temporal range of the Late Cretaceous (150 km x 200 km; upper Campanian – lower Maastrichtian), the large manual morphological disparity of Nemegt forms (68.7% PD for phalanges and 49.9% PD for unguals) within the entire Ornithomimosauria demonstrates a high diversity of hand shape-functions among them. This high diversity may be a result of adaptations to different ecological demands, as morphology, function, behavior, and ecology are closely related to each other (Sibbing et al., 1998).

Both phylogenetically and taxonomically, the hand structure of ornithomimosaurs is one of the important features. The morphologically different manual unguals of MPC-D 100/121 and MPC-D 100/133 can be inferred as evidence of a possible new taxon or new species. The manual unguals of MPC-D 100/133 and MPC-D 100/134 show similarities to the ornithomimid, ZPAL MgD-I/65 from the Upper Cretaceous, Tsagaan Khushuu locality (Bronowicz, 2011). Bronowicz (2011) is suggested that the morphology of the unguals which are almost straight and flat ventrally, but other morphological features are differentiated this new ornithomimid from *Anserimimus planinychus*. If those features are case of

validity, together with specimens MPC-D 100/133, MPC-D 100/134 and a new ornithomimid (ZPAL MgD-I/65) may possible to be as a fourth taxon from the Nemegt Formation (Fig. 59).

Even though a primitive but toothless non-ornithomimid ornithomimosaur *Garudimimus brevipes* is the earliest only known valid taxon from the early Late Cretaceous Bayanshireenian time (Cenomanian-Santonian) of Mongolia (Kobayashi and Barsbold, 2005a), true ornithomimid (arctometatarsalian condition) ornithomimosaurs, such as informally called "*Gallimimus mongoliensis"* ornithomimid (Kobayashi and Barsbold, 2006) and a new ornithomimid (in this study Chapter II), are coexisted in this time. In addition, late Early Cretaceous Khukhtekian toothed primitive ornithomimosaur, *Harpymimus okladnikovi*, is may replaced by the Bayanshireenian forms by the beginning of early Late Cretaceous. Comparing to less abundant and less diverse ornithomimosaur specimens from the Early Cretaceous beds of Mongolia (it is possible that less fossil occurrences are related to the taphonomic bias), early evolutionary stages of ornithomimid ornithomimosaurs were began diversified in the beginning of the Bayanshireenian time (from Cenomanian to Turonian) where was the climate more prevailed humid and wet. By the Djadokhtan time (Campanian), a number of dinosaur groups were required to migrate to the preferable places to live due to the climatic shifts. *Aepyornithomimus* was the one of the immigrants who are travelled together from Asia to North America during Campanian time (Tverdokhlebov and Tsybin, 1974; Jerzykiewicz and Russell, 1991; Shuvalov, 2000; Tsogtbaatar et al., 2014).

When the Nemegtan time, the climate was underwent more mesic environments, more places of vegetation and habitation are occupied the area, and permitted to open a new living places for certain dinosaur groups, including hadrosaurids and ornithomimids.

CHAPTER VIII

CONCLUSION

The Baishin Tsav ornithomimosaurs bonebed is the first ornithomimosaur bonebed reported from the Gobi Desert of Mongolia, and the fifth ornithomimosaur bonebed is known to date in the world. The morphologically different manus structure of two specimens described from the bonebed, which demonstrated that coexistence of ornithomimosaurs during early Late Cretaceous of Mongolia. It indicates a niche-partitioning was one of the major drives of ornithomimosaur evolution in early Late Cretaceous time. One of the individual (MPC-D 100/139) is represented the smallest adult ornithomimosaur based on the histologic analysis. The result shows that the individual was a dwarfed ornithomimosaur in terms of a niche-partitioning in early rapid diversification of ornithomimosaur dinosaur in the lower Upper Cretaceous Bayanshiree Formation.

A new taxon, *Aepyornithomimus tugrikinensis* gen. et sp. nov. is the first evidence of an ornithomimosaur, could have tolerated more diverse climatic conditions that were shifting from humid to more arid conditions. As well as, Upper Cretaceous Djadokhta Formation *Aepyornithomimus tugrikinensis* is replaced a missing gap of Asian ornithomimosaur evolution from the of the Gobi Desert of Mongolia, as well as the new taxon increased vertebrate fauna of the aeolian-influenced Tögrögiin Shiree locality.

New ornithomimid, MPC-D 100/121, from the Upper Cretaceous Nemegt Formation described here is found to be a member of Ornithomimidae and it provides evidence for the recognition of a new genus and species within Ornithomimosauria. In addition, it has several automorphic characters, in which can be potential to be a fourth valid ornithomimosaur from the Upper Cretaceous Nemegt Formation of Mongolia. A number of new characters of Bügiin ornithomimid provides it unique among the known ornithomimosaur taxa of Asia and North America. As well as, it also increases ornithomimid diversity of late Campanian to early Maastrichtian in Asia.

The Upper Cretaceous Nemegt Formation of Mongolia has a higher diversity of ornithomimosaur dinosaurs than any other places where ornithomimosaur specimens have been discovered. Seven morphologically different mani of ornithomimosaurs are identified from the formation in this study. The quantitative and statistical analyses demonstrate large manus variations within the Nemegt ornithomimosaurs. Moreover, Nemegt ornithomimosaurs contribute to about half of the manual morpho-functional disparity among Ornithomimosauria, suggesting that ornithomimosaurs were particularly diverse in the Nemegt Formation. Based on the wide morphological variation of hand structures, the Nemegt ornithomimosaurs are inferred to have been adapted to different functional and ecological niches related to their feeding.

LIST OF APPENDICES

Figure-A1. Possible dispersal patterns of derived ornithomimosaurs between Asia and North America. Topologies of four most parsimonious trees, including a position of *Aepyornithomimus tugrikinensis* gen. et. sp. nov. with ornithomimosaurs. *Explanation:* (384(0), 448(1)… 271(0)), the character numbers with changing character codes in every stages.

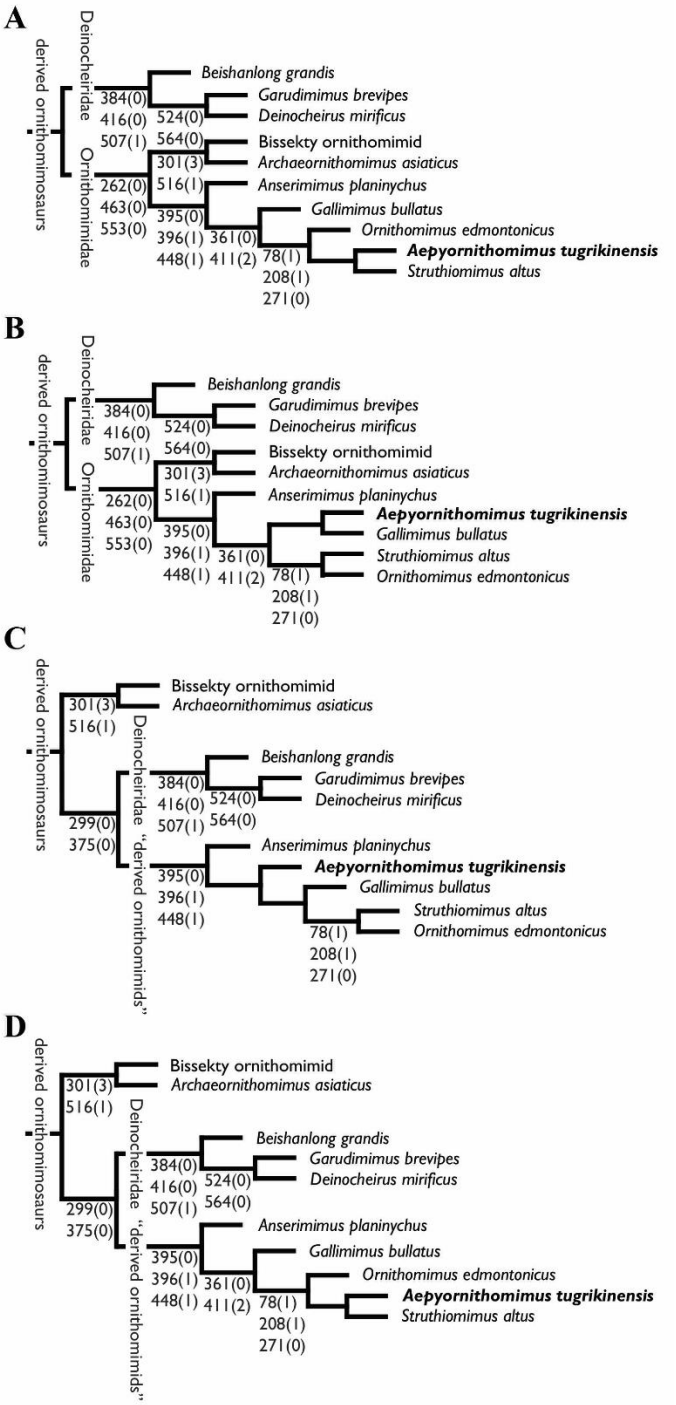

Figure-A2. Field view of Bügiin ornithomimid, (MPC-D 100/121).

Figure-A3. Geometric morphometrics of ungual I. All other individuals are with specimen numbers of MPC-D. *Abbreviations*: see the list of abbreviations on page vi.

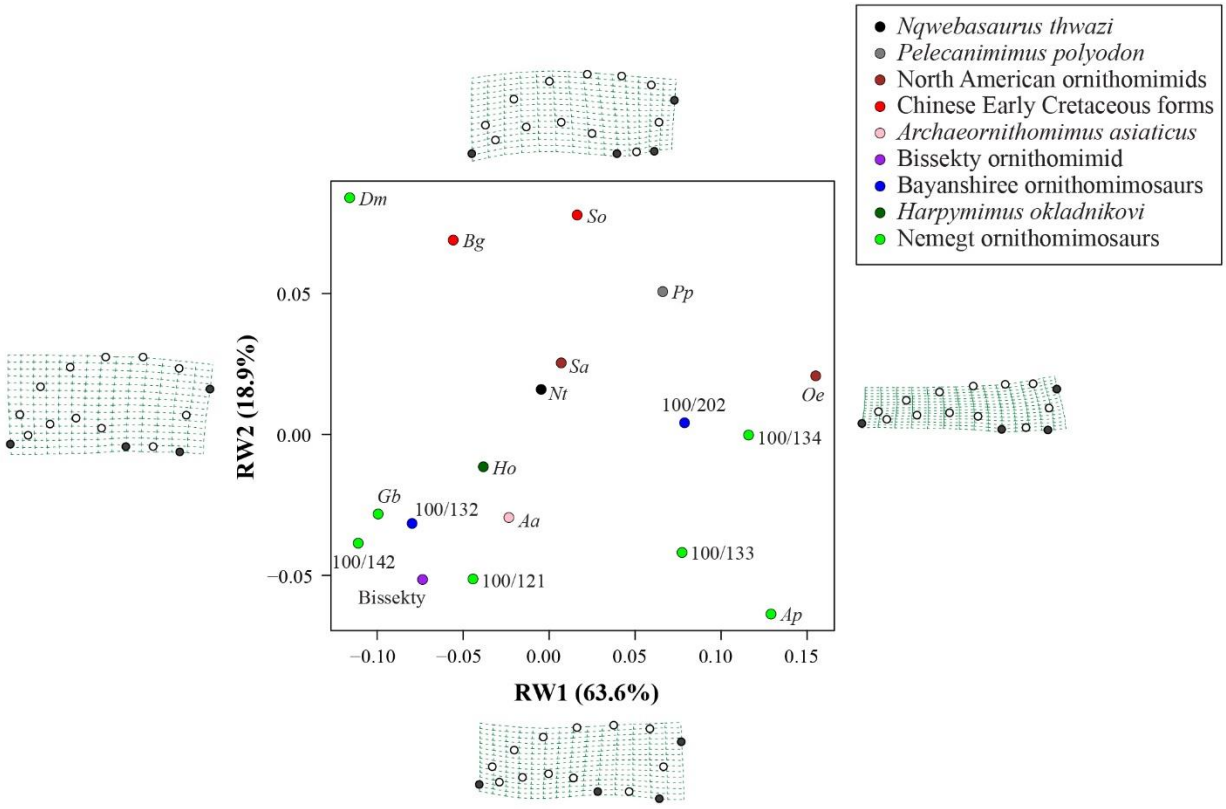

Figure-A4. Relationship of ungual I shapes (RW1 scores) and mechanical advantage obtained from the geometric morphometrics. An ordinary least squares line is fit on the plots. All other individuals are with specimen numbers of MPC-D. *Abbreviations*: see the list of abbreviations on page vi.

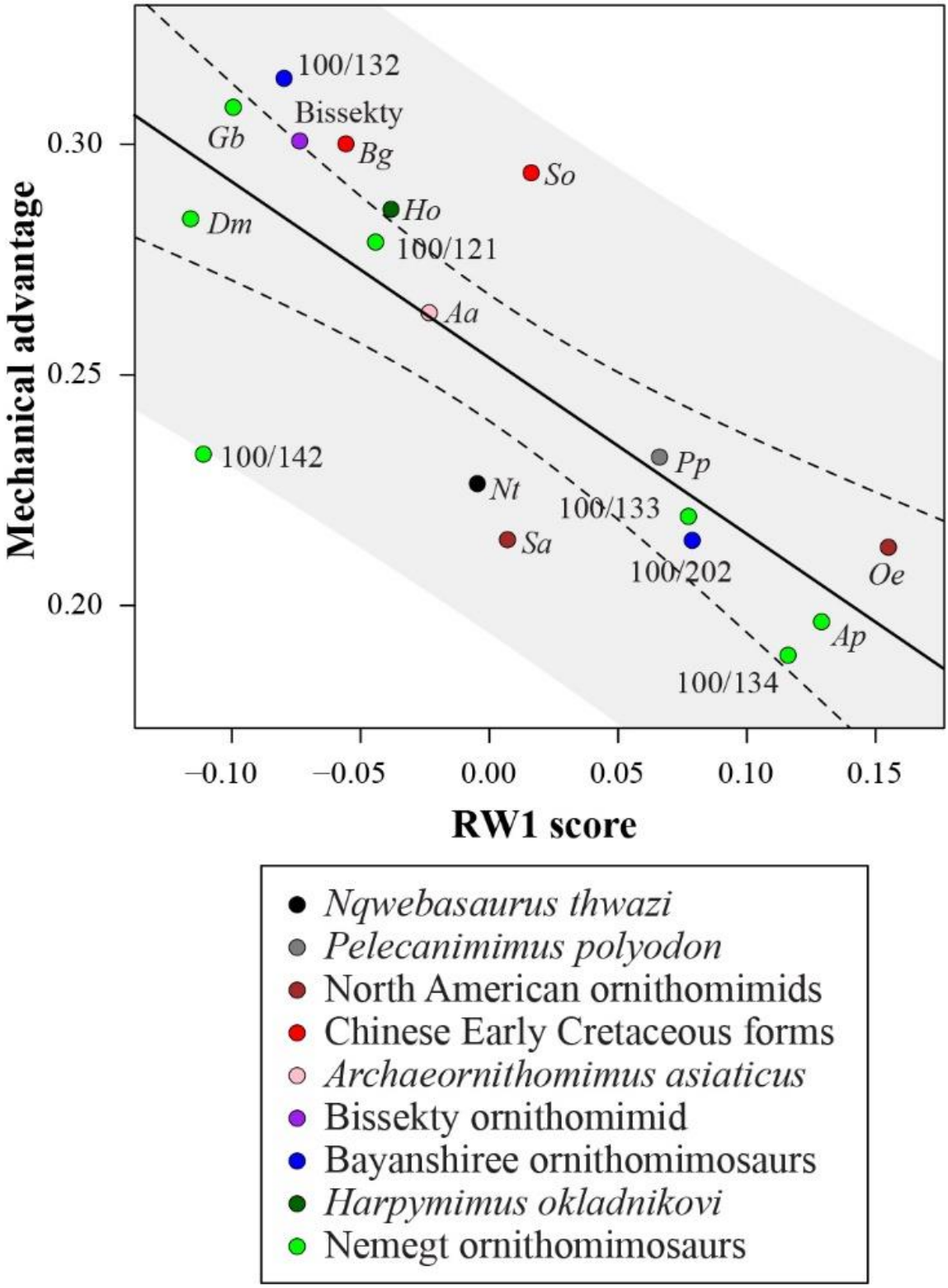

Table-A1. Measurements (mm) of the vertebral column of the BTs ornithomimosaur bonebed specimens. Note that: asterisk (*), behind the numbers refer to the incomplete elements.

No.	Length of centrum			Anterior width of centrum			Anterior height of centrum			Height of neural spine		Anteroposterior length of a tip of neural spine	
	100/139	100/144	100/146	100/139	100/144	100/146	100/139	100/144	100/146	100/139	100/146	100/144	100/146
Cv.7	48.10	-	-	21.69	-	-	5.49	-	-	7.25	-	-	-
Cv.8	42.81	-	-	-	-	-	-	-	-	13.42	-	-	-
Cv.9	43.36	-	-	12.37	-	-	12.74	-	-	-	-	-	-
Cv.10	36.31	-	-	17.63	-	-	13.74	-	-	-	-	-	-
Dv.1	31.82	-	-	18.63	-	-	18.82	-	-	11.42	-	-	-
Dv.2	29.88	-	-	19.29	-	-	17.08	-	-	-	-	-	-
Dv.3	31.04	-	-	18.48	-	-	18.44	-	-	-	-	-	-
Dv.4	28.30*	-	-	17.49	18.34	-	19.73	18.72	-	-	-	23.85	-
Dv.5	-	39.45*	35.00	-	-	17.49	-	-	19.30	-	-	-	-
Dv.6	32.75*	-	35.99	15.29	-	17.77	19.22	-	20.84	-	-	-	-
Dv.7	35.93	-	36.38	16.97	22.22	16.86 *	19.25	26.12	20.95*	-	19.78	-	29.63
Dv.8	35.45	50.18	40.79	17.60	26.33	21.43	19.46	24.16	24.47	-	22.99	-	32.19
Dv.9	36.68	41.66*	41.31	18.03	23.19	24.94	20.92	25.25	26.06	-	23.95	30.15	32.35
Dv.10	36.16*	43.56	37.00	18.81*	26.09	22.42	19.93*	32.43	26.00	-	24.62	-	32.62
Dv.11	37.09	45.08	-	19.91	27.05	-	22.90	34.98	-	-	-	-	-
Dv.12	37.82	-	-	19.97	25.62	-	27.87	-	-	-	-	-	-
Dv.13	39.04	43.58	-	21.83	25.89	-	26.66	32.22	-	-	-	35.53	-
Sv.1	40.93	47.75	-	?	?	-	?	?	-	-	-	-	-
Sv.2	41.94	47.50	-	?	?	-	?	?	-	-	-	-	-
Sv.3	36.80	42.25	-	?	?	-	?	?	-	-	-	-	-
Sv.4	35.02	42.61	-	?	?	-	?	?	-	-	-	-	-
Sv.5	39.05	49.56	-	?	?	-	?	?	-	-	-	-	-
Sv.6	41.90	56.88	-	24.76	?	-	26.30	?	-	-	-	-	-
Ca.1	34.71		-	24.08	-	-	26.68	-	-	33.63	-	-	-
Ca.2	31.03		-	22.34	-	-	25.96	-	-	30.10	-	-	-
Ca.3	29.81		-	22.13	-	-	24.08	-	-	29.47	-	-	-
Ca.4	28.18		-	18.97	-	-	20.73	-	-	-	-	-	-
Ca.5	27.98		-	17.70	-	-	19.69	-	-	-	-	-	-
Ca.6	28.10		-	16.44	-	-	18.27	-	-	-	-	-	-
Ca.7	27.48		-	16.76	-	-	17.11	-	-	-	-	-	-
Ca.8	29.23		-	16.85	-	-	17.63	-	-	-	-	-	-
Ca.9	28.52		-	15.80	-	-	15.44	-	-	14.83	-	-	-
Ca.10	28.54		-	15.51	-	-	13.28	-	-	15.78	-	-	-
Ca.11	28.45		-	15.53	-	-	11.98	-	-	11.68*	-	-	-
Ca.12	28.61		-	15.51	-	-	12.54	-	-	17.31*	-	-	-
Ca.13	28.74		-	15.88	-	-	11.33	-	-	-	-	-	-

Table-A2. Measurements (in mm) of the appendicular skeleton of the BTs ornithomimosaur bonebed specimens. Note that: asterisk (*), behind the numbers refer to the incomplete elements.

Skeletal elements	Measured section	100/139	100/143	100/144	100/145	100/147
Scapulocoracoid	Length	197.51	-	-	240.22*	-
	Proximal width	22.77	-	-	-	-
Humerus	Length	176.15	-	-	233.04	-
	Proximal width	35.31	-	-	48.55	-
	Shaft diameter	38.41	-	-		-
Ulna	Length	139.04	-	-	182.68	126.10
	Shaft diameter	9.01	-	-		-
Radius	Length	135.62	-	-	177.61	-
	Shaft diameter	7.30	-	-		-
Radiale	Length	11.29	-	-	-	-
	Width	5.44	-	-	-	-
Intermedium	Length	8.05	-	-	-	-
	Width	5.18	-	-	-	-
Centrale	Length	7.16	-	-	-	-
	Width	5.75	-	-	-	-
Pisiform	Length	5.71	-	-	-	-
	Width	4.56	-	-	-	-
Distal carpals II and III	Length	8.05	-	-	-	-
	Width	17.91	-	-	-	-
Metacarpal I	Length	38.12	-	-	50.69	-
	Distal width	11.66	-	-	17.19	-
	Distal height	11.54	-	-	14.49	-
Metacarpal II	Length	44.32	-	-	61.87	-
	Distal width	10.21	-	-	13.13	-
	Distal height	10.56	-	-	12.76	-
Metacarpal III	Length	42.92	-	-	60.31	-
	Distal width	8.23	-	-	10.07	-
	Distal height	9.64	-	-	12.56	-
Phalanx I-1	Length	59.60	-	-	72.17	-
Phalanx I-2, ungual-I	Length (straight)	41.88	-	-	47.55	-
Phalanx II-1	Length	20.85	-	-	28.35	-
Phalanx II-2	Length	46.09	-	-	56.73	-
Phalanx II-3, ungual-II	Length (straight)	34.30	-	-	42.14	-
Phalanx III-1	Length	16.21	-	-	19.96	-
Phalanx III-2	Length	-	-	-	18.98	-
Phalanx III-3	Length	-	-	-	42.08	-

Phalanx III-4, ungual-III	Length (straight)	20.71*	-	-	44.13	-
Ilium	Length	242.48	-	206.38*	225.42*	-
Ilium, between supracetabular crest and dorsal edge	Height	93.77	-	-	-	-
Ilium, acetabulum	Length	52.32	-	-	-	-
	Height	57.55	-	-	-	-
Pubis	Length	195.91*	301*	318.00	243.61	-
Pubic boot	Length	-		114.50	73.81	-
Ischium	Length	199.59	-	211.65*	94.22*	-
Ischial foot	Length	39.95	-	34.16		-
Femur	Length	257.63	-	-	-	-
	Shaft diameter	78.00	-	-	-	-
Tibia	Length	257.74	-	-	-	-
	Shaft diameter	75.81	-	-	-	-
Tibiotarsus	Length	269.27	-	-	-	-
Fibula	Length	253.23	-	-	-	-
	Proximal width	41.85	-	-	-	-
	Shaft diameter	4.02	-	-	-	-
Astragalus, ascending process	Height	67.43	-	-	-	-
Astragalus	Width	41.14	-	-	-	-
Astragalus, lateral condyle	Length	27.69	-	-	-	-
Astragalus, medial condyle	Length	27.11	-	-	-	-
Calcaneum	Length	27.26	-	-	-	-
	Height	18.73	-	-	-	-
Distal tarsal-III	Length	20.70	-	-	-	-
	Width	20.52	-	-	-	-
Distal tarsal-IV	Length	20.32	-	-	-	-
	Width	20.52	-	-	-	-
Metatarsal-II	Length	145.84	-	-	-	-
Metatarsal-III	Length	170.15	-	-	-	-
Metatarsal-IV	Length	157.95	-	-	-	-
Metatarsal-V	Length	51.06	-	-	-	-

Table-A3. Collected skeletal elements recovered from the BTs ornithomimosaur bonebed specimens by individuals.

Skeletal elements	Count			
	Ornithomimosaur		Unknown hadrosauroid	
	Count #	%	Count #	%
Cervical vertebrae	6	2.66		
Dorsal vertebrae	32	14.22		
Sacral vertebrae	16	7.11		
Caudal vertebrae	36	16		
Chevrons	8	3.55		
Scapulocoracoid	4	1.77		
Humeri	4	1.77		
Ulnae	4	1.77		
Radii	3	1.33		
Carpal bones	6	2.66		
Metacarpals	6	2.66		
Manual phalanges	26	11.55		
Dorsal ribs	12	5.33		
Ilia	5	2.22		
Pubes	8	3.55		
Ischia	5	2.22		
Femorae	3	1.33		
Tibiae	3	1.33		
Fibulae	2	0.88		
Distal tarsals	4	1.77		
Astragalus	2	0.88	1	0.13
Calcaneum	2	0.88		
Metatarsals	8	3.55		
Pedal phalanges	20	8.88		
Sub total	**225**	**99.87**	**1**	**0.13**
Total	**226**			

Table-A4. The histologic checklist of MPC-D 100/139 and other ornithomimosaurs.

Specimens	Catalog No.	Age	Formation	Sampled elements	Side	Measurement (mm)	Vascularization type	Number of LAGs	Medullary cavity	Periosteal	Secondary osteons - remodeling around periosteal
BTs Bonebed ornithomimosaur specimen	MPC-D 100/139	Cenomanian Turonian	Upper Cretaceous, Bayanshiree Fm.	Fibula	Right	253	dominantly longitudinal and some reticular	5-6	not-known		highly remodeling

	highly remodeling		not-known	13-14	from inner cortex reticular to outer cortex Longitudinal	662	Right	Fibula	Lower Cretaceous, Xinminpu Group	Aptian - Albian	FRDC-GS GJ (06) 01-18	*Beishanlong grandis*
	highly remodeling		poor	5	plexiform	448	Right	Fibula	Upper Cretaceous, Horseshoe Canyon Formation	late Campanian	ROM 851	*Ornithomimus edmontonicus*
	existed, greater vascularization towards the periosteal margin		poor	4	from plexiform to reticular	393	Left	Fibula	Horseshoe Canyon Formation	early Maastrichtian	CMN 12068	Dry Island Bonebed ornithomimid specimen
				4	dominantly longitudinal and some reticular		Left	Fibula	Upper Cretaceous, Ulansuhai Fm.	late Turonian - early Campanian	IVPP11797-24	*Sinornithomimus dongi*

Table-A5. Cortex thickness of MPC-D 100/139 and accumulation percentages of the spacing between annuli and LAGs. *Abbreviations*: see the list of abbreviations on page vi.

	um	**%**	**accum %**
A1			
A2			
A3 est	1192	30.93%	30.93%
A4	284	7.37%	38.30%
A5 est	322	8.35%	46.65%
L1	376	9.76%	56.41%
L2	523	13.57%	69.98%
L3	500	12.97%	82.95%
L4	333	8.64%	91.59%
L5	146	3.79%	95.38%
L6	128	3.32%	98.70%
EFS	50	1.30%	100.00%
Total	3854		

Table-A6. Measurements of skeletal elements.

Taxon	Specimen # (measurements)	Data source (measurements)	Specimen # (ungual photos)	Data source (ungual photos)	mcI	mcII	PhIII-1	PhII-1	PhII-2	PhII-3	PhIII-1	PhIII-2	PhIII-3	PhIII-4	mcs	Pteridine (=arctometatarsalian)
Nqwebasaurus thwazi	AM 6040	de Klerk et al. 2000	AM 6040	Choiniere et al. 2012	16.7	26.5	20	?	?	?	?	?	?	?	x	x
Pelecanimimus polyodon			LH 7777	first hand observation	?	?	?	?	?	?	?	?	?	?	x	x
Shenzhousaurus	NGMC 97-4-002	Ji et al. 2003	NGMC 97-4-002	Ji et al. 2003	?	?	50	35+	29	60	45	19	18	43+	29+	x
Harpymimus okladnikovi	MPC-D 100/29	Kobayashi's personnel	MPC-D 100/29	first hand observation	48.1	94.3	102.6	119.2	73.6	50.8	104	80	31	37	81	77	x	x
Beishanlong grandis	FRDC-GSGJ (06)01-16	Makovicky et al. 2009	FRDC-GSGJ (06)01-18	Makovicky et al. 2009	?	?	?	?	?	?	?	?	?	?	?	?	x	x
Deinocheirus mirificus	MPC-D 100/18	Osmólska and Roniewicz 1970	MPC-D 100/18	first hand observation	210.65	230.2	248.19	308.94	252.68	136.69	207.93	235.03	96.23	78.07	164.17	215.64		
Shromithomimus sloani	IVPP V11797-10	Kobayashi and Lu 2003			41.2	54.7	53.8	76.3	?	19.9	59.9	48.3	13.9	14.6	42.9	46.9		
Anserimimus planinychus	MPC-D 100/300	first hand measurements	MPC-D 100/300	first hand observation	73.82	72.74	74	101.82	71.06	49.08	68.3	58.6	28.04	20.28	42.42	?		
Gallimimus bullatus	MPC-D 100/11	first hand measurements	MPC-D 100/11	first hand observation	355.55	109.73	103.88	123.31	73	43.31	31.64	67.53	29.31	26.61	61.97	90		
Gallimimus bullatus	MPC-D 100/12	Kobayashi's personnel			69.7	72.5	69.2											
Ornithomimus	CMN 8632	Kobayashi's personnel			96.1	89.51	85.33	100.4	66	34.23	81.32	84	25.98	24.43	67.35	65e		
Ornithomimus	ROM 851	Kobayashi's personnel	ROM 851	first hand observation	107.1	104.4	100.5	107	61.27	33.1	88.8	65.61	20.9	29.1	72.1	55.22		
Ornithomimus velox	YPM 548	Claessens et al. 2015			56	53	51	?	?	?	?	?	?	?	?	?		x
Struthiomimus altus	AMNH 5339	Claessens et al. 2015			89	103	103	110	65	40	90	85	25	35	75	80		
Struthiomimus altus	TMP 90.26.1	Kobayashi's personnel			102.31	106.27	108.67	109	63.5	43	87.3	85	28	28	72	85		
Struthiomimus altus	UCMZ (VP) 1980.1	Kobayashi's personnel	CDZH-14a, 1980	Sues and Averianov 2009	105.1	113.3	110.2											
Bissekty ornithomimid					?	?	?	?	?	?	?	?	?	?	?	?		
Ornithomimidae indet.	MPC-D 100/121	Kobayashi's personnel	MPC-D 100/121	first hand observation	86.6	91.1	87.9	99.2	55	34	87	64	25.6	25.43	65.77	72.11		
Ornithomimidae indet.	MPC-D 100/133	first hand measurements	MPC-D 100/133	first hand observation	54.01	62.64	59.84	71.28	41.89	21.61	59.11	48.84	14.35	14.97	42.74	45.13		
Ornithomimidae indet.	MPC-D 100/134	first hand measurements	MPC-D 100/134	first hand observation	83.4	86.25	77.46	56.8	64.22	36.15	?	65.8	23.89	23.26	63.63	48.12+		x
Ornithomimidae indet.	MPC-D 100/142	first hand measurements	MPC-D 100/142	first hand observation	63.1	65.21	64.2	93.74	36.08	39.33	80.39	75.4	23.8	27.63	53.11	61.48	x	
Ornithomimidae indet.																		
("*Gallimimus*" Ornithomimidae indet.	MPC-D 100/14	first hand measurements			77.72	82.19	76.64	111.28	74.45	35.35	93.31	60.65	26.66	30	67.01	54.66	x	
	MPC-D 100/132	first hand measurements	MPC-D 100/132	first hand observation	?	?	84.2	92.78	53.09	?	?	57.92	21.57	18.82	47.2	44.53	x	x

Supplementary Data-S1A. Character list and character matrix that used in this study after modified Xu et al., 2011.

Character list

1. Premaxillary teeth: present (0) or absent (1) (Holtz 1994)

2. Posterior end of maxillary process of premaxilla terminates anterior to anterior border of antorbital fossa (0) or extends more posteriorly (1), (Kobayashi and Lü, 2003).

3. Maxillary teeth: present (0) or absent (1), (Holtz,1994).

4. Maxilla participates in external narial opening (0) or separated from opening by maxilla-nasal contact (1), (Xu et al., 2002).

5. Series of foramina along ventral edge of lateral surface of maxilla: present (0) or absent (1), (Kobayashi and Lü, 2003).

6. Prominence on lateral surface of lacrimal: present (0) or absent (1), (Xu et al., 2002).

7. Area of exposed prefrontal in dorsal view: less than that of lacrimal (0) or approximately the same (1), (Xu et al. 2002).

8. Parasphenoid bulla: absent (0) or present (1), (Osmólska et al. 1972).

9. Ventral reflection of anterior portion of dentary, resulting in a gap between upper and lower jaws when jaws are closed: absent (0) or present (1), (Pérez-Moreno et al., 1994).

10. Dentary teeth: present (0) or absent (1), (Holtz, 1994).

11. Dentary subtriangular in lateral view (0) or with subparallel dorsal and ventral borders (1), (Currie 1995).

12. Dorsal border of dentary in transverse cross-section: rounded and lacks “cutting edge” (0) or sharp with “cutting edge” (1), (Kobayashi and Lü, 2003).

13. Accessory mandibular condyle, lateral to lateral condyle of quadrate: absent (0) or present (1), (Kobayashi and Lü, 2003).

14. Foramen on dorsal edge of surangular dorsal to mandibular fenestra: present (0) or absent (1), (Hurum, 2001).

15. Posterior surangular foramen: absent (0) or present (1), (Sereno, 1999).

16. Number of accessory antorbital fenestra: one (0) or two (1).

17. Mandibular fenestrae: heart-shaped with a short and wide process of dentary at anterior part of external mandibular fenestra (0) or oval-shaped without the process (1).

18. Neck length: less (0) or more (1) than twice skull length (Pérez-Moreno et al., 1994).

19. Anteroposterior lengths of cervical neural spines: more (0) or less (1) than one third of neural arch lengths.

20. Posterior process of coracoid: short (0) or long (1), (Pérez-Moreno et al., 1994).

21. Biceps tubercle of coracoid: positioned close to base of posterior process (0) or more anteriorly (1), (Kobayashi and Lü, 2003).

22. Depression on dorsal surface of supraglenoid buttress of scapula: present (0) or weak/absent (1), (Nicholls and Russell, 1985).

23. Infraglenoid buttress of coracoid: aligned with posterior process (0) or is offset laterally from line of posterior process (1), (Kobayashi and Lü, 2003).

24. Robustness of humerus, ratio of width of proximal end to total length: greater (0) or less than 0.2 (1) (Kobayashi and Lü, 2003).

25. Deltopectoral crest of humerus: strong (0) or weak (1).

26. Radial condyle of humerus: larger than ulnar condyle (0), approximately equal (1), or smaller (2).

27. Entepicondyle of humerus: weak (0) or strong (1).

28. Length of metacarpal I: approximately half or less than metacarpal II (0), slightly shorter (1) or longer (2), (Russell, 1972).

29. Distal end of metacarpal I: laterally (0) or medially (1) rotated (Pérez-Moreno and Sanz, 1995).

30. Distal end of metacarpal I forms ginglymoid articulation with distinct condyles (0) or relatively large convex phalangeal articulation with reduced condyles (1), (Pérez-Moreno and Sanz, 1995).

31. Metacarpal II: shorter (0) or longer (1) than metacarpal III.

32. First phalanx of manual digit I: shorter (0) or longer (1) than metacarpal II (Pérez-Moreno et al. 1994).

33. Flexor tubercles of manual unguals: positioned at proximal end (0) or distally placed (1), (Nicholls and Russell, 1985).

34. Pubic shaft: nearly straight (0) or curved (1), (Norell et al. 2002).

35. Ventral border of pubic boot: nearly straight or slightly convex (0) or strongly convex with ventral expansion (1).

36. First pedal digit: present (0) or absent (1).

37. Proximal end of metatarsal III exposed in anterior view (0) or covered by metatarsals II and IV anteriorly (1), (Norell et al., 2002).

38. Length of pedal phalanx II-2: more than 60% of pedal phalanx II-1 (0) or less (1).

39. Ischium straight (0) or ventrally curved anteriorly (1), (Ji et al., 2003)

40. Angular exposed almost to end of mandible in lateral view reaches or almost reaches articular (0) or excluded from posterior end angular suture turns ventrally and meets ventral border of mandible rostral to glenoid (1), (Ji et al., 2003)

41. Brevis fossa poorly developed adjacent to ischia peduncle and without lateral overhang medial edge of brevis fossa visible in lateral view (0), or fossa well developed along full length of postacetabular blade, lateral overhang extend along full length of fossa medial edge completely covered in lateral view (1), (Ji et al., 2003)

42. Mid-caudal vertebrae short prezygapophyses extend less than one half centrum length (0) or moderate prezygapophyses extend more than one half but less than one centrum length (1), (Kobayashi and Barsbold, 2005a).

43. Anterior extension of the pubic boot; nearly absent (0) or present (1).

44. Distal end of pubic shaft is curved (0) or straight (1).

45. Acute angle between pubic shaft and boot is small (0) or large (1).

46. Tip of anterior extension of the pubic boot is at the level of anterior border of pubic shaft (0) or is more extended anteriorly (1).

47. Pedal unguals curved in lateral view (0) or straight (1), (Makovicky et al., 2009)

48. Shaft of MT III with straight medial border in dorsal view (0) or with a medial expansion forming a convexity or bulge along the distal part of the shaft (1), (Kobayashi and Barsbold, 2005b; Makovicky et al., 2009)

Character matrix

Allosaurus fragilis	00000000000000000000000000000000000000000100010100
Tyrannosaurids	000100000000000000000000(12)(01)000?0000010(01)10101000(01)
Anserimimus planinychus	??????????????????11101002121101100111?111???11
Archaeornithomimus asiaticus	??????????????????0101001201101?110?1?1?1?100011
Beishanlong grandis	??????????????????101001?1?????1??00?????????00
Gallimimus bullatus	11111111111110000111111(01)12(01)111111001111011110011
Garudimimus brevipes	1111111111111111?0?????????????00001?01?100001
Harpymimus okladnikovi	1011110?10101011110?0100110000011O??00?010?0??00
Ornithomimus edmontonicus	1111011?11111111111100011202111110111111111111111
Pelecanimimus polyodon	0?0??0?10010???0?1?1????1??110111??????0????????
Qiupalong henanensis	??????????????????????????????????0?1???1?011101
Sinornithomimus dongi	1111111111111?01?1110(01)0112011011100111111101??011
Shenzhousaurus orientalis	1?1101??101?1??1???????????1??0?100???0?0?0000??
Struthiomimus altus	1111001?1111110111110100l?0111111011111(01)111???11
DI bonebed	??????????????????????????????????011111?11111111
BTs bonebed A (MPC-D 100/139)	??????????????????1100110001001110?1111?00????01
BTs bonebed B (MPC-D 100/145)	??????????????????1?0110001001110O?????0?1100??

Supplementary Data-S2A. Character list used in phylogenetic analyses of *Aepyornithomimus tugrikinensis* and Bügiin ornithomimid, after modified from Lee et al. 2014, Sues and Averianov, 2016, and McFeeters et al. 2017 for used this matrix in *Deinocheirus* (2014), Bissekty ornithomimid (2016), and *Rativates* (2017) phylogeny).

1. Contour feathers

0: absent

1: present

2. Vaned feathers on forelimb

0: symmetric

1: asymmetric

3. Shape of premaxillary body (portion in front of the external naris)

0: wider than high, or approx. as wide as high

1: significantly higher than wide

4. Premaxillae

0: unfused

1: fused

5. Premaxillary-nasal suture dorsal view

0: v-shaped

1: w-shaped

6. Premaxillary-maxillary suture

0: scarf or butt joint

1: interlocking joint

7. Premaxillary body in front of external nares

0: rostrocaudally shorter than body below nares and angle between anterior margin and alveolar margin more than 75 degrees

1: rostrocaudally longer than body below the nares and angle less than 70 degrees, naris overlaps premaxillary tooth row

2: much longer than body below naris, naris located posterior to premaxillary tooth row

8. Ventral process at the posterior end of premaxillary body (gives the posterior process a forked appearance in lateral view)

0: absent

1: present

9. Maxillary process of premaxilla

0: contacts nasal to form posterior border of nares

1: reduced so that maxilla participates broadly in external naris

2: extends posteriorly to separate maxilla from nasal posterior to nares

10. Internarial bar

0: dorsoventrally rounded

1: dorsoventrally flat

11. Crenulate margin on buccal edge of premaxilla

0: absent

1: present

12. Caudal margin of naris

0: farther rostral than the rostral border of the antorbital fossa

1: nearly reaching or overlapping the rostral border of the antorbital fossa

13. Premaxillary symphysis

0: acute, V-shaped

1: rounded, U-shaped

14. Subnarial foramen

0: absent

1: present

15. Groove on lateral surface of premaxilla, extending ventrally from the narial fossa

0: absent

1: present

16. Maxillary fenestra

0: absent

1: present

17. 'Maxillary fenestra

0: recessed within a shallow, caudally

1: or caudodorsally open fossa,

18. Longitudinal position of maxillary fenestra

0: situated at rostral border of antorbital fossa

1: situated posterior to rostral border of antorbital fossa

19. Latitudinal position of maxillary fenestra

0: situated approximately mid-height of the antorbital fossa

1: displaced dorsally in antorbital fossa

20. Foramen on caudal edge interfenestral bar between the maxillary and antorbital fenestrae

0: absent

1: present, pierces ventral portion of bar

21. Promaxillary fenestra (fenestra promaxillaris)

0: absent

1: present

22. Palate formed by

0: premaxilla only

1: premaxilla, maxilla and vomer

23. Palatal shelf of maxilla

0: flat

1: with midline ventral "tooth-like" projection

24. Ventrolateral margin of the maxilla posterior to ascending process

0: flat or rounded as it grades onto tooth row

1: developed as a sharp, ventrolaterally-projecting ridge

25. Anteroposterior length of palatal shelf of maxilla

0: short

1: long, with extensive palatal shelves

26. Orientation of the maxillae towards each other as seen in dorsal view

0: acutely angled

1: subparallel

27. Ascending process of the maxilla

0: confluent with anterior rim of maxillary body and gently sloping posterodorsally

1: offset from anterior rim of maxillary body

28. Form of anterior projection of maxilla

0: offset from anterior rim of maxillary body, with anterior projection of maxillary body shorter than high

1: offset from anterior rim of maxillary body, with anterior projection of maxillary body as long as high or longer

29. Ascending process of maxilla

0: prominent, exposed laterally and medially

1: weakly developed, lacking lateral exposure and only slight medial exposure

30. Anterior margin of maxillary antorbital fossa

0: rounded or pointed

1: square

31. Dorsal border of the internal antorbital fenestra lateral view

0: formed by lacrimal and maxilla

1: formed by nasal and lacrimal

32. Dorsal border of the antorbital fossa lateral view

0: formed by lacrimal and maxilla

1: formed by nasal and lacrimal

2: formed by maxilla, premaxilla and lacrimal

33. Lateral exposure of lamina of the ventral ramus of nasal process of maxilla

0: present, large broad exposure

1: present, reduced to small triangular exposure

34. Maxillary antorbital fossa in front of the internal antorbital fenestra

0: 40% or less of the length of the external antorbital fenestra

1: more than 40% of the length of the external antorbital fenestra

35. Extent of antorbital fossa on jugal ramus of maxilla

0: less than half the dorsoventral height of jugal ramus

1: more than half dorsoventral height of jugal ramus

36. Maxilla, pneumatic region on medial side of maxilla posteroventral to maxillary fenestra

0: absent

1: present

37. Horizontal ridge on the lateral surface of maxilla at the ventral border of the antorbital fossa

0: absent

1: present

38. Medial constriction between articulated premaxillae and maxillae in dorsal or ventral view

0: absent

1: present

39. Subnarial gap between maxilla and premaxilla at the alveolar margin

0: absent

1: present

40. Maxillary paradental plates

0: unfused

1: fused

41. Medial surface of maxillary paradental (interdental) plates

0: smooth or finely pitted

1: dorsoventrally striated

42. Maxillary paradental (interdental) plates, ventral extent

0: to the same ventral level as lateral maxillary wall

1: dorsal to ventral level of maxillary wall

43. Maxillary paradental plates, dorsal margin of anterior end

0: horizontal

1: inclined anteroventrally

44. Ventral edge of maxillary body and ventral ramus

0: ventrally flat

1: ventrally convex

45. Nasals

0: unfused

1: fused

46. Dorsal surface of the nasals

0: smooth

1: rugose

47. Nasal crest

0: absent

1: present, single median crest

2: present, bilateral crests along lateral nasal margins

48. Pneumatic foramen in ventrolateral margins of the nasals

0: absent

1: present

49. Shape of nasals

0: expanding posteriorly

1: of subequal width throughout their length

50. Pronounced lateral rims of the nasals, sometimes bearing lateral cranial crests

0: absent

1: present

51. External nares (new state)

0: facing laterally

1: facing anterolaterally

2: facing dorsally (new state)

52. Length of nares

0: less than 20 percent skull length

1: greater than 20 percent skull length

53. Jugal pneumatic recess in posteroventral corner of antorbital fossa

0: present

1: absent

54. Medial jugal foramen

0: present on medial surface ventral to postorbital bar

1: absent

55. Sublacrimal part of jugal

0: tapering

1: bluntly squared anteriorly

2: expanded

56. Anterior end of jugal

0: reaches internal antorbital fenestra

1: excluded from the internal antorbital fenestra

57. Form of anterior end of jugal

0: without anterior process underneath antorbital fenestra

1: expressed at the rim of the internal antorbital fenestra and with a distinct process that extends anteriorly underneath it

58. Jugal antorbital fossa

0: absent or developed as a slight depression

1: large, crescentic depression on the anterior end of the jugal

59. Jugal

0: broad, plate-like

1: very slender, rod-like

60. Jugal contribution to postorbital bar

0: contribute equally to postorbital bar

1: ascending process of jugal reduced

61. Anteroposterior width of postorbital bar

0: subequal to preorbital bar

1: expanded, greater than twice width of preorbital bar

62. Rugosity on ventrolateral surface of jugal below orbit

0: absent

1: present

63. Jugal and quadratojugal

0: separate

1: fused and not distinguishable from one another

64. Quadratojugal

0: hook-shaped, with a dorsoventrally tall, mediolaterally short process that wraps around the lateral margin of the quadrate and is visible in posterior view

1: with a dorsoventrally short, anteroposteriorly long process only visible in lateral view

65. Quadratojugal and quadrate

0: sutural connection present

1: sutural connection absent

66. Anteriormost level of jugal process of quadratojugal relative to infratemporal fenestra

0: ventral to

1: anterior to

67. Supraorbital crests on lacrimal in adult individuals

0: absent

1: present

68. Form of supraorbital crests

0: dorsal crest above orbit

1: lateral expansion anterior and dorsal to orbit

69. Enlarged foramen or foramina opening laterally at the angle of the lacrimal

0: absent

1: present

70. Lacrimal foramen number

0: single

1: paired

71. Lacrimal foramina

0: exposed laterally

1: developed within a pocket formed by a lateral lacrimal sheet of bone and a rostrally open pocket in the lacrimal angle

72. Height of the lacrimal

0: significantly less than height of the orbit, and usually fails to reach the ventral margin of the orbit

1: as high as the orbit, and contacts jugal at the level of the ventral margin of orbit

73. Orientation of jugal ramus of lacrimal

0: strongly sloping anteroventrally

1: subvertical

2: sloping posteroventrally

74. Dorsoventral thickness of maxillary ramus of lacrimal

0: very slender, much less than anteroposterior thickness of jugal ramus

1: moderate, less than or subequal to anteroposterior thickness of jugal ramus

2: greater than anteroposterior thickness of jugal ramus

75. Suborbital spur on posterior edge of ventral ramus of lacrimal

0: absent

1: present

76. Lacrimal posterodorsal process

0: absent

1: present

77. Length of lacrimal posterodorsal process

0: subequal in length to maxillary ramus

1: much shorter than maxillary ramus

78. Direction of lacrimal posterodorsal process

0: projects horizontally

1: projects posterodorsally or completely dorsally

79. Passage of the nasolacrimal duct

0: leading through the body of the ventral process of the lacrimal

1: ventral process of lacrimal not pierced, lateral side depressed below the level of the surrounding bones, and nasolacrimal duct passes lateral to the process

80. Jugal ramus of lacrimal

0: broadly triangular, articular end nearly twice as wide anteroposteriorly as lacrimal body at

lacrimal angle

1: strut-like, roughly same width anteroposteriorly throughout ventral ramus

81. Prefrontal

0: absent

1: present

82. Size of prefrontal

0: small, forms anterolateral rim of orbit with descending process proceeding along medial surface of the descending process of the lacrimal

1: small, forms small portion of skull roof and not expressed at orbital margin, no descending process

2: hypertrophied, forms portion of orbital rim and skull roof, with descending process

83. Configuration of lacrimal and frontal

0: lacrimal separated from frontal by prefrontal

1: lacrimal contacts frontal

84. Frontals (ORDERED)

0: narrow anteriorly as a wedge between nasals

1: end abruptly anteriorly, suture with nasal transversely oriented

2: nasals extend further medially than laterally, invading anteromedial contact between frontals

85. Frontal supratemporal fossa

0: limited extension of supratemporal fossa onto frontal

1: supratemporal fossa covers most of postorbital process of the frontal and extends anteriorly onto the dorsal surface of the frontal

86. Groove on orbital rim of frontal, possibly for reception of frontal process of postorbital

0: absent

1: present

87. Anterior emargination of supratemporal fossa on frontal

0: straight or slightly curved

1: strongly sinusoidal and reaching onto postorbital process

88. Frontal postorbital process (dorsal view):

0: smooth transition from orbital margin

1: sharply demarcated from orbital margin

89. Orbital margin of frontal

0: without groove

1: with groove for articulation with frontal process of the postorbital

90. Frontal edge

0: smooth in region of lacrimal suture

1: edge notched

91. Postorbital in lateral view

0: with straight anterior (frontal) process

1: frontal process curves anterodorsally and dorsal border of temporal bar is dorsally concave

92. Lateral surface of anterior process of postorbital

0: thin and unornamented

1: dorsoventrally thickened into a laterally projecting and rugose platform

93. Contact between lacrimal and postorbital

0: absent

1: present

94. Cross-section of the ventral process of the postorbital

0: triangular

1: U-shaped

95. Jugal process of the postorbital

0: ventrally directed and tapering

1: with suborbital anterior spur

96. Postorbital jugal process anterior suborbital spur

0: small

1: large curving flange

97. Supraorbital shelf formed mostly by an additional ossification (palpebral)

0: absent

1: present

98. Orbit

0: circular in lateral or dorsolateral view

1: dorsoventrally long

99. Parietals

0: separate

1: fused

100. Parietal supratemporal fenestra (ORDERED)

0: separated by a horizontal plate formed by the parietals

1: contact each other posteriorly, but separated anteriorly by an anteriorly widening triangular plate formed by the parietals

2: nearly confluent over parietals and only separated by a thin line of bone along the sagittal suture

101. Anteromedial corner of supratemporal fossa

0: open dorsally

1: roofed by shelf of frontoparietal

102. Sagittal crest

0: dorsal surface of parietals smooth with no sagittal crest

1: sagittal crest present

103. Form of sagittal crest

0: parietals dorsally convex with very low sagittal crest along midline

1: dorsally convex with well-developed sagittal crest

104. Posteriorly placed, knob-like dorsal projection of the parietals

0: absent

1: present

105. Connections of quadratojugal process of squamosal

0: contacts quadratojugal

1: does not contact quadratojugal

106. Infratemporal fenestra shape

0: rectangular, postorbital bar parallels quadratojugal and squamosal articular area

1: lower temporal fenestra constricted mesially by squamosal and quadratojugal approaching postorbital bar

107. Shape of quadratojugal process of the squamosal

0: tapering

1: broad, and usually somewhat expanded

108. Posterolateral shelf on squamosal overhanging quadrate head

0: absent

1: present

109. Quadrate head

0: covered by squamosal in lateral view

1: quadrate cotyle of squamosal open laterally exposing quadrate head

110. Descending process of squamosal

0: parallels quadrate shaft

1: nearly perpendicular to quadrate shaft

111. Supratemporal fenestra

0: bounded laterally and posteriorly by the squamosal

1: supratemporal fenestra extended as a fossa on to the dorsal surface of the squamosal

112. Quadrate

0: solid

1: hollow

113. Mandibular joint

0: approximately straight below quadrate head

1: significantly posterior to quadrate head

2: significantly anterior to quadrate head

114. Quadrate medial pneumatic recess (depression and foramen in the area of the mandibular condyle on medial surface)

0: absent

1: fossa adjacent to mandibular condyle, foramen at base of pterygoid ramus

115. Quadrate posterior pneumatic recess

0: absent

1: present as a lens-shaped fossa extending dorsally or dorsomedially from the quadrate foramen

116. Dorsal end of the quadrate

0: with a single head that fits into a slot on the ventral side of the squamosal

1: double-headed, medial head contacts the braincase

117. Quadrate foramen

0: absent

1: present

118. Quadrate foramen

0: developed as a distinct opening between the quadrate and quadratojugal

1: almost entirely closed in the quadrate

119. Ectopterygoid

0: slender, without ventral fossa

1: expanded, with a ventral depression medially

2: expanded, with a deep groove leading into the ectopterygoid body medially

3: deeply excavated and medial opening constricted into a foramen

120. Dorsal recess on ectopterygoid

0: absent

1: present

121. Ectopterygoid

0: posterior to palatine

1: lateral to palatine

122. Palatine and ectopterygoid

0: separated by pterygoid

1: contact

123. Contact between pterygoid and palatine

0: continuous

1: discontinuous in the mid-region, resulting in a subsidiary palatal fenestra

124. Flange of pterygoid

0: well developed

1: reduced in size or absent

125. Shape of palatine in ventral view

0: plate-like trapezoidal or subrectangular

1: tetraradiate

2: jugal process strongly reduced or absent

126. Suborbital fenestra

0: similar in length to orbit

1: reduced in size or absent

127. Infratemporal fenestra

0: smaller than or subequal in size to orbit

1: strongly enlarged, more than 1.5 times the size of the orbit

128. Postorbital part of the skull roof

0: as high as orbital region

1: deflected ventrally in adult individuals

129. Preorbital region of the skull in post-hatchling individuals

0: elongate, nasals considerably longer than frontals, maxilla at least twice the length of the premaxilla

1: shortened, nasals subequal in length to frontals or shorter, maxillary length less than twice the length of the premaxillary body

130. Occipital region of the skull faces

0: posteriorly

1: posteroventrally

131. Basipterygoid processes

0: well-developed, extending as a distinct process from the base of the basisphenoid

1: abbreviated or absent

132. Basipterygoid processes well developed and

0: anteroposteriorly short and finger-like (approximately as long as wide)

1: longer than wide

2: significantly elongated and tapering

133. Basipterygoid processes

0: ventral or anteroventrally projecting

1: lateroventrally projecting

2: caudally projecting

134. Basipterygoid processes

0: solid

1: hollow

135. Basipterygoid recesses on dorsolateral surfaces of basipterygoid processes

0: absent

1: present

136. Basisphenoid bulla

0: absent

1: present

137. Basisphenoid recess

0: absent or poorly developed

1: deep and well-developed

138. Passage of internal carotids between posterior end of skull and pituitary fossa

0: no bony tubes present

1: enclosed by bony tubes extending along ventral surface of basisphenoid

139. Basisphenoid recess position

0: between basisphenoid and basioccipital

1: entirely within basisphenoid

140. Posterior opening of basisphenoid recess

0: single

1: divided into two small, circular foramina by a thin bar of bone

141. Basisphenoid between basal tubera and basipterygoid processes

0: approximately as wide as long, or wider

1: significantly elongated, at least 1.5 times longer than wide

142. Basisphenoid in lateral view

0: oriented subhorizontally

1: anterior portion located much more ventrally than posterior portion, recess visible in posterior view

143. Base of cultriform process

0: not highly pneumatised

1: expanded and pneumatic (parasphenoid bulba)

144. Vestibular and Cochlear branches of CN VIII

145. Exits of CN X-XII

0: flush with surface of exoccipital

1: located together in a bowl-like basisphenoid depression

146. Exits of CN X and XI

0: laterally through the jugular foramen

1: posteriorly through a foramen (metotic foramen) lateral to the exit of cranial nerve XII and the occipital condyle

147. Exoccipital lateral to occipital condyle

0: forms roof over exits for CN X and XII

1: unexpanded and does not form roof

148. Supraoccipital sagittal crest

0: with pronounced sagittal crest

1: sagittal crest reduced or absent

149. Paroccipital process shape

0: elongate and slender

1: short, deep

150. Paroccipital process direction

0: straight, projects laterally or posterolaterally

1: project ventrolaterally

2: pendant

151. Paroccipital process dorsal edge

0: with straight dorsal edge

1: distal end twists rostrally, distal ends of the processes oriented transversely rather than vertically

152. Ventral rim of the basis of the paroccipital processes

0: above or level with the dorsal border of the occipital condyle

1: situated at mid-height of occipital condyle or lower

153. Foramen magnum

0: subcircular, slightly wider than tall

1: oval, taller than wide

154. Foramen magnum size

0: smaller than or subequal in width to occipital condyle

1: larger in width than occipital condyle

155. Occipital condyle

0: without constricted neck

1: subspherical with constricted neck

156. Infracondylar fossa of occipital condyle

0: absent

1: present

157. Form of infracondylar fossa of occipital condyle

0: narrow and groove-like

1: broad depression approximately two-thirds the width of the occipital condyle

158. Basal tubera

0: present

1: absent

159. Basal tubera composition

0: equally formed by basioccipital and basisphenoid and not subdivided

1: subdivided by a lateral longitudinal groove into a medial part entriely formed by the basioccipital, and a lateral part, entirely formed by the basisphenoid

160. Basal tubera spacing

0: set far apart, level with or beyond lateral edge of occipital condyle and/or foramen magnum

1: tubera small, directly below condyle and foramen magnum, and separated by a narrow notch

161. Subcondylar recess

0: absent

1: present in basioccipital/exoccipital lateral and ventral to occipital condyle

162. Subcondylar recess form

0: isolated from nervous foramina CNX-CNXII

1: subcondylar recess and cranial nerves exit together in a deep depression encompassing multiple pneumatic fossae and enclosed by a well developed rim

163. Exit of mid-cerebral vein

0: included in trigeminal foramen

1: vein exits braincase through a separate foramen anterodorsal to the trigeminal foramen

164. Brain proportions

0: forebrain small and narrow

1: forebrain significantly enlarged and triangular

165. Anterior tympanic recess in the braincase

0: absent

1: present

166. Prootic pneumatic recess

0: absent

1: present

167. Form of pneumatic prootic recess

0: dorsally open fossa on prootic/opisthotic

1: deep, posterolaterally directed concavity

168. Crista interfenestralis

0: confluent with lateral surface of prootic and opisthotic

1: distinctly depressed within middle ear opening

169. Accessory dorsal tympanic recess (dorsal to crista interfenestralis)

0: absent

1: present

170. Form of dorsal tympanic recess

0: small pocket present

1: extensive with indirect pneumatisation

171. Caudal (posterior) tympanic recess

0: absent

1: present

172. Form of caudal tympanic recess

0: present as opening on anterior surface of paroccipital process

1: extends into opisthotic posterodorsal to fenestra ovalis, confluent with this fenestra

173. Exoccipitals ventral to posterior pneumatic recess

0: no lip

1: form anteriorly projecting, posterodorsally curling, dorsally concave, tablike process

174. Otosphenoidal crest

0: vertical on basisphenoid and prootic, and does not border an enlarged pneumatic recess

1: well-developed, crescent-shaped, thin crest forms anterior edge of enlarged pneumatic recess

175. Subotic recess (pneumatic fossa ventral to fenestra ovalis)

0: absent

1: present

176. Depression (possibly pneumatic) on ventral surface of postorbital process of laterosphenoid

0: absent

1: present

177. Interorbital region in adults

0: unossified

1: ossified

178. Prominent endocranial expansion of vertical semicircular canal

0: absent

1: present

179. Mandibular foramen

0: absent or reduced

1: large

2: hypertrophied, greater than 50% dentary length

180. Shape of mandibular foramen

0: oval

1: subdivided by a spinous rostral process of the surangular

181. Paradental plates of dentary

0: lack paradental plates

1: with paradental plates on the medial surface of the tooth row

182. Internal mandibular fenestra

0: small and slit-like

1: large and rounded

183. Shape of anterior end of dentary

0: blunt and unexpanded

1: dorsoventrally expanded, rounded and slightly upturned

2: with anteroventral process giving a "squared off" appearance in lateral view

184. Dorsal edge of anterior end of dentary in lateral view

0: dorsally flat

1: with dorsally expanded, arcuate eminence

185. Symphyseal region of dentary

0: Broad and straight, paralleling lateral margin

1: medially recurved

186. Degree of medial recurvature of dentary symphysis

0: medially recurved slightly

1: strongly recurved medially

187. Dentary symphyseal fusion

0: absent

1: present

188. Dentary anterior end in lateral view

0: in line with main part of buccal edge

1: anterior end deflected ventrally

189. Width of dentary symphyseal region

0: no broader than transverse width of post-symphyseal region

1: broader than post-symphyseal region

190. Orientation of dentary symphysis in lateral view

0: vertical to subvertical

1: projects strongly cranially, oblique with respect to dentary ventral margin

191. Posterior end of dentary

0: without posterodorsal process dorsal to mandibular fenestra

1: with dorsal process

192. Form of dentary posterodorsal process

0: developed only above anterior end of mandibular fenestra

1: with elongate dorsal process extending over most of fenestra

193. Labial face of dentary

0: flat

1: with lateral ridge and inset tooth row

194. Nutrient foramina on external surface of dentary

0: superficial

1: descend strongly posteriorly within a deep groove

195. Form of nutrient foraminal groove

0: thin groove of constant height as it extends posteriorly

1: posterior end of groove is dorsoventrally expanded

196. Dentary shape in lateral view

0: with subparallel dorsal and ventral edges

1: subtriangular in lateral view

197. Form of triangular dentary

0: low triangular

1: high triangular

198. Ventral edge of dentary in lateral view

0: straight or nearly straight

1: descends strongly posteriorly

199. Dentary paradental groove separating interdental plates from medial wall of dentary

0: absent

1: present

200. Pronounced coronoid eminence on the surangular

0: absent

1: present

201. Foramen in lateral surface of surangular rostral to mandibular articulation

0: absent

1: present

202. Number of surangular foramina

0: one

1: two

203. Laterally inclined flange along dorsal edge of surangular for articulation with lateral process of lateral quadrate condyle

0: absent

1: present

204. Anterior portion of the surangular

0: less than half the height of the mandible above the mandibular fenestra

1: more than half the height of the mandible at the level of the mandibular fenestra

205. Retroarticular process of the mandible

0: narrow, rod-like

1: broadened, with groove posteriorly for the attachment of the m. depressor mandibulae

206. Attachment of the m. depressor mandibulae on retroarcticular process of mandible

0: facing dorsally

1: facing posterodorsally

207. Retroarticular process

0: points posteriorly

1: curves gently posterodorsally

208. Articular

0: without elongate, slender medial, posteromedial, or mediodorsal process from retroarticular process

1: with process

209. Angular

0: exposed almost to end of mandible in lateral view, reaches or almost reaches articular

1: excluded from posterior end angular suture turns ventrally and meets ventral border of mandible rostral to glenoid

210. Coronoid ossification

0: absent

1: present

211. Form of coronoid ossification

0: large

1: thin splint

212. Splenial

0: not widely exposed on lateral surface of mandible

1: exposed as a broad triangle between dentary and angular on lateral surface of mandible

213. Foramen in the ventral part of the splenial (mylohyal foramen)

0: absent

1: present

214. Form of mylohyal foramen

0: completely enclosed in the splenial

1: opened anteroventrally

215. Posterior end of splenial

0: straight

1: forked

216. Articular glenoid fossa

0: as long as distal end of quadrate

1: twice or more as long as quadrate surface, allowing anteroposterior movement of mandible

217. Palatal teeth

0: present

1: absent

218. Premaxillary teeth

0: present

1: absent

219. Number of premaxillary teeth

0: three

1: four

2: five

3: more than five

220. First premaxillary tooth size

0: slightly smaller or the same size as 2 and 3

1: much smaller than 2 and 3

2: much larger than 2 and 3

221. Second premaxillary tooth

0: approximately equivalent in size to other premaxillary teeth

1: markedly larger than third and fourth premaxillary teeth

222. Premaxillary tooth direction

0: decumbent or ventrally projecting

1: procumbent

223. Serrations on premaxillary teeth

0: present

1: absent

224. In cross section, premaxillary tooth crowns

0: sub-oval to sub-circular

1: D-shaped with flat lingual surface

225. Maxillary teeth

0: present

1: absent

226. Length of maxillary tooth row

0: extends posteriorly to approximately half the length of the orbit

1: ends at the anterior rim of the orbit

2: completely antorbital, tooth row ends anterior to the vertical strut of the lacrimal

3: ends below the junction between the maxillary body and the ascending process

227. Number of maxillary teeth (ORDERED)

0: 10-14

1: 15-19

2: 20 or more

228. Maxillary tooth direction

0: ventrally or posteriorly inclined

1: procumbent

229. Maxillary and dentary teeth, mesial (anterior) carina

0: present

1: absent

230. Mesial (anterior) carina of maxillary and dentary teeth present and

0: extends to base of crown

1: terminates ventrally at approximately mid-crown level or more dorsally

231. Shape of maxillary teeth (ORDERED)

0: mediolaterally flattened, dorsoventrally taller than anteropostiorly wide

1: lanceolate and subsymmetrical (as in therizinosaurs)

2: simple, conical, incisive crowns (as in Alvarezsaurs)

232. Degree of curvature of maxillary tooth crowns

0: crowns curve posteriorly as they extend distally

1: very little curvature or crowns straight

233. Serrations on maxillary and dentary teeth

0: present

1: some without serrations anteriorly

2: absent

234. Maxillary tooth implantation

0: separate alveoli

1: set in an open groove

235. Roots of maxillary and dentary teeth

0: mediolaterally compressed

1: circular in cross-section

236. Dentary tooth row (ORDERED)

0: fully toothed

1: only teeth rostrally

2: edentulous

3: fully toothed with short edentulous anterior portion

237. Number of dentary teeth

0: large, fewer than 25 in dentary

1: moderate number of small teeth (25-30 in dentary)

2: relatively small and numerous (more than 30 in dentary)

238. Dentary teeth distribution

0: homodont

1: increasing in size anteriorly, becoming more conical in shape

2: Decreasing in size anteriorly, becoming more densely packed

239. Shape of dentary teeth (ORDERED)

0: mediolaterally flattened, dorsoventrally taller than anteroposteriorly wide

1: lanceolate and subsymmetrical (as in therizinosauroids)

2: simple, conical, incisive crowns (as in Alvarezsaurs)

240. Third dentary alveolus

0: subequal in size to other alveoli

1: circular and enlarged relative to other alveoli

241. Dentary tooth implantation

0: separate alveoli

1: set in an open groove

242. Dentary tooth direction

0: dorsally or posteriorly inclined

1: procumbent (anteriorly inclined)

243. Serrations on maxillary and dentary teeth

0: simple, denticles convex

1: distal and often mesial edges of teeth with large, hooked denticles that point toward the tip of the crown

244. Serration size

0: large

1: small

245. Constriction between tooth crown and root

0: absent

1: present

246. Enamel of tooth crowns

0: smooth

1: horizontally wrinkled, especially flanking the serrations

247. Form of enamel wrinkles

0: bands extending across labial and lingual tooth surfaces

1: adjacent to carinae but do not extend across labial and lingual tooth surfaces

248. Vertical striations of enamel of tooth crowns

0: absent

1: present

CERVICALS

249. Axial diapophyses

0: moderate

1: reduced or absent

250. Axial parapophyses

0: prominent or moderate

1: reduced or absent

251. Axial neural spine

0: flared transversely and sheet-like

1: compressed mediolaterally, anteroposteriorly reduced, and rodlike

252. Epipophyses on axis

0: absent

1: present

253. Form of axial epipophyses

0: present as small ridges

1: strongly pronounced (overhanging the zygapophyses)

254. Pleurocoel in axis

0: absent

1: present

255. Number of cervical vertebrae

0: 10

1: More than 10

256. Pleurocoels in cervical vertebrae

0: absent

1: present

257. 'Number of pleurocoels in 'cervicals

0: one

1: two

258. Arrangement of two foramina in cortical surface of cervical centra

0: one in anterior half of lateral surface, one in posterior half

1: both foramina in anterior half

259. Pleurocoels developed as

0: deep depressions

1: foramina

260. Interior pneumatic spaces in cervicals

0: Structure camerate (few chambers)

1: Structure camellate (many chambers separated by delicate lamellae) (Ornithomimus)

261. Ventral surface of anterior cervicals (ORDERED)

0: keeled

1: smooth

2: ventral depression

262. Posterolateral crests on lateral surfaces of cervical centra

0: absent

1: present

263. Anterior cervical centra length

0: less than twice transverse centrum width

1: between two and three time transverse width (Nqwebasaurus)

2: three to five times transverse width (Ornithomimus, Gallimimus)

264. Anterior articular facet of anterior cervical vertebrae

0: approximately as high as wide or higher

1: significantly wider than high

2: wider than high and higher laterally than medially (kidney-shaped), with neural canal emarginating dorsal aspect

265. Anterior cervical centra relative length

0: level with or shorter than posterior extent of neural arch

1: centra extending beyond posterior limit of neural arch

266. Articulation surfaces of cervical centra

0: amphi- to platycoelus

1: opisthocoelus

2: heterocoelus

267. Carotid process on posterior cervical centra

0: absent

1: present

268. Epipophyses in anterior cervical vertebrae

0: absent or poorly developed

1: well-developed

269. Form of well-developed cervical epipophyses

0: proximal to postzygapophyseal facets

1: strongly overhanging postzygapophyseal facets

270. Prezygapophyseal-epipophyseal lamina on dorsal surface of neural arch

0: absent or poorly developed

1: extending anteriorly from epipophysis as a mediolaterally thin ridge that separates dorsal surface of diapophysis from rest of dorsal neural arch

271. Postzygapophyses of cervical vertebrae 2-4

0: well-separated, or connected only at the base

1: medially connected along their entire length by a intrazygapophyseal lamina that is dorsally concave for attachment of the interspinous ligaments

272. Cervical neural spines

0: anteroposteriorly long (Harpymimus, Struthiomimus, Ornithomimus)

1: anteroposteriorly short and centered on neural arch, giving arch an "X" shape in dorsal view (Nqwebasaurus, Beishanglong, Gallimimus)

2: extremely short anteroposteriorly, less than 1/3 length of neural arch

273. Cervical neural spine height

0: dorsoventrally tall, subequal to or exceeding height of neural arch from centrum to base of neural spine

1: moderate, less than neural arch height

2: strongly reduced, less than half height of neural arch (not including spine itself)

274. Prezygapophyses in anterior cervicals

0: transverse distance between prezygapophyses less than width of neural canal

1: prezygapophyses situated lateral to the neural canal

275. Prezygapophyses in anterior postaxial cervicals

0: straight

1: anteroposteriorly convex, flexed ventrally anteriorly

DORSALS

276. Pneumaticity of dorsal neural arches

0: absent to moderate

1: extreme

277. Hypapophyses in anterior dorsals

0: absent or poorly developed

1: pronounced

278. Pleurocoels in dorsal vertebrae

0: absent

1: present in anterior dorsals ('pectorals')

2: present in all dorsals

279. Dorsal centra articular surfaces

0: amphiplatyan

1: opisthocoelous

280. Ventral keel in anterior dorsals

0: absent or very poorly developed

1: pronounced

281. Shape of dorsal centra in anterior view

0: subcircular or oval

1: significantly wider than high

2: triangular

282. Posterior dorsal vertebrae

0: strongly shortened, centra much shorter than high

1: relatively short, centra approximately as high as long, or only slightly longer

2: significantly elongated, much longer than high

283. Posterior dorsal vertebrae, basal webbing of neural spines

0: absent

1: present (Ichthyovenator, Baryonyx, Suchomimus) maybe by elongation of neural spines

284. Posterior dorsal vertebrae, orientation of neural spines

0: vertically or posteriorly

1: anteriorly

285. Anterior dorsal vertebrae height of prezygodiapophyseal lamina

0: less than or subequal to height of centrum

1: hypaxially inflated, height significantly greater than centrum height

286. Anterior dorsal vertebrae, anterior and posterior infrazygapophyseal fossae

0: single

1: with one or more accessory centrodiapophyseal laminae dividing fossa into multiple chambers

287. Transverse processes of anterior dorsal vertebrae

0: subhorizontal to vertically inclined

1: pendant

288. Parapophyseal facets of anterior dorsal vertebrae

0: moderate in size (less than half height of centrum)

1: hypertrophied (greater than two thirds centrum height)

289. Hyposphene-hypantrum articulation in dorsal vertebrae

0: absent

1: present

290. Step-like ridge lateral to hyposphene running posterodorsally from the dorsal border of the neural canal to the posterior edge of the postzygapophyses of dorsal vertebrae (visible in lateral view)

0: absent

1: present

291. Postzygapophyses of the dorsal vertebrae in posterior view

0: without lateral flanges

1: with lateral, small, flange-like lateral extensions of postzygapophyseal facets

292. Postzygapophyses of dorsal vertebrae

0: abutting one another above neural canal, opposite hyposphene meet to form lamina

1: zygapophyses placed lateral to neural canal and separated by groove for interspinous ligaments, hyposphene separated

293. Neural spines on posterior dorsal vertebrae in lateral view

0: rectangular or square

1: anteroposteriorly expanded distally, fan-shaped

294. Neural spines of dorsal vertebrae in dorsal view

0: not expanded distally

1: expanded laterally in dorsal view to form "spine table"

295. Scars for interspinous ligaments

0: terminate at apex of neural spine in dorsal vertebrae

1: terminate below apex of neural spine

296. Neural spines of posterior dorsals

0: broadly rectangular and approximately as dorsoventrally high as anteroposteriorly long

1: high rectangular, significantly dorsoventrally higher than anteroposteriorly long

297. Hook-like extension on anterior end of dorsal neural spines in lateral view

0: absent

1: present (with associated depression immediately caudal to the projection for spinous ligament attachment)

298. Parapophyses of posterior dorsal vertebrae

0: flush with neural arch

1: distinctly projected on pedicels

299. Parapophyses in posteriormost dorsals

0: on same level as transverse process

1: distinctly below transverse process

300. Transverse processes of anterior dorsal vertebrae

0: proximodistally long and anteroposteriorly thin

1: proximodistally short, anteroposteriorly wide

301. Notarium of dorsal vertebrae

0: absent

1: present

SACRUM

302. Number of sacral vertebrae

0: two

1: three

2: four

3: five

4: six

5: seven

6: eight

7: nine or more

303. Pleurocoels in centra of sacral vertebrae

0: absent

1: present on anterior sacrals only

2: present on all sacrals

304. Ventral surface of posterior sacral centra

0: gently rounded, convex

1: flattened ventrally, sometimes with shallow sulcus

2: centrum strongly constricted transversely, ventral surface keeled

305. Transverse dimensions of mid-sacral centra relative to other sacral centra

0: subequal

1: mediolaterally narrower

2: mediolaterally wider

306. Sacral vertebrae

0: with unfused zygapophyses

1: with fused zygapophyses forming a sinuous ridge in dorsal view

307. Last sacral centrum

0: with flat posterior articulation surface

1: convex articulation surface

308. Fenestrae between neural spines of sacral vertebrae

0: present

1: absent

309. Sacral ribs

0: slender and well-separated

1: forming a more or less continuous sheet in ventral or dorsal view

2: very massive and strongly expanded

310. Sacral neural arch pneumaticity

0: absent to moderate

1: extreme

311. Number of caudal vertebrae

0: more than 40

1: 25-40

2: fewer than 25

312. Pygostyle (need to clarify)

0: absent

1: present, centra of distal caudal vertebrae fused

313. Pleurocoels in centra of anterior caudal vertebrae

0: absent

1: present

314. Caudal centra

0: amphiplatyan

1: procoelus

315. Shape of anterior caudal centra

0: oval

1: subrectangular and box-like

2: laterally compressed with a ventral keel

316. Ventral surface of anterior caudals

0: rounded

1: with a distinct keel sometimes bearing a narrow, shallow groove on its midline

2: grooved

317. Relative length of distal caudal centra

0: significantly elongated in relation to centrum height

1: not elongated in relation to centrum height

318. Caudal vertebrae

0: with distinct transition point, from shorter centra with long transverse processes proximally to longer centra with small or no transverse processes distally

1: homogeneous in shape, with no transition point

319. Position of transition point

0: distal to the tenth caudal vertebra

1: between the 7th and 10th caudal vertebrae

2: proximal to the 7th caudal vertebra

320. Location of transverse processes of proximal caudals

0: centrally positioned on centrum

1: anteriorly displaced

321. Centrodiapophyseal laminae of anterior caudal vertebrae

0: weak

1: prominent, as well developed as those of dorsal vertebrae

322. Neural spines on distal caudals

0: form a low ridge

1: spine absent

2: midline sulcus in center of the neural arch

323. Neural spines of caudal vertebrae

0: simple, undivided

1: separated into anterior and posterior alae throughout much of caudal sequence

324. Neural spines of mid-caudals

0: rod-like and posteriorly inclined

1: rod-like and vertical

2: subrectangular and sheet-like

325. Prezygapophyses of distal caudal vertebrae

0: between 1/3 and whole centrum length

1: with extremely long extensions of the prezygapophyses (up to 10 vertebral segments in some taxa)

2: strongly reduced as in Archaeopteryx lithographica

326. Anterior margin of neural spines of anterior mid-caudal vertebrae

0: straight

1: with distinct kink, dorsal part of anterior margin more strongly inclined posteriorly than ventral part

RIBS AND GASTRALIA AND CHEVRON

327. Long, hair-like cervical ribs

0: absent

1: present

328. Shaft of cervical ribs

0: slender and longer than vertebra to which they articulate

1: broad and shorter than vertebra

329. Posterior cervical ribs and centra

0: separate

1: fused

330. Ossified uncinate processes

0: absent

1: present

331. Ossified sternal ribs

0: absent

1: present

332. Lateral gastral segment

0: shorter than medial one in each arch

1: distal segment longer than proximal segment

333. Cranial process at base of chevrons

0: absent

1: present

334. Proximal surface of chevrons

0: distinct transverse ridge dividing surface into anterior and posterior facets

1: no ridge, low mounds may be present laterally

335. Proximal end of chevrons of proximal caudals

0: short anteroposteriorly, shaft cylindrical

1: proximal end elongate anteroposteriorly, flattened and plate-like

336. Mid-caudal chevrons

0: rod-like or only slightly expanded ventrally

1: L-shaped

337. Distal chevrons

0: rod-like or L-shaped

1: skid-like

338. Distal caudal chevrons

0: simple

1: anteriorly bifurcate

2: bifurcate at both ends

339. Ossified sternal plates

0: separate in adults

1: fused

340. Ventral keel on sternum

0: absent

1: present

341. Sternum

0: without distinct lateral xiphoid process posterior to costal margin

1: with lateral xiphoid process

342. Furcula (need to clarify))

0: absent

1: present

343. Furcula shape

0: v-shaped

1: u-shaped, with bowed epicleidea

344. Hypocleidium on furcula

0: absent

1: present

SCAPULAR AND CORACOID

345. Articular facet of coracoid on sternum (conditions may be determined by the articular facet on

coracoid in taxa without ossified sternum (재확인)

0: anterolateral or more lateral than anterior

1: almost anterior

346. Anterior edge of sternum

0: grooved for reception of coracoids

1: without grooves

347. Coracoid in lateral view

0: subcircular, with low ventral blade and no or small posterior process

1: shallow ventral blade with elongate posterior process

2: subquadrangular with extensive ventral blade

3: strut-like, very tall ventral blade with little or no posterior process

348. Posterior edge of coracoid

0: not or shallowly indented below glenoid

1: posterior edge of coracoid deeply notched just ventral to glenoid, glenoid lip everted

349. External surface of coracoid ventral to glenoid fossa and along dorsal margin of posteroventral blade

0: unexpanded

1: expanded, forms triangular subglenoid fossa bounded laterally by coracoid tuber

350. Coracoid tubercle

0: absent

1: present

351. Coracoid tubercle form

0: anteroposteriorly short, mound-like

1: anteroposteriorly elongated, ridge-like

352. Coracoid foramen

0: present

1: absent

353. Scapula shape

0: short and broad (ratio length/minimal height of shaft <9)

1: slender and elongate (ratio >10)

354. Scapulocoracoid junction anterior surface

0: indented or notched between the scapular acromial process and the coracoid suture

1: smoothly curved and uninterrupted across the contact between the scapula and coracoid

355. Acromion margin of scapula

0: continuous with blade

1: anterior edge enlarged and projects anteriorly at approximately a right angle

356. Flange on supraglenoid buttress on scapula (see Nicholls and Russell, 1985) (Osmólska: present as a weak swelling)

0: absent

1: present

357. Distal end of scapula

0: expanded

1: not expanded

358. Glenoid fossa

0: faces posteriorly or posterolaterally

1: faces laterally

359. Scapula and coracoid

0: separate

1: fused into scapulocoracoid

360. Scapula and coracoid orientation

0: continuous arc in posterior and anterior views

1: coracoid inflected medially, scapulocoracoid L shaped in lateral view

361. Scapula length

0: longer than humerus

1: shorter than humerus

HUMERUS

362. Deltopectoral crest length

0: less than one quarter humeral length

1: approximately one third humeral length

2: greater than one half humeral length

363. Deltopectoral crest

0: large and distinct, proximal end of humerus quadrangular in anterior view

1: less pronounced, forming an arc rather than being quadrangular

2: very weakly developed, proximal end of humerus with rounded edges

3: extremely long (as in Shuvuuia and Mononykus)

364. Deltopectoral crest orientation

0: longitudinal

1: oblique distolaterally and distal end of crest oriented laterally rather than anteriorly from the humeral shaft

365. Lateral surface of distal end of deltopectoral crest

0: smooth

1: with distinct muscle scar near lateral edge along distal end of crest for insertion of biceps muscle

366. Ratio femur/humerus

0: more than 2.5

1: between 1.2 and 2.2

2: less than 1

367. Outline of proximal articular facet of humerus

0: broadly oval (more than twice as broad transversely than anteroposteriorly)

1: distinctly rounded, often globular (less than twice as broad anteroposteriorly than transversely)

368. Internal tuberosity of humerus

0: small and confluent with humeral head

1: offset from humeral head by distinct notch, often projects proximally above humeral head

2: hypertrophied but not distinct from humeral head (as in Suchomimus)

369. Shape of internal tuberosity on humerus in anterior view

0: triangular, often rounded

1: rectangular

370. Humerus in lateral view

0: sigmoidal

1: straight

371. Transverse width of distal humerus

0: greater than 2.7 times shaft width

1: between 2 and 2.5 times humeral shaft width

2: less than twice shaft width

372. Ectepicondyle of humerus (lateral epicondyle)

0: small, often rectangular and does not form articular surface

1: large, rounded and forms articular surface

373. Entepicondyle of humerus (medial epicondyle)

0: absent or small and tabular

1: large, projects medially from ulnar condyle as a distinct process and is distally separated from ulnar condyle by a groove

374. Distal humeral condyles

0: primarily developed on distal end of humerus, but may also have some articular surface extending to anterior edge

1: limited to anterior surface, condylar surfaces not present on distal end

ULNA

375. Ulnar shaft

0: straight

1: bowed

376. Olecranon process of ulna

0: absent or weakly developed

1: well-developed

2: hypertrophied

377. Shape of olecranon process

0: transversely broad

1: mediolaterally thin, blade-like

378. Crest extending along posterior surface of ulnar shaft from olecranon process

0: absent

1: present

379. Proximal surface of ulna

0: single continuous articular facet

1: divided into two distinct fossae

380. Proximal end of the ulna in proximal view

0: without extensive coronoid process and radial process on radial side of proximal end

1: coronoid and medial processes large

381. Distal articular surface of ulna

0: flat

1: convex, semilunate surface

382. Distal condyle articular surface of ulna

0: unexpanded or spatulate, articular surface limited to distal end

1: bulbous, trochlear articular surface extends onto dorsal surface of ulna

RADIUS

383. Radius length

0: more than half the length of humerus

1: less than half the length of humerus

384. Radial shaft

0: straight

1: bowed laterally

385. Radius and ulna

0: well-separated

1: with distinct adherence or syndesmosis distally

CARPUS

386. Ossified carpals

0: absent

1: present

387. Lateral proximal carpal (ulnare?)

0: quadrangular

1: triangular in proximal view

388. Trochlea on the proximal surface of distal carpal 1

0: absent

1: present

389. Two distal carpals

0: in contact with metacarpals, one covering the base of Mc I (and perhaps contacting Mc II), the

other covering the base of Mc II

1: two distal carpals not present, single distal carpal capping Mc I and II

390. Distal carpals

0: not fused to metacarpals

1: fused to metacarpals, forming carpometacarpus

METACARPALS AND PALANGES

391. Rectangular buttress on ventrolateral surface of proximal end of Mc I

0: absent

1: present

392. Length of Mc I

0: approximately half the length of Mc II

1: subequal in length to Mc II

393. Shape of Mc I

0: significantly longer than broad

1: very stout, approximately as long as broad

394. Contact between Mc I and Mc II

0: metacarpals contact each other at their bases only

1: Mc I closely appressed to Mc II, at least the proximal half of McI flattened

395. Medial tab on proximal end of Mc I ('proximo-radial process of Gishlick and Gauthier, 2007)

0: absent or poorly developed

1: well-developed, extending far medially

396. Distal end of Mc I

0: condyles more or less symmetrical

1: condyles strongly asymmetrical, the medial condyle being positioned more proximally than the lateral

397. Distal articular end of metacarpal I

0: ginglymoid

1: rounded and smooth

398. Medial side of Mc II

0: expanded proximally

1: not expanded

399. Distal articular end of McII

0: ginglymoid

1: without ginglymus

400. Shaft of Mc III

0: subequal in width to Mc II

1: considerably more slender than Mc II (less than 70% of the width of Mc II)

401. Proximal articular end of Mc III

0: expanded and similar in width to Mc I and II

1: not expanded, very slender when compared to Mc I and II

402. Proximal outline of Mc III

0: subrectangular

1: triangular, apex dorsal

403. Shaft of Mc III

0: straight

1: bowed laterally

404. Extensor pits on the dorsal surface of the distal end of metacarpals

0: absent or poorly developed

1: deep, well-developed

405. Number of manual digits with one or more phalanges

0: five

1: four

2: three

3: two

406. Number of metacarpals

0: five

1: four

2: three

407. Paired flexor processes on proximal ventral surfaces of proximal most phalanges

0: absent

1: present

408. Flexor surface of manual phalanx I-1

0: convex or flat

1: concave, 'axial furrow' along proximodistal axis

409. Shaft diameter of phalanx I-1

0: less than shaft diameter of radius

1: greater than shaft diameter of radius

410. Proximodistal length of phalanx I-1/length of Mc I

0: 1 or less

1: between 1 and 1.5

2: more than 1.5

411. Penultimate phalanx of the second finger

0: shorter than first phalanx

1: longer than first phalanx

412. Penultimate phalanx of the third finger

0: as long as, or shorter than, more proximal phalanges

1: longer than each of the more proximal phalanges

2: longer than both proximal phalanges taken together

413. Length of third manual digit

0: longer than second finger

1: shorter than or equal in length to second finger

414. Proximal articular surface of manual ungual I-2

0: dorsoventrally much taller than mediolaterally wide

1: mediolaterally as broad as tall

415. Unguals on all manual digits

0: generally similar in size

1: digit I bearing large ungual and unguals of other digits distinctly smaller

416. Transverse ridge immediately dorsal to the articulating surface of unguals

0: absent

1: present

417. Flexor tubercle placement

0: proximal

1: distal

2: absent

418. Curvature of ventral surface manual ungual I

0: strongly curved

1: weakly curved

2: straight

419. Curvature of ventral surface of manual unguals II and III

0: strongly curved

1: weakly curved

2: straight

420. Flexor tubercle size

0: large (> 1/3 articular facet height)

1: small (< 1/3 articular facet height)

421. Lateral grooves of manual ungual I-2 in ventral view

0: unenclosed

1: proximal end of grooves partially enclosed by lateral notches

2: proximal end of grooves passes through foramina on ventral surface of ungual

ILIUM

422. Fusion of pelvic elements in adults

0: absent

1: present

423. Ilium

0: brachyiliac

1: dolichoiliac

424. Ilium pneumaticity

0: little or none

1: large external pneumatic foramina and internal spaces

425. Dorsal margin of ilium

0: subhorizontal or gently inclined relative to axis of pubic and ischial contact

1: rises steeply as it extends anteriorly, at least 30 degree angle from the axis of the pubic and ischial contact

426. Ventral edge of anterior ala of ilium

0: straight or gently curved

1: ventral edge hooked anteriorly

427. Form of hook of preacetabular ala of ilium

0: weak

1: strong

428. Preacetabular part of ilium

0: significantly shorter than postacetabular part

1: subequal in length to postacetabular part

2: significantly longer than postacetabular process

429. Anterior rim of ilium

0: shallowly convex or straight

1: strongly convex or pointed anteriorly

430. Dorsally-positioned, anteriorly-concave notch on anterior rim of ilium

0: absent

1: present

431. Preacetabular part of ilium (height)

0: approximately as high as postacetabular part (excluding the ventral expansion)

1: significantly higher than postacetabular part

2: significantly lower than the postacetabular part

432. Cuppedicus fossa

0: absent

1: present

433. Form of cuppedicus fossa

0: deep, ventrally concave

1: fossa shallow or flat, with no lateral overhang

434. Cuppedicus fossa position

0: ridge bounding fossa terminates rostral to acetabulum or curves ventrally onto anterior end of pubic peduncle

1: rim extends far posteriorly and is confluent or almost confluent with acetabular rim

435. Preacetabular portion of ilium

0: parasagittal

1: moderately laterally flaring

436. Brevis fossa shape

0: shelf-like, narrow with subparallel margins

1: deeply concave, expanded posteriorly with lateral overhang

437. Brevis fossa lateral view

0: Poorly developed adjacent to ischial peduncle, without lateral overhang and medial edge of the brevis fossa is visible

1: well developed fossa along full length of postacetabular blade, lateral overhang extends along full length of fossa, medial edge of brevis fossa covered in lateral view

438. Medial brevis shelf

0: strongly developed, projects medially

1: low ridge on medial surface of postacetabular ala

439. Shape of postacetabular ala of ilium in lateral view

0: squared

1: acuminate

440. Postacetabular ala of ilium in lateral view

0: ventral edge flat

1: ventral edge concave

2: ventral edge concave and distal end extends ventrally below level of the ventral margin of the ischial peduncle

441. Articulation of iliac blades with sacrum

0: vertical, well-separated above sacrum

1: strongly inclined mediodorsally, almost contacting each other or sacral neural spines at midline

442. Vertical ridge on iliac blade above acetabulum

0: absent

1: low ridge with associated foramina

2: well-developed

443. Shape of pubic peduncle of ilium

0: transversely broad and roughly triangular in outline

1: anteroposteriorly elongated and narrow

444. Iliac pubic peduncle length relative to iliac ischial peduncle

0: significantly longer than ischial peduncle, ischial peduncle tapering ventrally and without clearly defined articular facet

1: subequal in length to ischial peduncle

2: anteroposteriorly shorter than the ischial peduncle

445. Articulation facet of pubic peduncle of ilium

0: facing more ventrally than anteriorly, and without a pronounced kink

1: with pronounced kink and anterior part facing almost entirely anteriorly

446. Anterior margin of pubic peduncle

0: straight or convex

1: concave

447. Supraacetabular crest

0: absent

1: present

448. Form of supraacetabular crest

0: forms hood over femoral head

1: reduced, not forming hood

449. Antitrochanter posterior to acetabulum

0: absent or poorly developed

1: prominent

450. Postacetabular blades of ilia in dorsal view

0: parallel

1: diverge posteriorly

451. Tuber along dorsal edge of ilium, dorsal or slightly posterior to acetabulum

0: absent

1: present

452. Dorsal margin of postacetabular ala in lateral view

0: convex or straight

1: concave, brevis shelf extends caudal to lateral ilium making it appear concave in lateral view

453. Caudal end of postacetabular ala in dorsal view

0: rounded or squared in dorsal view

1: lobate, with brevis shelf extending caudally beyond caudal terminus of the postacetabular ala

454. Ilium and ischium articulation

0: flat or slightly concavo-convex

1: with process projecting into socket in ischium

455. Pubic orientation

0: propubic

1: vertical

2: moderately posteriorly oriented

3: opisthopubic

456. Strongly expanded pubic boot

0: absent

1: present

457. Pubic boot projects

0: anteriorly and posteriorly

1: with little or no anterior process

2: only expanded anteriorly

458. Ratio length of pubic boot to length of pubic shaft

0: less than 0.3

1: more than 0.5

459. Pubic boot outline, distal view

0: triangular

1: narrow, with subparallel margins

460. Pubic apron

0: present

1: absent

461. Form of pubic apron

0: extends medially from middle of cylindrical pubic shaft

1: shelf extends medially from anterior edge of anteroposteriorly flattened shaft

462. Pubic apron

0: about half of pubic shaft length

1: less than 1/3 of shaft length

463. Pubic apron

0: completely closed

1: with medial opening distally above the pubic boot

464. Pubic obturator foramen

0: present

1: absent

465. Form of pubic obturator foramen

0: completely enclosed

1: open ventrally (obturator notch)

466. Pubic fenestra below obturator foramen

0: absent

1: present

467. Pubic shafts in lateral view

0: straight

1: anteriorly convex

2: anteriorly concave

468. Lateral face of pubic shafts

0: smooth

1: with prominent lateral tubercle about halfway down the shaft

469. 'Length of Ischium

0: more than two-thirds pubis length

1: two thirds or less of pubic length

470. Obturator process of ischium

0: absent

1: present

471. Position of obturator process (ORDERED)

0: proximal in position

1: located near middle of ischiadic shaft

2: located at distal end of ischium

472. Ischial shaft

0: Rodlike

1: anteroposteriorly wide and plate like

473. Lateral blade of ischium

0: flat or laterally convex

1: laterally concave

2: with longitudinal ridge subdividing lateral surface into anterior (including obturator process) and posterior parts

474. Ischium, lateral view

0: straight

1: distally curved anteriorly

2: distally curved posteriorly

475. Ischium, anterior view

0: straight

1: laterally convex

2: twisted at midshaft and with flexure of obturator process toward midline so that distal end is horizontal

3: laterally concave

476. Contact of obturator process of ischium

0: does not contact pubis

1: contacts pubis

477. Ventral notch at distal edge of ischial obturator process

0: absent, grades smoothly into ischial shafts

1: present

478. Obturator process on ischium

0: confluent with pubic peduncle

1: offset from pubic peduncle by a distinct notch

479. Morphology of offset triangular obturator process of ischium

0: wide base along ischiac shaft, rostral process short

1: narrow base, rostral process elongate

480. Distal end of ischium

0: strongly expanded, forming ischial "boot"

1: slightly expanded

2: tapering

481. Distal ends of ischia

0: form symphysis

1: approach one another but do not form symphysis

2: widely separated

482. Distally placed process on caudal margin of ischium

0: absent

1: present

483. Tubercle on anterior edge of ischium

0: absent

1: present

484. Posterior process (ischial tuberosity) on posteroproximal part of ischium

0: absent

1: well-developed

485. Form of posteroproximal ischial process (ischial tuberosity)

0: small, tablike

1: large, proximodorsally hooked and separated from the iliac peduncle by a notch

486. Semicircular scar on posterior part of the proximal end of the ischium

0: absent

1: present

FEMUR

487. Femoral length

0: longer than tibia

1: shorter than tibia

488. Femoral head (new state)

0: without fovea capitalis

1: circular fovea present in center of medial surface of head

2: vertical ridges on anterior and posterior edges of medial surface of head (new state)

489. Oblique ligament groove on the posterior surface of femoral head

0: absent or very shallow

1: deep, bound medially by a well-developed posterior lip

490. Femoral head and greater trochanter

0: confluent with greater trochanter

1: separated from greater trochanter by a distinct cleft

491. Femoral head direction anteroposterior

0: directed anteromedially

1: directed strictly medially

492. Femoral head direction dorsoventral

0: ventromedial

1: horizontal

2: dorsomedial

493. Greater trochanter

0: anteroposteriorly narrow and narrowing from medial to lateral

1: anteroposteriorly expanded, forming a trochanteric crest

494. Lesser trochanter

0: separated from greater trochanter by a deep cleft

1: trochanters separated by small groove

2: completely fused (or absent) to form crista trochanteris

495. Lesser trochanter shape

0: alariform

1: cylindrical in cross section

2: very short and ridge-like

496. Proximal extent of lesser trochanter

0: at distal end of femoral head

1: more proximally placed, but distal to greater trochanter

2: as proximal or more proximal than greater trochanter

497. Accessory trochanteric crest on distal end of lesser trochanter

0: absent

1: present

498. Posterolateral trochanter

0: absent or represented only by rugose area

1: posterior trochanter distinctly raised from shaft, mound-like

499. Fourth trochanter on femur

0: present

1: absent

500. Broad groove on extensor surface of distal femur

0: absent or poorly developed

1: well developed

501. Femoral medial epicondyle (medial distal crest, expanded medial lamella)

0: stout ridge or absent

1: flange like, medially extensive

502. Popliteal fossa on distal end of femur

0: open distally

1: closed off distally by contact between distal condyles

503. Infrapopliteal ridge present posteriorly between medial condyle and crista tibiofibularis

0: absent

1: present

504. Distal end of femur

0: anteroposteriorly broad and distally flattened

1: less broad and well rounded

505. Lateral femoral distal condyle

0: distally rounded

1: distally conical

506. Distal projection of lateral femoral distal condyle

0: approximately the same level as the medial condyle

1: distinctly further than medial condyle and distal surface of medial condyle is flattened

TIBIA

507. Anteroposterior length of proximal end of tibia in proximal view

0: exceeds mediolateral width

1: less than mediolateral width

508. Cnemial crest proximal projection

0: approximately at the same level as posterior condyles

1: projects strongly proximal to posterior condyles

509. Anteroposterior length of cnemial crest

0: prominent but not expanded

1: anteroposteriorly expanded

510. Accessory ridge on lateral surface cnemial crest

0: absent

1: present

511. Medial cnemial crest and lateral cnemial crest (also called the cranial cnemial crest in birds)

0: absent

1: present

512. Fibular condyle (lateral condyle) on proximal end of tibia

0: confluent with cnemial crest anteriorly in proximal view

1: strongly offset from cnemial crest

513. Medial proximal condyle on tibia

0: round in proximal view

1: arcuate and posteriorly angular in proximal view

514. Posterior cleft between medial part of the proximal end of the tibia and fibular condyle

0: absent

1: present

515. Fibular crest (fibular flange) (ridge on lateral side of tibia for connection with fibula)

0: absent

1: present

516. Form of fibular crest

0: extending from proximal articular surface distally

1: clearly separated from proximal articular surface

517. Shape of fibular crest

0: quadrangular

1: low and rounded

518. Fibular crest distal extension

0: proximally positioned

1: extends to midshaft of tibia

519. Fibular crest length

0: short, less than one fifth tibial length

1: long, between one quarter and one third tibial length

520. Bracing for ascending process of astragalus on anterior side of distal tibia

0: distinct 'step' running obliquely from mediodistal to lateroproximal

1: anterior side of tibia flat

2: Step-like ridge running proximodistally rather than obliquely

FIBULA

521. Fibula

0: reaches proximal tarsals

1: short, tapering distally, and not in contact with proximal tarsals

522. Lateral surface of proximal fibula

0: shallow longitudinal trough situated posteriorly

1: trough absent or weak groove present, surface convex

523. Proximal fibular margin

0: sub-horizontal

1: cranial portion extends proximally beyond level of posterior portion

524. Fibular proximal dimensions in proximal view (new state)

0: anterior portion subequal to posterior portion in mediolateral width

1: anterior portion mediolaterally wider than posterior portion

2: posterior portion mediolaterally wider than anterior portion (new state)

525. Insertion of m. iliofibularis on fibular shaft

0: not especially marked

1: present as a well-developed anterolateral tubercle

526. Position of insertion of m. iliofibularis on fibular shaft

0: proximal

1: mid-shaft

527. Ridge on medial side of proximal end of fibula, that runs anterodistally from the posteroproximal end

0: absent

1: present

528. Medial surface of proximal end of fibula

0: concave along long axis

1: flat

529. Deep oval fossa on medial surface of fibula near proximal end

0: absent

1: present

ASTRAGALUS AND CALCANEUM

530. Astragalus and Calcaneum

0: condyles indistinct or poorly separated

1: distinct condyles separated by prominent vertical tendinal groove on anterior surface

531. Astragalus and calcaneum

0: separate from tibia

1: fused to each other and to the tibia in late ontogeny

532. Fibular facet on astragalus

0: large and facing partially proximally

1: reduced and facing laterally or absent

533. Height of ascending process of the astragalus

0: lower than astragalar body

1: higher than astragalar body

2: more than twice the height of astragalar body

534. Shape of ascending process of the astragalus

0: broad, covering most of anterior surface of distal end of tibia

1: narrow, covering only lateral half of anterior surface of tibia

535. Notch on medial edge of ascending process of the astragalus

0: absent

1: present

536. Fossa on anterior surface of mesial base of ascending process of astragalus, sometimes bearing accessory fenestrations

0: absent

1: present

537. Ascending process of astragalus and astragalar body

0: confluent or only slightly offset from astragalar body

1: offset from astragalar body by a pronounced groove

538. Astragalar condyles

0: almost entirely below tibia and face distally

1: significantly expanded proximally on anterior side of tibia and face anterodistally

539. Horizontal groove across astragalar condyles anteriorly

0: absent

1: present

540. Calcaneum

0: without facet for tibia

1: well-developed facet for tibia present

TARSALS

541. Distal tarsals

0: separate, not fused to metatarsals

1: form metatarsal cap with intercondylar prominence that fuses to metatarsal early in postnatal ontogeny

542. Metatarsals coossification

0: not co-ossified

1: coossified

543. Shafts of metatarsals II-IV

0: not closely appressed beyond proximal half of metatarsus

1: closely appressed throughout most of metatarsus, adjacent surfaces flattened for contact

544. Maximum length of metatarsals

0: greater than 50% tibia length

1: less than 50% tibia length

545. Metatarsal I

0: present

1: absent

546. Metatarsal I

0: attenuates proximally, without proximal articulating surface

1: proximal end of Mt I similar to that of Mt II-IV

547. Metatarsal I

0: contacts the ankle joint

1: does not contact the ankle joint

548. Position of distally-placed Mt I

0: reduced, elongated and splint-like, articulates in the middle of the medial surface of Mt II

1: broadly triangular and attached to the distal quarter of Mt II

549. Metatarsal II proximal end of flexor surface

0: flat or small tab present

1: large quadrangular flange present

550. Distal end of metatarsal II

0: smooth, not ginglymoid

1: with developed ginglymus

551. Tuber along extensor surface of MtII

0: absent

1: present

552. Posteromedial margin MtII diaphysis

0: well-developed flange absent or area rugose

1: with flange projecting caudally or medially

553. Distal end of metatarsal III

0: smooth, not ginglymoid

1: with developed ginglymus

554. Metatarsal III

0: subequal in width to Mt II and IV proximally

1: pinched between II and IV and not visible in anterior view proximally

2: does not reach the proximal end of the metatarsus

3: mediolaterally much wider than either II or IV

555. Metatarsal III shape of proximal end

0: rectangular, medial and lateral surfaces pinched

1: hourglass-shaped, medial and or lateral surface(s) concave

556. Medial side of anterior surface of distal end of Mt III

0: unexpanded

1: expanded

557. Metatarsal III shape of shaft in cross section

0: rectangular

1: wedge-shaped, plantar surface pinched

558. Shaft of Mt IV

0: round or thicker dorsoventrally than wide in cross section

1: shaft of Mt IV mediolaterally widened and flat in cross section

559. Length of Mt IV

0: subequal to Mt II

1: markedly longer than Mt II

560. Posterolateral margin of Mt IV diaphysis

0: well-developed flange absent or area rugose

1: with flange projecting caudally or laterally

561. Metatarsal V

0: with rounded distal articular facet

1: strongly reduced and lacking distal articular facet

2: short, without articular surface, transversely flattened and bowed anteriorly distally

562. Pedal digit IV

0: significantly shorter than III and subequal in length to II, foot is symmetrical

1: significantly longer than II and only slightly shorter than III, foot is asymmetrical

563. Extensor ligament pits on dorsal surface of phalanges of pedal digit IV

0: shallow, extensor ridges not sharp

1: deep and extensive proximally, corresponding extensor ridges sharply defined in dorsal view

564. Pedal phalanges of digit IV

0: anteroposteriorly short, with proximal and distal articular surfaces very close together, particularly in distal elements

1: anteroposteriorly long, proximal and distal articular surfaces well-separated

565. Shape of ventral surface of pedal unguals

0: ventrally concave in lateral view

1: straight in lateral view

566. Ungual and penultimate phalanx of pedal digit II

0: similar to those of III

1: highly modified for extreme hyperextension, ungual more strongly curved and about 50% larger than that of III

567. Ventral surface of pedal unguals

0: without a flexor fossa, ventral surface of proximal end convex

1: with a pronounced flexor fossa on ventral surface of proximal end

568. Form of flexor fossa on pedal unguals

0: without development of flexor tubercle

1: small flexor tubercle present within flexor fossa

Supplementary Data-S2B. Character matrix of *Aepyornithomimus tugrikinensis* gen. et sp. nov., and Bügiin ornithomimid added in the character matrix after modified from Lee et al. (2014), Sues and Averianov, (2016a), and McFeeters et al. (2016) for used this matrix in *Deinocheirus* (2014), Bissekty ornithomimid (2016), and *Rativates* (2017) phylogeny. Taxa names which are bolded are species of Ornithomimosauria in the list.

Herrerasaurus ischigualastensis

??000000?00??100???????0010?00000000000????0?00000001?2010000000000?0??01100??0010000???0

??00?0?00?00??00?1????01???11??000?0?0000?0????0???000???01?1?0?0?0?000????0???????????0???1

?000?0?0011???????010?000??????????1010?000?010000000???0?000??00?0000100?0????0010?001000

?000000000000000000100?0??1??0?00000???200000000?000?0000?????????00?????????0??0?00?1010?00

110?1000010??0100?0?00001?0??010000?10000011000?11100000???0000?0?0??0????00?000001001???

?00??1010???00000?0101????00?1?1?0???010000?2000000000000000?0000????0?0??100????00100000

0??000?0?0?00?0000?000?01000?

Acrocanthosaurus atokensis

???010100?0??101?0??10?0?10??0?1?0110001001000?0?0?0112011??0?00001010??1110???11?0??0??0

?01101111?00??10110??01001?1120?0??1?0??0?????01?0?0????1??0101?0?10000????10???????????0???

??200??0000??10???0?10111???0??0?0??101??000021001?00?0?0??1?0???1000?1??1?111110??001?11?

?0?10??2?1??01????10?1?00??01?0?1?????????0?02??????10?1?0????1?010?????????0???1?101?10?0?1

00000??10???02??00?101??0?0??01111?0?10100220002??100?0???00???10?????????????10??????????

101010??0?0{01}0??0????00?11?10?00???01012?1001?011?0??00100?101?????0?0?????0??0??100????
001?000?00??0?1010??2?01000?

Afrovenator abakensis

?????0???????1?101001??0??11010100110?00000?1???????0?201100??0?0010100111 00??00??????????0
0010?01??0????010000001?010????????0?0???
??02000100000???????0100?0110110?10?1?0001?1?11???0100?
{01}?1010?????1?00?????0???????????0???0??0?0?0?100???????11?00?????????????????????????0??0?
01??????00??????????1???011?1?0?????12100?2???0100000001001 00??0????00?00010000100?000000?0
?0?01???000100010011010000??0?0?11000100010001 00????0?0??????001????00?0000100?111??1?0?1
10????01?????2???0???

Albertosaurus sarcophagus

??1????0000011??0????10?1???0??0??0100000101110?11??00201100110001111101120 1??000?1200000
10111100112010101?0010101001030000010000000000 01?00010?1??1000?00110000100?10??00???000
0?001??00??0?00?00?10000101 11?011100???010??00?10?00??0?0000000?0001010???011?0???????000
0011?00????0?0?0???????1??0000?00?00410?00???10??0??00??0??0?00?0????0??0000??0100001 0???00
?000011?001???????00??0?00??0100000001 0?0???????320?0????0000????????10101?100000000?20???
1000000?010??0001???000100000001020001 01?1101100110000100100000001?1110011001?1000100?2
000110?001?00110000011110 00?0?1000?

Allosaurus fragilis

??0010{01}01001010?0000?0000?1000010?110?0100100001?1?011?1?000000000101???{01}100???111
0100000?01000?010?0???01?0100010101120?00010??000100101?00?00?10?0010100110 0100?1?10??0?
0??000000010000??0000?00?1000011111?000100101010200000021001000000000000010100000111010
?10000001011000010011010001000010000001001003000000000000200000010010 00???1?0100???100
??000110101000000100000000100000000000000101000011110001010121000211100000000010010100
0100010000010000100000000101000?10100001000000110100 00?000101100011001100100010001011 1
0000?000100000001100011 10?1?00110000001010?02001000?

Alvarezsaurus calvoi

??

??

??0????00?0?0?0?0012100?0?1?????????

???????????3020????????12100?0?1002???????????1??????????000?01?00?000?????????????????????

????????????????????????????????1?011?1101000?10020??01100210020011?01?00?????????????????????

???????????00?11?1??001?????????????????????10????????1011??11111001??????00?00?01110??10000?

Alxasaurus elesitaiensis

????????????????????????????????????0??

??1?00110101??1

0?101?0????????????????????????????00110?10211000101?0?????????????????0?????????0?00?010010

011??00001001004?1??0??????????01??00?2?01??????0000?????????0???????0????01000100111011011?

???00??0?100010000000?11101220?02???00100100???110100?110101?0???????0???000?2????????1????

?011110?1?1?220?0????????111?00???0??0?10?????????????????1?????????????????00?010??00?00???0?0

?001?0??

Anserimimus planinychus

??

??

??

0??0????????111110???1000001100????12??0???????????

10000?10100111111?00221??111110012210????10100?100?11?0???????10?0000?010????00???00?10001

00010??000??001?1????00?0101100??0??1???

Apsaravis ukhaana

???????0??

0?????????????????1??0??0010100111

00?0?0?????????????????????????????????2?????????????????110?1?001?12110??1?11?00??0?????

???????????0???501210?0?210?10?0200???2?0110????????11????103000?1110011010110?0001101110
0010100001111110001???1?11?1?????????????????11000?01010??0???1?1?1?000?10????312??1???1?00
000?00000?1?22000??11?11112?2001????1100???????????11????????11?????110?111?00??000110?110
10?001000?

Archaeopteryx lithographica

1100001010010001010?1?00?00?000100010001???0000010001100111100021?0?0??1100111110?11010
000??0?0?000000?010?00?000???0?210??12?010?0?0?????????0?0?01110001???0???????1001011?00??
10010000??0000?00?0?0?00?0?1?0?00?0??00101000100200l?21201000?00??10?0??1???0?0???????10
??????0???????0???????????00???0??04????0???20?01??01??1??2?00?0????1?1110??101?2011?0110001
111110020??1?00010????000?011?10?00?0?0?1???1?22??0??2??0000000???00?010???1001?1??0????0?
01100?2?1????11???00112100000l0?2101001??????11?0110?0??0?00??0??????0010?????00?000200011
0?11110011?00?00?0?010?0??010?

Archaeornithomimus asiaticus

??
??
??202?1000?0112110000??2000000
10??00?000110301010?0??0000200?0000?00??0????????????????111110??1??000?120??00?120000100
000000???????10101010111100?2?0?1?????01??1??100??1???1000110??1000001000????0100?0?0?1??00
010001?00101?000??1?10110001100?000100010001??111001?????????0???????1??001?????100001011
000??001???

Avimimus portentosus

??????????1?1?1??11??1?????????????????????0?000?????0?
?01??????0?00?000???11?????????????1?1?0?1?10?00?01??120?0?0??0?00??110?????????0??00????11??
???????11??10?0?0?00???????111?????????????????2??2?????????????110?11101001200011O?1121101001
0100011110000000000110601010?0?2?0000???00?????????????????????????2001001100001001100l001
0100010010000000l?111????0???????0??2?????????????????0100??1???10000111010100011111?00?01001

00011?000111102300l0?0000?011011210110100000101000001001100011?11100010112000110111100

?11000102?110102010100?

Beipiaosaurus inexpectus

??

??0??????????????????0???1?00???1?1??1

0?101??100?????????????11??????022000110013201000101O?0??????????????????????????1???0???????0?

??????????????0????????????????????????????0???????????00??1001001?10000?0100?????????10????

????0????00100?????????0?22?????1?00?0000?01011110011??????1?????????????????????0?????????

??????0???????1??????00???0?0?0??0????0?????010????????10?0??0??????001???11?????????????????

0?

Beishanlong grandis

??

??

??1?11?????????????

????????????????????????1?????????????????????1??????????1111101?11000?0020??0000100001000000

001???????????0?????0?????0????00010110??0?1???

??1?0????10?0?10002100110?100010101??11000101O?100010???0001101?010001???0?00??10????0010

11

Bissekty ornithomimid

??1??0010010??????

??

??10?10202210O0?01121100001020001

00100000000011?30?01?000?0000000?0100200??0????????????????1111101?11?000??200?0001????01

0000???????????101?101111100??10???????01??1??10???????100?110???0000?100?????????????????

??????????????????0101100011001000110000001011110?1?100??0010?02000110?001?????100001?11

0?0??001?11

Buitreraptor gonzalezorum

?????????0000??1?10???0?1???0??????????1???????0???????????00????0??????????????????1?10?010??
0?001?0????0???0?10?001?????????????????????????????????????0?????????????????????????1?0?0??0?
???01010???????????????????????????0??01?0020???00?00??00?0??110?010???201210110??12??010???
????0??1????0???1?1??01??0???????1??01??10?2?01??????1??2????10??2?1????11??10111001????????
?0??1??????1?110??????????????22???????????????0100??????????01?10?0????111?111?1????010?????2
0112122??0112?0?1001???????1??1??????????????????????1????????11?20001????01?0011?10??1?0100
1?0???1??

Byronosaurus jaffei

??0000001100000010001?100110?000001110001????00001000??0000???0????110??11101110?0??0?????
??????????????????????????????????????000?11?0?1???0??011?100111????010???11001010111?????0?
000?00000?0110?0?010??????????????101?001002201?002000120010??10?0??10??????????2??0??????2
10?1???????????1??1?????0???????????????????0???2??
???1???
?????????????????????????1???????????0?0?01??11???????????0????????????????????????????????????
???1??

Carnotaurus sastrei

??1000000000001000???0??00?0100001000100001???1?1001110??200000000?000?10101000???10?110000
00001?1101100101000010000??00????0????1000??2??0?????0??????00?1001??0?0????????????????1?1
01100??00?01000?100?01000??0?1101000101000??01000000?0?0000000???0?000010101101?10?00??
11102?10100?00100?10?10000111?110040?11?0??????00????0?????0000???0??????00??0?0000??01001
010?221?0110?200000?000111000???????????????????????????????????11000?0000??????00?00??00??0
?00000100????1000000100?000?0?00000???000?10000?0111011??011?00?110?0?????????????????????
?????????????????????????????

Caudipteryx zoui

100000??0?111?0?0000????????0?0?0?11??????????00???01?????000?01?0??????1?0101?10??10?00001

0??0?00??0???00????000??0?????????????1?????????????????????????????0?????????????????0?201?001

101111100?110?1??0???0?0?????0?10???1101??????12??2????01???0????????0?0?????1??00????????0?

{01}0???00?????????????????04?1??0???2100??11????0??00?0???1?011?00?110??00????1?001?0?0????1

??10?0??0000?0??0001?110?0000?0111110?22??021?100?000000100101001???0?1?10?0?000?????00??

??????01???2011110??00102?0?0??100?111111?0?????10??00?????????011???10????0120001 1?1001??0

????01?1?0???1?0??000?

Ceratosaurus nasicornis

??10100010001100???00?00?0100000001000010001111010101101?100000000111 0?11100??001001 0?0

00000010?0111010100101000 10?00?0?00?0??1000?02??01???000??0???1?1???10?00???0????????????1

?????000????0???0?10?001000?0??????100?100??000?11000?0000??0?0?0??00?0000111?110110000000

11??0?00101?00100????10000011011004001?0?1?000?01000?0?01000010??10000????????00010?0100

1000??????????????10001100101????0100?100010101110??1??????2????1100??0000????1?000000100

1000000000?000101000100100000010?00000?0?1100000000001101100011101111 0?0?0000?1000???00

1000011?????????????00?0???????0?0?

Chirostenotes pergracilis

??1????????1?00??????1101??

??????????????????????????????????????1?0100??01?1??0???120?011??0?00?1?110??????1????10?0?011111

11100?100?10?0?0??00??0????????????1??????????2?????????????????????110??211??0?????12????1?????

??010?1??1?????????5210????0??1?0?????????????0?????????????????????20?100???0?10?????????????????

?????????????????????0????????2200???????10000??1000?100010000??1??010000?000000?12??00?????20

111102300112 1000?01????0?0??????0?0?11??0?0??????00??????????00?????1???0?1??0???00?01?010?0

?0??00??

Citipati osmolskae

??10000000101001 01?0?110100?00020111000????0000100101?00101000010 00?1101100101?10?11110

000100?0?001200?000?000000??010?011011111101?0??01?01010?0101120000 00?0?001??11111110?00

00021?02011011111100?110?10?01010001100?0111??????1???????????2?????????????10??110??????210

010??1????1?0?1???????1??1000??0?1?52???0???10?????1???0??2?01?1????0??00011111200?????00?1
10010?1?????1?00?0???000??0?1?10?00???0?????0?22??0????0010000?????0?100????001?1???????0?01
000?110??0110???20?11102300102?000?01??????2110010?0?10?????0?????????????????0000??000????0
01??0???00?00?0?0?0?0??000?

Coelophysis bauri

??000011??0??000???????0?00?0101001?1?10???0?00001001????000000000?0??11100??00100??0??0?
000?0?01?00??0??0?????0???????0?????0000?0???01?????0????1???0?0?1000?????????????????0?001?0
00?0?0011???10?100??000??????????1010?010?020000000?????000??00?1??0100?11000?02??0010?0?1
0000{01}0002001000????0??00?0?03?00???10000002O?000100?01?0??????00?????????0????0011?00?0
?1?0?1000010??0100????000??1?0000001?00?0?0?100??111100?0???001000?0000????1000000011O1??
?000??0?00???0001101100????10?1?0?0???1100?0??0?0000000?00101?0?110???0??0?001????00100000
0??0???10???0?0?0????1001000?

Compsognathus longipes

??00?011000????1010?1?00??1101000???0000???000000000??00001000000?0?0??111?0????1?1101??1
?000?0?001000?0?0??????0?????????????????0???????1?????????????????010??0?????????????????????00110
00??0?00?00?0?000100?0?000??1210?10100010021011001000000000100?0??0??1010?1?0?0?00010??
0?1?0?10?0200????????100010?103????0??0000?0?000?01000010000?1?1000???1????00010?111?00000
?0??1???1?0??01???000000????0?0101??0?10?1?22??12??10000011001??0?1000???0???0??0?0???????0
0?01111???0010000100010001010O?0??1??????000??1????1???00?0??????00?0??????0?0001000?10?00
1?0011000?00?0?0?02001000?

Conchoraptor gracilis

???0????0011100?0?00??1?????0?020?????????????01????1????110??010?0????????101?10??10?00001?
??0??01??????0?000000??0?????????1??1?????????????0?????0?2????1?????00???110????????0??21?0?01
101??1100?110?1??0?0?000??0???111??????1??????????2?????????????????????????????????0??????????1??
?????????????01??0????11??0???????1?????????????????????????0?????1?12?010???0??0100?0?1???????0
0?0???0?????????????????0?????0????0?????00100100????0?100?11?001?1???????0?10000?110??00?1??

?20???1????010??000?0???????11?001??0?10?????0?????????????????????0??????????01??0???00?00?0??

?0?0??0???

Confuciusornis sanctus

11?000?01?000000????0?01?0??00110011000????00000?0?01?11?111001?1?0?0???1?0????10???00?00?

10??0?000?0????0?00?000??1?????????0??0?????????????????????1?????0?????????????????????0?10??00

0??0011000?100?0100?1?000??0???011??????1???????????2?????????????????????0?????????????????????0?

???0??0????0??100???1??05????0???20?01??1??0?????010110?????11111010?0?????1?0?1111110020?

?1101110001?1000011?11?00?0?0?????1?22??0?????000000?1?000?010????0?1?1???????0???100?30???

??1????0010?1?????1?211011?11?????2?20?1?????0??0??1??????00???????01??1??2110???111100??001

?10?01??0?0??000?

Cryolophosaurus ellioti

??????????????????????????????????1??1?1??000??0??0????0?2?????0?00001011??1100??001000??????000

00?01?00??10?10??00????10?0?0???????0?????????????????10101?????000??????????0?????0?????????

?????????????0?0110??0?????????????????0{12}??0?0000?????????????????????10?1{01}????00?????0??

?0??????00????10010??1?10?0???????00???0????????00?0?0????0?00?????????????????????????????0?

???????10000???00?????????????0?0??1??10?????00????????

00????????00????10??????01001?010??011?0??0000??????????0??????????00110000?????????????????

????????????

Daspletosaurus torosus

??10002010011111010??00?10?00000101?000???11101??????2??000110001111101110110000 11?01?01

0?000?0?01120101011 0?1?101001030???01?0000???????????0?????????????????100?10??0?10?0000??

?1?000?0000??00?100001011????????211?10100001020000000000000000010100?????????????0???0??

??0????????????????????????????0?????????????????????????????????1?111????????????1?????????????????

01??0??????????????????????20????????????????

??????????????????????????????01?0002???1?0?10?????01?111???2????????????????????????1????????????1

????????0?0?

Deinocheirus mirificus

??000000210010010000010111O?0013011?000????10000102011010011001O0?0?0??1010110011200010
010000?0?000000?0010010010010111????????010?0?0???1?1?????????0000001??000?????????????????
10??00110111O?00?000?00?1?1??000?0???011??????1??????????2?????????????????010?10201210000
?11211112000111010010001001011004120100211100020000000000110?10100????111??2001001110
0010012001000120000000000000011?000101010111110022100211101000000110111000110001100?00
000010000001010000001000000?0010????10000?100100100011001000100010001011101l?010200001
01020000100001O?????00000010000?0000010

Deinonychus antirrhopus

??000000200001?111101000?00?0000000100010000000100001l0??100000101O?0??1???100?110??1???
0?10??0?00??0???1001000?0??11031?110100?0??????????1????????00??0????0?0??????????10??????00
11?00??000??00?0?000101?1001???11010101100000210O?00100000O?000100?0001111?10?0010120001
1?0101100201000000001001011101100?????0?????00120010010?1001?1????1?12??????1?21110??110?
101010?1?0???100010001000?00?111000011101011111220002l2?0010000001?00?1??1100001?1??0?00
00?111001210??0101???0011112220010210l0?0101011111111100001000001011111?00101??10?00000
2000110100110011?10?100011101001010?

Dilong paradoxus

0?100020000110?101001100?10?00000011100????0102101000120110011000O0?11011100??001000110
01000000?001200?0011?01010??011??0?????00000100101?00000??????1?1??1??0001??0????????????0
?0?11000?00000?00?0?0000?11111111101010101000010200000000000100000100?0???????10?1?10000
0010??0010?0?0101?????????????1????0?????????????0?0???????2?000?0??1?????????????0?????1?1000
?011???10001?????????????????????????1?1?1?1110022???21????00000??1?0??1??010000??0??20000100
?0?0??11?????????????0??????0??0????11?11?0001?00??0?10??0?001?111??010???10???00020001l1??
01???????0?00?0??0?2???000?

Dilophosaurus wetherilli

??001020?00??0?0????1?????0?010?0010011{01}0{01}1??0?0?1001?2010001000010?0??1111???0010?

0????0?00010?01?0????111????000?011????????0000?0???01???000??1?1?0?0?0?10000??101?????0???

????1?1?1?0????0???0?10?00101?01??????????1010?000?1000000000??1?10???00?0110110?1101?0011

?0011?0??0?011000200?10?10000??1100?03000???0?0000020?000?01000?0???10?0??????????0??10001

0?00?0?100?10000100?0100?0??010?01?00?0001?00100011000?1?11000?????11000????0????1?00?000

1101????100?0?00???100?00?100????10?????0???11000001000000000?0000??00110?000?0??100????00

1000000??0?0?10??0??0000?0?2001000?

Dromaeosaurus albertensis

????????2?0??1??1?1??100????0???0?010??10100??0????011???100??0101??????1???????0?121?1101??

?????0??0?????????000??01031???0?0??000100001?00000?0?0?0011?01010000?1110?10?10000000001

1000?00000?00?0?000100111010111101010?000110?000?000000000000?0100?0???????????0??????????

??????????????????????????0??

??1????????????????????????

??

???010?

EK troodontid

??

??????????????1????11??????????0???????0??????????????????10????1????1??0?????01????????????????

????????100???0????1?????????????????????????0????????1???????0????????????????????????????????

??

???1000010?01????1?22?0?2???0000???0?????????????????

??0011?00?1????0???1???10?

Eoraptor lunensis

??000000000?000????0?00?0100100000100????000000001?01?000000000?0??11100??001001??0??

?000?0?00??0??00000000?0???10???0???0000???0?101?

000?00?0??00?0?0?010?0??0?0???????10100000001000000000???0011?0?0?????0?0?????????0?10????

?0?00??0?00????????0??0????01???????0????0???0?00???0??0??????00?????????0?????00??00?0???0?1

0?0??????????0??0????????10?01???0??0110???0100???0????00000?0??0???????0?00?100?????????0???

???00000?010?????00?1???0?????0????2??0?0???0??????????0?????????00??????????????????????0??????

0??????????0???

Epidexipteryx hui

??00???0???????0?001?00??????????????????0???0?0?0??0

?001??10????????00???0??10?2?0?00???1?1

0?00?10001??001?00???????010?011100?01??2120?101?0?1??00?0??????0?????????????????12??000???

100????????00?0????04??0?0?0?2100???020?1??2??100????????10??????2?1?????0?100?101?02?????00

010?0?0??001????????0??????????22??0??????00001?010?0?200011???????????0???????0??00??????????

0?010102?????110????1?????????????????????0????????????0?????????1??0001???111000110????0?0???

0????????

Erlikosaurus andrewsi

??100000100110000??0?101110?00001101000????0?00????11????100000101O?0???1100???110?100000

010000?00100??0000010000?0??0???1012100001???010????00?0?1000000000???00?????????10??000?1

010?011?1011010?101000?011?0000?0100011??????0220001?0013111?001010????????????????????

??1??10??

??

??0????????0??0?????

?????0????

Eustreptospondylus oxoniensis

??0??020100?1100????00000?1100??0001001000?0???????1??????????000?1?11011000??0011011?00?0

00010?010?0????010?00000?00?????????0??0?????01?00010?01010001?0111?100???10?00?10000??0??

1?110??0????0101001????????????0?????010000002000?00000001010001O0?0110111010?11100101011

?00?10001000200000011000001000?03000?0?0?{01}00002???00?00?????????????????????????????1?00

100?0200010001?000??10???0??0???01000?000000110

0000001000000101000010001 0?0?01?000?0101001000000010001000100000111000000011000000001 0 0011??00?????000001000 00?001000?

Falcarius utahensis

??????????????????????0???????????010??001?0??10?0000?0?00 ?00??0??????????1?10010??????????????1?0??00?00?1?01000?000??0?011?110?10011010??0??1?0010 0000??00?1010?????????????????????????0?20001{01}0010111000111 0?0???????1101?212100010?112 1111201020011101001010?0010041101000?1000120010011000010???101111???1010?10010?1?101001 ?1001?0010001111001100?0001100100101000111102200021110010000001011110011101010 1?000000 11010??1110010101010001121023001022000?010?0110101100000010000010111110001 0?11??0100001 0001101000100110 0??001000???001000?

Gallimimus bullatus

??00?0002100100101 00?101110?0000011?000????1000000001 1001?110?00010?0??11101110112000100 10000?0?000000?0010010112??0????01101001010?110?1?00001?0100000000 0?00011??110?0?100010 ??00?00010?1011000?0?0?01?1?1?1000?0???011??????1??????????2????????????0101110 10?1?2022100 0001121100000020000001000000 0?01104010100001 00?0000000020001 00??010110????????11110011 1110001020010001200001000000001110??00101011?11110022?0001210001111 0?100101000100011000 1000001000000000100001001??0001000100010100 00?110101100011001000110000001011110010100 00 ?010??2000110100101???10000101100020001010

Garudimimus brevipes

??0000002100100100001101110?00000111000????100000000??0100110000010?0??11101110112000 10 010000?0?00?000?00100100?0010113?01?01001000?11?0???0001?01?000010001100011?????????0???0 0?00?0001001010?00?000?00?101?1000?0?1?011??????1??????????2????????????000101?????????????0 ????2?1000010100010 01???0000001?04010100?0?00002???00?0??0??0?????????????????????????????? ??1001110001001110 0?1000001001000 10100100011??00?????????????????1010110001100100011001000101110000 0?0100?010?02000110?00 100011100000?1000020000011

Giganotosaurus carolinii

???0?00????????0????10????10???1?001000100??01?1?0????2???????????1010??1110????1?0???????01
101111?01??1???????1?0??10{12}??????????1????????????0???0???101????????????1?????0?????1?????2
01??0?0???10???0???1?11????????????1???000200?0?10?0?0??0?0???110001??1?111110??{01}?1?11??
0?100?2?0??0?????10010??1?01?????0???0?000?01??????000???0???1000??????????0???????1?10?0???
??0???10000?110?1??0?0?000?11?????1010
10??010100?0???????11?1???????01012?100??01??0?????0??10111???0?0??1?00????1??????????????
??????????????????

Gigantoraptor erlianensis

??
??20?00011110111
00?110?1??000?00?0?????????????????????????2??
??????????????????????101012?0000?0??0??????????1?????????????????1?0?100??110?110002???00?000
00000?????000101000??
?????????????111110????10001?????????????????????????????????????1?????????????????????0?0?

Gorgosaurus libratus

??10102010001 1?10100110011 0?000000010000???1110?11101?00110011000 1111?11110????0??121?00
00001?0?00?20101011??10?0?????3?0000100000000??01?00000?????????????000?????????????????0?0
0??000?00000?00?100001011110?0??0????10100001020000000000000000000?????????0???????0?0????
??00??0??0??0000?0?????00?1????0?????????????????????????000???????????10?????????1???0??????
??32??????????????????100101011100????0?12100?100?000?01
01?0001???00?10010?0010?????????????????????????????00???????????0?0?10?????????????????01000110
??????1????????0?0?

Guanlong wucaii

??10100000011111010011001111 0000?01110000100101100010120110001000 00?11011100??0?1000100
00?00000?001200?00110?1012??0??300?1???00000100001?00000?11010001000??000100010?10010?00

00?001?000?00000?010100?00?1111??1??0????101000010200{01}1001000?000000100?1?????010?101

01000010?100100100101000000100100110010030001O?00100000000?0??2000000?????11?????????000

10?1?10000?0100110000100111000100000101000001010101110021000212100O????00100101010100000

000?021001100100001101100010000001000000000?10001001 1?0110001100110010000010111110O?200

0?1?00100011001111001?00110000001010002101000?

Haplocheirus sollers

??00??00110111110101110011100001001110O0?0?0000100001?01?1100000000?0??1000111?11201000

0??10000?00??00??010011000??010?00110100000021?001?00010?010?0111??00?00110??????1?110??0

0?1011110?0000100100?00011101001 1??02100101000100120110010001101000100?0??????00????101?

00?10?101110100101??00001??1?????10103000?0?0?{01}?00??00100?00?00000??1?01???????????11010

011100001010011011011100?00?1100001?100000011011111002201121210101000101O???????11??010

02?000001001??00011010100??0100110000011011O?0?01??0110101000000?1110001011110?00101101

0??000?20???1?10010?????00?00?0100020010O0?

Harpymimus okladnikovi

??0000002100100l0?0?1101110?00000111?00?????00000000???????10?????0?0??1110111?1120001001

0000?0?00?000?00100100??????????????????10??0?00100

01001011000?000000010???000000?0011??????1?????????11?0??0????????????1010?1??0??0000??102?

100001?2000000????00?000110401?10???10000200O?002000100??0?0110?????????11???1?111000012

00?00012000010000000011?100000101010111002210021110001111O?100101001????11?0010??00100?

00000????010????00?????????????????????0101?00?????????????????????????10????????0?0?000110?001

0????100000010000?0001011

Huaxiagnathus orientalis

??0???000001?0?10100??00??11000???11??0????0000?1000?????110?0000?0?0???1?0????1???1???????

???0??0??0????0?????????????????????????0???0?001?000?

00?00?00?0?0?????????????????10??0??00?0?1?00100000000?0100?0??????0????????????11??10??0??

0?0100????????10?01??10???????????0????00?0?120?1000??1?0000???100??00010?111000000100?????

?????00????00?00?0100?001??0??10?1?22??12111?000000?01?00?10001010???0??0?0??02??000?111??
??????000100000001010000??1??????0?????????????0?????????????0???0????00?2000110?001?0011?0?
?00?0???020??000?

Incisivosaurus gauthieri

??10000001011101000001001l0?000111110001???0000100001100010000?1000?10012000010000?10100
00010000?00100100000000010010102011012101101?00001?0110??11?012001000??0010?11??1100???
0?0?2011?01111111000?0?0000?000?0?0110??0?101200?00?00??1?2001101?10??10?????????????????
??
??0??????????????????0?????
??
???1?????????

Limusaurus inextricabilis

??10001010011101O1?00?000?11?0?1?01?000????00000?000??01??000000000?10012100??00120??0???
?00000?00?1????0000?0?020?00??????01?000??0?20??
00??01?1110??0?1000??0?10?0??0????11??????1?????????????????????000??0?1101?1?2?0000???01?
0?0??????????????00?1????0?????????10000?000???020000000?0??1101000?1??000100011010000?100
11011?00?00000?000000?????0000?00010101{123}10?00011??02???000000?000110001000?100100100
100000100???0?0000?00???000?0?00?00?1???00?010?0?0?????00011????????????0??10??????1???????0
01?0???00??0??00???2?00000?

Linheraptor exquisitus

???000002000?1?1101?1?00?10?00000001000????000?0100???000100010101O????1110100?10?1?10000
?100?0?00?200?00001010?0?0?10????????0000?????????????????1?10101?????????????????????????0??0??
000?000???00?0?0?01011????0??111???01?????02101?0?1000000??00100????1111010?1??00?0??11?11
??1?????????????????00?????10?????????10?0???000??001000?1101???1?111???????????1???1????10?1
1???01???1?????10?????????????????????????????2????????????1?0?????????????????????????????2????0

10????01??????????????????1??????????????????00?101??111??10???10???0??2000110??011001??10?1

0?0?10???01010?

Mahakala omnogovae

??10??000??????

??????????????????????????????0??????????????????1001??1???????????10?0?10?????????????????

??

????????????401??0???????1??01??10?2?????????1?????????????????????????????????????1???10???

???1110?0?????????????????????????????1000?0???0???11?1???????0?11100?????????????????????

??????????????1?11?111?0?0???0?0????????00??????0???00??0001????01?00??010?10??1??0?0??010?

Majungasaurus crenatissimus

??10100010001000????10000010000100010001110 0?10110101120100000000 10?101?1010??010?11000

0?0011?1101111101100010001 0?00?0000001?1000012??01?00000?1??1?????0???0?0?????0??????????0

?10110???0?00?????10?0?1000100001001000101000000110000000000000000100?0000111010?1?10000

?011?0200010100010011 01?0000010110030??1?00110000200000011000000 0?100100????????000?00

??0?0?0022100100120 00??????????0??????????????????11??????????????0100100000100010000?0001

00100000010????????????0???0?????????0???????????000000??00100011101101010000111100010000 1

00010??0??0???0000000?0??0?0000011

Mapusaurus roseae

?????0?????????0????10????10?0???001000100?1?1?1?0??1?2??1???????01010????1????1100???????01

1?1111?????????????1?01?10??201??

0?????10???0???1?1???0??0101????????0?00?0?10?0?0??0?0???110??1????11111???001?11??0?100?2?

???0?????10010001?0????1?????????0?01??????1001??????1???0????10?????????1?1??0???100?0???11?

1??????????????????????0??0?????????????0?????0???10000?110????????00??110????10???????????

???????00?11?10?00???0?012?1001?011?0????10??10?110000?00?0?00???1?100011??0???????????0?1?1

0??????????

Masiakasaurus knopfleri

???????????????0????100???0?00???0100??10000??????????????????????????????????????0??????????????

??1?110?01?11

100?1000?????????????0???????????0?00?0?00?000?00010100?0???????1101?10??00?0?1?2110?0???01

??00001??00010?01?0???01?0?110?0020????0??0?0????????????????????00010???????????100?1001????

??110?01000000??

??????????????????0100100010000100100011101011000000?????????1??1001111001?????000?0???00?

???001?0?

Megalosaurus bucklandii

?????000100?1?000???????0?1000????1100001101???

???1?000??00?

??00???010100????0?????????????????0?0001000000?0000?010100????????0?????????????????????0?{01}?

1??00?????100?????0???300010100??0??2????0??0?1?????????????????????0??0??0?0??????2011?0201??

????00?0???010?10000110000000?01000?100000100??00000??

??000100010?1??0??????00000100000001000100?1010101100??0??????????????????????????????????001

?00?0????????

Mei long

??00000011011?00????0?00?12100000?11000?????00001000??01??11?0?11?0?0??12?01110?0?1100?00

0??0???001100?0???????10???11??????????0???????????????????110??????0????????????????0??0??????

00?0000??0110?0??????100????1????10?0?0?001201?0020???0???0???0?0??110000????101210110??10

1001?0?11000?00????00?00111040??1??0?1000?0001??2??0?0?0?1?0???12???1111?20110?1100110100

00010?11100110???????0??????????????1???????2??????????0000001????????0??00??1?0011000?011000

0????01001?0101??10???0??20??10?10?01??1110110?0?11?000?????????011?0?100??0112000110?0010

0011???1?1??10112101010?

Microraptor gui

100????01000???1??????00??0?0??????????????00000???0?????1?0?0???????????1?0??????????????0??0??

0?00?????????????????????????????0??10?0???000

??00?0?0????????01???1????10???01?02?0??0?10000???00??10?????????????????0?111??1????00??01?

????????100?0?1?004???1????10??1?001??1??1?01?1??????120011101??0??????1??111110?11???0???11

0??????000?110000000101?0??0?22??02??100100000100101?0?111??1?1???????0?011?1?20???010?1?

0011121?2??011011010?1??????11?111????10???0?0??????00??????0?0?0???0001???10110011?10?11?0

??01?101010?

Microvenator celer

??

??{12}0????11?110

1100?????00?00?????????????????????0???????2??2?????????????1101?110??????0010?01?1?102??110

00?001001000??0?10?0???????????1?11??00??2?????????????????????2001????00?0?0?010110??02?001

0000?000?0???????0???0?????????????2???0010?00001000?1001101001???1010000?00?0010100?0101??

?20????????0?????????1??11?10121010000100??000???11?001??00100000012000l101?????????????

??????????0?

Monolophosaurus jiangi

??0010001001O1?10000?00?01110001000?0000??00111100010020110000000l111??11100??001000000

00?000110011000?0011000001??010????????0000?????01???00?????1010100?100000?????????????????0?

0011110??0000?00?100?01001????0100211?1010000002000?000000000000?010100??1101?10?1?100?01

011?000100010101000011?0000?1001003000?0?????0?02????0?????0?????????????????????????????

??0100100000100100?0?01000010000

00000???0101000100100?00110?100?0??

????????????????????????

Mononykus olecranus

??

??1100?????????????1001011??0??1?????????????

??1?212?1??0??????10?0???????0????1010?11????12110101102001

0000??101???1010??2??1?????0121?0?1??????????????????110???001000?01?10100002300001011?00
21000111011?10101111101101100221112??111011?120?0?0??????????????????1?00111??00?30??????1??
?00?0?0000????????0??10011112?200100101110000110111110011?11???1011??1101101001?001100010
2?11000?010100?

Neovenator salerii

??00?0101000010100001000?11000100110001010001011?0??????????????????????????????????????
?????????0??????????????????????????1??1?100??
000??00???00??????????????????102100000?10010000000010?0101000011110111111000010 11?000100
02000001000110110111001 00?010???????000100000100010?10??100100????????0001101?101010?????
??0110100??010001000??000001000??110101
00101010000100000011000000?000101200011001100101010101111100100011010 01????100?????01??
????000?01?100020010 00?

Nothronychus graffami

??
??
??212?????????2????20?0?0011111?
??????10???04?10?0?0?2010??10?0??0?000100?????00????101??00?1?00???10000110?1?111101??100?
100000?????????0?????????22????????000000001011120011??1???1?0??100???1100?1101000111??2?01
21?0?11102?10???0??112111100??00?000?0010110???111??1101?0??0?2000?1??0001010?0000001?011
0?0?0??0?

Nqwebasaurus thwazi

????????2??????1000??1011?0?00??00?1???????0??????????????????????0?10?1?2011101100201001 0??
0????010?0?0???????0?00?10?????????????????????????010?00?101???0000????????????????????????
????????????????????????????????????03?11?21211?????????00?0???????10?1??01200?0??11111?100
10???0???????0???????????1011101?10000??100?100?010?
10??0?00000010?0000001101010101221011110010101 10?????????????????????????????????1???0?0??

??00?????????????????1??0??1?????000001000001011111?0010?0010?0?0?0200l110?001?0011000000001000?0101010

Ornitholestes hermanni

??00?0000?01?00101011100??10000?01101000000000?0?00111000110000010?10011100??00101?01000?10000?000201000?001000000011{23}0????100000???0?0?????0?0?01111101?100????????????????????0010?10??0000?00?100?00?011100011010001012011102101?00100000?010100?????????10?1?1012000011??1111?11?101??01001??10010101l0?0??10?0?10?0020000?10?0??????????1?1?????????????????????010?1100001001?0??0?0?0?0?????0?????????????????????????????????1?0101??0100000?0?0010011000000?1????010?01000010?000001?10000?0?????????????10?0?10?????????????????00??0???????????????001??????0?100?0?0?0?0010?0?

Ornithomimus edmontonicus

??00?000210000010{01}0?1?01?10?0000011?000????10000000011001111000000?0?0??111?1111112?00100100?0?0?000000?00100101?2??011????????01010?11??1?00??1?0??000000100?0?0???1110?0?10?010??00?000100101100O?000?01?101?1110?0???011??????1??????????2????????????010111010?1?2022100??0112??0000?0?0001??1??0?00??0?00401?00???10000?0000?0020?01000???0110????????1111101?1100001020010012??000??000000110?000101001?111?0022??01121000122l0?10010100010001100O?0????1000000?0100?010????000100010001010000?110?????0011001?0?10?00000??????00?0?0??0?010???00011??00101???100001?1?00020?010{01}{01}

Oviraptor philoceratops

???100??0?11?????1????10????0?0?0??10??????0??01????1????01000???00?????1?0101?????1???00??0??0?001?0????0??0??00???10???1?1?1??1?1?0?1?????????????????????0????00?????????????????0?21???0111?1111100?110?10?0?0?00???0????11??????1??????????2??1???????????0?????????????0?????????????????????????10?????????1111??????????0??1??1??0???????00?0???0????0???1???????0?????0?????0????00?0000?????0?1???????0??1???0?10?????0?????????????????????????????????01?????????????????????

??

Parvicursor remotus

??

??

??{01}1??2?0???

?0???????010???????1?????0121???10??

??0???????0????????2?01?0?0??1????30???1???1??0000?0000?

???1{12}00???1?011112?200100101110000101111100011000?01?101211011010010????000102?11001?

001100?

Patagonykus puertai

??

???0????????????????????1???????????????

???0?00?01?0????10

000????1???302011000??012100?002??????????????????????0?1000?0?????001???0??011?11100210001

1???????00?10?10??????1??1112?????011?11010???????1?0???????00100101????0211011???01001?????

??????????0?0??????1112000100011100001111111??10111??000010{12}001100110??????1????000????

??010?0?

Pelecanimimus polyodon

??000000210001010001110110?0?00010011100????00000?00000001111?000??0?0??1120111011202?1?0

1?000?0?00???????????????0?010?00???1??10???????1?00?01???????????1???01????1?????10????0?000

?001000?1??00?0?0001010??1?0??0????1030001103201?102110201010??10?0???101010?1?????000?0?

1???1000?1?????????????????????0?????????????????????????000?10??????000???101??1??1?11000?0?2

00?0001?00?0100?0000011??00?101000101110022100112100011110????????????????????????????????

?????????????????????????????0??

??????????????????

Piatnitzkysaurus floresi

?????0?????????1??????????1000????110?00100?1??????????????????????????????????????0???????????

?????0??????????????????????????????0?????01???0????10??1?1?0?10?0010?010??????????00????0?10???

?????????0??????????????????????????0?1?01?00?0??0?0????0100111110?10?1010?1?0011????10001?10

10?????11000??1?00??30?0???0???0?02????0??????????????????????????0??11?0?0?00?0?1?0?10?00??0?

?100????0??0100??0???????????010000?????????1?00????0000?

010?????11?1???0???110010?0100010?0100??0??10111???0?0????0?????????????????????????01?0???

????????

Proceratosaurus bradleyi

??10??000000011101001100111000?001110000???0??1???010?0011000100000?????01?0????01?????????

???00??0??????0110?0000???112?0??0??0?000110101??011?????????????????0?????????????????????0?001?

000?00001000?100000?1111100??0???0101000010210 1?0010000000010100?0??????????????????????????

??

??

??

?????

Qiupalong henanensis

??

??

??

??

??

????????????????????????1?0???????1?0?110?0?0????100??0??0100?0?0?00000?????????????

??????????????????????000001011110010????????0?020001101001 0????100001??1000????0?0?

Rahonavis ostromi

??????????0???????????0??

??

??0120111000000?1

0010010010?041001?000??10120010010020??????1?1112?????????????1100110??????2????????10001

010000?????????????????????????????00??????01000?2101111001110001000?01110021 1??00111??001
12100000111210110100011 12?2011000010000010111111001110010010001200011010011001101111101
01110?001010?

Rativates evadens

??00000?21?0??01000??101110?0000????0???????00000000?????????????0?0??1110111111?00???????
??????????????????????????????????????0?????????????1????????????????????????????????????0??00
??1??00?000?????????????????11??????1??????????2??
??????????????????4??0?0?????00?000000?0?????????0?0???
??1100101000100011000 10?0??10000???0????01001?00001
000100010?0000??1??????00110010001??00?001??1110010100??0??01??????10?00101???100001?1100
020001000

Rinchenia mongoliensis

???1?????011100?0?00??1?????????????0?????????01????1????0100?010?0?10?????101?0????0?00?????
?0??0??????00?000?00????????1???1??1??????????0??????????0?????????????????????????????21?0?011?
11111?0???0?10?0?0?0?0?0??0???111??????1??????????2???
??????????????????????????0?????????????????????1?????????????11??????????0??1?0?0?0??????????0?
??0????????1?????????????????????????00?000??????102???111?01?1?????????????????????????????
????????????????????????????0????????0?????????????????????????????0??????????????????0??????

Sapeornis chaoyangensis

??0000000?010??1?1??0???????0??????1?00?????00001000??????11?002?00????12?0????10?11???0??10
0?0?0000?0?0???10??00100
1010?00?0?0?00?0?1?101??0??0010100?100?011?2120?2?????????0?0??????0???????????2??????211???0
?????0?????????????????05??01??0?210?0??1?0000??????0???????????111??2010??1100110111101 2?001?
011100?1000000111110001010111 1?1022??020010010000001000?11010????1?1??010000?0?100?31101
01101?01010?1000101101001101 0?11112?2?11??00100?0????????????1????????11??1001???11100010?
?0?10??10?0?0??000?

Saurornithoides mongoliensis

??1000??1100000??10?01?0????0???0?01???01000???0?????????1?????????????110?????????????0????
?0?00??0?????????????????????1?01????00?11????????1????????????0?0??0?????????0??11?0?000?0?100
000??011??0?0???????????1?????0?000??02101?001000100010101?0?????????????????????????1???0?00
?????0000?00??0?000??0?010?000???001????00???
??0??01?1???0??
111023001020000?0???1111111011???01?????????1???0???1
???1??

Saurornitholestes langstoni

??1??????0??????????1?????????????????????????1?11?1??????
?????????????????????????1???0??????????????0????1??00??0????
?????0????0???????????1????1???0???0??0?1000000?000100????1111010?1?1??200011?11?10?12??00?
?????1??101110110?411010100????1??0???1??2?01?1????1??1????????20?????????????????0?????1??00?
0?00?1?000??1?0?00?010??1111022?002???00100000?10?10210110100??1?001001110010??????????
???0???1????0?0??0?????????????????????????01011111???101??1?011001100011001010?0011?10?10?
001?0?001?10?

Segnosaurus galbinensis

??
??1?????????????????????0010?????1?1??1
??101??0?0?1?000??0???0????????0???001?0?10111?00101?????????????????????????????2?????????????
??????????????????1??0??2????????1???1??11?0?0??110110??????
????????????????????????22????????00????????10111100111020100001010000?01000?21010????010000111
10?1?102?101??0?????????????????0?0??1??0???????11???11?????0??10000????001010??00000??0110200
1????

Shenzhousaurus orientalis

??0000002100000100?01011?0?000?0011000????000000001?????1???????0?0??1120111?1????0?00?

00?0?????00?0?0???0001????0????0???1???0????????????????????????????0????????????????????0?001?0

01000010?00?0?000??1?1??????0?????1??????1???1?????11001001??00?0?????????????????0?????????0

?001?200?0??????00?0001?0301??0????0?000?0000?0??0???0??0?01?????????????????????????????????

????????????????????????????????0?110?221???12100010110?10010100010101101????100100?000101001

0100?1?0101000000000010000????1????001100??00100???

????????????????

Shuvuuia deserti

??000000110000010101?10110210000?11000????000000000011000?11001?1?100??1220111011202000

00?10000?001000?0100000000??10???01?1200000021010012?010?011111?00100?0010???11001011110

001100?001000001000?0?0000?00100111102??001????0??03201?212110202?10??10?0??10???10?10100

211110?11210?101?0???0???0??100??01?105020?1?00100121001101002001012???1110110???001000?0

11000000023000010 1?1?002????110?11?10101111?01101??0221112???1101121201000?10020??011102

1012001111000?30???1??11?00000?0000????22000?010011112?200100101???0??1???101?001??????10

111211011010010001100010 2?11000?011100?

Sinornithoides youngi

????????1?000???????????1???0?00?????????????00?????????????01?????????????????0?????????????

??0??????10?????????0??0?????????????1????000??00??000

??0110?0?????????????????????0?000??0?101???1??0100?10?010?????????10????0??101?????????1??????

??????????????????0?????0???10??1??01??1??0??1?0????1?12???????1?20110???00?1??001???????2?0?10

???????????10?0010?01??????22??02????0?0000?????????????001?1???????0?1???0?0??????01???00?

1210??00?0210?0??1???????1?011???????00?????????00??????0???0???????????0100011?0?10????011?

101010?

Sinornithomimus dongi

??0000002?00100101001??1?10?0000011?000????1000??000110011110000010?0??11?01?1?112000100

10000?0?000000?0010010110010 11????????0101????????????1????000000?????????????????10??????00

??00100101 0?00?0?0?00?101?1?00?0???0?1??????1??????????2?????????????011?010?1?20221000?01

12110000?020?0000??0??0??0??104010???0?10000000?00002000100?0???10????????1111001?11100?

1020?10001200000?0?0000011??00?101010?111?00221002121?00?1111??100101000100011000100000100

00?00010100?010?1??000100010001010000??10101100011001000110000001011110010100??010??20

0011?100101???1000010?10?020001010

Sinornithosaurus millenii

?000??001?000??1111?1000??0?00001?11??01???0?00010????0000000?010?0?0??1??0100??10111?100

0100?0?00120110 1?0?0??0??0010??????????0?????????????0?????????????????????????????????0?101?

000?00000?00?0?0?01010??0?0??1????101010000?10010?1?00000?000100?0?????????????????????11

???1?????????????????????????04????0???????1??0??????2?????????????00111?1120110???10?101110???

?????????0????????0????0000???1?????1?22??02?2?00?0000?????0?1???11??01?0???????0?11??0?211??

???1???011121????011211010?1?????????1?????????????????????????????????0??1001???001?00???10?

?1?0???1?001?10?

Sinosauropteryx prima

000000000001?001??0?0?????0?0000????0?0????0000???????????100????00?0???1100????11?????????0

??0?00??????00??00012?0?10??????????0?????????????????????0???????0?????????????????0?001?000?

00?0??0??0?0?0?????????????????10100?1002101?0?1000000?000100?0??????010?1?1?0?10?10??11??0?

20??100????????10?01???03????????000?0?000??1120?10000?1?1110????????00010?111010000200?00

?00????01?0??00000?1100?0111101?1110?22??121110100010001000?1000???0???0??0?001020?000?11

1?????1???000100000011?100?0??1??01?0001??0??0?1????0?01??10?00?0???0??0?00?20001101001?00

1100??00?0??0020??000?

Sinovenator changii

??1???0001010??0010?1100111000?11???000??????000???011????????0?????????????????0????0?000??

?????01????????00??12??011??????????0?0?00100????00?0??0100?110??0?10???1001010?001??1?0??

0???000??011100?0??0?1?0?0??????0101?00??0?2?1?0?10?010??1?01?0??????????10???0?210?10??01?

??00??????00?01??100???0?1?401?00???10??1??01??2??0???????????1????????20110???10?101???????

??????????????????0???10?001?????????????????????????0000???????????111????1???????0?11?00?211??01

0????0011210??0011210010?10?01?11110110?0?11?00??11?111?0011???1000?10??0001???001??????0
0?10???1?1?1???1??

Sinraptor dongi

??001000000000?10000000?010?000110110000?0000001000000200000000100101??11210???11001100
00?0100100110000?0001000001 0?0113000001000010000101?00000?10?0010100010010 0???10??0?0??0?
00?1011000??0000?010100?0111010000??0101010100000021 00?000000000?0101001101110 10?1010
0001011?0011001101010101001100000 1?0100300000?????0002?00?0??1?1001???1??1??10????000????
?1010100?0??????0?????????????????????????????0??11101210?????1000000100100101001???000?0??1
0000100000000110 0??1101000010000001101000 0?00010?1000110011001000101010111?000000?00?00
000010000110 00?0011000000101 0?0100?000?

Juratyrant langhami

??
??
??10?1?100?00011?00???0010001000??1
?0???00?00??030001000???000????00???????0???1??
??0100110??1100?0100??2100110 0?0000011?1000?0000101000
1000001?0?101????????0????1100101010101011000 1??0??
??

Struthiomimus altus

??00?0002100000100001101110?0000011?000????100000000110011110?00010?0??1110111111200010
010000?0?000000?0010010112?1011??01?0??010?0????01000??1?0100000?0100?00010??110?0?10001
0?000?0001001011000?000?010101?1010?0???011??????1??????????2??????????????????010??????210
0???0?2???000?????0???1??0000??0?00401?00???10000?0000?0020?01?00???0110????????1111101?11
1000002001000120000100000000110?00010100{01}1111100221001121000112101100101000100011100
010????100000000100100001??0001000100010100 00?110?01?00011001?0010?00000???1110010?0?10?
010??200011??00101???10000101100020001 0{01}0

Suchomimus tenerensis

???101201????0?0?????1?0?111???0?01?001000?01??????????????????000??0???????0????100????????00
0?????0??1?????????????10????????0???110????
?0????????????1??????????????3???00022000?01?1?2????0???0?1?01??1?10???0??????11??0?1?0?1?1??
10????11000001?01?0???????????0???????0??0???0????0100??????????0??0??0?0????00101010?1??0?
?21001??10?????????????????100???0?????0100????0?0?10000?????1??0?01?0????0?0???00?????0?{01
}{01}00?0????00?11?10??0???01011?1001?010?0??0??0??10111???1?1??0?00????110001?????????????
????????????????

Megapnosaurus rhodesiensis

???0?0211?0??000???0???0000?0101001?1110??1010?001001?11?0000000000?0??122?0??00120100???
??0000?00?00??0110????00??010??00??1?0000?0???01???100??0?0?0?0?0?10000??0010????0?????????
1?100???0011?100??10101000??????????1010?010?010??00000??1??00??00?0110??0?1100?00???00100
0?0000010002??100010?00??0?00?03010???1?0000020?000?00001?1?0?1??00?????????0??1000?1000?
0?1?0?10001100??1???0??0?0??1??000001?001000110?0?11110000???011000?0000????1000?0001101?
??0001?0?00???000110110001011001000?0?110000??00000{01}010000101?10110?000?10?1010??100
1000000?10?0?100?0??000????1001000?

Tanycolagreus topwilsoni

??1??000?00?00?????????????????????????????1?0000???0??????????00000?1??12201?00?????????0?00?
110?1?????????????000?010???
??????????????1000????101??01??0?10??0??000?0???????????011???1??0???1?????????????0?0?001
00????1001100?001?0?0?????????00?0???????20?00????1????????????00010?1?10000??101110?011?0
111000000010??11000010100?110002210?20?100000000?????????????????????????????????111101?1?
???0?????????????????1010110001100010010000?010111?0010001100010?2000111100100010?0?00
010?0002001000?

Tarbosaurus bataar

??0???0000001101000?100110?000000??0000????1100101001201100110000?111101???100001??01000

??0?1010?112?111011001010??0103100001000?000??01?10010?1?000001001??0000???????0??????0?

?0011?00??0000?00?100001?111101110010101010000102002?0?0000000?00010?????????????????????

????????????????????????????????????0??0??????????

?0????????????????????????????0?????????32??

??1?????1??????1

??????000?0?

Tawa hallae

??0001201000??00????01001?11000?00000?1????0?000?0011?200?00100001 0?0??12100???1100??0???

?000?0?00?0?0???11010000??0????????????0?020?001???000??????000??1??0??????1?????????????10?

?000?00000?00?100?00??0????0????????00??00002000?0000?0000?000100?0???????1100?00??00?1???

??0?0?????????????1????1???0???????0???????0??00????0?0?00?????????????????????1?10100?01001

10000????????????0??1????000??10??00?01110001110?000000000000?0???0???0?00??00000100?000?0

110????????10?????????????????????001??2000000??100?????????????????????0001000000000?010?

?00?00???00?1???????

Torvosaurus tanneri

??001010???????0??????????1100????00000101??????????1?2??10000???0101??1100???00???????????0

010?00?????????????0?1?0?0???0?0??

??????0?????????????????????????00??0??0?0001?00?0????1????010000???1?10?1000?1?1?11????10002?

10100????11000??1?0??03???????????1?02??0?0??0?1??????11?0??????????0??0?0000??????2?0??0201?

00?0200?1?01001?????01111?0?10?01?????0????10????00100110??0????00?0?000000?????000?0?00???

0000000100?10?00?1?0?0????0??1????0?010?0??0??0??00111???0?0????00???011000111?????????????

01?0???????????

Troodon formosus

??0???001?0?0?010?011100?10?0000?1??0??1??????00???0????????00????110??????100??0??00?00?01?

?00??01??0?0???0?0?1???01030??1?11??0?0011000???001?010?1000001???010?1110?10?10?111??1?1?

?010?100??0110?00????????0????????101?00?00?201?0?1000220?001010?????111?10?111??210110?01

?10?100101??????1??1011??0?10501?10?0????011?0?0?20?0??1?????????2??????????????1?00110???0?

1?0?10??01?0????????0????000010?0???????220??????001?????????0????????????????????????????010?

?0001???0??11??23??1?21000?0?0001?11120110?0?1???0?00110101??1????1?0100012000110?001?????

100111?1?011?1??010?

Tsaagan mangas

??00000020000?011010?100110?000000010001???00000100?1?0001000101010?0??1100?????0?111000

01100?0?001200?000010?000?00103????0?000000100101001000?11010101100???0000??10110?100000

0?001?000?00000?00?0?0?0100111010111111?010101?0002101?0?1000000?000100???????????????00?0

?????110??1?

???

???

?????????????

Tyrannosaurus rex

??10?0000000110101011100110?0000000100000101110110100020110011000111110111011 0?1111010

000?011?100112011101100101010 0103?00001000000100101?10?00?100000010010?0?010?010??0?100

000000011000?00000?00?1000010111?0111001010101000010200000000000000000010100000111010?1

1?00000011?00010001000000000000100000010010031000 00?0100000100000020000000?100110???101??

0001001010000000110001 0012?000100010010 01?0?0000101000????03200021??00000?00010010101110

000000?1200011000000101011000101000010000000102100101011012001210010001000100010111?00

10?0??0?010002000110 1001?0011100001?110002000000?

Unenlagia comahuensis

???

???

??0?20?1100????10

011011011??4000?01?0??????????????????????10??????????????????1?00110?010011021?????????????

??????????????????????????????????????01000?21001010011100010001010111011101010 11?010?11102

10011????1101000100l0?1110000100?????????????1???

?

Velociraptor mongoliensis

??00000020000?01111011001l0?000000110001???0000010001l0000?00101010?0??1120100?10?11101

100100?0?000?0???00?10?000?0010?1?1?0100?00??0010?001?00?1?01001?000??0?00???11110?100000

010011000?00000?00?0?000100?1?0?01111010l0?110000?00110010000000000100?0??111?010????012

000????10??01???1?00??0?1001011?01?00501010?0010001??010?1????01?110??1?1200110010201l0??

100?111010?1?0??01?0010??1100??0?1?10000???010???0?220002?2?00100000010l00?1100111001l0?0

0?1000?0110002110?01011?0001111022001021010?0111??1?11?11?000010000010?1???100???0????00

00?20001???101?00111100100011111?001010?

Zanabazar junior

??10000011000001010101001110000001110001????00001000??1???1?????????????????111?????00?00?0

100?0?00120100?0000?0?????????????????????0011000????01?0??11000101l0?0010???10????0??1110???0

?001000000?0110?000???????????1100?10100011021l01?00100010001010l0?0????????????????????????

??????????????????????????????401010?00???0??00???2??0?????????1?12????????????????????????????

??

???????1??????0???20001?????1?????????????1????

????????

Zuolong salleei

??00??00?00?0101010l0?0?0?0?000000111000000?????00???????0??010?0?0??1?10111011????00?0?

00000?0?1100?00?10000000101130l??0????0??

??????????????????????????????????10100001020?0000100???????010100???????10?0?10110001l??0?10

??00?01?????????????????????40001?000??000000??0?00?????????????????????????1?1?1???010001??

?010???????00?000?????????????????????????????0???00100???????????00?0???0???100?0000011?001

0112?00?????????????????????1?011000100001001000001010111?0???011??000????????????010????1000

10101000????0???

Aepyornithomimus tugrikinensis

??

??

??

??

??

???000???10111001?1???100001?01011?0010010

Bügiin ornithomimid, (MPC-D 100/121)

???0???02100??0100????01??0?0??0????000?????000000?0?10011??0?0001??0??1110111111 2000?0010

0?0?0?000??0????0??0?12???1???0??????101?????????????1?0?0???????00????????????????0?????00?0?0

1001011000?000?00?101?1?00?0????11??????1???????????????????????????????10?1??02010000001211

000000200??0?10000001011?0311010???100010000000020000000?010110??????????????????1????????

?????200001000000001??000101011111100221001121010112101100?????1100011000100000100100

000100100001??000100010????00000??101111000110010001100000010111100101 0000?0101?2000110

?00101???10000101100020001010

Supplementary data-S3A. List of characters used in this study (Modified from Kobayashi and Lü, 2003; Makovicky et al. 2010).

1. Premaxillary teeth: present (0) or absent (1), (Holtz, 1994).
2. Posterior end of maxillary process of premaxilla terminates anterior to anterior border of antorbital fossa (0) or extends more posteriorly (1).
3. Maxillary teeth: present (0) or absent (1), (Holtz, 1994).
4. Series of foramina along ventral edge of lateral surface of maxilla: present (0) or absent (1).
5. Prominence on lateral surface of lacrimal: present (0) or absent (1), (Xu et al., 2002).

6. Area of exposed prefrontal in dorsal view: less than that of lacrimal (0) or approximately the same (1), (Xu et al., 2002).
7. Parasphenoid bulla: absent (0) or present (1), (Osmólska et al., 1972).
8. Ventral reflection of anterior portion of dentary, resulting in a gap between upper and lower jaws when jaws are closed: absent (0) or present (1), (Pérez-Moreno et al., 1994).
9. Dentary teeth: present (0) or absent (1), (Holtz, 1994).
10. Dentary subtriangular in lateral view (0) or with subparallel dorsal and ventral borders (1), (Currie, 1995).
11. Dorsal border of dentary in transverse cross-section: rounded and lacks "cutting edge" (0) or sharp with "cutting edge" (1).
12. Accessory mandibular condyle, lateral to lateral condyle of quadrate: absent (0) or present (1).
13. Foramen on dorsal edge of surangular dorsal to mandibular fenestra: present (0) or absent (1) (Hurum, 2001).
14. Posterior surangular foramen: absent (0) or present (1), (Sereno, 1999).
15. Number of accessory antorbital fenestra: one (0) or two (1).
16. Mandibular fenestra: heart-shaped with a short and wide process of dentary at anterior part of external mandibular fenestra (0) or oval-shaped without the process (1).
17. Neck length: less (0) or more (1) than twice skull length (Pérez-Moreno et al., 1994).
18. Anteroposterior lengths of cervical neural spines: more (0) or less (1) than one third of neural arch lengths (Makovicky, 1995).
19. Posterior process of coracoid: short (0) or long (1), (Pérez-Moreno et al., 1994).
20. Biceps tubercle of coracoid: positioned close to base of posterior process (0) or more anteriorly (1).
21. Depression on dorsal surface of supraglenoid buttress of scapula: present (0) or weak / absent (1), (Nicholls and Russell, 1985).
22. Infraglenoid buttress of coracoid aligned with posterior process (0) or is offset laterally from line of posterior process (1).

23. Robustness of humerus, ratio of width of proximal end to total length: greater (0) or less than 0.2 (1).
24. Deltopectoral crest of humerus: strong (0) or weak (1).
25. Radial condyle of humerus: larger than ulnar condyle (0), approximately equal (1), or smaller (2).
26. Entepicondyle of humerus: weak (0) or strong (1).
27. Length of metacarpal I: approximately half or less than metacarpal II (0), slightly shorter (1) or longer (2), (Russell, 1972).
28. Distal end of metacarpal I: medially (0) or laterally (1) rotated (Pérez-Moreno and Sanz, 1995).
29. Distal end of metacarpal I forms ginglymoid articulation with distinct condyles (0) or relatively large convex phalangeal articulation with reduced condyles (1), (Pérez-Moreno and Sanz, 1995).
30. Metacarpal II: shorter (0) or longer (1) than metacarpal III.
31. First phalanx of manual digit 1: shorter (0) or longer (1) than metacarpal II (Pérez-Moreno et al., 1994).
32. Flexor tubercles of manual unguals: positioned at proximal end (0) or distally placed (1) (Nicholls and Russell, 1985).
33. Ventral border of pubic boot: nearly straight or slightly convex (0) or strongly convex with ventral expansion (1).
34. First pedal digit: present (0) or absent (1).
35. Proximal end of metatarsal III exposed in anterior view (0) or covered by metatarsals II and IV anteriorly (1) (Norell et al., 2002).
36. Length of pedal phalanx II-2: more than 60% of pedal phalanx II-1 (0) or less (1).
37. Pedal unguals curved in lateral view (0) or straight (1).
38. Flexor tubercles in pedal unguals: without or weakly developed (0) or well-developed (1).
39. Distal end of metatarsal II: smooth, not ginglymoid (0) or with developed ginglymus (1).
40. Distal end of metatarsal III: smooth, not ginglymoid (0), developed ginglymus (1), or with semi-developed ginglymus (2).

41. Shaft of metatarsal IV: round or thicker dorsoventrally than wide in cross-section (0) or mediolaterally widened and flat in cross-section (1).

Supplementary Data-S3B. Character matrix used in phylogenetic analysis of Bügiin ornithomimid.

Allosaurus fragilis	00000000000000000000000000000000000000000
Aepyornithomimus tugrikinensis	??????????????????????????????????11111000
Anserimimus planinychus	????????????????1110100212110110111111000
Archaeornithomimus asiaticus	????????????????0101001201101?10?1?10000
Beishanlong grandis	????????????????101001?1?????1?00?00000
Deinocheirus mirificus	101011?1110011?11101110010110010010?00?
Gallimimus bullatus	11111111111000011111[01]12[01]111111011111000
Garudimimus brevipes	1111111111111111?0????????????00010?00?
Harpymimus okladnikovi	101110?10101011110?0100110000011??000000?
Ornithomimus edmontonicus	111011?11111111111100011202111111111110000
Pelecanimimus polyodon	0?0?0?10010???0?1?1????1??110111?????0???
Qiupalong henanensis	????????????????????????????????0?1?00000
Rativates evadens	1110111?111?????????????????????????11?10000
Shenzhousaurus orientalis	1?101??101?1??1???????????1??0?10????????
Sinornithomimus dongi	111111111111?01?1110[01]01120110111011111000
Struthiomimus altus	111001?11111101111101001?0111111111111000
Tototlmimus packardensis	????????????????????????????????1?111020
Bügiin ornithomimid (MPC-D 100/121)	1?101?11111?11?1????????10101111111111000

Supplementary Data-S4A. List of characters used in this study (modified from (Kobayashi and Lü, 2003))

1. Premaxillary teeth: present (0) or absent (1), (Holtz 1994).
2. Posterior end of maxillary process of premaxilla terminates anterior to anterior border of antorbital fossa (0) or extends more posteriorly (1).
3. Maxillary teeth: present (0) or absent (1), (Holtz, T. R., 1994).
4. Maxilla participates in external narial opening (0) or separated from opening by maxilla−nasal contact (1) (Xu et al. 2002).
5. Series of foramina along ventral edge of lateral surface of maxilla: present (0) or absent (1).
6. Prominence on lateral surface of lacrimal: present (0) or absent (1) (Xu et al. 2002).
7. Area of exposed prefrontal in dorsal view: less than that of lacrimal (0) or approximately the same (1) (Xu et al. 2002).
8. Parasphenoid bulla: absent (0) or present (1) (Osmólska et al., 1972).
9. Ventral reflection of anterior portion of dentary, resulting in a gap between upper and lower jaws when jaws are closed: absent (0) or present (1) (Perėz-Moreno et al., 1994).
10. Dentary teeth: present (0) or absent (1) (Holtz, T. R., 1994).
11. Dentary subtriangular in lateral view (0) or with sub-parallel dorsal and ventral borders (1) (Currie 1995).
12. Dorsal border of dentary in transverse cross−section: rounded and lacks “cutting edge” (0) or sharp with “cutting edge” (1).
13. Accessory mandibular condyle, lateral to lateral condyle of quadrate: absent (0) or present (1).
14. Foramen on dorsal edge of surangular dorsal to mandibular fenestra: present (0) or absent (1), (Hurum, 2001).
15. Posterior surangular foramen: absent (0) or present (1) (Sereno, 1999).
16. Number of accessory antorbital fenestra: one (0) or two (1).
17. Mandibular fenestra: heart−shaped with a short and wide process of dentary at anterior part of external mandibular fenestra (0) or oval−shaped without the process (1).

18. Neck length: less (0) or more (1) than twice skull length (Perěz-Moreno et al., 1994).
19. Anteroposterior lengths of cervical neural spines: more (0) or less (1) than one third of neural arch lengths (Makovicky, 1995).
20. Posterior process of coracoid: short (0) or long (1), (Perěz-Moreno et al., 1994).
21. Biceps tubercle of coracoid: positioned close to base of posterior process (0) or more anteriorly (1).
22. Depression on dorsal surface of supraglenoid buttress of scapula: present (0) or weak/absent (1), (Nicholls and Russell, 1985).
23. Infraglenoid buttress of coracoid: aligned with posterior process (0) or is offset laterally from line of posterior process (1).
24. Robustness of humerus, ratio of width of proximal end to total length: greater (0) or less than 0.2 (1).
25. Deltopectoral crest of humerus: strong (0) or weak (1).
26. Radial condyle of humerus: larger than ulnar condyle (0), approximately equal (1), or smaller (2).
27. Entepicondyle of humerus: weak (0) or strong (1).
28. Length of metacarpal I: approximately half or less than metacarpal II (0), slightly shorter (1) or longer (2), (Russell, 1972).
29. Distal end of metacarpal I: medially (0) or laterally (1) rotated (Pérez-Moreno and Sanz, 1995).
30. Distal end of metacarpal I forms ginglymoid articulation with distinct condyles (0) or relatively large convex phalangeal articulation with reduced condyles (1), (Pérez-Moreno and Sanz, 1995).
31. Metacarpal II: shorter (0) or longer (1) than metacarpal III.
32. First phalanx of manual digit I: shorter (0) or longer (1) than metacarpal II (Perěz-Moreno et al., 1994).
33. Flexor tubercles of manual unguals: positioned at proximal end (0) or distally placed (1), (Nicholls and Russell, 1985).
34. Pubic shaft: nearly straight (0) or curved (1), (Norell et al., 2002).

35. Ventral border of pubic boot: nearly straight or slightly convex (0) or strongly convex with ventral expansion (1).
36. First pedal digit: present (0) or absent (1).
37. Proximal end of metatarsal III exposed in anterior view (0) or covered by metatarsals II and IV anteriorly (1), (Norell et al., 2002).
38. Length of pedal phalanx II−2: more than 60% of pedal phalanx II−1 (0) or less (1).

Supplementary Data-S4B. Character matrix used in phylogenetic analysis of Ornithomimosauria (after (Kobayashi and Lü, 2003).

Allosaurus fragilis	00000000000000000000000000000000000
Tyrannosaurids	000000000000000000[12][01]00000000?00001000
Aepyornithomimus tugrikinensis	??????????????????????????????????111
Anserimimus planinychus	????????????????????1110100212110110011 1
Archaeornithomimus asiaticus	????????????????????0101001201101?110?1?
Beishanlong grandis	????????????????????101001?1?????1?00?00
Deinocheirus mirificus	101011?1110011?11101110010110000010 10?
Dromiceiomimus brevitertius	1111?11?111??101???10001110?????101111
Gallimimus bullatus	11111111111100001111 11[01]12[01]111111011111
Garudimimus brevipes	11111111111111111?0??????????????00001
Harpymimus okladnikovi	1011110?10101011110?01001100000110??00
Ornithomimus edmontonicus	1111011?11111111111100011202111110111 1
Pelecanimimus polyodon	0?0??0?10010???0?1?1????1??110111?????
Qiupalong henanensis	????????????????????????????????0?1?00
Rativates evadens	1110111?111?????????????????????????11?10
Shenzhousaurus orientalis	1?101??101?1??1????????????1??0?10?????
Sinornithomimus dongi	111111111111?01?1110[01]0112011011100111
Struthiomimus altus	1111001?11111101111101001?011111101111
Tototlmimus packardensis	????????????????????????????????????1?111
Bügiin ornithomimid, (MPC-D 100/121)	1?1?0??1?1111?1?110??????1010111101111
MPC-D 100/139	????????????????????1100110001001110?111
MPC-D 100/145	????????????????????1?01100010011100???

REFERENCE

Allain, R., R. Vullo, A. Leprince, D. Neraudeau, and J.-F. Tournepiche. 2011. An ornithomimosaur dominated bonebed from the Early Cretaceous of southwestern France. 71st Annual Meeting of Society of Vertebrate Paleontology in Los Angeles 61.

Andrare, R. C., R. A. M. Bantim, F. J. de Lima, L. dos S. Campos, L. H. de S. Eleutério, and J. M. Sayão. 2015. New data about the presence and absence of the external fundamental system in archosaurs. Cadernos de Cultura e Ciencia 14:200–211.

Barsbold, R. 1976. On the evolution and systematics of the late Mesozoic dinosaurs [in Russia]. Trudy Sovm. Sov.-Mong. Paleontol. Eksped. 3:68–75.

Barsbold, R. 1981. Toothless carnivorous dinosaurs of Mongolia. Nauke, Trudy Issue Sovm. Sov.-Mong. Paleontol. Exped. 15:28–39.

Barsbold, R. 1988. A new Late Cretaceous Ornithomimid From the Mongolian People's Republic. Paleontological Journal 1:124–127.

Barsbold, R., and A. Perle. 1984. On first new find of a primitive ornithomimosaur from the Cretaceous of the MPR. Paleontologicheskiy Zhurnal 2:121–123.

Barsbold, R., and H. Osmólska. 1990. Ornithomimosauria; pp. 225–244 in The Dinosauria. California University Press.

Barsbold, R., H. Osmólska, M. Watabe, P. J. Currie, and Khishigjav. 2000. A new oviraptorosaur (Dinosauria, Theropoda) from Mongolia:the first dinosaur with a pygostyle. Acta Palaeontologica Polonica 45:97–106.

Behrensmeyer, K. A. 1978. Taphonomic and ecologic information from bone weathering. Paleobiology 150–162.

Bell, P. R., and N. E. Campione. 2014. Taphonomy of the Danek Bonebed: a monodominant Edmontosaurus (Hadrosauridae) bonebed from the Horseshoe Canyon Formation, Alberta. Canadian Journal of Earth Sciences 51:992–1006.

Benton, M. J., N. J. Minter, and E. Posmosanu. 2006. Dwarfing in Ornithopod dinosaurs from the Early Cretaceous of Romania. 1–9.

Berkey, C. P., and F. K. Morris. 1927. Geology of Mongolia. pp.

Bronowicz, R. 2011. New material of a derived ornithomimosaur from the Upper Cretaceous Nemegt Formation of Mongolia. Acta Palaeontologica Polonica 56:477–488.

Brownstein, C. D. 2017. Description of Arundel Clay ornithomimosaur material and a reinterpretation of Nedcolbertia justinhofmanni as an "Ostrich Dinosaur": biogeographic implications. PeerJ 5:e3110.

Brusatte, S. L., T. D. Carr, G. M. Erickson, G. S. Bever, and M. A. Norell. 2009. A long-snouted, multihorned tyrannosaurid from the Late Cretaceous of Mongolia. Proceedings of National Academy of Sciences, USA 106:17261–17266.

Buffetaut, E., V. Suteethorn, and H. Tong. 2009. An early "ostrich dinosaur" (Theropoda: Ornithomimosauria) from the Early Cretaceous Sao Khua Formation of NE Thailand. Geological Society of London Special

Publications 315:229–243.

Burch, S. H. 2014. Complete forelimb myology of the basal theropod dinosaur Tawa hallae based on a novel robust muscle reconstruction method. Journal of Anatomy 225:271–297.

Chiba, K., M. J. Ryan, D. R. Braman, D. A. Eberth, E. E. Scott, C. M. Brown, Y. Kobayashi, and D. C. Evans. 2015. Taphonomy of a monodominant centrosaurus apertus (Dinosauria: Ceratopsia) bonebed from the Upper Oldman Formation of southeastern Alberta. Palaios 30:655–667.

Chinsamy, A., D. B. Thomas, A. R. Tumarkin-Deratzian, and A. R. Fiorillo. 2012. Hadrosaurs were perennial polar residents. Evolutionary Biology 295:610–614.

Chinzorig, T., Y. Kobayashi, M. Saneyoshi, K. Tsogtbaatar, Z. Batamkhatan, and T. Ryuji. 2017a. Multitaxic bonebed of two new ornithomimids (Theroda, Ornithomimosauria) from the Upper Cretaceous Bayanshiree Formation of southeastern Gobi Desert, Mongolia. 77th Annual Meeting of Society of Vertebrate Paleontology, August 23-26. Poster Session-II 97.

Chinzorig, T., Y. Kobayashi, K. Tsogtbaatar, P. J. Currie, M. Watabe, and R. Barsbold. 2017b. First Ornithomimid (Theropoda, Ornithomimosauria) from the Upper Cretaceous Djadokhta Formation of Tögrögiin Shiree, Mongolia. Scientific Reports 7:1–14.

Chinzorig, T., Y. Kobayashi, K. Tsogtbaatar, P. J. Currie, T. Ryuji, T. Tanaka, M. Iijima, and R. Barsbold. 2018. Ornithomimosaurs from the Nemegt Formation of Mongolia: manus morphological variation and diversity. Palaeogeography, Palaeoclimatology, Palaeoecology 494:91–100.

Choiniere, J. N., C. A. Forster, and W. J. De Klerk. 2012. New information on Nqwebasaurus thwazi, a coelurosaurian theropod from the Early Cretaceous Kirkwood Formation in South Africa. Journal of African Earth Sciences 71–72:1–17.

Claessens, L. P. A. M., and M. A. Loewen. 2015. A redescription of Ornithomimus velox Marsh, 1890 (Dinosauria, Theropoda). Journal of Vertebrate Paleontology e1034593.

Codron, D., J. Codron, J. A. Lee-Thorp, M. Sponheimer, D. De Ruiter, J. Sealy, R. Grant, and N. Fourie. 2007. Diets of savanna ungulates from stable carbon isotope composition of faeces. Journal of Zoology 273:21–29.

Cohen, K. M., S. C. Finney, P. L. Gibbard, and J.-X. Fan. 2017. The ICS International Chronostratigraphic Chart. Episode 36:199–204.

Cormack, D. 1987. Ham's histology. 732.

Cullen, T. M., M. J. Ryan, C. Schröder-Adams, P. J. Currie, and Y. Kobayashi. 2013. An ornithomimid (Dinosauria) bonebed from the Late Cretaceous of Alberta, with implications for the behavior, classification, and stratigraphy of North American ornithomimids. PLoS ONE 8:1–9.

Cullen, T. M., D. C. Evans, M. J. Ryan, P. J. Currie, and Y. Kobayashi. 2014. Osteohistological variation in growth marks and osteocyte lacunar density in a theropod dinosaur (Coelurosauria: Ornithomimidae). BMC Evolutionary Biology 14:1–14.

Currie, P. J. 1985. Cranial anatomy of Stenonychosaurus inequalis (Saurischia:Theropoda) and its bearing on the

origin of birds. Canadian Journal of Earth Sciences 22:1643–1658.

Currie, P. J. 2000. Theropods from the Cretaceous of Mongolia; pp. 434–455 in M. J. Benton, D. M. Shishkin, Unwin, and E. N. Kurochkin (eds.), The age of dinosaurs in Russia and Mongolia. Cambridge University Press, Cambridge.

Currie, P. J. 2016. Dinosaurs of the gobi: Following in the footsteps of the Polish-Mongolian Expeditions. Palaeontologica Polonica 67:83–100.

Currie, P. J., and J. H. Peng. 1993. A juvenile specimen of Saurornithoides mongoliensis from the Djadokhta Formation (Upper Cretaceous) of Northern China. Canadian Journal Earth. Sciences 30:2224–2230.

Currie, P. J., and D. A. Eberth. 1993. Palaeontology, sedimintology and palaeoecology of Iren Dabasu Formation (Upper Cretaceous), Inner Mongolia, People's Republic of China. Cretaceous Research 14:127–144.

Currie, P. J., and K. Padian. 1997. The Encyclopedia of Dinosaurs. 869 pp.

Dashzeveg, D., L. Dingus, B. D. Loope, C. C. Swisher III, T. Dulam, and M. R. Sweeney. 2005. New stratigraphic subdivision, depositional environment, and age estimate for the Upper Cretaceous Djadokhta Formation, southern Ulan Nur Basin, Mongolia. American Museum Novitates 3498:1–31.

Dingus, L., B. D. Loope, D. Dashzeveg, C. C. Swisher III, C. Minjin, M. J. Novacek, and M. A. Norell. 2008. The geology of Ukhaa Tolgod (Djadokhta Formation, Upper Cretaceous, Nemegt Basin, Mongolia). American Museum Novitates 3616:1–40.

Dodson, P., C. A. Forster, and S. S.D. 2004. Ceratopsidae, The Dinosa. Berkeley: University of California Press, 494-513 pp.

Eberth, D. A. 1993. Depositional environments and facies transitions of dinosaur-bearing Upper Cretaceous redbeds at Bayan Mandahu (Inner Mongolia, People's Republic of China). Canadian Journal of Earth Sciences 30:2196–2213.

Eberth, D. A. 2018. Stratigraphy and paleoenvironmental evolution of the dinosaur-rich Baruungoyot-Nemegt succession (Upper Cretaceous), Nemegt Basin, southern Mongolia. Palaeogeography, Palaeoclimatology, Palaeoecology 494:29–50.

Eberth, D. A., and P. J. Currie. 2010. Stratigraphy, sedimentology, and taphonomy of the Albertasaurus bonebed (upper Horseshoe Canyon Formation; Maastrichtian), southern Alberta, Canada. Canadian Journal of Earth Sciences 47:1119–1143.

Eberth, D. A., D. Badamgarav, and P. J. Currie. 2009. The Baruungoyot-Nemegt transition (Upper Cretaceous) at the Nemegt type area, Nemegt Basin, south central Mongolia. Journal of the Paleontological Society of Korea 25:1–15.

Efremov, I. A. 1954. Nekotorie zamechaniya po voprosam istoricheskovo razvitiya dinosaurov. Trudy Sovm. Sov.-Mong. Paleontol. Eksped., Acad. Nauk SSSR. XLVIII:125–141.

Elizabeth J. Kleynhans, A. E. Jolles, M. R. E. Bos, and H. Olff. 2011. Resource partitioning along multiple niche dimensions in differently sized African savanna grazers. Oikos 120:591–600.

Elzanowski, A. 1999. A comparison of the jaw skeleton in theropods and birds, with a description of the palate in

the Oviraptoridae. 4th International Meeting of Society of Avian Paleontolgy and Evolution, Washington, D.C. June 4-7, 1996 311–323.

Erickson, G. M., P. J. Makovicky, P. J. Currie, M. A. Norell, S. A. Yerby, and C. A. Brochu. 2004. Gigantism and comparative life-history parameters of tyrannosaurid dinosaurs. Nature 430:772–775.

Evans, D. C., D. W. Larson, and P. J. Currie. 2013. A new dromaeosaurid (Dinosauria: Theropoda) with Asian affinities from the latest Cretaceous of North America. Die Naturwissenschaften 100:1041–9.

Fanti, F., P. J. Currie, and D. Badamgarav. 2012. New specimens of Nemegtomaia from the Baruungoyot and Nemegt formations (Late Cretaceous) of Mongolia. PLoS One 7.

Fanti, F., P. J. Currie, and M. E. Burns. 2015. Taphonomy, age, and paleoecological implication of a new Pachyrhinosaurus (Dinosauria: Ceratopsidae) bonebed from the Upper Cretaceous (Campania) Wapiti Formation of Alberta, Canada. Canadian Journal of Earth Sciences 52:250–260.

Fanti, F., L. Cantelli, and L. Angelicola. 2017. High-resolution maps of Khulsan and Nemegt localities (Nemegt Basin, southern Mongolia): Stratigraphic implications. Palaeogeography, Palaeoclimatology, Palaeoecology XX–XX:(this volume).

Fastovsky, D. E., D. Badamgarav, H. Ishimoto, M. Watabe, and D. B. Weishampel. 1997. The paleoenvironments of Tugrikin Shireh (Gobi Desert, Mongolia) and aspects of the Taphonomy and Paleoecology of Protoceratops (Dinosaurian: Ornithishichia). Palaios 12:59–70.

Fiorillo, A. R. 1988. Taphonomy of Hazard Homestead Quarry (Ogallala Group), Hitchcock County, Nebraska. Rocky Mountain Geology 26:57–97.

Foote, M. 1993. Contributions of individual taxa to overall morphological disparity. Paleobiology 19:403–419.

Fowler, D. W., H. N. Woodward, E. A. Freedman, P. L. Larson, and J. R. Horner. 2011. Reanalysis of Raptorex kriegsteini: A Juvenile Tyrannosaurid Dinosaur from Mongolia. PLoS One 6:e21376.

Funston, G., S. E. Medonca, P. J. Currie, and R. Barsbold. 2018. Oviraptorosaur anatomy, diversity and ecology in the Nemegt Basin. Palaeogeography, Palaeoclimatology, Palaeoecology 494:101–120.

Funston, G. F., P. J. Currie, D. A. Eberth, M. J. Ryan, T. Chinzorig, D. Badamgarav, and Nicholas R. Longrich. 2016. The first oviraptorosaur (Dinosauria: Theropoda) bonebed: evidence of gregarious behaviour in a maniraptoran theropod. Scientific Reports 6:1–13.

Geist, V. 1974. On the relationship of social evolution and ecology in ungulates. American Zoologist 14:205–220.

Gilmore, C. W. 1920. Osteology of the carnivorous Dinosauria in the United States National Museum, with special reference to the Antrodemus (Allosaurus) and Ceratosaurus. Bulletin of the United States National Museum 110:1–159.

Gilmore, C. W. 1933. On the dinosaurian fauna of the Iren Dabasu Formation. American Museum of Natural History 67:23–78.

Goloboff, P., J. S. Farris, and K. C. Nixon. 2008. TNT, a free program for phylogenetic analysis. Cladistics 24:774–786.

Goloboff, P. A., and S. A. Catalano. 2016. TNT version 1.5, including a full implementation of phylogenetic

morphometrics. Cladistics 32.

Gower, J. C. 1975. Generalized Procrustes analysis. Psychometrika 40:33–51.

Gradziński, R. 1970. Sedimentation of dinosaur-bearing Upper Cretaceous deposits of the Nemegt Basin, Gobi Desert. Palaeontologica Polonica 21:147–229.

Gradziński, R., and T. Jerzykiewicz. 1974a. Dinosaur- and mammal-bearing aeolian and associated deposits of the Upper Cretaceous in the Gobi Desert (Mongolia). Sedimentological Geology 12:249–278.

Gradziński, R., and T. Jerzykiewicz. 1974b. Sedimentation of the Barun Goyot Formation. Palaeontologica Polonicaeon 30:111–146.

Gradziński, R., J. Kazmierczak, and J. Lefeld. 1969. Geographical and geological data from the Polish-Mongolian paleontological expeditions. Paleontologia Polonica 19:33–80.

Gradziński, R., Z. Kielan-Jaworowska, and T. Maryánska. 1977. Upper Cretaceous Djadokhta, Barun Goyot and Nemegt Formations of Mongolia, including remarks on previous subdivisions. Acta Geologica Polonica 27:281–318.

Gradzínski, R., and T. Jerzykiewicz. 1974. Dinosaur- and mammal-bearing aeolian and associated deposits of the Upper Cretaceous in the Gobi Desert (Mongolia). Sedimentological Geology 12:249–278.

Harland, B. W., R. L. Armstrong, A. V. Cox, L. E. Craig, A. G. Smith, and D. G. Smith. 1990. A geologic time scale. Cambridge University Press 263.

Hicks, J. F., D. L. Brinkman, D. J. Nichols, and M. Watabe. 1999. Paleomagnetic and palynologic analyses of Albian to Santonian strata at Bayn Shireh, Burkhant, and Khuren Dukh, eastern Gobi Desert, Mongolia. Cretaceous Research 20:829–850.

Holtz, T. R., J. 1994. Arctometatarsalian pes, an unusual structure of the metatarsus of Cretaceous Theropoda (Dinosauria: Saurischia). Journal of Vertebrate Paleontology 14:480–519.

Holtz, T. R., J. 2004. Tyrannosauroidae; pp. 111–136 in D. B. Weishampel, P. Dodson, and H. Osmólska (eds.), The Dinosauria, 2nd editio. University of California Press [AQ1], California.

Horner, J. R., and K. Padian. 2004. Age and growth dynamics of Tyrannosaurus rex. Proceedings. Biological Sciences / The Royal Society 271:1875–1880.

Horner, J. R., D. B. Weishampel, and C. A. Forster. 2004. Hadrosauridae, The Dinosa. (D. B. Weishampel, P. Dodson, and H. Osmólska (eds.)). Berkeley: University of California Press, 438-463 pp.

Hübner, T. R. 2012. Bone histology in Dysalotosaurus lettowvorbecki (Ornithischia: Iguanodontia)–variation, growth, and implications. PLoS ONE 7:e29958.

Hurum, J. H. 2001. Lower jaw of Gallimimus bullatus.; pp. 34–41 in D. H. Tanke and K. Carpenter (eds.), In Mesozoic vertebrate life. Indiana University Press.

Hurum, J. H., and K. Sabath. 2003. Giant theropod dinosaurs from Asia and North America: Skulls of Tarbosaurus bataar and Tyrannosaurus rex compared. Acta Palaeontologica Polonica 48:161–190.

Ian Macdonald, and P. J. Currie. 2018. Description of a partial Dromicceiomimus (Dinosauria: Theropoda) skeleton with comments on the validity of the genus. Canadian Journal of Earth Sciences.

Van Itterbeeck, J. V., D. J. Horne, P. Bultynck, and N. Vandenberghe. 2005. Stratigraphy and palae¬onvironment of the dinosaur-bearing Upper Cre¬taceous Iren Dabasu Formation, Inner Mongolia, People's Republic of China. Cretaceous Research 26:699–725.

Jerzykiewicz, T. 2000. Lithostratigraphy and sedimentary settings of the Cretaceous dinosaur beds of Mongolia; pp. 279–296 in M. J. Benton, M. A. Shishkin, D. M. Unwin, and E. N. Kurochkin (eds.), The Age of Dinosaurs in Russia and Mongolia. Cambridge.

Jerzykiewicz, T., and D. A. Russell. 1991. Late Mesozoic stratigraphy and vertebrates of the Gobi Basin. Cretaceous Research 12:345–377.

Jerzykiewicz, T., P. J. Currie, D. A. Eberth, P. A. Johnston, E. H. Koster, and J. J. Zheng. 1993. Djadokhta Formation correlative strata in Chinese Inner Mongolia: an overview of the stratigraphy, sedimentary geology, and paleontology and comparisons with the type locality in the pre-Altai Gobi. Canadian Journal of Earth Sciences 30:2180–2195.

Ji, Q., M. A. Norell, P. J. Makovicky, K. Gao, S. Ji, and C. Yuan. 2003. An early ostrich dinosaur and implication for ornithomimosaur phylogeny. American Museum Novitates 3420:1–19.

Khand, Y., D. Badamgarav, Y. Ariunchimeg, and R. Barsbold. 2000. Cretaceous System in Mongolia and Its Depositional Environments (H. Okada and N. J. Mateer (eds.)). Amsterdam, 49-79 pp.

King, T. D., and E. D. Jones. 1997. Late Cretaceous dinosaurs of the southeastern United States. Gulf Coast Association of Geological Societies Transactions 47:263–269.

Kobayashi, Y., and J. Lü. 2003. A new ornithomimid dinosaur with gregarious habits from the Late Cretaceous of China. Acta Palaeontologica Polonica 48:235–259.

Kobayashi, Y., and R. Barsbold. 2004. Phylogeny of Ornithomimosauria and its paleobiogeographic implications. Proceedings of the 19th International Congress of Zoology, Beijing, China, 23–27 August 2004 50–52.

Kobayashi, Y., and R. Barsbold. 2005a. Reexamination of a primitive ornithomimosaur, Garudimimus brevipes Barsbold, 1981 (Dinosauria: Theropoda), from the Late Cretaceous of Mongolia. Canadian Journal of Earth Sciences 42:1501–1521.

Kobayashi, Y., and R. Barsbold. 2005b. Anatomy of Harpymimus okladnikovi Barsbold and Perle 1984 (Dinosauria; Theropoda) of Mongolia; pp. 97–126 in K. Carpenter (ed.), The carnivorous dinosaurs. Indiana University Press, Indianapolis.

Kobayashi, Y., and R. Barsbold. 2006. Ornithomimids from the Nemegt Formation of Mongolia. Journal of Paleontological Society of Korea 22:195–207.

Kobayashi, Y., K. Kubota, and R. Barsbold. 2009. Ornithomimid materials from the Bayanshiree Formation at Shine Us Khudak, Dornogov', Southeastern Mongolia. Abstracts of 2009 Goseong International Dinosaur Symposium 26–29.

Kobayashi, Y., Y.-N. Lee, J.-C. Lü, M. J. Ryan, and P. J. Currie. 2010. A nearly complete skeleton of a new ornithomimid from the Nemegt Formation of Mongolia. Journal of Vertebrate Paleontology 30:1A–198A.

Koen Stein, Z. Csiki, K. C. Rogers, D. B. Weishampel, R. Redelstorff, J. L. Carballido, and P. M. Sander. 2010.

Small body size and extreme cortical bone remodeling indicate phyletic dwarfism i nMagyarosaurus dacus (Sauropoda: Titanosauria). PNAS 107:9258–9263.

Köhler, M., N. Marín-Moratalla, X. Jordana, R. Aanes, I. Macdonald, and P. J. Currie. 2012. Seasonal bone growth and physiology in endotherms shed light on dinosaur physiology. Nature 487:358.

Kolesnikov, C. M. 1982. Mesozoic Lacustrine Basins of Mongolia.; pp. 101 in G. G. Martinson (ed.), Nauke. Leningrad.

Ksepka, D. T., and M. A. Norell. 2004. Ornithomimosaur cranial material from Ukhaa Tolgod (Omnogov, Mongolia). American Museum Novitates 3448:1–4.

Kurzanov, S. M. 1981. Catalog No: 3907/1; incomplete skeleton; MNR, Udan-Sayr, Upper Cretaceous, Nemgetinsk suite. Material. Besides the holotype, paratype #3906/1 from the location Shara-Tsav, individual fragments of the postcranial skeleton; MNR, Upper Cretaceous, Nemgetinsk. .

Kurzanov, S. M. 1987. Avimimids and the problem of the origin of birds. Trudy Issue Sovm. Sov.-Mong. Paleontol. Eksped 31:5–95.

Lee, Y.-N., R. Barsbold, P. J. Currie, Y. Kobayashi, H.-J. Lee, P. Godefroit, F. Escuillié, and T. Chinzorig. 2014. Resolving the long-standing enigmas of a giant ornithomimosaur Deinocheirus mirificus. Nature 515:257–60.

Lefeld, J. 1971. Geology of the Djadokhta Formation at Bayn Dzak (Mongolia). Results of the Polish-Mongolian Palaeontological Expeditions, Part III. Palaeontologica Polonica 25:101–127.

Lü, J.-C., Z. Dong, Y. Azuma, R. Barsbold, and Y. Tomida. 2002. Oviraptorosaurs compared to birds. Science Press 175–189.

Makovicky, P. J. 1995. Phylogenetic aspects of the vertebral morphology of Coelurosauria (Dinosauria: Theropoda). pp.

Makovicky, P. J., and M. A. Norell. 1998. A partial ornithomimid briancase from Ukhaa Tolgod (Upper Cretaceous, Mongolia). American Museum Novitates 3247:1–16.

Makovicky, P. J., and M. A. Norell. 2004. Troodontidae; pp. 184–195 in The Dinosauria.

Makovicky, P. J., Y. Kobayashi, and P. J. Currie. 2004. Ornithomimosauria; pp. 137–150 in D. B. Weishampel, P. Dodson, and H. Osmólska (eds.), The Dinosauria, 1st ed. University of California Press [AQ1], Berkeley.

Makovicky, P. J., D. Li, K.-Q. Gao, M. Lewin, G. M. Erickson, and M. A. Norell. 2009. A giant ornithomimosaur from the Early Cretaceous of China. Proceedings of the Royal Society B: Biological Sciences 277:191–198.

Maleev, E. A. 1955. Giant carnivorous dinosaurs of Mongolia. Doklady, Academy of Sciences USSR. 104:634–637.

Marsh, O. C. 1881. Classification of the Dinosauria. The American Journal of Science, Third Series 23:81–86.

Marsh, O. C. 1890. Description of a new dinosaurian reptile. The American Journal of Science, 3:81–86.

Martinson, G. G. 1982. Pozdnemelovye molliuski Mongolii (The Upper Cretaceous mollusks of Mongolia). In Sovmestnaya Sovetsko-Mongolskaya Paleontologicheskaya Ekspeditsia (eds. Nevesskaya, L. A. et al.). Tudy 17:5–76.

Maryánska, T., and H. Osmólska. 1981. Cranial anatomy of Saurolophus angustirostris with comments on the Asian Hadrosauridae (Dinosauria). Palaeontologica Polonica 42:5–24.

McFeeters, B., M. J. Ryan, C. Schröder-Adams, and T. M. Cullen. 2016. A new ornithomimid theropod from the Dinosaur Park Formation of Alberta, Canada. Journal of Vertebrate Paleontology 4634:e1221415.

McFeeters, B., M. J. Ryan, C. Schröder-Adams, and P. J. Currie. 2017. First North American occurrences of Qiupalong (Theropoda: Ornithomimidae) and the palaeobiogeography of derived ornithomimids. Facets 2:355–373.

Mikhailov, K. E. 1991. Classification of fossil eggshells of amnoitic vertebrates. Acta Palaeontologica Polonica 36:193–238.

Nagy, K. A., I. A. Girard, and T. K. Brown. 1999. Energetics of free-ranging mammals, reptiles, and birds. Annual Review of Nutrition 19:247–277.

Nicholls, E. L., and A. P. Russell. 1980. A new specimen of Struthiomimus altus from Alberta, with comments on the classificatory characters of Upper Cretaceous ornithomimids. Canadian Journal of Earth Sciences 18:518–526.

Nicholls, E. L., and A. P. Russell. 1985. Structure and function of the pectoral girdle and forelimb of Struthiomimus altus (THeropoda: Ornithomimidae). Palaeontology 28:643–677.

Norell, M. A., P. J. Makovicky, and P. J. Currie. 2001. The beaks of ostrich dinosaurs. Nature 412:873–874.

Norman, D. B. 2000. The Evolution of Mesozoic Flora and Fauna.; pp. 204–230 in the Scientific American book of Dinosaurs, First edit. St. Martin's Press, New York.

Okada, H. 2000. Cretaceous Environments of Asia. Elsevier Developmen:49–79.

Osborn, H. F. 1917. Skeletal adaptations of Ornitholestes, Struthiomimus, Tyrannosaurus. American Museum of Natural History 35:733–761.

Osborn, H. F. 1924. Three new Theropoda, Protoceratops zone, central Mongolia. American Museum Novitates 144:1–12.

Osmólska, H. 1980a. The Late Cretaceous vertebrate assemblages of the Gobi Desert, Mongolia. Mem. Soc. Geol. Fr., N.S. 139:145–150.

Osmólska, H. 1980b. Late Cretaceous vertebrate assemblages of the Gobi Desert. Mem. Soc. Geol. Fr., N.S. 139:145–150.

Osmólska, H. 1997. Ornithomimosauria. Encyclopedia of Dinosaurs 499–503.

Osmólska, H., and E. Roniewicz. 1970. Deinocheiridae, a new family of theropod dinosaurs. Acta Palaeontologica Polonica 21:5–19.

Osmólska, H., E. Roniewicz, and R. Barsbold. 1972. a New Dinosaur , Gallimimus bullatus n . gen . , n . sp . (Ornithomimidae) from the Upper Cretaceous of Mongolia. Acta Palaeontologica Polonica 27:103–143.

Ostrom, J. H. 1966. Functional morphology and evolution of the ceratopsian dinosaurs. Evolution 20:290–308.

Ostrom, J. H. 1969. Osteology of Deinonychus antirrhopus, an unusual theropod from the Lower Cretaceous of Montana. Bulletin of Peabody Museum of Natural History 30:1–165.

Ostrom, J. H. 1970. Stratigraphy and paleontology of the Cloverly Formation (Lower Cretaceous) of the Bighorn Basin area, Wyoming and Montana. Peabody Museum of Bulletin 35:1–234.

Owen, R. 1842. Report on British fossil reptiles. Part II. Report of the British Association for the Advancement of Science 11:60–204.

Peabody, F. E. 1961. Annual growth zones in living and fossil vertebrates. Journal of Morphology 108:11–62.

Perěz-Moreno, B. P., J. L. Sanz, A. D. Buscalioni, J. J. Moratalla, F. J. Ortega, and D. Rasskin-Gutman. 1994. A unique multitoothed ornithomimosaur dinosaur from the Lower Cretaceous of Spain. Nature 370:363–367.

Perle, A. 1977. On the first discovery of Alectrosaurus from the Late Cretaceous of Mongolia. Problems of Mongolian Geology 3:104–113.

Perle, A., M. A. Norell, L. M. Chiappe, and J. M. Clark. 1993. Flightless bird from the Cretaceous of Mongolia. Nature 362:623–626.

Peyer, K. 2006. A reconsideration of Compsognathus from the upper Tithonian of Canjuers, southeastern France. Journal of Vertebrate Paleontology 26:879–896.

R Core Team. 2016. R: A language and environment for statistical computing. .

Rohlf, F. J. 2013a. tpsDig version 2.17. Department of Ecology and Evolution, State University of New York, Stony Brook, NY. .

Rohlf, F. J. 2013b. tpsRelw version 1.53. Department of Ecology and Evolution, State University of New York, Stony Brook, NY. .

Rohlf, F. J., and D. Slice. 1990. Extensions of the Procrustes method for the optimal superimposition of landmarks. Systematic Zoology 39.

Russell, D. A. 1972. Ostrich dinosaurs from the Late Cretaceous of Western Canada. Canadian Journal of Earth Sciences 9:375–402.

Ryan, M. J., A. P. Russell, D. A. Eberth, and P. J. Currie. 2001. The taphonomy of a Centrosaurus (Ornithischia: Ceratopsidae) bonebed from the Dinosaur Park Formation (Upper Campanian), Alberta, Canada, with comments on cranial ontogeny. Palaios 16:482–506.

Sander, P. M., O. Mateus, T. Laven, and N. Knotschke. 2006. Bone histology indicates insular dwarfism in a new Late Jurassic sauropod dinosaur. Nature Letters 441:739–741.

Saneyoshi, M., and M. Watabe. 2008. Eolian deposits and paleo-wind-direction of the Upper Cretaceous Djadokhta Formation in the central Gobi desert, south Mongolia. Journal of the Geological Society of Japan 114:V–VI.

Sereno, P. C. 2017. Early Cretaceous Ornithomimosaurs (Dinosauria: Coelurosauria) from Africa. Ameghiniana 54:576–616.

Serrano-Brañas, C. I., E. Torres-Rodríguez, P. C. Reyes-Luna, I. González-Ramírez, and C. González-León. 2016. A new ornithomimid dinosaur from the Upper Cretaceous Packard Shale formation (Cabullona Group) Sonora, México. Cretaceous Research 58:49–62.

Shapiro, M. D., H. You, N. H. Shubin, Z. Luo, and J. P. Downs. 2003. A large ornithomimid pes from the Lower Cretaceous of the Mazongshan area, Northern Gansu province, People's Republic of China. Journal of

Vertebrate Paleontology 23:695–698.

Shuvalov, V. F. 2000. The Cretaceous stratigraphy and palaeobiogeography of Mongolia; pp. 256–278 in J. M. Benton, M. A. Shishkin, D. M. Unwin, and E. N. Kurochkin (eds.), The Age of Dinosaurs in Russia and Mongolia. Cambridge University Press.

Shuvalov, V. F., and T. V. Nikolaeva. 1985. On the age and territorial distribution of Cenozoic basalts in the south of Mongolia. Vestnik Leningradskogo Universiteta: Geologiya, Geografiya 7:52–59.

Sibbing, F. A., L. A. J. Nagelkerke, R. J. M. Stet, and J. W. M. Osse. 1998. Speciation of endemic lake Tana barbs (Cyprinidae, Ethiopia) driven by trophic resource partitioning; a molecular and ecomorphological approach. Aquatic Ecology 32:217–227.

Smith, D., and P. Galton. 1990. Osteology of Archaeornithomimus asiaticus (Upper Cretaceous, Iren Dabasu Formation, People's Republic of China). Journal of Vertebrate Paleontology 10:255–265.

Sochava, A. V. 1975. Report of Joint Soviet-Mongolian Paleontological Expedition. Transactions of the Joint Soviet-Mongolian Paleontological Expedition 13:113.

Sues, H.-D., and A. Averianov. 2016a. Ornithomimidae (Dinosauria: Theropoda) from the Bissekty Formation (Upper Cretaceous: Turonian) of Uzbekistan. Cretaceous Research 57:90–110.

Sues, H.-D. D., and A. Averianov. 2016b. Ornithomimidae (Dinosauria: Theropoda) from the Bissekty Formation (Upper Cretaceous: Turonian) of Uzbekistan. Cretaceous Research 57:90–110.

Du Toit, J. T., and H. Olff. 2014. Generalities in grazing and browsing ecology: using across-guild comparisons to control contingencies. Oecologia 174:1075–1083.

Tsogtbaatar, K., D. B. Weishampel, D. C. Evans, and M. Watabe. 2014. A new Hadrosauroid (Plesiohadros djadokhtaensis) from the Late Cretaceous Djadokhtan fauna of southern Mongolia; pp. 108–135 in Hadrosaur. Indiana University Press, Indianapolis.

Tsuihiji, T., R. Barsbold, M. Watabe, K. Tsogtbaatar, T. Chinzorig, Y. Fujiyama, and S. Suzuki. 2014. An exquisitely preserved troodontid theropod with new information on the palatal structure from the Upper Cretaceous of Mongolia. Naturwissenschaften 101:131–142.

Turner, A. H., S. J. Nesbitt, and M. A. Norell. 2009. A large Alvarezsaurid from the Late Cretaceous of Mongolia. American Museum Novitates 3648:1–14.

Tverdokhlebov, V. P., and Y. I. Tsybin. 1974. Genesis of the Upper Cretaceous dinosaur localities Tugrugiin Us and Alag Teeg. Trudy Sovmestnoi Sovestsko-Mongol'skoi Paleontologicheskoi Ekspeditsii 1:314–319.

Varricchio, D. J., P. C. Sereno, Z. Xijin, T. Lin, J. A. Wilson, and G. H. Lyon. 2008. Mud-trapped herd captured evidence of distinctive dinosaur sociality. Acta Palaeontologica Polonica 53:567–578.

Watabe, M., S. Suzuki, and K. Tsogtbaatar. 2006. Geological and geographical distribution of bird-like theropod Avimimus in Mongolia. Journal of Vertebrate Paleontology 26:136A.

Watabe, M., K. Tsogtbaatar, S. Suzuki, and M. Saneyoshi. 2010. Geology of dinosaur fossil-bearing locations (Jurassic and Cretaceous, Mesozoic) in the Gobi desert: results of the HMNS − MPC Joint Paleontological Expedition. Hayashibara Museum of Natural Sciences Research Bulletin 3:41–118.

Watanabe, A., G. M. Erickson, and P. S. Druckenmiller. 2013. An ornithomimosaurian from the Upper Cretaceous Prince Creek Formation of Alaska. Journal of Vertebrate Paleontology 33:1169–1175.

Weishampel, D. B., P. Dodson, and H. Osmólska. 2004a. The Dinosauria, 2nd ed. (D. B. Weishampel, P. Dodson, and H. Osmólska (eds.)). University of California Press [AQ1], ix-xv pp.

Weishampel, D. B., D. E. Fastovsky, M. Watabe, D. Varricchio, F. Jackson, K. Tsogtbaatar, and R. Barsbold. 2008. New oviraptorid embroys from Bugin-Tsav, Nemegt Formation (Upper Cretaceous), Mongolia, with insights into their habitat and growth. Journal of Vertebrate Paleontology 28:1110–1119.

Weishampel, D. B., P. M. Barrett, R. A. Coria, J. Le Loeuff, X. Xu, X. Zhao, A. Sahni, E. M. P. Gomani, and C. R. Noto. 2004b. Dinosaur distribution; pp. 517–606 in D. B. Weishampel, P. Dodson, and H. Osmólska (eds.), The Dinosauria, 2nd ed. University of California Press [AQ1], Berkeley.

Wilson, J. P., D. C. Woodruff, J. D. Gardner, H. M. Flora, J. R. Horner, and C. L. Organ. 2016. Vertebral Adaptations to Large Body Size in Theropod Dinosaurs. PLoS One 11:1–15.

Wilson, M. C., and P. J. Currie. 1985. Stenonychosaurus inequalis (Saurischia: Theropoda) from the Judith River (Oldman) Formation of Alberta: new findings on metatarsal structure. Canadian Journal of Earth Sciences 22:1813–1817.

Xu, L., Y. Kobayashi, J. Lü, Y.-N. Lee, Y. Liu, K. Tanaka, X. Zhang, S. Jia, and J. Zhang. 2011. A new ornithomimid dinosaur with North American affinities from the Late Cretaceous Quipa Formation in Henan province of China. Cretaceous Research 32:213–222.

Zelditch, M. L., D. L. Swiderski, and H. D. Sheets. 2004. Geometric Morphometrics for Biologists: A Primer., 2nd ed. Amsterdam, pp.